VLÁKNA a TEXTIL

4

Volume 27.
December
2020

FIBRES AND TEXTILES

STU FCHPT

TECHNICAL UNIVERSITY OF LIBEREC
Faculty of Textile Engineering

Trenčianska univerzita Alexandra Dubčeka v Trenčíne
Fakulta priemyselných technológií v Púchove

VÚCHV

VÚTCH CHEMITEX

Spoločnosť priemyselnej chémie ZSVTS

CHEMOSVIT FIBROCHEM

Indexed in:
SCOPUS
Chemical Abstracts
World Textiles

ISSN 1335-0617
print version

ISSN 2585-8890
online version

Fibres and Textiles
Vlákna a textil

Published by

- Slovak University of Technology in Bratislava, Faculty of Chemical and Food Technology
- Technical University of Liberec, Faculty of Textile Engineering
- Alexander Dubček University of Trenčín, Faculty of Industrial Technologies
- Slovak Society of Industrial Chemistry, Bratislava
- Research Institute of Man-Made Fibres, JSC, Svit
- VÚTCH – CHEMITEX, Ltd., Žilina
- Chemosvit Fibrochem, JSC, Svit

Vydáva

- Slovenská technická univerzita v Bratislave, Fakulta chemickej a potravinárskej technológie
- Technická univerzita v Liberci, Fakulta textilní
- Trenčianska univerzita Alexandra Dubčeka v Trenčíne, Fakulta priemyselných technológií
- Slovenská spoločnosť priemyselnej chémie, Bratislava
- Výskumný ústav chemických vlákien, a.s. Svit
- VÚTCH – CHEMITEX, spol. s r.o., Žilina
- Chemosvit Fibrochem, a.s., Svit

Editorial office and distribution of the journal
(Redakcia a distribúcia časopisu)

Ústav prírodných a syntetických polymérov
Fakulta chemickej a potravinárskej technológie
Slovenská technická univerzita v Bratislave
Radlinského 9, 812 37 Bratislava, SK
Tel: 00 421 2 59 325 575
e-mail: marcela.hricova@stuba.sk

Order and advertisement of the journal
(Objednávka a inzercia časopisu)

Slovenská spoločnosť priemyselnej chémie,
člen Zväzu vedecko-technických spoločností
Radlinského 9, 812 37 Bratislava, SK
Tel: 00 421 2 59 325 575
e-mail: marcela.hricova@stuba.sk

Order of the journal from abroad – excepting Czech Republic
Objednávka časopisu zo zahraničia – okrem Českej Republiky

SLOVART G.T.G, s.r.o. EXPORT-IMPORT
Krupinská 4, P.O.Box 152, 852 99 Bratislava, SK
Tel: 00421 2 839 471-3, Fax: 00421 2 839 485
e-mail: info@slovart-gtg.sk

Typeset and printing *(Sadzba a tlač)*

FOART, s.r.o., Bratislava

Journal is published 4x per year
Subscription 60 EUR

Časopis vychádza 4x ročne
Ročné predplatné 60 EUR

Evidenčné číslo MKCR SR Bratislava EV 4006/10

IČO vydavateľa 00 397 687

Fibres and Textiles (4) 2020
Vlákna a textil (4) 2020
December 2020

Content

APPROXIMATION OF A MATHEMATICAL MODEL OF THE THERMO-MECHANICAL FUSING PROCESS IN THE SEWING INDUSTRY

Snezhina Angelova Andonova[1] and Silvia Baeva[2]

[1]*Faculty of Engineering, South-West University "Neofit Rilski", 66 Ivan Mihailov Str., 2700 Blagoevgrad, Bulgaria*
[2]*Faculty of Applied Mathematics and Informatics, Technical University of Sofia, 8 Kl. Ohridski Blvd, 1000 Sofia, Bulgaria*
andonova_sn@swu.bg, sbaeva@tu-sofia.bg

Abstract: *The use of optimization in various fields of the sewing industry is becoming more accessible, due to the rapidly growing IT industry. A frequently used and effective method for optimizing a technological process is the method of approximation. With this method the investigation of various (unknown or extremely complex) numerical characteristics and qualitative properties of the original objects reduces to working with other objects whose characteristics and properties are already known or more convenient to work with. The aim of the present work is to investigate the nature of the function describing the thermo-mechanical fusing (TMF) process and to derive an effective approximation of this function. This will allow the relatively complex mathematical model of the TMF process to be replaced by its simpler approximation in real production.*

Keywords: *approximation; thermo-mechanical fusing process.*

1 INTRODUCTION

The application of mathematical methods for analysis, evaluation and mathematical modeling in the sewing technologies is increasingly relevant today. Deriving a mathematical model of a technological process creates conditions for increasing the efficiency of this process. In this way, high levels of quantitative and qualitative indicators are provided with minimal expenditure of financial, material, labor, energy and time resources. The desired benefits for each technological problem can be expressed as a function of certain variables, which leads to the task of finding its maximum or minimum value by using mathematical apparatus. In addition, the conditions under which the task is solved are determined for this function [1-4]. The use of optimization in various fields of the sewing industry is becoming more accessible, due to the rapidly growing IT industry.

A frequently used and effective method for optimizing a given function is the method of approximation. With this method the investigation of various (unknown or extremely complex) numerical characteristics and qualitative properties of the original objects reduces to working with other objects whose characteristics and properties are already known or more convenient to work with. The application of approximation for different technological processes is expressed in the application of numerical methods and functional analysis, which deal with the approximation of functions; geometry and topology, in which the approximation of curves, surfaces, spaces and images is considered. The realization of the approximated objects and their characteristics is much easier and is not a secondary choice of solution. Approximated solutions on the one hand can help to see if an exact method is really needed, and on the other hand, an approximate solution can be used to improve the formulation of the task. Examples of good approximations applied to technological processes in the textile and clothing industry are presented in [5-9]. The authors of [5] applied approximation to the process of accelerating the drying of textile materials. They applied a linear approximation of the obtained experimental dependence of the correction value to the mass of the moisture content. The nonlinear approximation of moisture yield by size in textile cutting processes is presented in [6]. In [7] the structural properties of fibers and tissues are analyzed. The authors investigated the possibility of describing the isotherms of water vapor absorption by different equations. They showed that the use of the Zimmerman equation for capillary-porous materials is most suitable for the approximation of the absorbed isotherms of different fibrous materials. They recommend this equation should be used in calculations of drying, extraction, soaking and other processes of thermo-chemical treatment of fibrous materials. In [10] a mathematical model of the thermo-mechanical fusing process (TMF) was created. The TMF process is one of the main technological processes in the sewing industry. The quality and productivity of the entire technological cycle for the production of clothing largely depends on the effective implementation of this process. In light of the above, it is important to find an approximation of the mathematical model of [10] that describes the TMF process in a simplified way. This will lead to a faster and more accurate solution of specific technological problems in real production.

The aim of the present work is to investigate the nature of the function describing the TMF process and to derive an effective approximation of this function. This will allow the relatively complex mathematical model of the TMF process [10] to be replaced by its simpler approximation in real production.

2 RESEARCH WORK

2.1 Methods

The present work uses the standard algorithm for approximating functions [11-13]:

1) Plot the graph of the function with the known points (if possible - in R^2 or R^3)]
2) Attempts to "guess" the type (class) of the sought function on the graph; it can resemble, for example, to: a polynomial of some degree (straight line - polynomial of 1st degree, parabola - polynomial of 2nd degree, etc.), trigonometric function, exponential, logarithmic, etc. (Figure 1 [11]).
3) Depending on the number of points, the class of the function and other characteristics of the approximate function, a different method is used for its approximation.
4) A formula is obtained that is "close" to the data.
5) The obtained approximation formula is used to calculate the values of the function at points where there are no data.

Taking into account the nature of the set aim, interpolation is used as a method of approximation in this work.

The numerical realization of the researched problem is rendered in software environments with the help of specialized software - Maple and MatLab.

2.2 Materials

Materials produced by the company NITEX-50 - Sofia were used for basic textile materials. They are 100% wool fabrics. Their characteristics are described in detail in [10].

A material produced by the company Kufner-B121N77 was used for an auxiliary TM (interlining).

The auxiliary TM is fabric, with mass per unit area 63 g/m^2, warp threads 100% PES, weft threads 100% PES [10].

2.3 Conditions for conducting the study

In the present work the function (1) describing the technological process TMF [10] is investigated:

$$Y = 22.4375 - 1.4375x_1 - 5.8125x_2 + \\ +6.9375x_3 - 1.8125x_2x_3 \tag{1}$$

The function (1) is derived in [10]. It provides the relationship between performance criterion *Y* (process execution time) and manageable process factors X_1 - pressure, *P* [N/cm^2], X_2 - temperature of the pressing plates, *T* [°C] , X_3 - mass per unit area of the basic textile materials, *M* [g/m^2].

The approximation of the function (1) is made by interpolation of approximate polynomials - linear and exponential.

The studied factors of the TMF process are three (X_1, X_2, X_3), therefore, three variants are considered. The studies were performed with the coded values (*CV*) of the factors. The relationship between the natural values (*NV*) and the *CV* of the factors is given in Table 1 [10].

In each variant, one of the factors assumes values in the range [-1; +1], and the other two factors are constants. The choice of constant values is based on the condition for optimization of the function (1) [14].

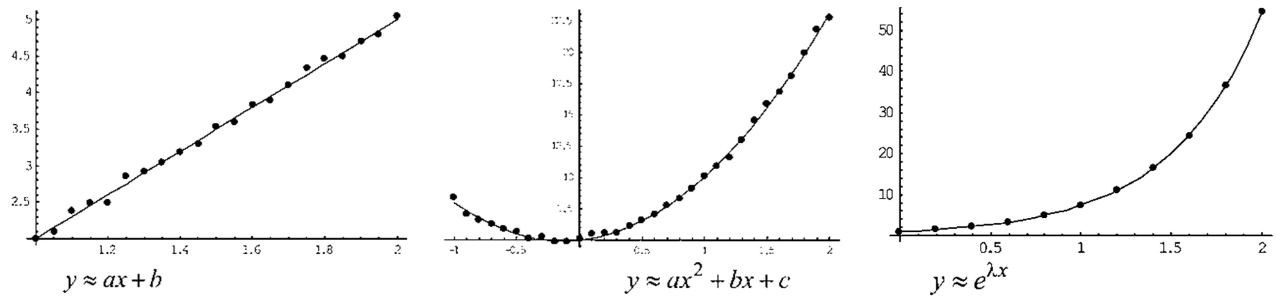

a) b) c)

Figure 1 Examples of the type of the function sought: a) linear function; b) quadric function; c) exponential function

Table 1 Levels of factors

Factors Levels	X_1 - P [N/cm²]		X_2 - T [°C]		X_3 - M [g/m²]	
	NV	*CV*	*NV*	*CV*	*NV*	*CV*
$X_{oi} + J_i$	40	+1	150	+1	213	+1
X_{oi}	25	0	135	0	193	0
$X_{oi} - J_i$	10	-1	120	-1	173	-1
J_i	15		15		20	

Y is the time for the TMF process to take place, therefore the optimal value of *Y* is Y_{min}. The coded values of the factors in which Y_{Rmin} is obtained are $X_1=(+1); X_2=(+1); X_3=(-1)$ [14].

Therefore, the linear and exponential approximation of the function (1) is performed in the following three variants:

-variant I $X_1 \in [-1;1];\ X_2 = 1;\ X_3 = -1;$

-variant II $X_2 \in [-1;1];\ X_1 = 1;\ X_3 = -1;$

-variant III $X_3 \in [-1;1];\ X_1 = 1;\ X_2 = 1.$

3 RESULTS AND DISCUSSION

3.1 Results of the approximation

The results of the linear and exponential approximation of the function (1) for the first variant are given in Table 2. and illustrated in Figure 2.

For the 1st variant: the linear and exponential approximation coincide, i.e.

$$\mathrm{Y}_{\mathrm{LinAppr}} = \mathrm{Y}_{\mathrm{ExpAppr}} \tag{2}$$

where:

$$Y_{LinAppr} = Y = -1.4375x_1 + 11.5 \tag{3}$$

$$Y_{ExpAppr} = Y = 11.44e^{-0.126x_1} \tag{4}$$

when:

$$-1.4375x_1 + 11.5 = 11.44e^{-0.126x_1} \tag{5}$$

only for values for x_1: x_1=0,8501345056 and x_1=–0.7788357158.

The function *Y* (for these values for x_1) takes values accordingly:

$$Y(x_1 = 0.8501345056) = 10.27793165 \tag{6}$$

$$Y(x_1 = -0.7788357158) = 12.61957634 \tag{7}$$

Table 2 Numerical results of the approximations of function (1) for variant 1

X_1	Linear approximation	Exponential approximation
	$Y = -1.4375x_1 + 11.5$	$Y = 11.44e^{-0.126x_1}$
-1.00	12.937500	12.976188
-0.75	12.578125	12.573809
-0.50	12.218750	12.183907
-0.25	11.859375	11.806096
0.00	11.500000	11.440000
0.25	11.140625	11.085257
0.50	10.781250	10.741513
0.75	10.421875	10.408429
1.00	10.062500	10.085674
R^2	0.9998	0.9987

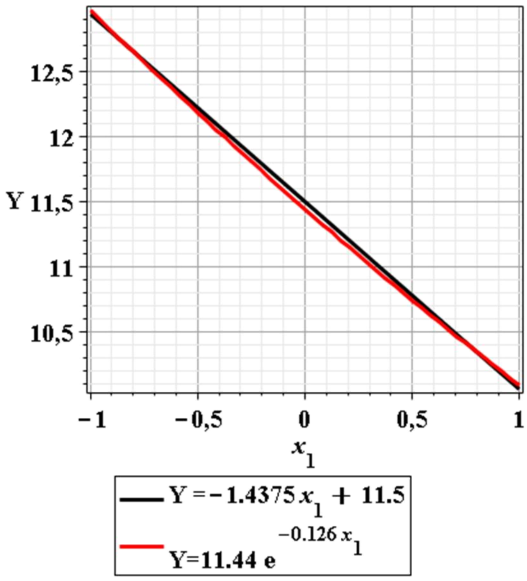

Figure 2 Graphical results of the approximations of function (1) for variant 1

The results of the linear and exponential approximation of the function (1) for the second variant are given in Table 3. and illustrated in Figure 3.

Table 3 Numerical results of the approximations of function (1) for variant 2

X_2	Linear approximation	Exponential approximation
	$Y = -4x_2 + 14.0625$	$Y = 13.673e^{-0.293x_2}$
-1.00	18.0625	18.327874
-0.75	17.0625	17.033348
-0.50	16.0625	15.830257
-0.25	15.0625	14.712141
0.00	14.0625	13.673000
0.25	13.0625	12.707255
0.50	12.0625	11.809722
0.75	11.0625	10.975583
1.00	10.0625	10.200361
R^2	0.9991	0.9931

For the 2nd variant: the linear and exponential approximation coincide, i.e.

$$Y_{LinAppr} = Y_{ExpAppr} \tag{8}$$

where:

$$Y_{LinAppr} = Y = -4x_2 + 14.0625 \tag{9}$$

$$Y_{ExpAppr} = Y = 13.673e^{-0.293x_2} \tag{10}$$

when:

$$-4x_2 + 14.0625 = 13.673e^{-0.293x_2} \tag{11}$$

only for values for x_2: x_2=0.8543639807 and x_2=– 0.7788090732.

The function *Y* (for these values for x_2) takes values accordingly:

$$Y(x_2 = 0.8543639807) = 10.64504408 \tag{12}$$

$$Y(x_2 = -0.7788090732) = 17.17773629 \tag{13}$$

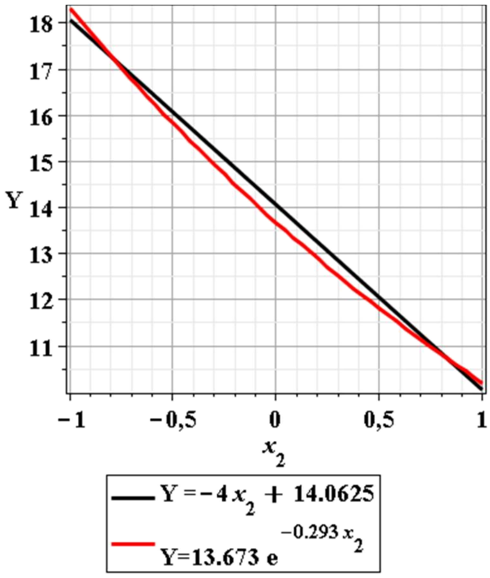

Figure 3 Graphical results of the approximations of function (1) for variant 2

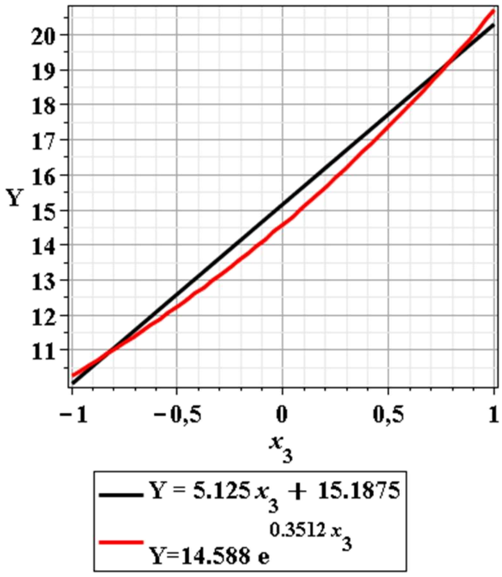

Figure 4 Graphical results of the approximations of function (1) for variant 3

The results of the linear and exponential approximation of the function (1) for the 3rd variant are given in Table 4. and illustrated in Figure 4.

Table 4 Numerical results of the approximations of function (1) for variant 3

X_3	Linear approximation $Y = 5.125x_3 + 15.1875$	Exponential approximation $Y = 14.588e^{0.3512x_3}$
-1.00	10.062500	10.267661
-0.75	11.343750	11.209922
-0.50	12.625000	12.238654
-0.25	13.906250	13.361792
0.00	15.187500	14.588000
0.25	16.468750	15.926737
0.50	17.750000	17.388330
0.75	19.031250	18.984052
1.00	20.312500	20.726214
R^2	0.9989	0.9902

For the 3rd variant: the linear and exponential approximation coincide, i.e.

$$Y_{LinAppr} = Y_{ExpAppr} \tag{14}$$

where:

$$Y_{LinAppr} = Y = 5.125x_3 + 15.1875 \tag{15}$$

$$Y_{ExpAppr} = Y = 14.588e^{0.3512x_3} \tag{16}$$

when:

$$5.125x_3 + 15.1875 = 14.588e^{0.3512x_3} \tag{17}$$

only for values for x_3: x_3=–0.8561650515 and x_3=0.7799220898.

The function Y (for these values for x_3) takes values accordingly:

$$Y(x_3 = -0.8561650515) = 10.79965411 \tag{18}$$

$$Y(x_3 = 0.7799220898) = 19.18460071 \tag{19}$$

The summarized numerical results for the value of the studied function (1) are presented graphically in Figure 5.

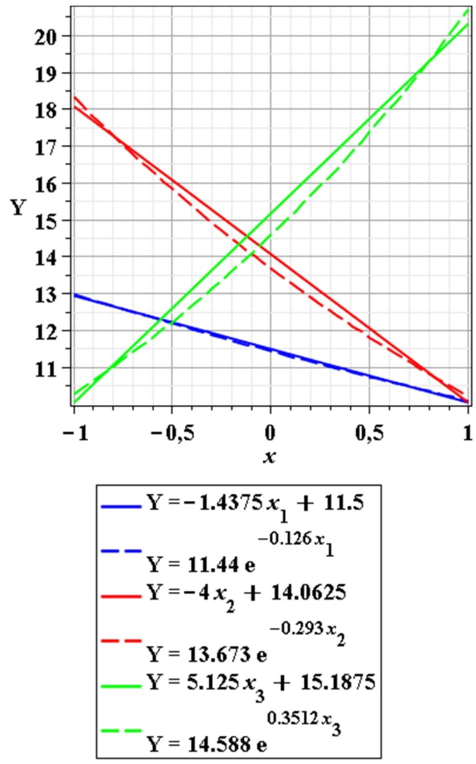

Figure 5 Movement of the value of the target function Y in the linear and exponential approximation

3.2 Discussion of the obtained numerical results

The study shows that the optimal value of the studied function Y is reached at a point with coordinates (1;1;-1) and this value is 10.0625, i.e.,

$$Y_{min} = Y(x_1 = 1; x_2 = 1; x_3 = -1) = 10.0625 \tag{20}$$

i.e. the minimum time for carrying out the TMF process at the selected technological factors is approximately 10 s. To evaluate the efficiency of the linear and exponential approximation, the values of the coefficients of determination for the two types of approximations are determined for each of the considered variants (Table 5).

Table 5 Values of the coefficients of determination in the linear and the exponential approximation

	1st variant	2nd variant	3rd variant
$R^2_{LinAppr}$	0.9998	0.9991	0.9989
$R^2_{ExpAppr}$	0.9987	0.9931	0.9902

The comparison of the values of the coefficients of determination proves that the linear approximation of the mathematical model (1) of the technological process TMF is more effective.

4 CONCLUSIONS

A mathematical model of the TMF process is studied in this work. It describes the relationship between the performance criterion *Y* (the time for the implementation of the TMF process) and three controllable factors. A linear and exponential approximation of the mathematical model for three variants of combinations of the manageable factors is made. For each of the variants, specific values of *Y* were obtained at the respective levels of the manageable factors. $Y_{LinAppr}$ and $Y_{ExpAppr}$ are illustrated as being close enough to the time obtained from the mathematical model of the process.

The linear approximation is proven to be more effective than the exponential one. This allows the relatively complex mathematical model of the TMF process to be replaced by its linear approximation. The use of the linear approximation of the mathematical model of the TMF process creates conditions for its easier and faster implementation in real production conditions. The linear approximation makes it possible for more faster and easier calculation of the time for the implementation of the TMF process for levels of manageable factors for which there are not sufficient experimental results.

The application of mathematical methods for analysis and evaluation in the presented study create conditions for faster solution of specific technological problems related to the TMF process.

This in turn, leads to increased efficiency of the sewing technology.

5 REFERENCES

1. Gries T., Lutz V., Niebel V., Saggiomo M., Simonis K.: Automation in quality monitoring of fabrics and garment seams, chapter 14 in: Automation in Garment Manufacturing, 2018, pp. 353-376, https://doi.org/10.1016/B978-0-08-101211-6.00014-8
2. Watcharapanyawong K., Sirisoponsilp S., Sophatsathit P.: A Model of mass customization for engineering production system development in textile and apparel industries in Thailand, Systems Engineering Procedia 2, 2011, pp. 382-397, https://doi.org/10.1016/j.sepro.2011.10.052
3. Quezada-García S., Espinosa-Paredes G., Polo-Labarrios M.A., Espinosa-Martínez E.G, Escobedo-Izquierdo M.A.: Green roof heat and mass transfer mathematical models: A review, Building and Environment 170, 2020, Article 106634, https://doi.org/10.1016/j.buildenv.2019.106634
4. Dimitrienko Yu.I., Dimitrienko I.D.: Modeling and simulation of textile composite plates under a punching load. Applied Mathematics and Computation 2020, 3641, Article 124660, https://doi.org/10.1016/j.amc.2019.124660
5. Kosheleva M., Golykh R., Novikova T., Dorovskikh R., Khmelev V., Shalunov A.: Ultrasonic drying of textile materials, Proceedings of 18th International Conference of Young Specialists on Micro/Nanotechnologies and Electron Devices, IEEE, 2017, https://doi.org/10.1109/EDM.2017.7981757
6. Yu-xian Zhang, Yong Li, Bin Cheng: A nonlinear approximation for size moisture regain using moving least squares method, Proceedings of 24th Chinese Control and Decision Conference (CCDC), IEEE, 2012, https://doi.org/10.1109/CCDC.2012.6244142
7. Kosheleva M., Dornyak O., Novikova T., Tsintsadze M.: Approximation of sorption isotherms of fiber materials by various equations, Fibre Chemistry 51(4), 2019, pp. 268-271, https://doi.org/10.1007/s10692-020-10092-y
8. Chizhik M., Yurkov V., Litunov S., Skuba P.: Nonlinear net models of multi-parametrical systems and processes, Journal of Physics: Conference Series of XIII International Scientific and Technical Conference "Applied Mechanics and Systems Dynamics", 2019, 1441, Omsk, Russian Federation, https://iopscience.iop.org/article/10.1088/1742-6596/1441/1/012053/pdf
9. Anoshkin Al., Pisarev P., Ermakov D., Roman Ks.: Forecasting Effective Elastic Properties of Spatially Reinforced Composite Materials Applying the Local Approximation Method, 28th Russian Conference on Mathematical Modelling in Natural Sciences - AIP Conf. Proc. 2216, 020008-1–020008-7, 2020, https://doi.org/10.1063/5.0004078
10. Andonova S.: Mathematical modeling of the thermo-mechanical fusing process, Vlákna a textil (Fibres and Textiles) 27(2), 2020, pp. 3-7
11. http://db.cs.duke.edu/courses/fall01/cps150/lectures/Interpolation.pdf (27 July 2020)
12. Giri P., Banerjee J.: Introduction to statistics, e-book, 6th ed., Academic Publishers: 2008, https://books.google.co.in/books?id=1CiL9H7mO7wC&printsec=frontcover#v=onepage&q&f=false
13. Agarwal B.L.: Basic statistics, e-book, 4th ed., New Age International (P) Limited: 2006, https://books.google.bg/books?id=qT2srNLLxB0C&printsec=frontcover#v=onepage&q&f=false
14. Andonova S., Baeva S.: Optimization of the thermo-mechanical fusing process, Vlákna a textil (Fibres and Textiles) 27(2), 2020, pp. 13-18

MORDANT AND FIXATION TEST OF BONE ASH ON NATURAL COLOURS TOWARDS COTTON AND SILK FABRIC

Nooryan Bahari[1], Rum Handayani[2], Ratna Endah Santoso[2] and Nadia Sigi Prameswari[3]

[1]Study Program of Fine Art, Faculty of Art and Design, Sebelas Maret University, Jl. Ir. Sutami 36 A, 57216 Surakarta, INDONESIA
[2]Study Program of Textile Craft, Faculty of Art and Design, Sebelas Maret University, Jl. Ir. Sutami 36 A, 57216 Surakarta, INDONESIA
[3]Visual Arts Department, Faculty of Languages and Art, Universitas Negeri Semarang, Jl Sekaran Raya, Gunung Pati, Sekaran, 50229, Semarang, INDONESIA
nooryanbahari@staff.uns.ac.id; rumhandayani@staff.uns.ac.id; ratnaendahsantoso@staff.uns.ac.id; nadiasigi@mail.unnes.ac.id

Abstract: *The environmental pollution due to synthetic textile dye waste has induced an increase in the use of natural dyes. In general, the fixation process using alum, lime and tunjung. The novelty of this research is to make bone ash as an initial mordant and fixator. The CaO in bone ash and its absorbent potential makes it worth testing as a pre-mordant and fixator for cotton and silk fibers using natural dyes. This study aimed to determine the effect of bone ash as a mordant and fixator on the immersion of natural dyes from chromolaena, mango leaves and garlic skin. The test stages include: preparation, extraction, fixation and pelorodan. The resulting colour tends not to change. However, the endurance level of the fabric towards washing, sweat, light and rubbing has improved (grades 4-5). It has been proven that bone ash, which is chemically composed of several metal oxides, (CaO) is quite similar to lime ($CaCO_3$), having a high pH (alkaline) level. Therefore, it can serve as an alternative fixator with sodium carbonate (Na_2CO_3) as the final mordant. The results showed that cow bone ash has a high potential of being used as a pre-mordant material and fixator in the colouring processes of cotton and silk fabrics.*

***Keywords**: bone ash, final mordant, natural dyes fixator, cotton, silk fabric.*

1 INTRODUCTION

The use of synthetic dye has existed in the textile industry since the rise of Industrial Revolution in Britain. This was turning point for industrial and economic growth in the world [1]. Textile dyes became very popular in the 21st century [2], as well as batik colouring, which relied on synthetic dyes [3]. Synthetic dyeing in textile industries has become a hereditary tradition in the process of colouring [4]. This is due to its sharpness and colour diversity [5]. An estimated 10,000 types of dyes are used in the textile industry [6]. Textile waste makes clear water colorful and toxic; thus it affects the ecosystem, bringing about chemical and biological changes as well as producing pollutants that disrupt the aquatic ecosystem [7, 8]. Environmental damage and pollution become a long debate in regards to the fulfilment of human economics. This is also known as anthropocentrism behavior, which prioritizes human interests [9]. The high market demand for the activities of textile industries makes it a source of state revenue. These activities contribute about 8.5% of gross domestic product [10]. Therefore, it is a key tool to spurring economic growth [11]. The textile industry needs to collaborate with other textile industries, convection business units, dye supply units and the government for economic progress [12]. The rapid progress of globalization is driving competition in the textile industry, including batik as one of the common commodities in the international market [13]. Many textile businesses have difficulties in economic growth, so innovation is needed [14]. The development of textiles gave rise to colour innovations, including synthetic colouring [12]. These innovations have helped in raising alternative choices of silk batik in long-sleeved and short-sleeved for consumers [15, 16]. This triggers a rapid increase in market demand. Therefore, it results in textile industries choosing synthetic dyes. The use of synthetic dyes can accelerate production, increase product quantity and facilitate economic circulation in the textile industry but conversely, it has an impact on environmental pollution due to its waste [17]. In addition, the use of synthetic dyes in the production process can also become a risk towards health, causing allergies and skin injury [18, 19]. Waste water contains various pollutants including surfactants, salts and acetic acids [20]. Among these components, synthetic dyes are the most difficult components to be melted. This is due to the fact that they are made from synthetic chemicals which have complex structures [21]. Environmental problems arising from accelerated industrial growth have led to the development of safer production strategies [22]. The dangers resulting from the use of synthetic colouring has led to the use of natural dyes by some industries [23]. The use of natural substances can provide a good and sharp colour pattern on the fabric [24]. Natural dye substances can be obtained from plants and animals. It can be extracted from plants through roots and twigs or leaves of many species [25]. Coconut oil can also be used as an enhancement on fabric to absorb natural dye [26]. Extreme climate change also encourages new colour changes on tree leaves [27], which is a natural phenomenon [28]. These dyes can also be obtained from animal skin extract as well as from animal fat [29]. Agents of natural dyes from animals can be found contained in pigments in the animal's body. Each contains substances with different shades [30].

Bone ash is a white powder which is a residue from the burning (calcination) of bone. It is one type of mineral made from cow bone waste consisting of calcium phosphate. Furthermore, it is a tricalcium phosphate in the form of $Ca_5(PO_4)_3OH$ hydroxyapatite. According to Saragih [32], cow bones contain 58.30% $Ca_3(PO_4)_2$; 7.07% $CaCO_3$; 2.09% $Mg_3(PO_4)_2$; 1.96% CaF_2 and 4.62% collagen. Chemically, bone ash consists of metal oxides in the form of 55.82% CaO; 42.39% P_2O_5; 1.40% MgO; 0.43% CO_2; 0.09% SiO_2; 0.08% Fe_2O_3 and 0.06% Al_2O_3. Bone ash which has a high CaO content can serve as a good absorbent based on the chemical composition of CaO [31].

In general, the fixation process using alum, lime and *tunjung*. The novelty of this research is to make bone ash as an initial mordant and fixator. The development led to many previous studies discussing textile colouring. The study aimed to examine the effect of bone ash as a mordant and fixator of natural dyes obtained from *chromolaena* (Kopasanda), mango leaves, and garlic skins applied to cotton and silk fabrics. White cotton fabric, commonly called *mori* or *Muslin* or cambric, which is made of cotton yarn, was used. It contains 10% mild starch which makes it easily removable while washing. It is a material from natural fibers with high affinity, absorption, heat resistance and heat conductivity. Tests were also carried out using silk that has some special properties which includes: (1) lighter than cotton, (2) having good insulating power against electricity and heat, (3) high water absorption level, and (4) high tensile strength [32].

From some previous studies, researchers did not discover that bone ash can be used as a pre-mordant and fixator in natural fabric colouring. Specifically, this study aims to determine whether bone ash can be used as a substitute for *tunjung* for the initial mordant process. Furthermore, the researcher wanted to find out whether bone ash could be used as an alternative material to replace lime and alum in the fixation process.

2 METHODS

2.1 Materials

Following are the physical properties of fabric primissima cotton: materials (warp 56/60 dtex, weft 50/56 dtex); density (warp 42/50 threads/cm, weft 42/50 threads/cm); 100% pure primissima cotton composition; weight 190 g/m^2. While the physical properties of silk fabric: materials (warp 22.2/24.4 dtex, weft 22.2/24.4 dtex; density (warp 115 threads/cm, weft 90 threads/cm); 100% pure silk composition; weight 175 g/m^2. From the material data, the fabric has met the requirements to do a color fastness test according to the Indonesian National Standard.

Pre-mordant raw materials: bone ash 2 g/L, alum 6 g/L. Raw colouring material: leveling agent, mango leaves, *chromolaena*, garlic skin with the ratio of 1:4. Raw final mordant material (fixator): alum 70 g/L, bone ash 50 g/L, *tunjung* 30 g/L. Equipments: scales, stainless steel pans, leaf grinding machines, process tubs, *pelorodan,* and filters.

2.2 Procedures

There are some processes that need to be passed, which includes: pre-mordant, extraction, fixation, and *pelorodan* (the release of wax).

<u>Pre-mordant process:</u> The mordanting process involves placing alum, lime, *tunjung* or other metal elements into the fabric fibre, therefore allowing them to react with the dye [33, 34]. In preparing ingredients for the mordant (according to the dosage recipe), they are dissolved in a predetermined amount of water and heated; cotton and silk are soaked in a leveling agent for about 10 minutes, then squeezed and placed into mordant solution at a temperature of 60°C; the fabric is heated in the solution for about 1 hour with a maintained temperature of 60-70°C before the source of heat is turned off. After that, it is left in the solution for about 24 hours. Finally, it was neatly washed with plain water, squeezed and dried.

<u>Extraction process:</u> This process began with the preparation of natural dyes according to the 1:4 ratio which was 1 kg of extracted material and 4 litres of water. Natural dyes were chopped and soaked overnight with predetermined amount of water. Furthermore, they were extracted by heating for about 1 hour after reaching the boiling point of water (100°C). The solution was filtered and cooled at room temperature and finally ready to be used as a natural dye. After that, the coloring process begins as shown in Table 1, cotton cloth, plain silk, or batik soaked with a leveling agent first, soak for about 10 minutes, then drain it; the cloth is evenly dipped back and forth and allowed to soak in the natural dye solution for about 10 minutes; the cloth is removed from the soaking solution of natural colors, drained and aerated to dry. Repeat coloring a predetermined number of repetitions (6, 12 and 18 times).

Table 1 Dyeing process test data

Coloring Type	Mordant	Fixator	Dyeing Number		
			6x	12x	18x
Chromolaena	alum 6 g/L	alum 70 g/L	√ (plain)	√	√
		bone ash 50 g/L	√ (plain)	√	√
		tunjung 30 g/L	√	X	X
	bone ash 2 g/L	alum 70 g/L	√	√	√
		bone ash 50 g/L	√	√	X
		tunjung 30 g/L	√	√	√
Mango leaves	alum 6 g/L	alum 70 g/L	√	√	√
		bone ash 50 g/L	√ (plain cotton & batik silk)	X	√
		tunjung 30 g/L	√ (cotton batik)	X	X
	bone ash 2 g/L	alum 70 g/L	√ (plain)	X	√
		bone ash 50 g/L	√	√	√
		tunjung 30 g/L	√ (plain)	X	√ (plain)
Garlic skin	alum 6 g/L	alum 70 g/L	√	√	√
		bone ash 50 g/L	√ (plain)	√	√
		tunjung 30 g/L	√	√	√
	bone ash 2 g/L	alum 70 g/L	√ (plain)	√	√
		bone ash 50 g/L	√ (plain)	√	√
		tunjung 30 g/L	√ (plain)	X	√ (plain cotton and batik silk)

Fixation process: The fixation process was carried out with mordant material (according to the dosage of the recipe), dissolved in predetermined amount of water, stirred evenly and allowed to stand overnight. A portion of the fixation solution was taken as a test sample. The natural-dyed cotton fabric and silk were put into each of the fixation solutions in a dry state. Afterwards, they were dyed back and forth for approximately 2-3 minutes. Thereafter, they were removed, aerated for about 1 minute and washed clean.

Pelorodan process: *Pelorodan* is a term from the Javanese language, Indonesia. *Pelorodan* is the process of removing the wax coating on fabrics. *Pelorodan* on coloured cotton and silk fabrics with water and then heated with bone ash as much as 5 g/L of solution. Afterwards, cotton fabric and batik silk were soaked in starch water solution for approximately 24 hours, squeezed and put into boiling water *pelorodan*. Fabric was stirred in the *pelorodan* solution until the wax was released. Then, it was lifted and put into a leveling agent solution. In addition, the *pelorodan* process should be repeated if wax was not completely released. Finally, the fabric was washed and dried. The results of the last stage of *pelorodan* can be seen in Table 2.

2.3 Data analysis

This research was carried out using the method of implementation experiment in Pilang Village, Masaran District, Sragen Regency and Indonesia.

In the trial, several analysis options can be done. One of them is the Kolmogorov-Smirnov normality test with statistics; if it is included in the test it makes this study not focus on the initial problems of this study. This study focuses more on bone ash as a substitute for mordant and fixator, so that researchers choose another appropriate method, namely the color resistance test based on the Indonesian National Standard to answer the focus of this research problem.

This study uses the standard of Gray Scale to assess the results of dyeing process. There are 4 color fastness tests based on the Indonesian government standard setting through the Indonesian National Standard (SNI) [35]. The quality testing includes color fastness of the fabric against washing (40°C) repeatedly (ISO 105-C06-2010), color fastness of the fabric to sweat (acid) (SNI ISO 105-E04: 2010), color fastness on fabrics against the light (daylight) (SNI ISO 105-B01: 2010) and color fastness on fabrics caused by rubbing (dryness) (SNI 0288-2008).

3 RESULT

3.1 Result of staining

Table 2 is the result of the coloring process starting from the initial mordant process, the extraction process in which there is a staining test process in Table 1, the fixation process, the *pelorodan* process (the release of wax). Based on the conducted dyeing results (Table 2), it showed that the differences were not significant, except for fixation with *tunjung* which appeared darker. There are several dyeing repetitions that show a darker colour with a smaller number of repetitions in the same mordant or type of fixation. This situation has led to a difficulty in making conclusions regarding the most appropriate dyeing technique. The fixation result also showed that batik silk fabric absorbs colour easily and therefore produces a darker shade than the batik cotton fabric.

Table 2 Test results of natural dyed fabric

Dyeing process	Type of fabric	Dyeing number 6x	Dyeing number 12x	Dyeing number 18x
bone ash - mango leaves - bone ash	cotton silk fabric	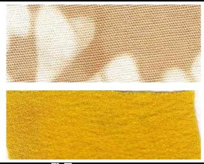	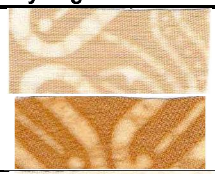	
bone ash - *chromolaena* - bone ash	cotton silk fabric			
bone ash - garlic skin - bone ash	cotton silk fabric	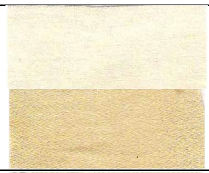		
bone ash - mango leave s- alum	cotton silk fabric		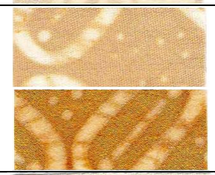	
bone ash - *chromolaena* - alum	cotton silk fabric	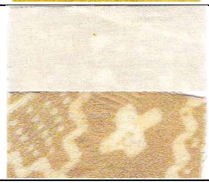		
bone ash - garlic skin - alum	cotton silk fabric	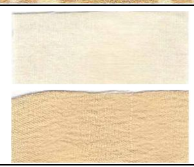	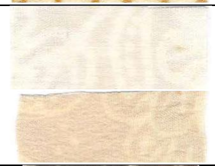	
bone ash - mango leaves - *tunjung*	cotton silk fabric			
bone ash – *chromolaena* - *tunjung*	cotton silk fabric	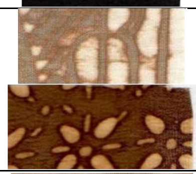	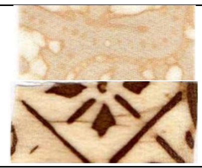	
bone ash - garlic skin - *tunjung*	cotton silk fabric		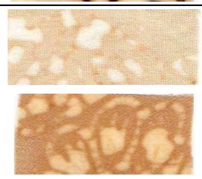	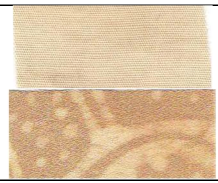
alum - mango leaves - bone ash	cotton silk fabric	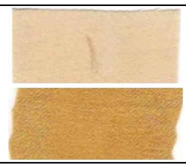	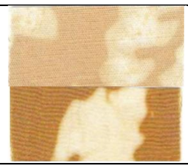	

Dyeing process	Type of fabric	Dyeing number 6x	Dyeing number 12x	Dyeing number 18x
alum - *chromolaena* - bone ash	cotton silk fabric	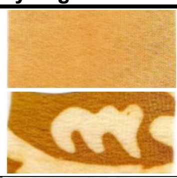	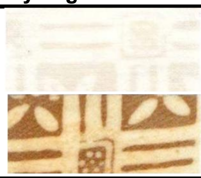	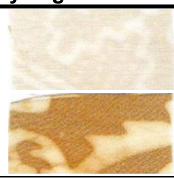
alum - garlic skin - bone ash	cotton silk fabric			
alum - mango leaves - alum	cotton silk fabric		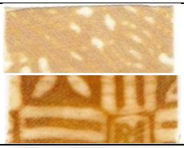	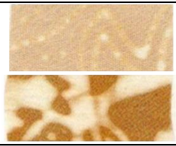
alum - *chromolaena* - alum	cotton silk fabric			
alum - garlic skin - alum	cotton silk fabric			
alum - mango leaves - *tunjung*	cotton silk fabric			
alum - *chromolaena* - *tunjung*	cotton silk fabric			

3.2 Color fastness test

There are 4 color fastness tests conducted in this study. Color fastness test based on the Indonesian government standard-setting through the Indonesian National Standard (SNI). The basis of colour fastness test lies in the overall difference or contrast between the original and the sample to be tested. Quality test for dyeing includes: fastness to washing (40°C), sweat (acid), light (daylight) and iron (wet). This test is based on SNI ISO 105-C06-2010, SNI ISO 105-E04: 2010, SNI ISO 105-B01: 2010 and SNI 0288-2008. Readings from the test results of colour dyeing and colour change was conducted in the form of gray scale with the following values:

In Table 3, the value 5 means there is no change in color change and so on until the value 1 means that there is a very large color change. The test results in Table 4 show color fastness to washing 40°C. The results on the types of cotton and silk fabrics scored 4-5 (good), the results of the color fastness test to acid sweat, on 7 samples of cotton fabrics, 2 samples got a value of 4-5 (good) and 5 samples got a value of 4 (good), while in 5 samples of types of silk fabric 4 samples scored 4 (good) and 2 samples scored 3-4 (quite good). From the results of the color fastness test to light (daylight), the results on the types of cotton and silk fabrics showed a score of 4-5 (good). From the results of the color fastness test to rubbing with dry cotton, 1 sample got a score of 4-5 (good), 3 samples got a score of 4 (good), 3 samples got a score of 3-4 (pretty good), while on silk, 1 The sample scores 4-5 (good) and 4 samples score 4 (good).

Table 3 The results of the color fastness value

Score	Different color	Tolerance for work standards	Reading
5	0	± 0.2	very good
4-5	0.8	± 0.2	good
4	1.7	± 0.3	good
3-4	2.5	± 0.3	good enough
3	3.4	± 0.4	enough
2-3	4.8	± 0.5	less
2	6.8	± 0.6	less
1-2	9.6	± 0.7	bad
1	13.6	± 1.0	bad

Table 4 The results of the color fastness value of the samples of marenggo shrubs, mango leaves and onion skin on cotton and silk fabrics

Type of fabric	Test type	Test results			
		40°C color fastness resistance to washing	***Color fastness resistance to acid sweat***	***Lightfastness (daylight)***	***Fastness resistance to dry rubbing cotton***
Cotton	bone ash - marenggo 18x - *tunjung*	4 -5	4	4 - 5	3 -4
	alum - 18x onion skin - alum	4 -5	4 – 5	4 – 5	4
	alum - 18x onion peel - bone ash	4 -5	4 – 5	4 – 5	4 -5
	bone ash - mango leaves 18x - bone ash	4 -5	4	4 – 5	4
	bone ash - mango leaves 18x - alum	4 -5	4	4 – 5	3 -4
	bone ash - mango leaves 18x - bone ash	4 -5	4	4 – 5	4
	bone ash - mango leaves 18x - bone ash	4 -5	4	4 – 5	3 -4
Silk	alum - onion skin 18x - alum	4 -5	4	4 – 5	4
	alum - 18x - bone ash - mango leaves	4 -5	3 -4	4 – 5	4
	bone ash - mango leaves 18x - alum	4 -5	4	4 – 5	4
	bone ash - mango leaves 18x - bone ash	4 -5	4	4 – 5	4 – 5
	bone ash - marenggo 18x - bone ash	4 -5	3 -4	4 – 5	4

From the test, samples were examined for colour density and colour fastness towards washing, sweat, rubbing and direct sunlight and the following results were obtained. From the results of table 4 on cotton fabric, it can be concluded that the most stable value was the use of alum as a pre-mordant with garlic skin and bone ash as the final mordant. This was due to the low content of colour pigments on garlic skin waste. Therefore, the possibility of colour loss due to fading process is minimal compared with colouring of *chromolaena* and mango leaves which contain more colour pigments.

Conversely, the highest value for silk fabric was found in mango leaf dyeing using bone ash a pre-mordant and colour fixator (final mordant) as well. This was a result of the presence of mangiferin pigment found in mango leaves which binds more strongly to the silk fibers in bone ash (mordant) through covalent bonds. The estimated result changes due to various factors, including suboptimal extraction, unstable treatment of the dyeing process, the condition of the material and its preparation process (the difference in wax used on a batik stamp). This can be minimized by maintaining similar natural materials, waxing on the initial preparation, and the treatment consistency during the dyeing process. With the combination of alum and bone ash, the dyeing results only compared the mordants (alum and bone ash) and fixators (alum, bone ash and *tunjung*). The results showed little difference except for fixations that showed darker results when tides was used. There are several dyeing repetitions that show more intense colour with fewer repetitions on the same type of mordant or fixation. Therefore, making a decision regarding the most appropriate colouring technique was difficult. Colouring results after fixation also showed that batik silk absorbs more colour extract thereby producing a darker colour than the cotton fabric.

4 DISCUSSION

Besides using synthetic dyes, the fabrication and dyeing process also utilizes natural mordant dyes which are generally extracted from plant parts, such as *Soga Alam*, Gambier, *secang* wood, indigofera leaves etc. This type of dye works optimally in colouring protein fibers (silk, wool) and polyamide fibers. In the natural mordant colouring process, the preliminary mordant (pre-mordant) and final mordant (fixation) processes are carried out [36]. This process was carried out to provide good washing resistance and colour determination. Binding of dyes to fibers is facilitated by the presence of metal ions from the mordanting process [37]. Metal ions act as electron acceptors to form coordination bonds with dye molecules, making mordants insoluble in water and ensuring colour fastness to the fabric [38]. In Sarwono's research, it was stated that alum, lime, and *tunjung* can be used as fixators [39].

The function of the initial mordant is to assist and increase the adhesion of the dye to the fabric. The purpose of mordanting in the fabric process is to increase color absorption, remove oil, grease, and wax that inhibit the color absorption process, increase color adhesion, connect natural dyes with fabric fibers so that affinity (the attraction of the dye increases to the fiber). Fixation is to strengthen the color and change the color of natural dyes according to the type of metal binder.

So far, a lot of cow bones have been wasted, not used. The results show new findings that bone ash can be used as an alternative material to substitute lime and soda ash for the final mordanting process, as a substitute for *tunjung* for initial mordant.

The test results also show that dyeing on cotton and silk fabrics without undergoing the *pelorodan* process did not experience a drastic colour reduction due to the absence of heat (temperature) which greatly affects the quality of natural colouring. The results of garlic skin dyeing gave a yellowish-white colour (ivory), mango leaves gave a light yellow colour [40], and the greenish yellow colour was shown in the dyeing results using *chromolaena* [41]. The use of the final mordant (fixator) alum gave a colour like the original colour before fixation, bone ash became slightly reddish yellow while *tunjung* became the darkest.

The colour direction obtained by the three types of natural dyes is as a result of the substance present in each material. The leaves of *chromolaena* and mango contain chlorophyll, a colouring pigment which is responsible for trapping sunlight energy which is used in photosynthesis. The leaves have other pigments, such as xanthophyll which gives a yellowish colour as shown in the results of *chromolaena* and mango leaf dyeing. Meanwhile, garlic skin which is a waste from white food does not have a pigment that can absorb certain colours. Therefore, the colour direction produced tends to be yellowish white. Garlic skin dyeing can be done by the traditional method of boiling in water [42]. However, the use of garlic skin waste as an alternative to natural dyes for batik became more optimal with pastel colours produced by a combination of *chromolaena* dyeing, mango leaves and garlic skin, from the initial level using alum fixation which later becomes darker with *tunjung* fixation.

Bones reflect an excellent affinity for pollutants. These pollutants become bound to the absorbent through the absorption process [43]. Bone ash is very important due to its unique cellular structure from bone which is maintained through calcination. Bone ash has excellent non-wetting properties for chemical moisture, free of organic material and has a very high heat transfer resistance [44]. The experimental results show that cow bone ash has high potential of being used as a pre-mordant material and a colour lock (fixator) as well in the process of colouring cotton and silk batik fabric. Bone ash is chemically composed of several metal oxides, one of which is CaO (55.82%), which implies that bone ash has a similarity with calcium oxide having a high pH (alkaline) and therefore can be an alternate fixator in substitution for calcium oxide and sodium carbonate as the re-mordant.

5 CONCLUSION

Synthetic staining can accelerate production and increase the quantity of products in the textile industry. Conversely, it contributes to environmental pollution due to its waste. The arising environmental problems caused by synthetic dyeing have led a number of producers in switching to natural dyeing. Natural dyeing can be obtained through elements of natural substances that can reduce production costs and are environmentally friendly with better quality. Natural substances provide various shades and stronger colouring. Bone ash reflects very good affinity for pollutants that are bound in the absorbent through the absorption process, and has some similarities with calcium oxide having high pH content. The test for the effects of mordant and fixation with bone ash on cotton and silk fabrics, using natural dyes obtained from *chromolaene*, mango leaves, and garlic skin, has shown results in colour direction which tends to change. Chemically, bone ash consists of several metal oxides (CaO) which is quite similar to lime ($CaCO_3$) with quite a high pH content (alkaline). Therefore, it can serve as an alternative fixator in substituting for lime ($CaCO_3$) and sodium carbonate (Na_2CO_3) as the final mordant. This was proven by the better value of fastness towards washing, perspiration, light, and iron (grades 4-5). The results showed that cow bone ash has a good potential as a pre-mordant material and fixator in the process of colouring cotton fabric and silk fabrics. This research was limited to cotton and silk fabrics. This condition allows the use of a more diverse fabric. Therefore, it can give a different colour dyeing and fastness in future research.

6 REFERENCES

1. Harley C.K.: Was technological change in the early Industrial Revolution Schumpeterian? Evidence of cotton textile profitability, Explorations in Economic History 49(4), 2012, pp. 516-527, https://doi.org/10.1016/j.eeh.2012.06.004
2. De Oliveira Neto G.C., Ferreira Correia J.M., Silva P.C., de Oliveira Sanches A.G., Lucato W.C.: Cleaner Production in the textile industry and its relationship to sustainable development goals, Journal of Cleaner Production 228, 2019, pp.1514-1525, https://doi.org/10.1016/j.jclepro.2019.04.334
3. Borshalina T.: Marketing strategy and the development of batik trusmi in the regency of cirebon which used natural coloring matters, The 6th Indonesia Int.ernational Conference on Innovation, Entrepreneurship and Small Business, Procedia - Social and Behavioral Sciences 169, 2015, pp. 217-226, DOI: 10.1016/j.sbspro.2015.01.305
4. Elliott I. M.: Batik: Fabled Cloth of Java, Hong Kong: Periplus Editions (HK) Ltd., 2013, 240 p.
5. Belfer N.: Batik and Tie Dye Techniques, New York: Dover Publications, 2012, 227 p.
6. Selvam K.; Swaminathan K., Chae K.-S.: Decolourization of azo dyes and a dye industry effluent by a white rot fungus Thelephora sp, Bioresource Technology 88(2), 2003, pp. 115-119, DOI: 10.1016/s0960-8524(02)00280-8

7. Mahmoodi N.M.: Photocatalytic ozonation of dyes using copper ferrite nanoparticle prepared by co-precipitation method, Desalination 279(1-3), 2011, pp. 332-337, https://doi.org/10.1016/j.desal.2011.06.027
8. Tóth A.J.: Liquid waste treatment with physicochemical tools for environmental protection, Ph.D. Thesis, BME OMIKK 000617279, 2015
9. Mazzarella F., Escobar-Tello C., Mitchell V.: Service Ecosystem: Empowering Textile Artisans' Communities Towards A Sustainable Future, NORDES Nordic Design Research 6, 2015, http://www.nordes.org/opj/index.php/n13/article/view/437/410
10. Afzal H.M.Y.: Impact of electricity crisis and interest rate on textile industry of Pakistan, Academy of Contemporary Research Journal 1(1), 2012, pp. 32-35
11. Pandit N., Tejani R.: Sustainable growth rate of textile and apparel segment of the Indian retail sector, Global Journal of Management and Business Research 11(6), 2011, pp. 39-44
12. Mulyanto, Prameswari N.S., Fenitra R.M.: The empowerment of design and management for non-machinary lurik weaving industry in Central Java Indonesia, Vlakna a textil (Fibres and Textiles) 25(2), 2018, pp. 64-73
13. Zucchella A., Siano A.: Internationalization and innovation as resources for SME growth in foreign markets, International Studies of Management & Organization 44(1), 2014, pp. 21-41, https://doi.org/10.2753/IMO0020-8825440102
14. Helia R., Farida N., Prabawani B.: .: The Effect of Market Orientation and Orientation Toward Competitive Advantage Through Enterprise Product Innovation as a Variable Between, Case Study on SMEs in Kampung Batik Batik Laweyan, Solo (Pengaruh Orientasi Pasar dan Orientasi Kewirausahaan Terhadap Keunggulan Bersaing Melalui Inovasi Produk sebagai Variabel Antara, Studi Kasus pada IKM Batik di Kampung Batik Laweyan, Solo, Jurnal Ilmu Administrasi Bisnis 4(4), 2015, pp. 281-290
15. Agnhage T., Perwuelz A., Behary N.: Eco-innovative coloration and surface modification of woven polyester fabric using bio-based materials and plasma technology, Industrial Crops and Products 86, 2016, pp. 334-341, https://doi.org/10.1016/j.indcrop.2016.04.016
16. Wadho W., Chaudhry A.: Innovation and firm performance in developing countries: The case of Pakistani textile and apparel manufacturers, Research Policy 47(7), 2018 pp. 1283-1294, https://doi.org/10.1016/j.respol.2018.04.007
17. Mulyanto, Prameswari N.S., Suharto M., Afatara N.: Long-Sleeved Shirt Pattern as Guidelines for Designing a Sanggit Motif Batik Shirt, Vlakna a textil (Fibres and Textiles) 25(4), 2018, pp. 61-70
18. Zhang C., Chen J., Wen Z.: Assessment of policy alternatives and key technologies for energy conservation and water pollution reduction in China's synthetic ammonia industry, Journal of Cleaner Production 25, 2012, pp. 96-105, https://doi.org/10.1016/j.jclepro.2011.11.056
19. McGuinness T.M., Newell D.: Risky Recreation: Synthetic Cannabinoids Have Dangerous Effects, Journal of Psychosocial Nursing and Mental Health Services 50(8), 2012, pp. 16-18, DOI: 10.3928/02793695-20120703-04
20. Santacroce R., Bosio E., Ferrero F., Mignone M.: Life (and death) in Pink: The dangerous rise of synthetic opioids in the new psychoactive substances panorama, European Neuropsychopharmacology 28(1), 2018, pp. 225-226, https://doi.org/10.1016/j.euroneuro.2017.12.008
21. Khan R., Bhawana P., Fulekar M.H.: Microbial decolorization and degradation of synthetic dyes: a review, Reviews in Environmental Science and Bio/Technology 12, 2013, pp. 75-97, https://doi.org/10.1007/s11157-012-9287-6
22. Abiri F., Fallah N., Bonakdarpour B.: Sequential anaerobic–aerobic biological treatment of colored wastewaters: case study of a textile dyeing factory wastewater, Water Science and Technology 75(5-6), 2016, pp. 1261-1269, DOI: 10.2166/wst.2016.531
23. Ahmed N.S.E., El-Shishtawy R.M.: The use of new technologies in coloration of textile fibers, Journal of Material Science 45, 2010, pp. 1143-1153, https://doi.org/10.1007/s10853-009-4111-6
24. Singh K., Arora S.: Removal of synthetic textile dyes from wastewaters: acritical review on present treatment technologies, Critical Reviews in Environmental Science and Technology 41(9), 2011, pp. 807-878, https://doi.org/10.1080/10643380903218376
25. Toussirot M., Nowik W., Hnawia E., Lebouvier N., Hay A.-E., de la Sayette A., Dijoux-Franca. M.-G., Cardon D., Nour, M.: Dyeing properties, coloring compounds and antioxidant activity of *Hubera nitidissima* (Dunal) Chaowasku (Annonaceae) Dyes and Pigments 102, 2014, pp. 278-284, https://doi.org/10.1016/j.dyepig.2013.11.010
26. Baishya D., Talukdar J., Sandhya S.: Cotton dying with natural dye extracted from flower of Bottlebrush (*Callistemon citrinus*), Universal Journal of Environmental Research & Technology 2(5), 2012, pp. 377-382, http://www.environmentaljournal.org/2...
27. Verma A.K., Dash R.R., Bhunia P.: A review on chemical coagulation/flocculation technologies for removal of colour from textile wastewaters, Journal of Environmental Management 93(1), 2012, pp. 154-168, https://doi.org/10.1016/j.jenvman.2011.09.012
28. Hammond W.M., Yu K.L., Wilson L.A., Will R.E., Anderegg W.R.L., Adams H.D.: Dead or dying? Quantifying the point of no return from hydraulic failure in drought-induced tree mortality, New Phytologist 223(4), 2019, pp. 1-10, https://doi.org/10.1111/nph.15922
29. McDowell N.G., Beerling D.J., Breshears D.D., Fisher R.A., Raffa K.F., Stitt M.: The interdependence of mechanisms underlying climate-driven vegetation mortality, Trends in Ecology & Evolution 26(10), 2011, pp. 523-532, DOI: 10.1016/j.tree.2011.06.003
30. Melo R.P.F., Barros Neto E.L., Moura M.C P.A., Castro Dantas T.N., Dantas Neto A.A., Oliveira H.N.M.: Removal of direct Yellow 27 dye using animal fat and vegetable oil-based surfactant,

Journal of Water Process Engineering 7, 2015, pp. 196-202, https://doi.org/10.1016/j.jwpe.2015.06.009

31. Benkhaya S., El Harfi S., El Harfi A.: Classifications, properties and applications of textile dyes: A review, Applied Journal of Environmental Engineering Science 3(3), 2017, pp. 311-320, https://doi.org/10.48422/IMIST.PRSM/ajees-v3i3.9681
32. Saragih S.A.: Production and Characterization of Activated Carbon from Riau Coal as Adsorbent (Pembuatan dan Karakterisasi Karbon Aktif dari Batubara Riau sebagai Adsorben), Jakarta: Universitas Indonesia, 2008
33. Sewan Susanto: Development of Batik Craft Arts (Pengembangan Seni Kerajinan Batik), Departemen Perindustrian BBKB, Yogyakarta, 1978
34. Kavak F, Onal A, Seyfikli D.: Usage of willow extract as mordant agent and dyeing of wooden and fiber samples with onion (*Allium cepa*) shell, Rasayan Journal of Chemistry 3(1), 2010, pp. 1-8
35. Suprapto H.: Mordantin's Knowledge (Pengetahuan Mordantin), Yogyakarta: Batik Natural Color BIXA, 2005
36. National Standardization Agency of Indonesia (Badan Standardisasi Nasional, Tekstil â€“ Benang Jahit), 2016, accessed: http://sispk.bsn.go.id/SNI/DetailSNI/10809
37. Djufri R., Kasoenarno G.A., Salihima A., Lubis A.: Bleaching, Dyeing and Dyeing Technology (Teknologi Pengelantangan, Pencelupan dan Pencapan), Bandung: Institut Teknologi Tekstil, 1976
38. Uddin M.G.: Effects of different mordants on silk fabric dyed with onion outer skin extracts, Journal of Textiles, article ID 405626m 2014, pp. 1-8, https://doi.org/10.1155/2014/405626
39. Mongkholrattanasit R., Krystufek J., Wiener J., Vikova M.: Dyeing, fastness, and uv protection properties of silk and wool fabrics dyed with eucalyptus leaf extract by the exhaustion process, Fibres and Textiles in Eastern Europe 86(3), 2011, pp. 94-99
40. Sarwono, Santosa S., Prameswari N.S.: The color fastness of cotton cloth dyed with dye extracted from skin of shallot (*Allium ascalonicum*), Biodiversitas Journal of Biological Diversity 20(9), 2019, pp. 2475-2479, DOI: 10.13057/biodiv/d200907
41. Banna B.U., Mia R., Tanni K.S., Sultana N., Shamim A.M., Turzo R.K., et al.: Effectiveness of dyeing with dye extracted from mango leaves on different fabrics by using various mordants, North American Academic Research 2(10), 2019, pp. 123-143, http://doi.org/10.5281/zenodo.3519880
42. Balogun S.W., Sanusi Y.K., Agboluaje B.A.: Green synthesis, characterization of zinc oxide nanoparticles using *Chromolaena odorata* extract and evaluation of its properties for photoanode of solar cells, IOP Conference Series: Materials Science and Engineering 805, 2020, pp. 1-12, https://doi.org/10.1088/1757-899X/805/1/012003
43. Pucciarini L., Ianni F., Petesse V., Pellati F., Brighenti V., Volpi C., Gargaro M., Natalini B., Clementi C., Sardella R.: Onion (Allium cepa L.) Skin: A Rich Resource of Biomolecules for the Sustainable Production of Colored Biofunctional Textiles, Molecules 24(3), 2019, pp. 1-18, DOI: 10.3390/molecules24030634
44. Salh D.M.: Adsorption of malachite green and methyl green on cow bone, Journal of Environment and Earth Science 4(8), 2014, pp.50-56

THE MECHANICAL VIBRATIONS OF THE SEWING MACHINE'S NEEDLE

PART 2: THE FREE LONGITUDINAL VIBRATIONS

Wael A. Hashima

Textile Engineering Department, Alexandria University, Egypt
wa_ahm2007@yahoo.com

Abstract: *It is well known that the free vibrations of the sewing needle are divided to lateral free vibration and axial (longitudinal) free vibrations. In this study a theoretical approach will be carried out concerning the sewing needle free longitudinal (axial) vibrations. The work will include the sewing needle with constant cross-section with classical and non-classical boundary conditions and needles with variable cross-sections - stepped - type. For all the different calculations scheme of the sewing needles, two items will be emphasized: the linear natural fundamental frequencies and the modal sewing needle shape (normal equations) and time - dependent vibratory pattern of the needle. The sewing process technology of the sewn fabrics has several parameters affecting the free longitudinal (axial) vibrations of the sewing needle as: sudden end breaks, the fabric resistance to the needle penetration: is it elastic or rigid or between both of them ... etc. In addition the penetrating needle force in the sewn fabric, how is it type of relationship with time of penetration? In this study we assumed it is as* $P = P_0 \sin wt$ *i.e sinusoidal. The effect of the needle linear speed on the modal shape of the sewing needle was evaluated. Also, it has been found the frequency equation of needle axial vibration under the effect of sewing thread break.*

Keywords: *Mechanical vibration; sewing needle; linear speed; axial vibrations; penetration.*

1 INTRODUCTION

It has numbered some factors in the sewing technology that have an influence on the vibrations pattern & their exciting of the sewing needle as the impact action between the needle tip and the sewn fabric before its penetration inside the fabric, the sudden leave (high speed) leave of the needle to the fabric surface, the sudden unexpected sewing threads breaks, the sewn fabrics movements, the resistance nature of the processed fabric to the needle penetration or the nature of interaction between the sewn fabrics and the swing needle, …etc. [1]. It has stated that the transfer of the industrial sewing needle from a bar with variable cross-section to a bar with constant cross-section could be carried out by applying the weighted average technique with percentage error 1% [2]. In addition, they mentioned the lowest linear natural lateral frequency for the sewing needle is ranging from 22 k to 180 k SPM [2]. Also, they reported that the first fundamental linear natural frequency of the lateral free vibrations of the sewing needle is too sufficient practically [2]. In his work has explained the vibrations of the continuous media; transverse vibrations of beams, orthogonality principle, torsional vibrations,…etc. [3]. Also, he studied the nonlinear vibrations, free undamped vibrations with nonlinear restoring forces, forced undamped vibrations with nonlinear restoring forces, self-excited vibrations and stability [4]. The elastic vibration of the different machine elements has been studied theoretically and experimentally by several authors as [5-10]. Referring to the vibrations of the textile machines elements, many authors and scientist have introduced works as [11-14],…etc.

2 THEORETICAL APPROACH

For the sewing needle with constant cross-section (Figure 1), the linear fundamental natural frequency is calculated by formula:

$$f_i = \frac{(2i-1)\,\pi}{2\ell}\sqrt{\frac{E}{\rho}} \tag{1}$$

where: i - variable = 1, 3, 5,…etc.; π - const. = 3.14; ℓ - needles length; E - needles material (steel) elastic modulus of elasticity = Young's modulus = 206 GPa; ρ - needles material (steel) density = 7850 kg.m^{-3}.

The general expression for longitudinal vibrations is:

$$U(x,t) = \sum_{i=1,3,5,..} \sin\frac{i\pi x}{2\ell}\left(A_1\cos\frac{i\pi at}{2\ell} + B_1\sin\frac{i\pi at}{2\ell}\right) \tag{2}$$

where: *U(x,t)* - longitudinal vibrations of the sewing needle as a function of needle general distance *x* & time *t* of vibrations (instantaneous); ℓ - needles length, $a = \sqrt{E/\rho}$.

Taking into consideration the actual sewing needle database that mentioned in the work [4] then we can find:

$$f_i = \frac{(2*1-1)\,\pi\,a}{2\ell} =$$
$$= \frac{\pi}{2\ell}\sqrt{\frac{E}{\rho}} = \frac{\pi}{2*0.045}\sqrt{\frac{206*10^9}{7850}} \qquad (i=1)$$
$$= 34.8889 \times 5122.6 = 1787250\ \ s^{-1}\ (Hz)$$
$$= 107235*10^6\ SPM \cong 107\ M.SPM$$

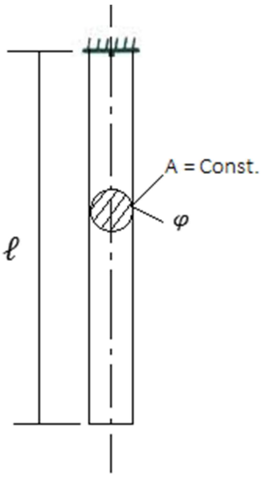

Figure 1 A sewing needle with constant cross-section; *A* - cross-sectional area CSA = const.; φ - needle diameter

3 FACTORS AFFECTING THE LONGITUDINAL VIBRATIONS OF THE SEWING NEEDLE WITH CONSTANT CROSS-SECTIONS

3.1 The sewn thread in the needle eye is suddenly ended down

This is taken place, usually, when ends down of the thread is happened. The rate of ends down during the sewing process is a bout 20-25 per (E+5) stitches [1]. From Figure 2a we can write the general longitudinal vibration of the sewing needle is:

$$U(x,t) = \frac{8\,\epsilon\,\ell}{\pi^2}\sum_{i=1,2,3,..}^{\infty}\frac{(-1)\,(i-1)^2}{i^2} * \sin\frac{i\pi x}{2\ell} * \cos\frac{i\pi a t}{2\ell} \quad (3)$$

where: *U(x,t)* - function of *x* (needle general length), *t* - time (depend, on initial conditions), ℓ - needle length; ϵ - needles strain due to thread tension *; i* - variable *i=1, 3, 5, 7,…*

The linear natural fundamental frequency is calculated by:

$$f_i = \frac{i\,\pi}{2\ell}.a = \frac{i\,\pi}{2\ell}\sqrt{\frac{E}{\rho}} \quad (4)$$

For *i=1*, first mode of free vibration $f_1 \cong 110\ M.SPM\ \ \cong 110\ M.SPM$,

where: $\left[a = \sqrt{\frac{E}{\rho}}\right]$, $(i = 1{,}3{,}5, \dots)$ and M - mega.

3.2 The sewn fabrics resistance to the needle penetration is ∞

In this case the lower free needle end will be treated as a built-in end as shown in Figure 2b.

The normal function that graphs the modal shapes is:

$$y(x) = \sum_{i=1,2}^{\infty} T_i\left[D_i \sin\left({f_i}/{a}\right) * X\right] \quad (5)$$

where:

$$a = Const. = \sqrt{E/\rho} \quad (6)$$

E - needles material Young's modulus (steel); ρ - needles material density (steel); f_i - natural frequency $= {i\,\pi a}/{\ell}$; T_i - period in sec; *X* - needle length in general position.

The equation (5) can be reformatted:

$$y(x) = D_i\,.\sin\left({i\,\pi a}/{\ell}\right) \qquad (i = 1{,}2{,}3, \dots.) \quad (7)$$

For $x = \ell,\ y(\ell) = 0$

$0 = \sum_{i=1,2}^{\infty} T_i\left[D_i \sin\left({f_i}/{a}\right) * X\right].$

The linear fundamental natural frequency of the needle is:

$$f_i = \frac{i\,\pi}{\ell}\sqrt{\frac{E}{\rho}} \quad (8)$$

where: *I = 1, 2, 3,…*

3.3 The sewn fabrics resisting elastically the needle penetration i.e. they have spring effect (spring const. S)

The frequency equation of the sewing needle shown in Figure 2c is:

$$\tan\left(\frac{f_i\,\ell}{a}\right) = -\frac{A\,E\,f_i}{S\ \,a} \quad (9)$$

where: f_i - natural linear frequency of the needle; ℓ - needle length

$$a\ = \sqrt{E/\rho} \quad (10)$$

A - needles cross-sectional area; *S* - spring stiffness (const.) due to elastic resistance of the fabric to needle penetration; *E* - steel Young's modulus = 206 GPa.

For actual needle [4] $A = \pi\,(0.89*10^{-3})^2/4 = 6.218*10^{-7};\ a = 16317,\ \ell = 0.045\ m$

then $\tan f_i\left(\frac{\ell}{a}\right) = -\frac{A\,E\,f_i}{S\ a}$ and:

$$tan\,f_i \times 2.7579*10^{-6} = -\frac{6.218*10^{-7}\ \times 206*10^9\,f_i}{16317\ *\ S}$$
$$= -7.8501\left({f_i}/{S}\right) \quad (11)$$

N.B:

If spring stiffness *S* is very small compared to that of the needle, then $\tan\left(\frac{f_i\ell}{a}\right) = \infty$

then $f_i\frac{\ell}{a} = \frac{i\,\pi}{2},\quad i = 1, 2, 3, \dots.$ and $f = \frac{i\,\pi\,a}{2\ell}$ (normal function for axial vibration of uniform sewing needle with one end (upper end) fixed built-in & the lower end is free.

N.B:

The final equation of the natural frequencies - frequency equation is:

$$tan\, f_i \times 2.7579 * 10^{-6} + 7.8501 \frac{f_i}{S} = 0 \tag{12}$$

The solution of equation (12) will give frequency f_i as a function of fabric elastic resistance *S*.

3.4 The effect of the sewing needle penetration speed V on its axial vibrations

To facilitate the theoretical approach we will assume that the sewing needle is built-in from both of upper end & lower end (see Figure 2b) while it moves with linear speed *V* during sewing process the needle speed could be calculated from the 4-bar mechanism or slider-crank mechanism or any mechanism that drives the needle.

The final longitudinal vibrations of the sewing needle (constant cross-section) are:

$$U(x,t) = \frac{4\,V\ell}{\pi^2 a} * \sum_{i=1,3,\ldots}^{\infty} \frac{1}{i^2} \sin\frac{i\,\pi\,x}{\ell} \sin\frac{i\,\pi\,a\,t}{\ell} \tag{13}$$

The natural frequency is governed by:

$$f_i = \frac{i\,\pi}{\ell}\sqrt{\frac{E}{\rho}} \tag{14}$$

The formula different items are defined previously.

3.5 The effect of the sewing needle extension due to sewing thread tension- on the axial vibrations when the thread breaks:

As shown in Figure 2d, the original needle length is ℓ when extended as a result of sewing thread tension, the length will be ℓ_0. The axial vibration of the needle is governed by formula:

$$U(x,t) = \frac{8(\ell_0 - \ell)}{\pi^2} * \\ * \sum_{i=1,3,\ldots}^{\infty} (-1)^{(i-1)/2} * \sin\frac{i\,\pi\,x}{2\ell} \cos\frac{i\,\pi\,a\,t}{2\ell} \tag{15}$$

where: *U(x,t)* - longitude elongation of the needle at general distance *x* and time *t*; ℓ - needle free length; ℓ_0 - extended needle length due to sewing thread tension; *i* - variable 1, 3, 5, …etc.

The natural frequency f_i is:

$$f_i = \frac{i\,\pi}{2\ell}\sqrt{\frac{E}{\rho}} \tag{16}$$

where: f_i - linear natural frequency of the sewing needle; i, ℓ, E, ρ - defined previously.

As mentioned previously, for the first mode of free vibrations (*i-1*), then f_i is as mentioned previously $f_i \cong 110\ M.SPM$.

3.6 Effect of penetration force as time independent on axial vibrations - Gorman [6] technique

The linear fundamental natural linear of sewing needle frequency f is:

$$f = \frac{\beta^2}{2\pi L^2}\sqrt{\frac{E\,I}{\rho\,A}} \tag{17}$$

where: β - Eigen value special graph [6]; *L* - Needle length; *E I* - sewing needle bending stiffness; *I* - sewing needles area moment of inertia of cross-section; *A* - needle cross-sectional area.

To calculate β from special graph [6] we need $\propto = \frac{P_{cr.}L^3}{\pi\,E\,I}$,

$$a = \sqrt{\frac{\pi^2 \propto}{2} + \sqrt{\frac{\pi^4 \propto^2}{4} + \beta^4}} \tag{18}$$

$$b = \sqrt{\frac{-\pi^2 \propto}{2} + \sqrt{\frac{\pi^4 \propto^2}{4} + \beta^4}} \tag{19}$$

β_n - special graph (3) (20)

The modal shape of the sewing needle as a function of (ζ) is:

$$r(\zeta) = \sin a\zeta - \frac{a}{b}\sin b\zeta + \\ + \frac{\sin a - \frac{a}{b}\sin b}{\cosh b - \cos a}[\cos a\zeta - \cosh b\zeta] \tag{21}$$

where $\left(\zeta = \frac{x}{L}\right)$, x - variable distance on the needle axis and $0 \leq \zeta \leq$.

The database of actual sewing needle of an industrial sewing machine is: *L = 0.045 m; φ = 0.89.10*$^{-3}$ *m; E = 206 GPa;* ρ*=7850 kg.m*$^{-3}$*; A = 6.2180 (E-7) m*^{2}*;* ℓ*xA = 4.8811*

$$EI = \frac{206 * 10^9 \times \pi \times (0.89 * 10^{-3})^4}{64} = 6.3413\ (E-3)$$

To calculate eigenvalue β, we need:

$$\propto = \frac{P_{cr.}L^3}{\pi\,E\,I} = \frac{62 \times (0.045)^3}{\pi \times 6.3413 * 10^{-3}} = 0.2837,$$

Critical load $P_{cr.}$*=62 N* [4]

$$a = \sqrt{\frac{\pi^2 \times 0.2837}{2} + \sqrt{\frac{\pi^4 \times (0.2837)^4}{4} + \beta^4}}$$

Then $a = \sqrt{1.400003 + \sqrt{1.9600094 + \beta^4}}$

$$b = \sqrt{\frac{-\pi^2 \times 0.2837}{2} + \sqrt{\frac{\pi^4 \times (0.2837)^4}{4} + \beta^4}}$$

Then $b = \sqrt{-1.400003 + \sqrt{1.9600094 + \beta^4}}$

Then $\beta/\beta_{cs} = 0.98,$

$$\beta_{cs} = 3.927 \;\; (n = 1)$$
$$= 7.069 \;\; (n = 2)$$
$$= 10.210 \;\; (n = 3)$$
$$= 13.352 \;\; (n = 4)$$

Then $\beta_1 = 0.98 \times 3.927 = 3.8485 \qquad (n = 1)$

and $\beta_2 = 0.98 \times 7.069 = 6.92762 \qquad (n = 2)$

The first natural frequency f_1:

$$f_1 = \frac{\beta^2}{2\pi L^2}\sqrt{\frac{E\,I}{\rho\,A}} = \frac{(3.8485)^2}{2\,\pi\,(0.045)^2} \times \sqrt{\frac{6.3413 * 10^{-3}}{7850\;\times\;6.2180 * 10^{-7}}}$$

$= 6.2618 \quad S^{-1} \quad (Hz) = 375.7 \quad SPM$

The second natural frequency f_2:

$f_2 = 20.2901\, S^{-1}\,(Hz) = 1217.4 \;\cong 1200\, SPM$

The third natural frequency f_3:

$\beta_3 = 0.98 \times 10.210 = 10.0058$

$f_3 = 42.327\, S^{-1}\,(Hz) = 2539.6 \;\cong 2540 \;\; SPM$

The fourth natural frequency f_4:

$\beta_4 = 0.98 \times 13.352 = 13.085$

$f_4 = 72.3875\, S^{-1}\,(Hz) = 4343.3 \;\cong 4340\, SPM$

If the average working speed of the sewing machine is 3k SPM, then $0.7 \times 4343.3 = 3040.3\, CPM$ that satisfies the safe running.

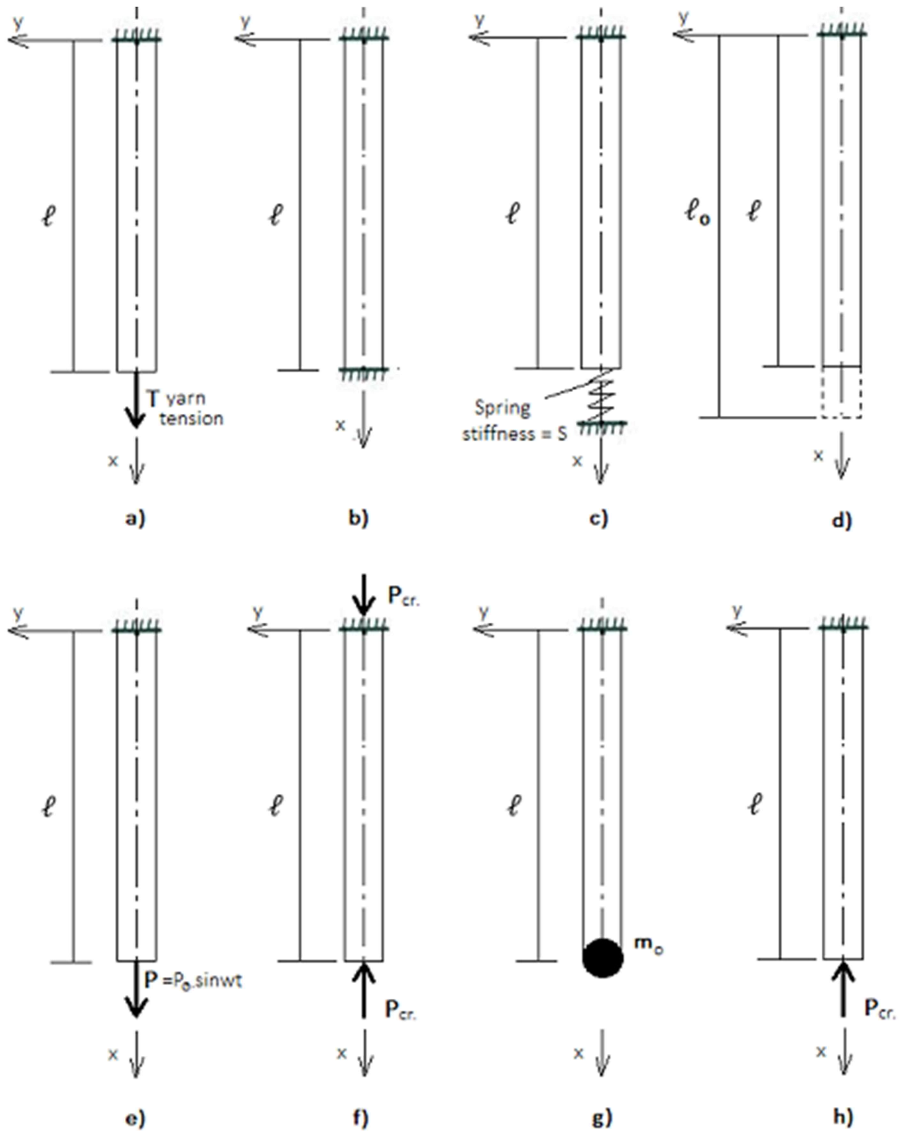

Figure 2 Different calculations schemes (line diagrams) of the sewing needles - constant CSA - for different cases

3.7 The effect of the penetration sewing needle force as time dependent on its longitudinal vibration

During the needle penetration into the sewn fabrics layers, starting from the upward to downward, it will take certain time. We will assume that the penetration force changes with time by a sinusoidal relationship as follow (see Figure 2e).

$$P = P_0 \sin \omega t \tag{22}$$

As shown in Figure 2e, the forced vibrations of the sewing needle are:

$$U(x,t) = \frac{P_0\, a}{A\, E\, \omega} \times \sec\frac{\omega \ell}{a} \times \sin\frac{\omega x}{a} \times \sin \omega t \tag{23}$$

where: ω - penetration force frequency (linear); A, ℓ, a & E - defined previously.

The natural frequency f_i is:

$$f_i = \frac{i\, \pi}{2\ell}\sqrt{\frac{E}{\rho}}, \qquad i = 1,2,3 \ldots. \tag{24}$$

where: f_i - linear natural frequency of the sewing needle; i, ℓ, E, ρ - defined previously.

When both of the penetrating force frequency and the needle natural frequency are equal, we will have a resonance at which the axial extension of the needle is ∞. Therefore we must select the working speed in the range:

$$0.7\, f_{1cr} \geq f_w \geq 1.4\, f_{2cr.} \tag{25}$$

When f_i, it is named critical linear frequency $f_{1cr} = 110\,(E+3)\, SPM$ for first mode of vibration $(i = 1)$.

3.8 Effect of the sewn fabric on supporting the free needles end (lower end)

Previously it was mentioned that the fabric during the sewing process can make different supporting actions or types on the lower end of the needle. These supports can be elastic (coil spring) or rigid (complete built-in). Now we will assume the sewn fabric will be intermediate between elasticity and rigidity i.e. the lower end of the needle will be simply supported as shown in Figure 2f. We studied this case previously - by the use of Gormens Eigen value [6].

3.9 Effect of concentrated mass at the lower end of the needle on axial vibration

We can apply Panovko [5] formula:

$$f_1 = \sqrt{\frac{EA}{m_0 \ell \left(1 + \frac{\alpha}{3}\right)}} = \sqrt{\frac{128091}{3.2943 * 10^{-6}\left(1 + \frac{\alpha}{3}\right)}} =$$

$$= \sqrt{\frac{3.8877 * 10^{10}}{\left(1 + \frac{\alpha}{3}\right)}} = {}^{197172}\!\Big/\!\left(1 + \frac{\alpha}{3}\right)^{1/2}$$

$\alpha = 0.10 \ \ldots 10$

$f_1 = 190812\, Hz \ \cong 191\, kHz, \qquad \alpha = 0.10$

$f_1 = 94718\, Hz \cong 95\ \ kHz, \qquad \alpha = 10$

Take $(\alpha = 0.3)$

$f_1 = 187996 * 10^{10}\ Hz \ \cong 188\, kHz = 5\, KSPM,$

$\alpha = 0.3$

N.B:

$$\alpha = \rho\, A\, \ell / m_0 = \frac{mass\ of\ needle}{m_0}$$

3.10 Effect of sewing needle penetration force on its - for interesting only - lateral vibrations

In this case the needle is subjected to axial load $P_{cr.}$, the combined frequency is calculated by see Figure 2h:

$$f_1 = \frac{0.562}{\ell^2}\sqrt{\frac{E\, I}{\rho\, A}\left(1 - \frac{5\, P_{cr.} \times \ell^2}{14\, EI}\right)} \tag{26}$$

where: f_1 - combined linear natural fundamental frequency due to lateral and axial vibration (it is the first mode of combined vibration), ℓ - sewing needle length; EI - bending stiffness of the needle (Young's modulus E = 206 GPa; I - area moment of inertia of the needle cross-section); $\rho\, A$ - mass per unit length of the needle (ρ - steel density $\rho = 7850\ kg/m^3$, *A* - needles cross-sectional area); $P_{cr.}$ - the Euler elastic axial load at which the needle loses its straight form. It will be taken 62 N for the actual needle as shown in the work [2].

The sewing needle (actual) has the following database: length $\ell = 0.045\, m$, diameter $\varphi = 0.89 * 10^{-3}\, m$ (mean value for constant cross-section needle), material of the needle is steel and the critical load $P_{cr.} = 62\, N$ [4].

Taking into consideration the previously mentioned database, we can write:

$$f_1 = \frac{0.562}{(0.045)^2}\sqrt{\frac{206{*}10^9 \times \pi \times (0.89{*}10^{-3})^4 \times 4}{64 \times 7850 \times \pi \times (0.89{*}10^{-3})^2} \times \times \left(1 + \frac{62 \times (0.045)^2 \times 64}{14 \times 206{*}10^9 \times \pi \times (0.89{*}10^{-3})^4}\right)}$$

$= 316.323\, S^{-1}\,(Hz) = 18980\, CPM \ \cong 19\, k\, SPM$

This relative low value is due to the presence of the penetration force.

3.11 Pisarenko [7] technique for different cases of sewing needle with constant cross-section area CSA, (axial vibrations)

The Table 1 has three columns:

a) First column describes the scheme of calculation or line diagram of sewing needle.

b) Column 2 gives the modal shape equation.

c) Column 3 illustrates the fundamental frequency of the sewing needle axial vibration.

Table 1 Sewing needles line diagram and natural linear frequency

Scheme or line diagram	Frequency equation	f_1
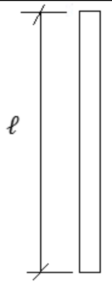 F - F	$\sin k\ell$	$= 56919\ Hz = 545\ kSPM$ $k\ell = i\pi,\ \ i = 1, 2, 3, \ldots$
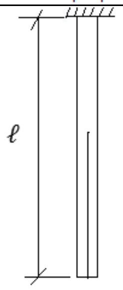 C - F	$\cos k\ell$	$= 28459\ Hz\ \cong 28\ kHz = 268\ kSPM$ $ki\ell = \frac{\pi(2i-1)}{2}, i = 1, 2, 3, \ldots$
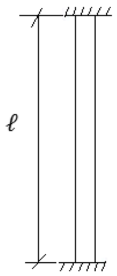 C - C	$\sin k\ell$	$= 56919\ Hz = 57\ kHz = 545\quad kSPM$ $k\ell = i\pi,\ \ i = 1, 2, 3, \ldots$
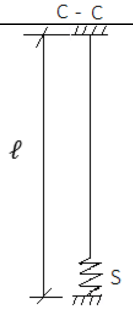 S - Spring const. of sewing fabric	$\tan k\ell = -\frac{k\ell}{\propto_0^\backslash}$	From graph $\propto_0^\backslash = 0,$ $S = 1000\ \ N/m,$ $\varphi = 0.89\ mm$ $f_i = 27191\ Hz = 27\ kHz$ $= 257962\ SPM \cong 258\ kSPM$
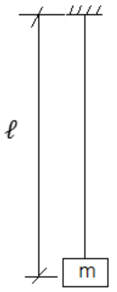	$k\ell \tan k\ell = \propto^\backslash$ $\propto^\backslash = \frac{\rho\ F\ \ell}{m}$	$\propto^\backslash = \frac{\rho\ F\ \ell}{m},\ \ m = \frac{1}{3}\ \rho\ F\ \ell$ $\therefore \propto^\backslash = 0.3 - by\ graph,\ \ ki\ell = 0.52$ $\propto^\backslash = \frac{7850 \times (0.89 * 10^{-3})^2\ \times 3.14 \times 0.045}{9}$ $\cong 0.01, \quad ki\ell = 0.10$ $f_i = 56919\ Hz\ \cong 57\ kHz \cong 545\ kSPM$

In the following section the sewing needle with variable cross-section will be constant. For the stepped sewing needle -2 sections- the linear fundamental natural frequency of axial free vibrations is determined by the solution of the next frequency equation:

$$\tan\left(f_i\ \frac{\ell_1}{a_0}\right) \times \tan\left(f_i\ \frac{\ell_2}{a_0}\right) = \frac{A_1}{A_2} \qquad (27)$$

where: f_i - natural frequency of free axial vibrations; ℓ_1, ℓ_2 &a_0 - see Figure 3; A_1, A_2 - sewing needle cross-sectional area at the upper and lower sections respectively.

The solution of formula (27), we can find:

$f_1 = 1.89,\ f_2 = 4.53, f_3 = 7.85, f_4 = 11.2$

$$P_1 = \frac{1.89}{\ell}\sqrt{\frac{206 * 10^9}{7850}} = 215153\ Hz = 215\ kHz$$

$$= 6.0\ M\ SPM$$

Assume: $a_0 = 45\ mm,\ \ \ell_1 = 40\%\ m,\ \ \ \ell_2 = 60\%\ \ mm$ of total length (a_0)

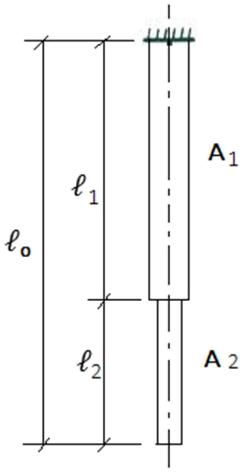

Figure 3 Stepped sewing needle

The database of the actual needle is:

$\varphi_1 = 1.5 * 10^{-3}\ m, \varphi_2\ = 0.8 * 10^{-3}\ m$

$\ell_1 = 0.015\ m, \ell_2\ = 0.025\ m$

$A_1 = 7.065 * 10^{-6},\ A_2 = 5.024 * 10^{-7}$

$\therefore\ {}^{A_1}/_{A_2}\ = 14.0625$

The frequency equation of the sewing needle is:

$$\tan 3.0643 * 10^{-6} f_1 \times$$
$$\times \tan 1.532 * 10^{-6} f_1 - 14.0625 = 0 \qquad (28)$$

By solving equation (28) we can obtain value f_1 and consequently linear natural frequency of longitudinal vibrations of the sewing needle.

For another approach for the stepped needle (see Figure 4) as written in Paramarev work [9]; the transcendental frequency equation is:

$$\cos\frac{f\ell_1}{a} \times \cos\frac{f\ell_2}{a} = \frac{A_1}{A_2}\sin\frac{f\ell_1}{a} \times \sin\frac{f\ell_2}{a} \qquad (29)$$

By assuming:

$$\frac{f\ell}{a} = k \qquad (30)$$

Then, we can write: $\frac{A_1}{A_2}\tan\left(\frac{\ell_1}{\ell}k\right) = \left(\tan\frac{\ell_2}{\ell}k\right)^{-1}$

or $\frac{A_1}{A_2}\tan\left(\frac{\ell_1}{\ell}k\right) \times \tan\left(\frac{\ell_2}{\ell}k\right) = 1$

i.e.

$$\tan\left(\frac{\ell_1}{\ell}k\right) \times \tan\left(\frac{\ell_2}{\ell}k\right) = \frac{A_2}{A_1} \qquad (31)$$

There is a similarity between both of equations (27 & 29). The graphical solution of equation (31) is shown in Figure 5.

The values of $k_{i\,(1-4)}$ are $k_1 = 1.89,\ k_2 = 4.53,$ $k_3 = 7.85,\ k_4 = 11.2$.

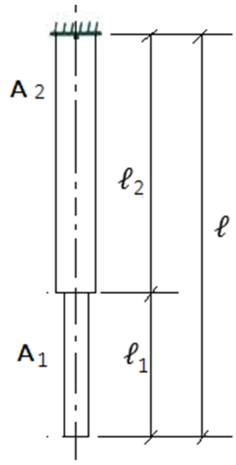

Figure 4 A stepped sewing needle

From formula (30) we can write:

$$f_i = \frac{k\ i}{\ell} * a = \frac{k\ i}{\ell}\sqrt{\frac{E}{\rho}} \qquad (32)$$

where: i - varies from 1, 2, 3, …n, f_i - natural linear frequency of the sewing needle (two-sections) axial vibrations, k_i - constant has different values from graphical solutions of equation (29) as mentioned previously, ℓ - total length of the needle, E - Young's modulus of the sewing needle material (steel) = 206 GPa and ρ - sewing needle material density (steel) = 7850 kg/m^3.

From database of the sewing needle;

$\varphi_1\ = 0.8 * 10^{-3}\ m,\qquad \varphi_2 = 1.5 * 10^{-3}\ m,$

$\ell = 0.040\ m,\qquad E = 206\ GPa,\qquad \rho = 7850\ \ kg/m^3,$

$$\sqrt{\frac{E}{\rho}} = 5122.69$$

$$f_i = \frac{1.89}{0.040} \times 5122.69 = 0.242\ MH = 14.523.10^6\ SPM$$
$$= 15\ M\ SPM$$

If we consider that the maximum allowable running speed of the industrial sewing machine is 15 k SPM, then the ratio will be 0.1033. This means that the running speed of the industrial sewing machine is too far from resonance i.e. too safe working speed. Practically the average running speed of the industrial sewing machines in the Garment industry is 3000 RPM. It is not necessary to calculate the higher linear natural frequencies i.e. $f_{2,}\ f_3 \&\ f_4$.

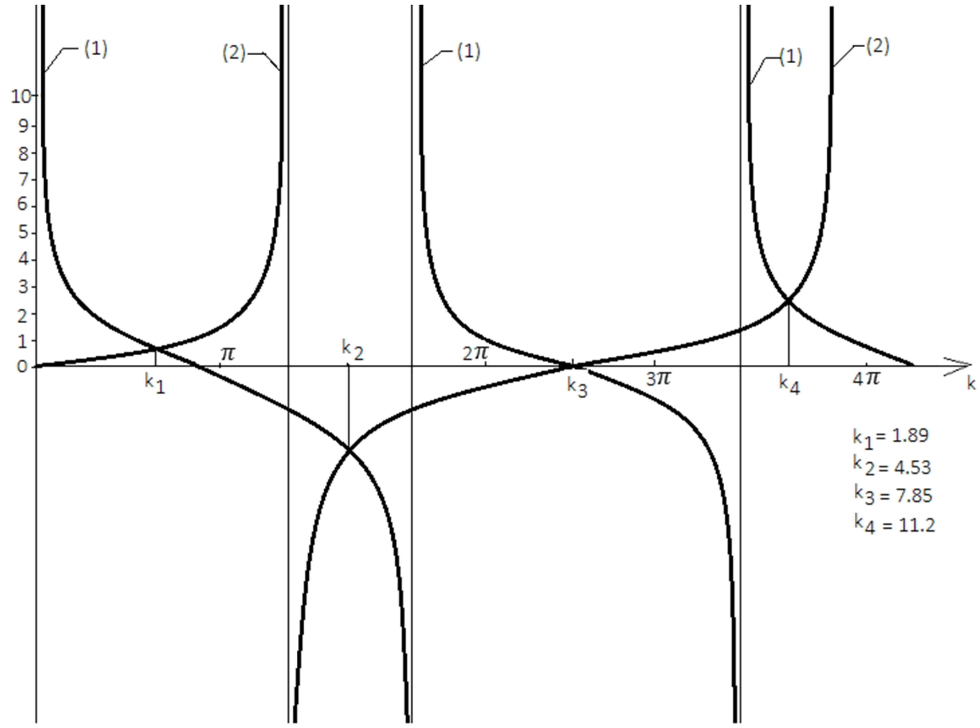

Figure 5 Graphical solution of equation (31) [9]. Legend: curve 1) $\cot\left(\frac{3}{5}\,k\right)$; curve 2) $\frac{1}{2}\tan\left(\frac{2}{5}\,k\right)$

4 CONCLUSIONS AND FUTURE VISIONS

From the previous theoretical and mathematical approaches of the sewing needles axial vibration the following conclusions and future visions can be drawn out:

1) The linear natural fundamental frequency for the sewing industrial needle is ranging from 19 k SPM (sewing needle is subjected to lateral vibrational) to 110 M. SPM (axial) depending upon other sewing needle engineering conditions (needles speed, sewing thread sudden breaks,…etc.).
2) The ratio between the highest linear frequency and the lowest linear natural frequency is 5789 ≅ 6 k rimes.
3) The first linear fundamental natural frequency is too high with respect to the sewing needle working speed.
4) For most geometrical engineering *conditions* of the sewing needle, the following constant (a) is valid in calculation the first mode of needle axial vibration: $a = \sqrt{\frac{E}{\rho}}$
   where: E - steel needles material Young's modulus = 206 GPa, ρ – sewing needle material density (steel) = 7850 kg/m^3.
5) The sewing stepped needle - two sections, natural linear axial frequency depend on the ratio of the cross-sectional areas at the upper end (built-in end) and the lower free-end.
6) The dealing - mathematical - with the sewing needle as a massive-less bar gave natural frequency for its longitudinal vibration = 30 k SPM.
7) The actual linear frequency equation for the sewing stepped needle (two-sections) is
   $$\tan 3.0643 * 10^{-6}\, f_1 \times \tan 1.532 * 10^{-6} f_i - \\ -14.0625 = 0$$
   where, f_i - the linear natural frequency of a stepped needle due to axial vibrations.
8) The frequency equation of the sewing needle (axial vibrations) with elastic resistance from the sewn fabric via spring constant is
   $$\tan f_i \times 2.758 * 10^{-6} + 7.8501\left(\frac{f_i}{S}\right) = 0$$
9) The sewing needle modal formula for axial vibration taking into consideration its linear speed V is
   $$U(x,t) = \frac{4\,V\ell}{\pi^2 a} * \sum_{i=1,3,\ldots}^{\infty} \frac{1}{i^2} \sin\left(\frac{\pi\, x}{\ell}\right) \sin\left(\frac{i\,\pi\, a\, t}{\ell}\right)$$
10) Most of the studied needles' configurations with their different geometrical – massive characteristics have equation of modal shape of free vibrations starting from the first mode to nth mode.

11) The sewn fabric is neither pure elastic material nor pure rigid (stiff) i.e. the expected sewn fabric spring constant *S* is ranging from *S = 0* complete free ends (F-F) to *S* = ∞ complete fixed end (C-C). Accordingly, in between both of these cases we can consider the lower end of the sewing needle is varying from a simply supported to a completely fixed.
12) The axial natural fundamental frequency of the sewing needle (as a complete - fixed upper end while its lower end is simply supported) is ranging from $f_1 = 376$ SPM to $f_4 = 4343$ SPM.
13) Seemingly, the mathematical approach for the axial free vibration of the sewing needle as a bar with built-in upper end and simply support at its lower end, can give satisfied linear natural frequency.
14) The ratio between the needle working speed (3 k RPM) and the fourth natural frequency (4343 CPM) is 0.691≅ 0.7, that satisfies condition of formula (25).

The future vision could be summarized as follow:

15) The elasticity of the sewing fabrics - in multi directions - (spring constant *S*) must be determined experimentally and intensively by using innovated techniques.
16) More attentions must be paid to the model shapes of the sewing needle vibrations, especially for the sewing needle with variable cross-sections. The same high attentions must be paid for these needles for calculating their natural linear frequencies at different modes.
17) Both of the sewing needle internal damping for vibrations and the fabric resistance as frictional - dry or wet - damping for the vibration are highly interested. For needles material internal damping, it could be assumed that $\sigma_x = E\varepsilon_x + C\,\dot{\varepsilon}$ where, *C* - is the internal sewing needle damping coefficient.

Acknowledgment: *The authors are willing to introduce thanks giving for prof. Dr. Eng. Ibrahim A. Elhawary and prof. Dr. Eng. Sherwet H. Elgolmy for invaluable and scientific help in carrying out the research work.*

5 REFERENCES

1. El Gholmy S.H.: Ready - made Garments and Apparels Modern Technology, Lecturers Notes, Textile Engineering Department (TED), Alexandria University, 2015, Egypt
2. El Gholmy S.H., El Hawary I.A.: The application of Gorman's Eigen values to the industrial sewing machine's needle vibration, Alexandria Engineering Journal 55 (2), 2016, pp. 983-989, https://doi.org/10.1016/j.aej.2016.02.028
3. Seto W.W.: Theory and Problem of Mechanical Vibrations, McGraw-Hill, USA, 1964, 200 p., ISBN: 9780070589131
4. El Gholmy S.H., El Hawary I.A.: A formula for calculating the critical load of the needles used in the garment and apparels sewing technology: Part 1: Pucarenko technique, Nature and Science 11(10), 2013, pp. 88-93, http://www.sciencepub.net/nature
5. Panovko I.A.: Elements of the applied theory of elastic vibrations, English copy, MIR Publisher, 1971, Moscow, RU, 317 p.
6. Gorman D.J.: Free Vibrations Analysis of Beams and Shafts, Wiley, Ottawa University, Canada, 1975, 386 p., ISBN-13 : 978-0471317708
7. Matveev V.V., Varvak P.M., Pisarenko G.C., Yakovlev A.P.: A Reference Book of strength of materials, Naukova Press, Kiev, Ukraine, 1975
8. Feodosev V.I.: Strength of Materials, English copy, MIR Publisher, Moscow, RU, 1968, 570 p.
9. Paramarev C.D., Buderman V.I., Lukharev K.K., Makyshin V.M., Malinin N.N., Fodoce V.N.: The basic modern methods of the machine design, Machine Design Press, Moscow, RU, 1952
10. Belyaev N.M.: Strength of Materials, Russian copy, Nauka Press, Moscow, RU, 1976
11. El Hawary I.A.: The Dynamic Balancing of the Heavy Packages of the Ply Constant Fil Yarns, Notes Lectures, TED, Alexandria University, Egypt, 2015
12. El Hawary I.A.: The Vibrations of the Heavy Twisting Spindles Used for Ply C.F. Yarn, Academy of Textiles, Moscow, RU, 1978
13. Rengasamy R.S.: Mechanics of Spinning Machines, NCUTE, IIT, Deli, India, 2002
14. Hashima W.A., El Hawary I.A.: The 3rd Penetration Phases of the Industrial Sewing Needle, Alexandria University, Egypt, under publication

EFFECT OF STYRENE ACRYLIC AND URETHANE POLYMER COATINGS FILLED WITH TITANIUM DIOXIDE ON THERMOPHYSICAL PROPERTIES OF FABRIC SURFACE

Ihor Horokhov, Irina Kulish, Tatyana Asaulyuk, Yulia Saribyekova, Sergey Myasnykov, Olga Semeshko, Natalia Skalozubova and Natalia Subbotina

Kherson National Technical University, Berislav Highway 24, 73008 Kherson, Ukraine
kulish.in.411@gmail.com

Abstract: *The goal of the work is to study the effect of styrene acrylic and urethane polymer films filled with titanium dioxide nanoparticles on the change in the thermophysical properties of the cotton fabric surface. Aqueous dispersions of styrene acrylic polymer Lacrytex 640 and polyurethane Aquapol 14 were selected as film-forming substances. Nanosized titanium dioxide was investigated as a thermophysical additive. The effect of the filler on the structural properties of polymer composites was investigated using the equilibrium swelling method. The mechanical properties of the obtained nanocomposites were evaluated in terms of breaking load and elongation at break. The surface morphology of the nanocomposite coated fabric before and after ignition was investigated using scanning electron microscopy. Based on the results of the study of the dependence of the structural and mechanical properties of polymer films on the nanofiller content, it was found that a high degree of polymer - filler interaction efficiency is observed at titanium dioxide concentrations up to 5 wt.%. It has been proven that the interfacial interaction of titanium dioxide with polyurethane Aquapol 14 is higher than that with styrene acrylic polymer Lacrytex 640. It was found that the introduction of nanosized titanium dioxide increases the tensile strength, but decreases the plasticity of nanocomposites in comparison with unfilled polymer matrices. It is shown that the studied styrene acrylic and polyurethane coatings filled with nano-sized titanium dioxide lead to the formation of coke residue on the fiber surface under the action of a flame, which makes it possible to preserve the fabric structure upon ignition. The obtained research results are of practical importance in the development of fire retardants for finishing textile materials.*

Keywords: *styrene acrylic polymer, polyurethane, nanocomposite, titanium dioxide, structural characteristics, mechanical properties, coke forming ability, fire retardant coating.*

1 INTRODUCTION

Concerns about the toxicity of fire retardants commonly used in the processing of textile materials have directed researchers towards creating more environmentally friendly compositions and finding effective solutions for fire protection technologies of fabrics [1, 2]. In this regard, nanostructured compositions are of interest, which can provide barrier properties to textile materials by reducing the penetration of oxygen from the fire zone to the surface of the fabric, and prevent droplet formation of the synthetic textile component during combustion. In addition, nanocomposites ensure the formation of a self-expanding thermophysical barrier on the surface, which can reduce heat and mass transfer from the atmosphere to the substrate. These advantages appear to be the most promising for the development of fire retardant compositions. Among modern coating technologies for textile materials, technologies have been developed based on the adsorption of nanoparticles (NP) and layer-by-layer assembly of components (LbL), the essence of which is one- or multi-stage surface adsorption of nanoparticles or polyelectrolytes from dilute (≤1 wt.%) aqueous suspensions or solutions. In [3, 4], a highly efficient starch-based LbL coating was considered, which demonstrated the self-extinguishing behavior of cotton after 4-8 stages of deposition. The creation of ultrathin nanostructured coatings is based on the stepwise layer-by-layer deposition of various polymers and nanoparticles, which can be nanoclays, glass fabrics, silsesquioxanes (POSS), and layered double hydroxides [5-10]. The technology for obtaining such coatings is also based on multiple and alternate immersion of a textile substrate in a polymer and nanoparticles to create multilayer organic-inorganic phases.

Despite the good fire retardant properties, the significant disadvantages of the listed technologies include the multistage deposition required to achieve the desired properties (about 20-40 processing stages), which is practically unrealizable in real production conditions. However, taking into account the undoubted advantages of precisely surface methods of protecting textile materials, an urgent task is to develop simple, quickly scalable technologies for the formation of coatings with an individual nanostructure based on readily available components with fire-fighting properties.

2 THE GOAL OF THE STUDY

The goal of the work is to study the properties of acrylic and urethane polymer films filled with nanosized titanium dioxide and the effect of the obtained polymer nanocomposites on the change in the thermophysical properties of the textile materials surface.

3 MATERIALS AND METHODS

A finely dispersed aqueous suspension of titanium dioxide was obtained by stirring on a magnetic stirrer at 600 rpm for 20 min, followed by ultrasonic treatment with an acoustic frequency of 20 kHz and exposure duration of 10 min.

An aqueous dispersions of styrene acrylic polymer Lacrytex 640 (OOO Polymer-Lak, Ukraine) and polyurethane Aquapol 14 (OOO NPP Makromer, Russia) were studied as film formers. Characteristics of the dispersions are given in Table 1.

Nanocomposites were prepared by introducing a suspension of titanium dioxide into polymer dispersions Lacrytex 640 and Aquapol 14 with stirring. Then, from the mixtures obtained, films were formed on a glass substrate and dried at 80°C. The thickness of the formed films was 0.7±0.05 mm.

The degree of interaction of the filler with the polymer matrix and the structural characteristics of the nanocomposites were studied using the equilibrium swelling method.

The polymer – filler interaction was evaluated by the change in the degree of equilibrium swelling of the obtained hybrid organic-inorganic films. For this purpose, film samples were immersed in isopropanol solvent for 24 hours. Then, after drying, the sample was weighed, placed in an oven for 24 hours at 60°C to remove residual solvent, and weighed again. The efficiency of polymer - filler interaction was calculated using the Lorentz and Parks equation [11]:

$$\frac{Q_f}{Q_g} = ae^{-z} + b \tag{1}$$

Subscripts *f* and *g* characterize filled and unfilled polymers, respectively; *z* is the weight ratio of filler to polymer; *a* and *b* are constants.

Q is determined in grams of solvent per gram of polymer and is calculated by the formula:

$$Q = \frac{M_s - M_d}{M_d} \tag{2}$$

where M_s is the mass of the swollen sample; M_d is the mass of the dry sample.

The mechanical properties of nanocomposites were investigated by determining the tensile strength and elongation at break of polymer films.

The formation of a nanocomposite coating on a textile material was carried out by impregnating a cotton fabric in a solution containing 10, 20 and 30 wt.% preliminarily dispersed nano-TiO_2 and 15 wt.% polymer dispersion, followed by squeezing to 80% and drying at 80°C for 10 min.

Fabrics with a nanocomposite coating containing TiO_2 were examined by scanning electron microscopy (SEM) to study the surface morphology and structure of the textile material before and after the flammability test.

4 RESULTS AND DISCUSSION

One of the most valuable flame retardant strategies used in volumetric addition relies on the production or accumulation of a heat resistant surface layer capable of acting as a barrier to mass and heat transfer [12]. This layer, often composed of inorganic nanoparticles, forms after the substrate is ignited due to decomposition of the surface layer of the polymer.

The combustion process of a textile material can be briefly described in two stages. In the first stage, reaching the surface of the fabric, heat from a flame or other heat source is transferred into its volume. In the second stage, volatile thermal decomposition products diffuse from the fabric volume over its entire surface to the gas phase, thereby feeding the flame.

Thus, it is the surface that is the region that controls the mass and heat transfer at the interface between the gas and condensed phases [13]. The thermophysical properties of the fabric surface play a dominant role at the stages of preliminary ignition and combustion of the textile material. Therefore, a change in these surface properties can provide an increase in the fire retardant properties of the fabric.

Mineral substances are often used as fire retardants due to the physical nature of their fire retardant effects at high temperatures. With an increase in temperature, endothermic decomposition of mineral fillers occurs with energy absorption, the release of non-combustible substances (water, carbon dioxide), which dilute flammable gases, and a protective ceramic or glassy layer is formed.

Table 1 Characteristics of polymer dispersions

Trade name	Chemical composition	Dry residue [%]	pH	Particle size [µm]	Viscosity [mPa.s]
Lacrytex 640	aqueous dispersion of acrylic copolymer, modified by the addition of an adhesion promoter	55-57	2-3	≈ 0.2	<5000
Aquapol 14	aqueous dispersion of aliphatic polyurethane	35	7.4	≈ 0.1	20.1

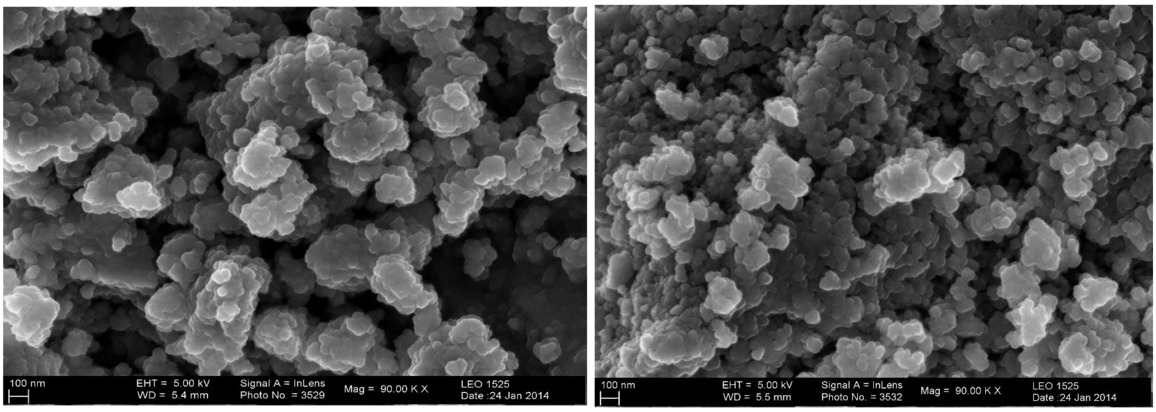

a) b)

Figure 1 Micrographs of the nanosized titanium dioxide suspension: a) before ultrasonic treatment; b) after ultrasonic treatment

The introduction of nanoparticles proved to be effective to improve the shielding ability of char. In addition, an increase in fire resistance is often accompanied by an improvement in related properties, such as mechanical strength, self-healing ability, thermal conductivity, etc.

One of the basic rules for obtaining compact insulating char on the surface of textile materials is a good dispersion of nanoparticles in the polymer matrix.

In this work, nanosized titanium dioxide was investigated as a thermophysical additive. Micrographs of the aqueous suspension of nanosized titanium dioxide obtained before and after ultrasonic treatment are presented in Figure 1.

Particles of titanium dioxide before ultrasonic treatment (Figure 1a) as a result of high surface energy are significantly aggregated and form large agglomerates in suspension, which can negatively affect the uniform distribution of the filler in the polymer matrix, increase the stress in the polymer system and worsen the operational properties. As a result of sonication (Figure 1b), titanium dioxide agglomerates are significantly reduced, which makes it possible to obtain a more finely dispersed aqueous system.

Methods for achieving fire retardant properties of textile materials should be based on predicting the direction of decomposition of a nanostructured surface coating. One of these methods is the formation of a bulk carbonaceous residue, which slows down heat transfer and thereby reduces the diffusion of flammable volatile gases, which makes it possible to achieve an increase in the fire retardant properties of the fabric. In this case, the use of polymers makes it possible not only to fix nanoparticles on the fiber surface, but also to promote the formation of a protective carbonaceous layer due to the organic nature of the film former.

In this work, we investigated aqueous dispersions of styrene acrylic polymers and polyurethanes capable of forming a carbonaceous residue in order to impregnate titanium dioxide nanoparticles on the surface of a textile material. Since the properties of composites are determined by the nature of the mixed components and their structure, it is necessary to study the degree of interaction between the components of the mixture.

The Q_f/Q_g ratio characterizes the degree of interaction between the filler and the matrix. Moreover, the higher the value of this ratio, the lower the efficiency of the interaction between the filler and the matrix. The calculation data are shown in Figure 2.

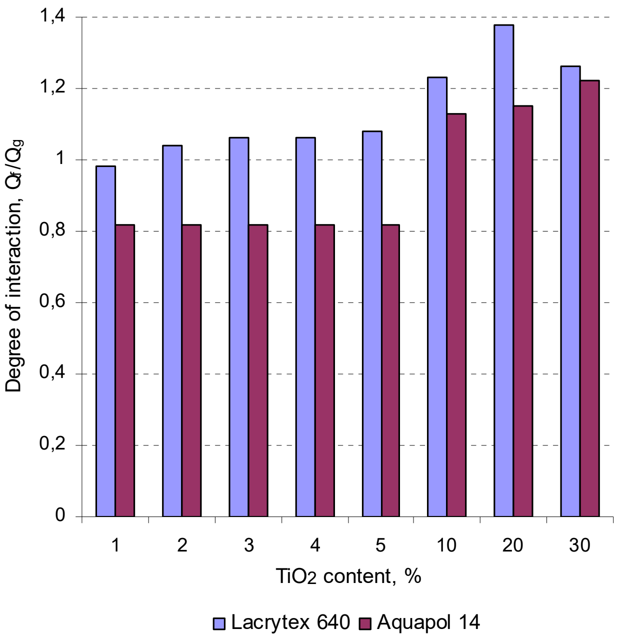

Figure 2 Degree of interaction between nanosized titanium dioxide and polymer matrix

Table 2 Structural parameters of polymers filled with TiO_2

TiO_2 content [%]	Lacrytex 640			Aquapol 14		
	Q_f/Q_g	M_c [g/mol]	$v \times 10^{-3}$ [mol/cm^3]	Q_f/Q_g	M_c [g/mol]	$v \times 10^{-3}$ [mol/cm^3]
–	–	50	10	–	1240	0.40
1	0.98	50	10	0.82	1032	0.48
2	1.04	52	9.6	0.82	967	0.52
3	1.06	67	7.5	0.82	922	0.54
4	1.06	81	6.2	0.82	913	0.55
5	1.08	95	5.3	0.82	944	0.53
10	1.23	103	4.8	1.13	1240	0.08
20	1.38	112	4.5	1.15	1432	0.08
30	1.26	128	3.9	1.22	1527	0.07

Q_f/Q_g - the degree of interaction between TiO_2 and polymer; M_c - the average molecular weight of the chain segment; $v \times 10^{-3}$ - the crosslinking density of the polymer.

Analysis of the data presented in Figure 2 shows that the introduction of nanosized titanium dioxide in an amount of up to 5 wt.% leads to low values of the Q_f/Q_g ratio, which explains the appearance of a rather high degree of polymer–filler effective interaction. It should be noted that the efficiency of the interaction of titanium dioxide with the urethane polymer of Aquapol 14 is in all cases higher than with the styrene acrylic polymer Lacrytex 640.

Based on the experimental results obtained using the equilibrium swelling method, the crosslinking density of the polymer and the average molecular weight of the chain segment enclosed between two crosslinks were calculated. The data are shown in Table 2. The results obtained (Table 2) indicate that the introduction of titanium dioxide nanoparticles into the styrene-acrylic polymer matrix does not improve the structural parameters of the nanocomposites. At a concentration of nanosized TiO_2 up to 1 wt.%, the average molecular weight of the chain segment and the crosslinking density remain unchanged. An increase in the nanofiller content leads to a decrease in the studied parameters.

However, in the case of using polyurethane as a polymer matrix, the polymer - filler interaction is 0.82 with a nanosized TiO_2 content of up to 5 wt.%. A decrease in the average molecular weight of the chain segment by 17 - 24% is also observed. This phenomenon is caused by an increase in the polymer - filler interphase interaction, which made it possible to reduce the rate of solvent transfer by lengthening the average diffusion path. TiO_2 content above 5 wt.% negatively affects the average molecular weight of the chain segment and lowers the crosslinking density.

The interface between nanoparticles and the polymer matrix plays a decisive role in the structure - property relationship and is one of the most important factors affecting the mechanical properties of nano-composites. The results of studying the effect of the concentration of nanofiller on the tensile strength and elongation at break of polymer composites are shown in Figures 3 and 4, respectively.

On the basis of the obtained experimental data (Figures 3, 4), it was found that nanocomposites have higher tensile strength, but lower plasticity compared to unfilled polymer matrices. With the content of nanosized TiO_2 up to 3 wt.% nanocomposites exhibit excellent mechanical properties. The tensile strength for Lacrytex 640 / TiO_2 is 12.74 MPa, which is 2 times higher than for unfilled styrene acrylic polymer. For Aquapol 14 / TiO_2, this indicator is 14.5 MPa, which exceeds the strength of unfilled urethane polymer by 1.5 times. It should be noted that with the introduction of TiO_2 nanofiller above 3 wt.% there is a decrease in tensile strength for all nanocomposites. This fact can be explained by the presence of aggregates of TiO_2 nanoparticles.

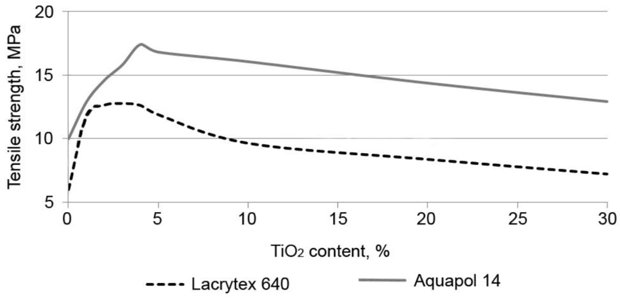

Figure 3 Effect of TiO_2 content on tensile strength of polymer composites

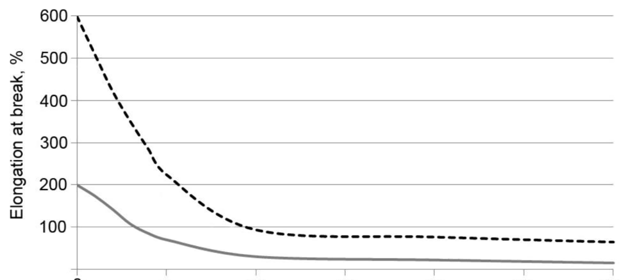

Figure 4 Effect of TiO_2 content on elongation at break of polymer composites

The aggregation of nano-TiO_2 in the polymer matrix can create zones of stress concentration and suppress the effect of interfacial interaction; therefore, the mechanical properties of nanocomposites decrease. Elongation at break of the studied nanocomposites (Figure 4) with nanoparticle content of 3 wt.% is reduced by almost 25% for the styrene acrylic polymer matrix Lacrytex 640 and by 50% for the Aquapol 14 polyurethane.

Analysis of the results of studying the mechanical properties of filled polymer films shows that the presence of nanosized TiO_2 in the polymer matrix limits the mobility of polymer chains, as a result of which the plasticity of nanocomposites decreases. If ignition occurs, the limited mobility of the polymer macromolecules will provide a reinforcing effect on the composite surface, which will help to reduce the drop formation of the synthetic component of the textile material.

At the next stage of the work, a study of the fire resistance of textile materials treated with the investigated polymer nanocomposites was carried out.

There is a significant difference in the size of the flame between the untreated samples and fabrics with polymer coating containing 10, 20 and 30 wt.% nano-TiO_2. The height of the flame for vertical combustion 6 s after ignition is lower on fabrics with a nanocomposite coating than on the untreated sample. In addition, after removal of the flame, a more intense residual glow was observed on the untreated samples. The residual smoldering time for untreated samples is 15 s, and for fabrics with nanocomposite coating it is 10 - 12 s.

Micrographs of untreated fabric sample and samples with nanocomposite coatings before and after thermal exposure are shown in Figure 5.

The flammability test shows that the untreated textile is completely destroyed by flame, so there is no micrograph of the surface of this sample after ignition. The results of SEM analysis of the fabric microstructure indicates that all samples with nanocomposite coating (Figures 5b, 5c) showed the presence of significant coke residue, which made it possible to prevent further thermal degradation of the fiber-forming polymer (Figures 5d, 5e).

A decrease in the flammability of a polymer under the action of nanoparticles occurs through several mechanisms, which consist in limiting the transition of combustible substances into a flame, the formation of a charred protective layer, etc. Analysis of the fabric samples surface with a nanocomposite coating (Figure 5) showed that the presence of 20 wt.% nanosized TiO_2 in the polymer matrix preserve fabric structure after ignition. However, a high concentration of nanofillers leads to uneven distribution and aggregation of nanoparticles on the fiber surface.

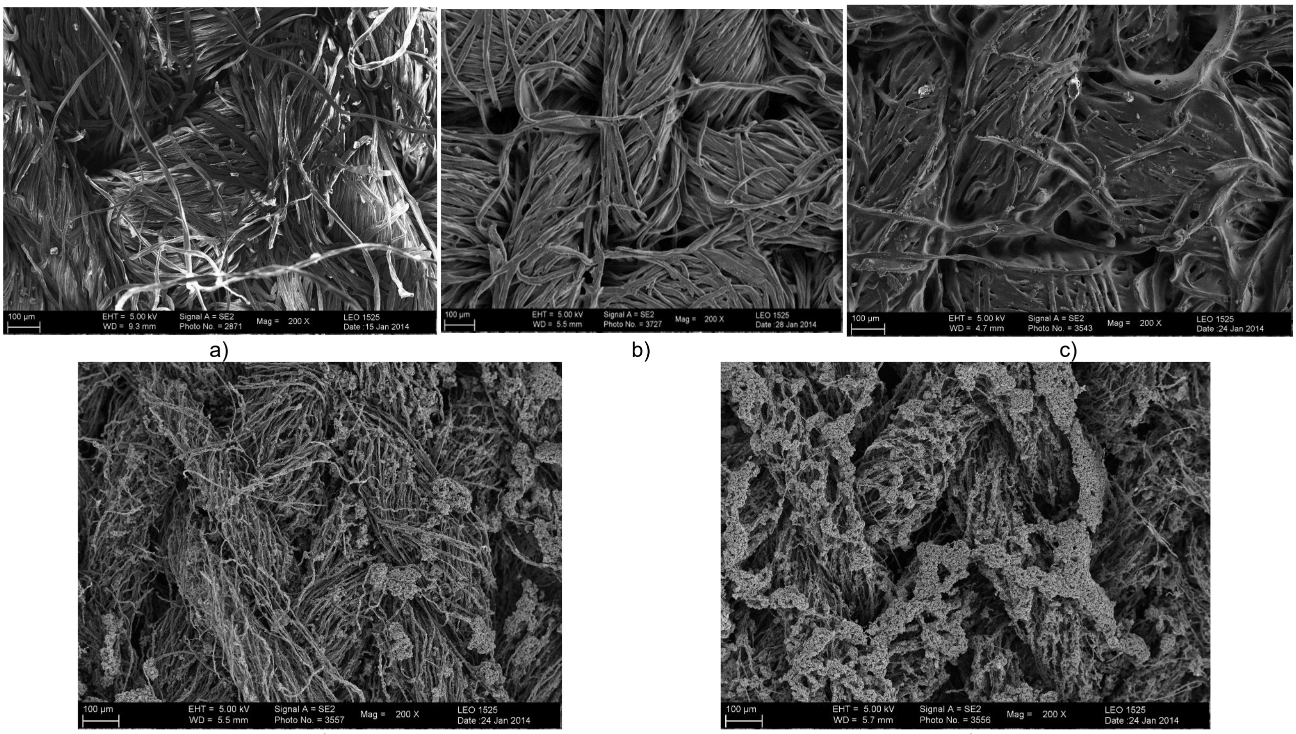

Figure 5 Micrographs of the fabric surface at 200x magnification: a) untreated sample before ignition; b) Lacrytex 640 / TiO_2 (20%) coated sample before ignition; c) Aquapol 14 / TiO_2 (20%) coated sample before ignition; d) Lacrytex 640 / TiO_2 (20%) coated sample after ignition; e) Aquapol 14 / TiO_2 (20%) coated sample after ignition

5 CONCLUSIONS

The results of studying the effect of polymer nanocomposite coatings on the change in the thermophysical properties of the fabric surface show that the introduction of titanium dioxide nanoparticles into the polymer matrix provides a reinforcing effect to the textile material. The presence of titanium dioxide nanoparticles in the polymer coating leads to the formation of coke residue on the fiber under the influence of the flame, which allows the fabric surface structure to be preserved after ignition.

6 REFERENCES

1. Kaspersma J., Doumen C., Munro S., Prins A-M.: Fire retardant mechanism of aliphatic bromine compounds in polystyrene and polypropylene, Polymer Degradation and Stability 77(2), 2002, pp. 325-331, https://doi.org/10.1016/S0141-3910(02)00067-8
2. Watanabe I., Sakai S.-i.: Environmental release and behavior of brominated flame retardants, Environment International 29(6), 2003, pp. 665-82, https://doi.org/10.1016/S0160-4120(03)00123-5
3. Alongi J., Horrocks A.R., Carosio F., Malucelli G.: Update on Flame Retardant Textiles: State of the Art, Environmental Issues and Innovative Solutions, Smithers RAPRA Technology, Shrewsbury, 2013, 364 p., ISBN: 978-1-90903-017-6
4. Alongi J., Tata J., Carosio F., Rosace G., Frache A., Camino G.: A comparative analysis of nanoparticle adsorption as fire-protection approach for fabrics, Polymers 7(1), 2015, pp. 47-68, https://doi.org/10.3390/polym7010047
5. Li Y.-C., Kim Y. S., Shields J., Davis R.: Controlling polyurethane foam flammability and mechanical behaviour by tailoring the composition of clay-based multilayer nanocoatings, Journal of Materials Chemistry A 1(41), 2013, pp. 12987-12997, https://doi.org/10.1039/C3TA11936J
6. Cui Z., Qu B.: Synergistic effects of layered double hydroxide with phosphorus-nitrogen intumescent flame retardant in PP/EPDM/IFR/LDH nano-composites, Chinese Journal of Polymer Science 28, 2010, pp. 563-571, https://doi.org/10.1007/s10118-010-9095-9
7. Aziz H., Ahmad F., Zia-ul-Mustafa M.: Effect of titanium oxide on fire performance of intumescent fire retardant coating, Advanced Materials Research 935, 2014, pp. 224-228, https://doi.org/10.4028/www.scientific.net/AMR.935.224
8. Li Y.C., Schulz J., Grunlan J.C.: Polyelectrolyte/nanosilicate thin-film assemblies: influence of pH on growth, mechanical behavior, and flammability, ACS Applied Materials & Interfaces 1(10), 2009, pp. 2338–2347, https://doi.org/10.1021/am900484q
9. Cain A.A., Plummer M.G.B., Murray S.E., Bolling L., Regevb O., Grunlan J.C.: Iron-containing, high aspect ratio clay as nanoarmor that imparts substantial thermal/flame protection to polyurethane with a single electrostatically-deposited bilayer, Journal of Materials Chemistry A 2(41), 2014, pp. 17609-17617, https://doi.org/10.1039/C4TA03541K
10. Carosio F., Fontaine G., Alongi J., Bourbigot S.: Starch-based layer by layer assembly: efficient and sustainable approach to cotton fire protection, ACS Applied Materials & Interfaces 7(22), 2015, pp. 12158-12167, https://doi.org/10.1021/acsami.5b02507
11. Halim S.F., Lawandy S.N., Nour M.A.: Effect of in situ bonding system and surface modification of montmorillonite on the properties of butyl rubber/montmorillonite composites, Polymer Composites 34(9), 2013, pp. 1559-1565, https://doi.org/10.1002/pc.22573
12. Malucelli G., Carosio F., Alongi J., Fina A., Frache A., Camino G.: Materials engineering for surface-confined flame retardancy, Materials Science and Engineering: R: Reports 84, 2014, pp. 1-20, https://doi.org/10.1016/j.mser.2014.08.001
13. Luda M.P., Zanetti M.: Cyclodextrins and cyclodextrin derivatives as green char promoters in flame retardants formulations for polymeric materials. A review, Polymers 11(4), 2019, pp. 1-29, DOI: 0.3390/polym11040664

IMPROVING THE DRIVE BELT CLEANING SYSTEM FOR THE POSITIVE FEED MECHANISM OF CIRCULAR WEFT KNITTING MACHINE: A NOBLE APPROACH

A.K.M. Mobarok Hossain[1], Md Imranul Islam[2] and Abu Rayhan Md. Ali[3]

[1]*Department of Textile Engineering, Ahsanullah University of Science and Technology, Dhaka, Bangladesh*
[2]*Textile Development and Marketing Department, Jay and Patty Baker School of Business and Technology, Fashion Institute of Technology, NY, USA*
[3]*Department of Mechanical Engineering, Bangladesh University of Engineering and Technology, Dhaka, Bangladesh*
mobarok@aust.edu; mdimranul_islam@fitnyc.edu; armali@me.buet.ac.bd

Abstract: *The yarn delivery rate required to knit fabric with a given stitch quality in a multi-feeder circular knitting machine is generally based on the drive belt speed of a positive yarn feed system. Even if the diameter of drive wheel (also known as Quality Adjustment Pulley (QAP) or Variable Diameter for Quality (VDQ) Pulley) of such system is well adjusted to maintain the required belt speed through positive drive, the stitch length measured on the fabric may not remain uniform as production continues. A key reason for this variation is the growing lint accumulation inside QAP that causes changing circumference of QAP gradually. Such deposition of lint may also occur on other parts of the yarn delivery system causing fluctuation in yarn tension and yarn delivery rate from different feeders, which ultimately causes fabric defect. To counteract such problem a typical brush associated cleaning system has been incorporated into some knitting machines by the manufacturers, which also possesses some inherent limitations. In this study, a noble approach has been carried out to develop an alternative cleaning tool for lint removal from the QAP system using compressed air. Further investigation through this study showed that the developed device exhibits better cleaning performance and is cost-effective than the traditional brush-shelf type cleaning apparatus.*

Keywords: *knitting, stitch length, QAP, lint/fluff, compressed air.*

1 INTRODUCTION

When a multi-feeder circular knitting machine knits a fabric, yarn ends from different packages are supplied to needles arranged around the cylinder of that machine. A number of knitting cams positioned around the cylinder define the travel path of the needles. The needles should receive a certain quantity of yarn supplied per revolution of the knitting machine for a smooth knitting process. The amount of yarn, supplied to the needles of a circular knitting machine, determines the quality of the fabric being knitted. To knit a denser fabric, the amount of yarn fed to the needles per revolution of the knitting machine is decreased and vice versa to knit a lighter fabric. Therefore, it is imperative to control the rate at which yarn is fed to a knitting machine in order to maintain the quality of knit fabrics.

In the negative feed system, the needles pulled yarns directly from yarn packages and this system has some serious drawbacks. For instance, the yarn feed rate and the tension of yarn from different packages are varied due to the relative spatial locations of the packages with respect to the circular knitting machine [1]. This varying yarn tensions and feed rates were the reasons for inconsistent product quality as well as low productivity through such feed systems. In order to solve this non-uniform feed rate problem, positive yarn feed system had been developed where yarn is fed to the needles at a controlled rate [1]. More specifically, a number of positive feed units, coupled with the motor through a belt and a drive wheel (Figures 1 and 2), can pull exact amount of yarn from yarn packages to be supplied to needles. This same amount of yarn then wraps around the positive feed wheels and, is subsequently distributed to needles (unlike the direct feeding of yarn to needles). Yarn delivery continues only when the positive feed units are rotating. The drive wheel is adjustable to differentiate the rotation rate of the positive feed units, and consequently, to adjust the amount of yarn supplied to needles. Hence, it is very much interrelated with fabric quality and consequently named as the quality wheel or quality pulley.

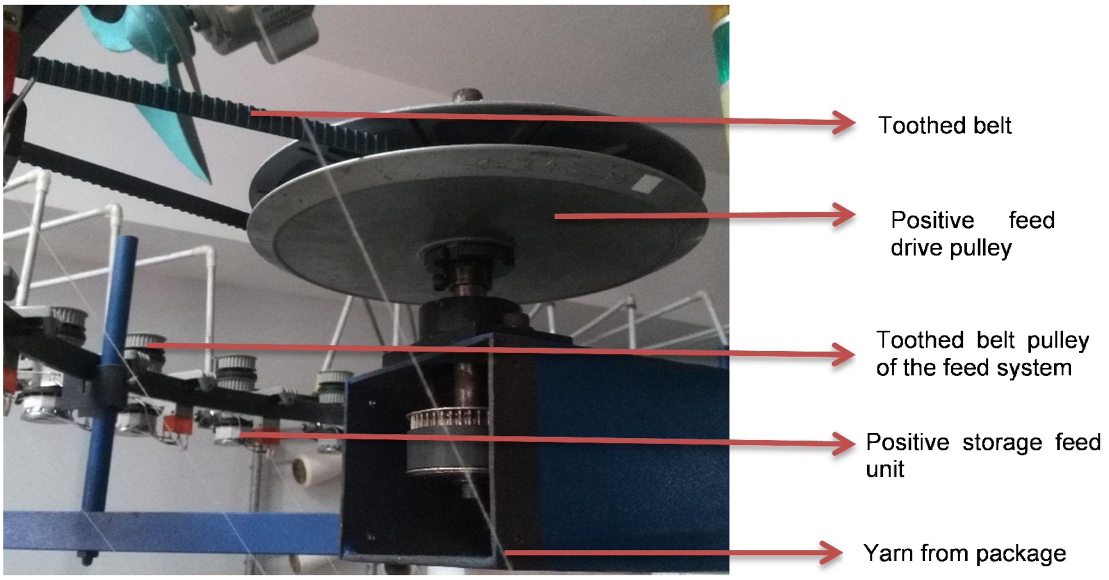

Figure 1 Drive pulley and toothed belt based positive storage feeding

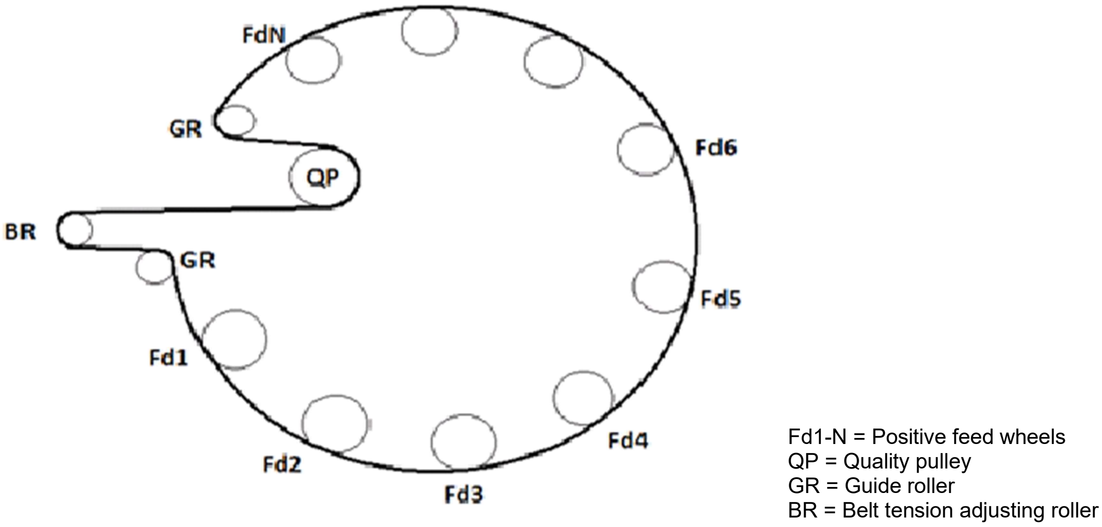

Figure 2 Schematic diagram of positive storage feed system [2]

A quality wheel, also known as Quality Adjustment Pulley (QAP) or Variable Diameter for Quality (VDQ) pulley, is illustrated in Figures 3-5. The quality wheel comprises of upper and lower plates with multiple movable segments between plates along with a lock nut to keep them in place. The upper plate includes a helical groove, while the lower plate includes radial grooves. The inner diameter of the quality pulley is adjustable to vary yarn feed rate. To increase the fabric areal density (e.g., Grams per Square Meter [GSM] or Ounces per Square Yard [oz/yd^2]), yarn supply is reduced by decreasing the inner diameter of the quality pulley through scrolled segments.

This results shorter stitches and hence denser fabric. In addition, couliering depth has to be reduced from cam box, to control high yarn tension caused by decreased yarn delivery. The couliering depth, that expresses the kinking of yarn into a needle loop and the subsequent knock-over of the old loop [3], can be controlled by adjusting the vertical position of the stitch cam to pull a longer or shorter loop. However, in case of positive feeding, the role of such adjustment is to bring tension balance on the feed yarn rather than controlling loop length.

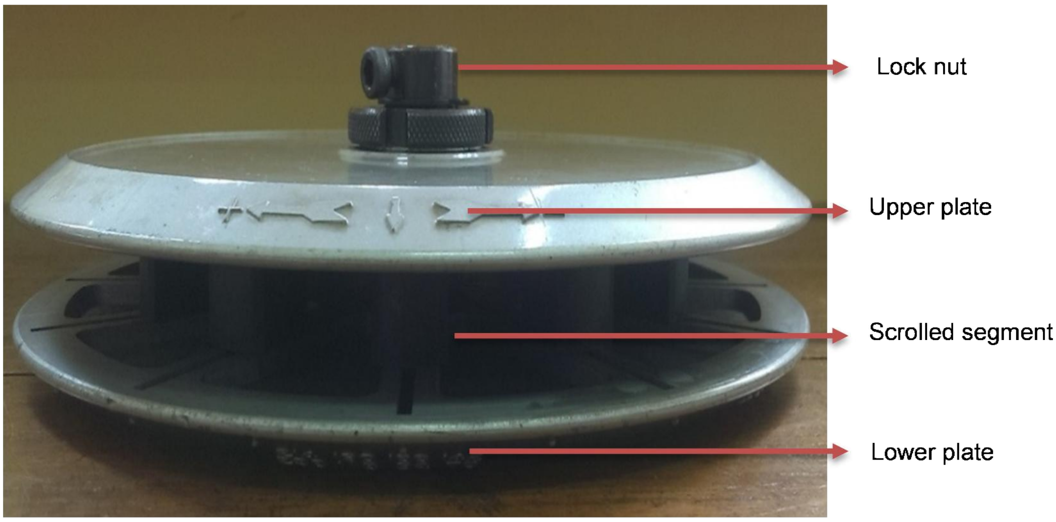

Figure 3 Quality Adjustment Pulley (QAP)

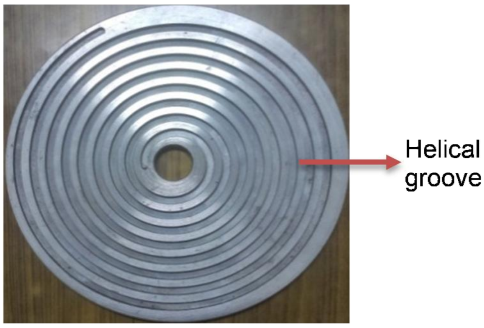

Figure 4 Inside view of upper plate of QAP

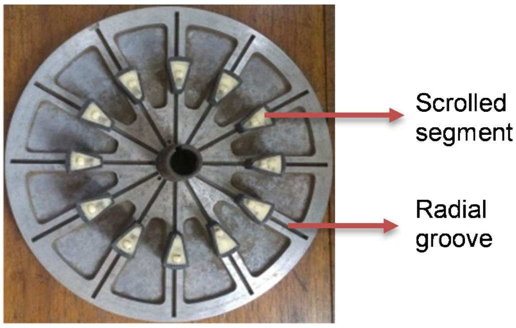

Figure 5 Inside view of lower plate of QAP

It is a common knowledge that the environment of a knitting floor is generally dusty with loose short fibers (i.e., lint), particularly when processing spun yarns. These dusty matters, sometimes known as fly, are sticky in nature, can be carried by the timing belt (Figure 6), even can be deposited and packed inside the grooves of toothed belt pulley. This fly accumulation eventually leads to slippage of toothed belt over toothed belt pulley, resulting poor control of positive feeding system. Moreover, such lint/fluff deposition may gradually grow inside the QAP (Figure 7), which apparently results a shift in pulley diameter and consequent variations in stitch length, even though the positive feed system operates at a fixed speed [4]. Furthermore, the increased belt tension due to the movement of belt over dust/lint deposited surface makes the belt prone to wear and tear and reduces its desired lifetime. Therefore, lint accumulation on yarn delivery system is quite warning and must be avoided to knit fabric with consistent quality.

Figure 6 A continuous QAP belt/timing belt [5]

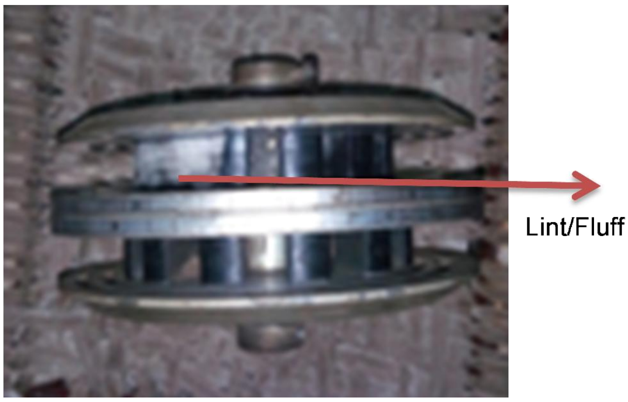

Figure 7 Fluff deposition inside QAP

Unfortunately, cleaning apparatus/methods for QAP system are quite rare till now and the effectiveness of the available one (a typical brush-based system) is questionable. While working in the knitting industry, the researchers observed and witnessed rapid deterioration of the cleaning performance of such brush-based devices. Eventually, it contributed to yarn tension and stitch variation and subsequent generation of two particular fabric faults, i.e. streakiness (Figure 8) and variation in fabric areal density. Both streakiness, i.e. narrow extended unintentional stripes [6], and variation in areal density throughout the fabric roll, would reduce the expected performance of the knitted fabric and could be a reason for customer dissatisfaction. Therefore, maintaining consistent yarn tension and stitch length throughout the knitting operation is imperative for the right quality of fabric. As a part of such effort, QAP belt cleaning system should be highly functional. Therefore, the purpose of this study is to develop a functionally better and cost-effective lint/fluff removal device for the QAP belt than the existing brush-based system. The system should resist the deposition of lint/fluff on the QAP system quite successfully.

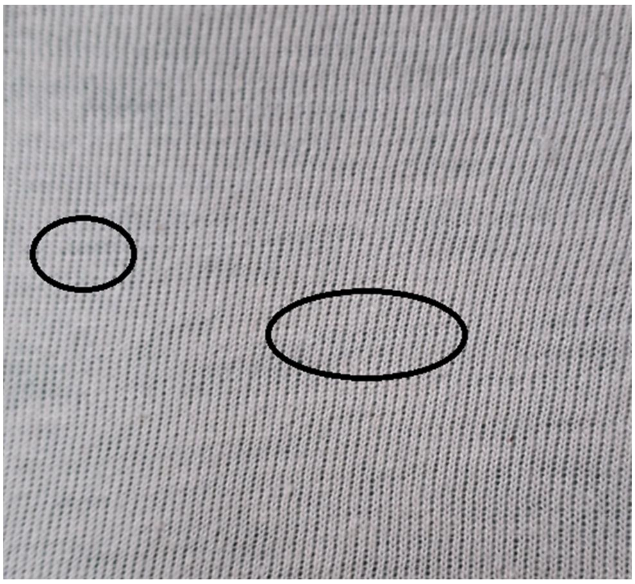

Figure 8 ‘Streak’ in grey cotton-knitted fabric

1.1 State of different cleaning systems for knitting machines

Numerous research works, mostly through patents, have been carried out over time to protect different parts of a knitting machine from environmental substances. Various dust/lint/fluff removing means (e.g., compressor and conduit, housings, fluid ejecting nozzle, air jet nozzle, filter, suction, blower, fan, airstream, etc.) were developed and are chronologically reviewed in this section.

Shortland’s invention comprised of a compressor and conduit to transmit compressed air at a relatively low pressure [7]. The compressor air directed to different machine parts to keep them clean from lint or fluff. Schmidt proposed housings in which the dust is raised and swirled up by an air steam and then, sucked off by a suction system [8]. The deposited dust is further collected in a dust bag or thrown away into the open air. The invention was based on the principle of raising the dust using a blower at the spot where it collects, followed by sucking the dust off through a suction fixture. This method claims the advantage of taking air from the blow tubes directly to relatively inaccessible spots without any damaging effects on the threads and stitch forming tools when the dust is moved from the spots.

Abrams and Tetrault showed a typical apparatus that was designed for blowing lint and other foreign objects away from the critical parts of the knitting machines with top creel arrangement [9]. Abrams, in another study, invented a lint removing device with fluid ejecting nozzles to prevent the accumulation of lint on the critical parts of the machine [10]. Nurk proposed a dust-collecting system for a circular knitting machine that has a needle cylinder and loop-forming instrumentalities which form loops along an annular loop-forming zone. A number of suction nozzles circles around the annular loop-forming zone to collect dust and fluff from the zone [11].

Yorisue and Morimoto invented a waste fiber removing device [12] with air jet nozzle which is flexible enough to impart a fluttering motion. The air jet nozzle is either stationary or rotating to prevent the accumulation of lint on various adjacent parts of the knitting machine. Rovinsky and Meszaros described a knitting machine attachment using pressure air that flow through a number of flutter tubes to control the accumulation of lint [13]. Each tube construction consists of an inner circular bore encircling elliptical wall which causes a flutter or pivotal traverse in a specified plan or path where lint is likely to accumulate.

Igarashi and Iida described a collector/remover of dust in knitting machine [14]. Fibers accumulated adjacent to the knitting zone and to yarn feeding devices of the knitting machine is blown to a filter next to the top of the machine. The lint is removed from the filter by a rotatable filter cleaner and then, is transported by suction to a vacuum device outside of the machine. In their (Igarashi and Iida) another research, an apparatus with suction/blowing attachment causes the fiber waste generated at the upper part of the knitting section moving upwardly through the suction duct associated with the suction-blowing segment [15]. Mutually spaced fiber waste collectors upon the knitting machine and on the creel of a knitting unit collect fiber waste, which is then withdrawn by a fiber waste remover. The waste remover is selectively connectable to different fiber waste collectors. Sensors can detect when the fiber waste collected by the collectors when the waste exceeds a predetermined amount.

An injection nozzle, invented by Izumi, is located on a rotating cylinder of a circular knitting machine to remove dust, lint and waste fibers as well as lubricating the knitting unit. The nozzle, located between the sinker cap and sinker cam, includes a tip opening located adjacent to the knitting unit. This nozzle also includes a receiving end located opposite to the tip opening. Mist-oil and air discharge at the tip opening of the injection nozzle for cleaning and lubricating the knitting unit [16]. Tsay showed a dust blower, mounted at the center of the circular knitting machine, to blow dust and fluff away from the annular loop forming zone. The dust blower includes a rigid guide tube and a swivel nozzle head. The rigid guide tube is connected to a compressed air source and rotates horizontally by a constant speed motion. The swivel nozzle head is mounted on one end of the rigid guide tube and rotates vertically when compressed air is driven out of its radial nozzles [17].

Baumann developed a fan-based cleaning system with a rotating arm, which is only suitable for the dimensions of circular knitting machine (not for flat-bed knitting machine) [18]. For double jersey circular knitting machine, Gutschmit explained some means for deterring lint and debris accumulation on the knitting elements [19]. According to his claim, the needle and dial slots can be significantly cleaned by enclosing an annular air chamber spanning between the cylinder and dial, and by delivering a pressurized air steam into the chamber. The air stream will blow lint, debris and contaminations away from the critical knitting elements (e.g. needles and sinkers) and prevent the accumulation of such materials within the cylinder and dial slots. Willmar, Sickinger and Berwald introduced a dust removal device which contains air distribution channels. These channels, configured in segments, are connected to a compressed air source via radial air supply channels [20].

From above discussion, it can be concluded that researchers and/or inventors used mainly two basic techniques- lint collecting and lint blowing means to control lint. Lint collecting technique was basically a lint suction system whereas lint blowing technique involved a system that applies jet of compressed air. Though some existing technologies (e.g., brush cleaning) incorporate the indirect way of keeping QAP away from dust via cleaning of QAP belt but, none of these previous studies mentioned any means of keeping QAP clean directly using compressed air. It is quite expected that an apparatus using pressured air flow will be able to obviate the accumulation of lint or fluff in any critical point of the knitting machine efficiently.

1.2 Traditional brush-based cleaning of QAP belt

Friction between yarn and various knitting machine's parts (e.g., yarn guide, feeder) with which the yarn comes into contact causes fibers breakage within the yarns. These broken as well as waste fibers are separated from the yarn and gets accumulated as lint or fluff in the contacted parts and adjacent areas of the machine. This fiber waste as well as other environmental dirt particles may also be attached on the toothed belt, carried away inside the QAP, and eventually accumulated over some scrolled segments. A significant amount of such elements (lint/dirt/fluff) deposited over the scrolled segments may create eccentricity increasing the circumference of the quality pulley. The increment of circumference leads to faster surface speed of the quality pulley and, subsequently increasing yarn delivery rate than the desired one. The periodic variation of yarn delivery rate due to the build-up eccentricity in QAP may also result fluctuation in yarn input tension and thereby, making the yarn delivery process unstable. A portion of the generated waste fiber during the knitting process may be collected on the grooves of some QAP belt pulleys through the belt, resulting faulty positive feeding through feed units. To overcome such problems, some knitting machines are provided with a typical brush-based cleaning apparatus (Figure 9) for the QAP system. As shown in figure 9, two rotating brushes attached in a brush-self are used to clean both sides of the QAP belt. Being surface driven by the moving QAP belt, the brushes remove fly or dirt from the belt.

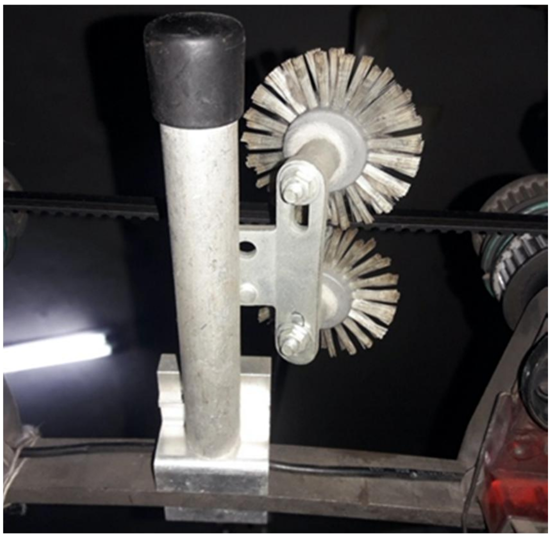

Figure 9 Single brush-shelf for circular knitting machine

1.3 Significance of the study

The typical brush-based cleaning apparatus for QAP system has some practical limitations. Firstly, the brushes are highly prone to wear on bristle side due to friction with moving belt. Secondly, the brushes get clogged frequently with dust//lint during operational hours and need frequent attention from the knitting machine operator.

Furthermore, the frequent manual handling of this cleaning aid might not fit ergonomically for all operators particularly those having comparatively shorter physical postures. Therefore, a need for an alternative cleaning apparatus is quite justified. On basis of previous studies, it may be assumed that a compressed air-based cleaning system would overcome the existing limitations of brush-based cleaning as well as show better cleaning performance. Therefore, the purposes of this study are i) to develop a compressed air-based cleaning system, and ii) to compare the cleaning performance and operating cost between brushed and air-based cleaning systems.

2 MATERIALS AND METHODS

2.1 Constructional elements

To develop a prototype compressed air-based cleaning apparatus, cheap and available material components have been used. Soft flexible plastic pipes with roller clamps have been used as conduit means. Polyvinyl Chloride (PVC) based board and channels have been utilized for housing. Hard plastic fittings like Tees and Elbows together with metal screws were used as joining aids. The device is developed in such a way that it can be mounted on the feed-units holder ring conveniently.

2.2 Constructional method

A sketch of the desired prototype device is shown in Figure 10. The width and total thickness the QAP toothed belt (not mentioned in the sketch) that would undergo cleaning, were considered as 10 mm and 3 mm respectively following the toothed belt dimensions of the renowned Memminger-IRO drive systems [5].

As in Figure 10, a base plate (1) is attached to a shaft (2) by screw (3a, 3b) to hold the entire device. An upper base plate (4) is attached by screw (5a, 5b) above the first base plate (1) for reinforcement purpose. These base plates (1, 4) are made of PVC composite board. A tee (6) is placed in the center of the upper base plate (4) to join pipe-segments (7, 8). With the pipe-segments (7, 8), two 90° elbows (9, 10) are attached. Another two PVC pipe-segments (11, 12) were attached with other ends of the elbows (9, 10). Two tees (13, 14) were joined on both open ends of the PVC pipe-segments (11, 12). At the top openings of the tees (13, 14), another two pipe-segments of PVC pipes (15, 16) were attached. On the other end of these PVC pipe-segments (15, 16), two elbows (17, 18) were attached. Air nozzles (19, 20) attached with flow tubes (21, 22) were incorporated with the side openings of tees (13, 14). Other air nozzles (23, 24) attached with flow tubes (25, 26) were incorporated with the openings of elbows (17, 18). The tubes (21, 22, 25, 26) act as conduit means and are connected to the air distributor of the machine. A roller clamp (not shown in the diagram) was used with each flow tube (21, 22, 25 and 26) to regulate the rate of air flow.

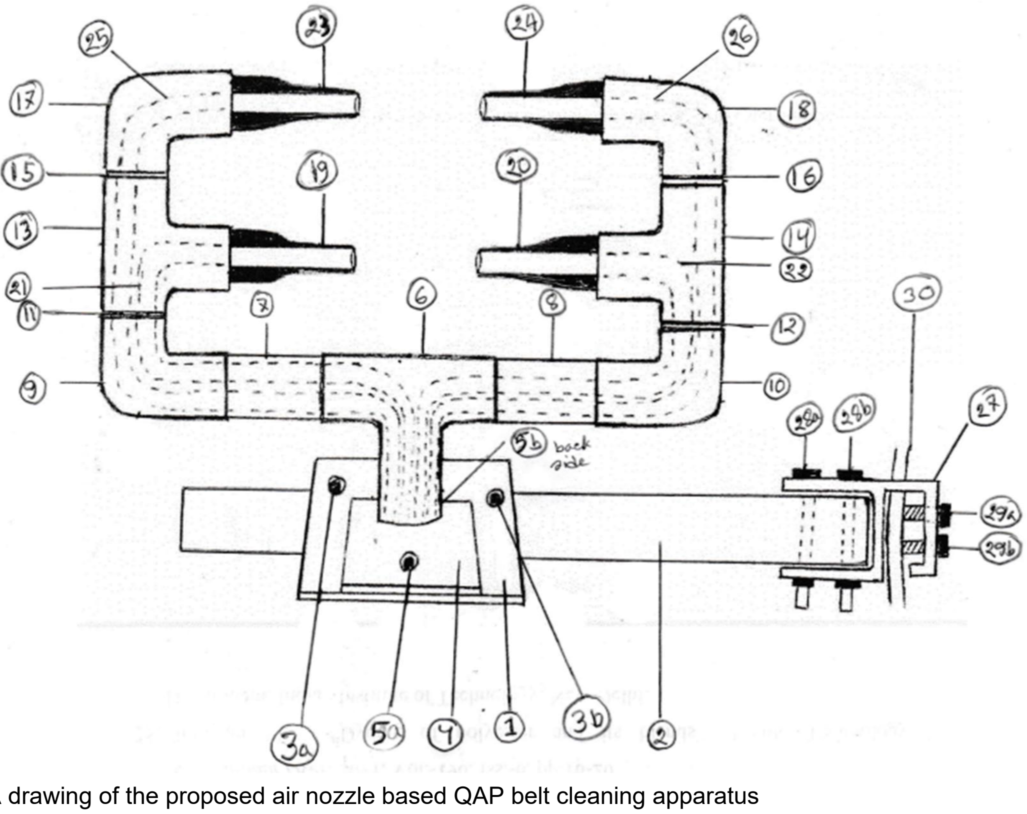

Figure 10 A drawing of the proposed air nozzle based QAP belt cleaning apparatus

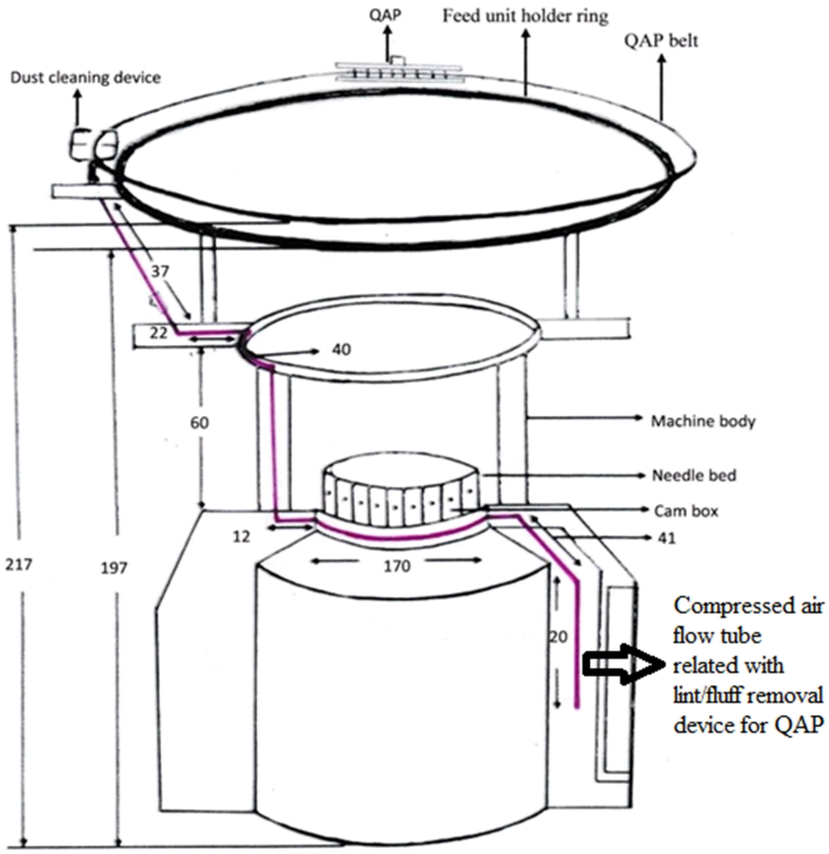

Figure 11 Proposed attachment of a compressed air-based lint removal device on a circular knitting machine with QAP based positive feed system (all measurements are taken in centimeters)

Typical diameters of PVC pipe-segments and nozzles are around 12.50 mm and 5 mm respectively. The distance between two face-to-face nozzles was kept at 23 mm so that the belt remains 10 mm away from any corresponding nozzle. This gap of 10 mm has been chosen according to the commonly practiced setting of lint blower (needle to air nozzle end) found through the periphery of needle cylinder of an industrial circular knitting machine. Based on the study by Torlach (1999), the compressed air pressure was maintained at around 210 KPa (around 2 bar) through air regulator unit [21]. It is because the air jets directed to the belt passing between face-to-face nozzles are strong enough to blow away attached lint without any damaging effect to belt or making any deviation to the belt's running condition. The position of whole base plate (1) can be adjusted somewhat by tuning the position of screws (3a, 3b). The shaft (2) is joined with feed unit holder ring (30) through a gripper (27). The gripper (27) is fixed with the shaft (2) by screws (28a, 28b). Two other screws (29a, 29b) are set at other side of the gripper (27). These screws (29a, 29b) are used for firm fitting of the gripper with the ring (30). A typical diagrammatic set-up for this device on a circular knitting machine (Orizio-Johnan, E 24) is shown on Figure 11.

3 RESULTS AND DISCUSSION

3.1 Installation of the device

An image of the developed prototype apparatus is shown in Figure 12. The device was first installed on a circular knitting machine in a lab setting for a trial run (Figure 13).

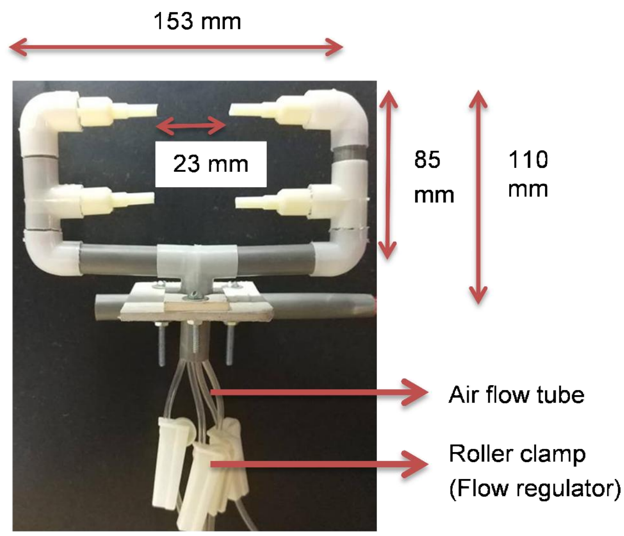

Figure 12 An image of the developed lint removal device for the QAP belt

Figure 13 The newly developed lint removal device attached to a knitting machine

3.2 Comparative cleaning performance between brush-based cleaning system and compressed air-based cleaning system

A comparative measurement of cleaning performances between brush-based cleaning system and compressed air-based cleaning system on the basis of dirt/fluff deposition over the scrolled segments inside QAP was carried out in an industrial environment. A circular knitting machine from a renowned knitting mill in Bangladesh was used for the intended purpose. In order to compare the cleaning performances, both the brush-based and compressed air-based cleaning devices were attached individually with same knitting machine [24 gauge, 34-inch (86.36 cm) diameter, 2556 needles, and 102 feeders] to produce the same single jersey structure fabric. Same yarn [60/40 cotton/viscose, 30/1 Ne (19.68 Tex)], same stitch length (2.72 mm) and other identical knitting parameters were maintained throughout the production hours consistently. Before attaching each of these cleaning devices, the scrolled segments inside QAP were cleaned properly, so that no dust/fluff can be pre-existed. Related data was collected for two consecutive days so that any significant change in room atmospheric condition and its effect on lint accumulation could be avoided.

For the brush-based cleaning device on day one for 24 hours (between 2 PM to 2 PM) duration, total actual production, total mass of dirt/fluff collected over the scrolled segments inside QAP, and mass of dirt/fluff collected over the scrolled segments inside QAP for 1 kg production of knitted fabric were 312.50 kg, 0.0818 gm and 0.00026 gm/kg respectively. Similarly, these outcomes for the compressed air-based device were 323 kg, 0.0601 gm and 0.00019 gm/kg respectively. Around 29 percent of less dust deposition was observed over the scrolled segments inside QAP due to installation of compressed air-based cleaning device instead of brush-based cleaning device. The outcomes of this study support better cleaning performance of compressed-air based device than that of the brush-based cleaning device. It is expected that the performance will be improved exponentially over a longer duration as less dirt/fluff deposition facilitates lesser further dirt/fluff deposition inside the QAP. Table 1 summarizes the comparative measurement of cleaning performances.

Since the compressed air-based cleaning apparatus is contactless to the QAP belt, any friction induced damage is impossible. Hence, frequent cleaning of QAP is not needed rather operator has to be aware of any leakage of compressed air. On the other hand, the belt, particularly the brushes are highly prone to wear on bristle side due to continuous friction between moving belt and brushes in the brush-based cleaning system. Frequent cleaning of brushes is required as dust collected by the brush causes jamming inside bristles resulting reduced cleaning efficiency.

Table 1 Comparative cleaning performances between traditional brush-based cleaning device and the developed compressed air-based cleaning device

Particulars obtained for Brush-based cleaning device	Particulars obtained for Compressed air-based device	Cleaning performances differences	Finding
*Production date and time =23/12/18 to 24/12/18 (2pm to 2 pm) *Avg. temp. = 25.5°C and R.H. 55% (approx.) respectively *Actual production=312.5 kg *Mass of lint/ fluff collected over the scrolled segments inside QAP during the production hours = 0.0818 gm *Mass of dirt/fluff collected over the scrolled segments inside QAP for 1 kg production of knitted fabric = 0.00026176 gm	*Production date and time =24/12/18 to 25/12/18 (2pm to 2 pm) * Avg. temp. = 25°C and R.H. 56% (approx.) respectively * Actual production=323 kg *Mass of lint/fluff collected over the scrolled segments inside QAP during the production hours =0.0601 gm *Mass of dirt/fluff collected over the scrolled segments inside QAP for 1 kg production of knitted fabric = 0.000186068 gm	0.0000757 gm less lint/fluff deposition inside QAP for 1 kg production of knitted fabric by the compressed air-based cleaning device over the selected time period of 24 hours	Due to installation of Compressed air-based cleaning device instead of brush-based cleaning device around 29 % less dust deposition was observed over the scrolled segments inside QAP

Most importantly, this frequent cleaning is not ergonomically feasible for workers, specifically of Bangladesh origin. The average height of Bangladeshi male is around 167.7 cm [22] and female is around 150.6 cm [23], whereas the brush-shelf/feed unit holder ring of a large diameter circular knitting machine is located more than 180 cm (like in Orizio-Johnan machine) above the ground.

3.3 Comparative cost analysis

To determine the feasibility of this study, a comparative cost analysis between traditional brush-based cleaning system and compressed air-based cleaning system has been conducted. After the successful trial run in lab setting, the developed device was attached to a knitting machine of a renowned knitting mill in Bangladesh to gather industry scale data. Therefore, all cost relevant to this experiment was calculated in a local currency (BDT), which then can be converted to USD (USD 1 = BDT 85 approximately) or EUR (EUR 1 = BDT 95 approximately).

<u>Operating cost</u>

The cost of compressed air consumed by the developed device was determined based on per unit cost of compressed air. The cost/m^3 of compressed air (at 10 bar) was calculated as BDT 0.67 using (1) (based on 100 percent compressor motor efficiency, 55 KW motor capacity, electricity cost of 8.15 BDT/kWh, 80 percent of operating hours running as fully loaded state, and volume of generated compressed air at 10 bar = 9.51 m^3/min).

The cost of compressed air per nozzle per year consumed by the developed device was calculated as BDT 1,305 using (2) (considering average knitting machine running time = 21 hours/day indicating the efficiency of 87.5 percent, yearly working days = 298 [excluding common official holidays of Bangladesh], distance between air nozzle to belt = 10 mm [indicating the common distance maintained for cleaning of knitting elements through compressed air jet], diameter of air nozzle = 5 mm, and average velocity of compressed air ejected from the nozzle, V = 22 m/s [measured by an anemometer, as shown in Table 2]).

From further calculation, it can be estimated that the developed device with four nozzles (applicable for a two QAP-based yarn delivery system) can cost BDT 5,250 and share about 0.19% of total cost need to generate compressed air by the compressor. On the other hand, cost evaluation for brush-based apparatus was done mainly based on the information provided by the authorized local agent of Memminger-IRO, the manufacturing company of this particular device. Four pieces of brush are required for a two QAP-based positive feed system, and the expected lifetime of each brush is one year, according to the supplier's warranty. As in this cleaning system, only brushes are required to be replaced when damaged/consumed, yearly cost for such system with four brushes stands at BDT 5,600 (price/brush = BDT 1,400). Therefore, annual cost for the developed device (i.e., BDT 5250 or USD 61.76) is 6.25% less than that (i.e. BDT 5,600 or USD 65.88) of the traditional brush-based cleaning device.

<u>Device price</u>

The asking price of a typical brush-based cleaning system (entire brush-self system with four brushes) was BDT 15,000 or USD 176.47(according to the supplier's invoice). On the other hand, the manufacturing price for the developed device was around BDT 1,650 or USD 19.41 (including parts and BDT 1,000 labor charge). As the device was built on prototype basis, the manufacturing components were purchased locally and hence, the reason for low cost. However, it was not evaluated in commercial scale as well as selling price is not considered in this study. Nonetheless, it is expected that the developed system will still be cheaper in price when it will compete with the brush-based apparatus through the same platform.

$$\text{Compressed air cost in BDT} = \frac{hp\ x\ 0.746\ x\ operating\ hours\ x\ \frac{BDT}{kWh}\ x\ (time\ \%)\ x\ (full\ load\ hp\ \%)}{Motor\ efficiency} \tag{1}$$

$$\text{Compressed air consumption per nozzle per year } = V\pi\left(\frac{d}{2}\right)^2 \times 60 \times 60 \times 21 \times 298\ m^3 \tag{2}$$

Table 2 Determination of the rate of air flow that will be ejected from a nozzle of the developed device

Reference position (distance)	Machine	Compressed air pressure [bar]	Air flow rate [m/s]	Average air flow rate [m/s]	Standard deviation
Needle to compressed air ejecting nozzle - end (10 mm)	Orizio-Johnan E 24	2	22.1	22	0.492161
			21.7		
			22.2		
			20.9		
			22.8		
			21.9		
			22.1		
			21.8		
			22.3		
			22.2		

4 CONCLUSION

An extensive root-cause analysis is carried out (as an extended part of this study) primarily for all recognized circular weft knitted fabric defects (e.g., hole, stain, press-off, snag, gout, miss knit, barrè, etc.). Two particular flaws/faults– areal density variation and streakiness have been isolated and scientifically investigated to consider the scope of rectifying them. The purpose of this study lies on conducting a machine modification to minimize the propensity of these two faults, whose root causes are directly related with lint accumulation in the drive wheel and belt based positive feed system of circular knitting machine. Therefore, a new lint removal device using compressed air for the cleaning of QAP belt, has been developed.

Based on the outcome of this study, the developed compressed air-based cleaning system for QAP belt is an excellent alternative to the currently available brush-based cleaning system. The prototype device developed in this study is cheaper, easy to install and operate, and entirely free from the risk of mechanical friction. It does not need any additional supporting system as the air distributor is already available in the machine as an integral part of it. Moreover, using this compressed-air based system eliminates the physical limitation of Bangladeshi circular knitting machine operators or people with short stature while setting up and changing brushed shelf cleaning system. Apart from better cleaning performance, the calculated operating cost of the compressed air-based cleaning system seems to be cheaper if the device is used as a replacement of brush-based cleaning apparatus for QAP belt. Finally, the developed device has been proven effective, convenient and economically feasible along with achieving better cleaning performance. Therefore, it is superior to the traditional device of its type and highly recommended for installation in circular knitting machines having positive feed drives. However, while working with such compressed air-based lint removal system, there is a higher possibility of the removed fiber to be settled upon nearby yarn or machine components. The venti-cleaners of the machine, more specifically the top one, should operate properly during knitting to overcome this.

4.1 Limitations of this study

The findings of this study have to be seen in light of some limitations. Firstly, there is a paucity of research available on the performance of brush-based clean system for the circular knitting machine. Secondly, a reliable source for some compressor related information (e.g., motor efficiency, compressor loading, and unloading duration) was unavailable to the particular knitting mill used in this study. This information was collected from the maintenance department without cross verification, which may lead to some erroneous judgement while calculating the cost of generated compressed air. However, it can be realized that these limitations are not so potential to hamper the research outcome significantly.

5 REFERENCES

1. Earl D., Earl W.D.: U.S. Patent No. 6151925, 2000
2. Dias T., Lanarolle G.: Stitch length variation in circular knitting machines due to yarn winding tension variation in the storage yarn feed wheel, Textile Research Journal 72(11), 2002, pp. 997-1001, https://doi.org/10.1177/004051750207201111
3. Spencer D.J.: Knitting Technology: A Comprehensive Handbook and Practical Guide, Woodhead Publishing, 2001, ISBN: 9781855733336
4. Assorted accessories for fabric quality improvement on fine gauge machines, The Indian Textile Journal 2010, accessed on 18 Mar. 2020, https://indiantextilejournal.com/articles/FAdetails.asp?id=2981
5. Memminger-Iro Gmbh. (n.d.): Drive Systems: TOOTHED BELTS, accessed on 18 Mar. 2020, https://www.memminger-iro.de/en/antriebssysteme/toothed_belt.php
6. American Society for Testing and Materials: ASTM D3990-12 (2016): Standard terminology relating to fabric defects, ASTM International, USA, 2016
7. Shortland A.: U.S. Patent No. 2846860, 1958
8. Schmidt R.: U.S. Patent No. 3220223, 1965
9. Abrams A., Tetrault R.L.: U.S. Patent No. 3269151, 1966
10. Abrams A.: U.S. Patent No. 3422640, 1969
11. Nurk S.: U.S. Patent No. 4312195, 1982
12. Yorisue S., Morimoto S.: U.S. Patent No. 4691536, 1987
13. Rovinsky W., Meszaros S.: U.S. Patent No. 4869080, 1989
14. Igarashi Y., Iida K.: U.S. Patent No. 5177985, 1993
15. Igarashi Y., Iida K.: U.S. Patent No. 5437732, 1995
16. Izumi T.: U.S. Patent No. 5388431, 1995
17. Tsay J.T.: U.S. Patent No. 5509281, 1996
18. Baumann J.: U.S. Patent No. 5680672, 1997
19. Gutschmit A.: U.S. Patent No. 5737942, 1998
20. Willmer R., Sickinger R., Berwald K.: U.S. Patent No. 7043941, 2006
21. Torlach J.M.: Safety Bulletin No. 49: Use of compressed air for cleaning purposes, Department of Mines, Industry Regulation and Safety, Government of Western Australia, 1999, https://www.dmp.wa.gov.au/Documents/Safety/MSH_SB_049.pdf
22. Khadem M.M., Islam M.A.: Development of anthropometric data for Bangladeshi male population, International Journal of Industrial Ergonomics 44(3), 2014, pp. 407-412, https://doi.org/10.1016/j.ergon.2014.01.007
23. Subramanian S.V., Özaltin E., Finlay J.E.: Height of nations: a socioeconomic analysis of cohort differences and patterns among women in 54 low-to middle-income countries, PLoS One 6(4), 2011, e18962, https://doi.org/10.1371/journal.pone.0018962

THE EFFECT OF DRAWING TEMPERATURE ON THE MECHANICAL PROPERTIES OF PLA FIBRES

Marcela Hricova, Erika Obertova and Anna Ujhelyiova

Slovak University of Technology in Bratislava, Faculty of Chemical and Food Technology, Department of Plastics, Rubber and Fibres, Radlinskeho 9, 812 37 Bratislava, Slovak Republic
marcela.hricova@stuba.sk

Abstract: *Polylactic acid (PLA) is one of the possible usable polymers that have the assumption to replace synthetic materials. Fibres made from PLA still do not achieve the properties of fibres made from synthetic polymers, and therefore the effort is to modify the production process of PLA fibres by additions of various additives. The aim of this work was to prepare the biodegradable fibres from PLA and to evaluate the influence of the preparation conditions on their mechanical properties. The special additives were added to the polymer mass to achieve better processability as well as better mechanical properties (tenacity and elongation at break) of PLA fibres. All prepared fibres were drawn at maximum drawing ratio λ_{max} at the drawing temperature 80; 90; 100 and 105°C. The effect of additives and the drawing temperature on the mechanical properties of the prepared PLA fibres was evaluated and discussed.*

Keywords: *Polylactic acid, biodegradable fibres, additives, mechanical properties.*

1 INTRODUCTION

People have been using polymers for thousands of years. In ancient times was used natural plant gum, later were using plant-derived polymers, and about since 1495 the natural rubber was known. The first synthetic polymer (Bakelite) was invented by Leo Hendrik Baekeland in 1907 [1]. The invention of catalytic polymerization has significantly contributed to the rapid development of polymer technology in the last decades of the 20th century. Because common polymers (PE, PP, PS, ...) are very cheap and have a wide range of uses, environment contamination with polymers has become a serious worldwide problem. Synthetic polymers take hundreds years to completely degrade to harmless soil components. This, together with the reduction of oil resources, is forcing to orient the research to field of renewable materials as well as biodegradable polymers.

The first step in solving the problems with plastic waste was mixtures of polymeric biomass, which had better degradability compared to conventional plastics. The second step is biodegradable polymers which can be divided into two categories 1) petroleum-derived and 2) microorganism-derived [2]. Biodegradable polymers can be defined as polymers that decompose into low-molecular products by the action of microorganisms and their enzymes. By combining the production of polymers from renewable sources and biodegradability, the possibility of extending the lifecycle of plastic products has emerged [3]. Most biodegradable polymers are in the polyesters group. Polylactic acid (PLA) is a biodegradable polymer, which has been receiving a lot of attention lately. PLA is made from lactic acid. Monomer - lactic acid can be produced by fermentation or chemical synthesis from carbohydrates. Fermentation of carbohydrates from agricultural crops such as sugar cane, potato and corn is more preferred [4, 5]. Polylactic acid (PLA) was discovered in the early 19th century by Pelouze. The first PLA companies began to emerge in the 1990s [1]. PLA is the first melt-processable natural-based fibre which can be derived from 100% renewable resources [5, 6]. The environmental benefit of PLA is determined by its applications. PLA can be processed using conventional processing technologies used for thermoplastic polymers. From PLA can be formed transparent foils, fibres, or bottles (by injection into bottle preforms), etc. PLA has also excellent organoleptic properties and it is excellent for contact with food and packaging applications [7]. As PLA is the largest produced biodegradable polymer in the world and attains a reasonable price, many food industries, particularly those involving single-use applications like food packaging, utilize PLA as a food packaging material. PLA is a suitable substitute for existing petrochemical polymers for the fabrication of cups, containers, and packaging. At the spinning of PLA, the conditions and the way in which this process is carried out are very important. PLA fibres have been manufactured using both solution-spinning and melt-spinning methods [8, 9]. During the spinning from melt, the degradation of such material is greater than during the spinning from solution, and the molecular weight decrease correlates with the decrease in strength. By using of processing technology from melt, the two types of fibres (mono and multifilaments) can be produced. Fibres made from PLA do not achieve the properties of fibres made from synthetic polymers (PP, PA, PET), and therefore, there is the attempt to modify not only the production process of PLA fibres but also the polymer mass, for example by the addition of various additives like fillers, plasticizers, pigments, nucleation agents, etc [10, 3].

This work was focused on the preparation of polylactic acid (PLA) fibres and modified PLA fibres with content of various additives. The influence of processing conditions and additives on mechanical properties (tenacity and elongation at break) of prepared PLA fibres was evaluated.

2 EXPERIMENTAL PART

2.1 Materials used

These materials were used in the experimental work:

Polylactid acid (PLA)

Additive 1 (A)

Additive 2 with lower concentration (B1) and additive 2 with higher concentration (B2)

2.2 Fibres preparation

PLA concentrates with final concentration of additives were prepared using LabTech extruder with diameter 28 mm (L/D = 40) at 190°C. Before spinning, PLA granulates were dried in a laboratory oven for 3 hours at temperature 80°C. PLA fibres and modified PLA fibres were prepared using a laboratory spinning plant at temperature 190°C with the take-up speed 150 $m.min^{-1}$. Fibres were drawn using a laboratory drawing machine at maximal draw ratios λ_{max} at drawing temperatures 80; 90; 100 and 105°C. The list and composition of fibres are presented in Table 1.

2.3 Method used

The Instron (Type 3343) was used for the measurements of the mechanical properties (tenacity and elongation at break) of fibres (according to ISO 2062:1993), evaluated from 15 measurements. The initial length of fibres was 125 mm and the time of deformation was about 20 sec.

3 RESULTS AND DISCUSSION

PLA fibres and modified PLA fibres with content of additives were prepared. The influence of drawing temperature and additives on mechanical properties of PLA fibres was investigated. With regard to the high sensitivity of polylactic acid on thermal degradation, the effect of real-time aging (during 90 days) on mechanical properties of prepared fibres was evaluated.

As we can see from the measured values in Table 1 and from the graphical dependence on Figure 1a, the tenacity of undrawn PLA fibres without the additives has a decreasing tendency depending on the aging time. The highest value of tenacity was measured after 14 days from the preparation of the fibres. The tenacity of PLA/A fibres increases slightly with increasing number of days. PLA fibres with the content of additive B also show similar dependences. The highest values of the tenacity of the undrawn modified PLA fibres were reached 90 days after spinning of fibres. In general, all undrawn PLA fibres containing additives showed lower tenacity than pure PLA fibre.

The addition of additives to the mass of PLA fibres caused an increase of the elongation at break for all modified fibres compared to pure PLA fibre (Table 1 and Figure 1b). The fibres containing the additive A show the highest values of elongation at break. The addition of additive B slightly reduces the elongation of the undrawn fibres, but these values are still higher than for pure PLA fibres.

Elongation at break for undrawn pure PLA fibres reached the lowest value after 90 days and the highest value after 21 days from fibre preparation. In general, modified PLA fibres show a decrease in elongation at break with on dependence on aging time. The exception is the elongation value 21 days after preparation, which is higher and comparable to the value immediately after fibre preparation and occurs for all PLA fibres with content of additives. The lowest values of elongation at break for these fibres were measured 90 days after fibre preparation (Figure 1b).

Table 1 Tenacity σ and elongation at break ε of **undrawn** PLA fibres measured during 90 days from spinning

No.	composition of fibres	σ [cN/tex]					ε [%]				
		*1 d**	*14 d*	*21 d*	*60 d*	*90 d*	*1 d*	*14 d*	*21 d*	*60 d*	*90 d*
1	PLA	6.7	7.3	6.6	6.4	5.6	181	164	189	166	142
2	PLA/A	5.1	5.4	5.3	5.5	5.8	240	223	240	214	202
3	PLA/A/B1	4.6	4.9	4.8	5.3	5.6	221	201	211	188	177
4	PLA/A/B2	5.1	5.3	4.8	5.3	5.8	230	219	224	197	181

*d – the number of days from spinning when the mechanical properties of the PLA fibres were measured

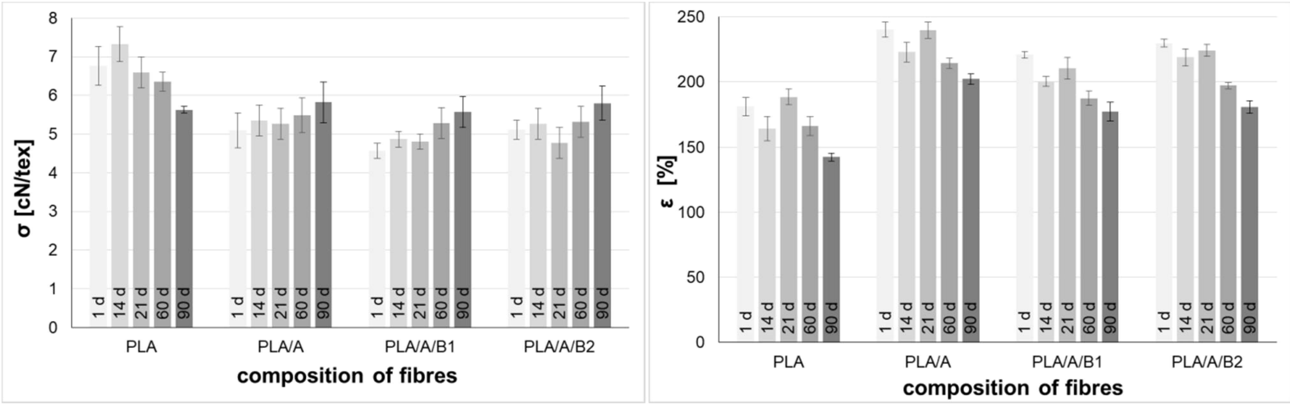

a) b)

Figure 1 Tenacity (a) and elongation at break (b) of **undrawn** PLA and modified PLA fibres

Table 2 Tenacity σ and elongation at break ε of **drawn** PLA fibres measured during 90 days from spinning

composition of fibres	drawing temperature [°C]	drawing ration λ_{max}	σ [cN/tex] 1 d*	14 d	21 d	60 d	90 d	ε [%] 1 d	14 d	21 d	60 d	90 d
PLA	80	2.0	16.3	15.9	15.6	17.5	16.3	65	60	65	55	60
PLA/A		2.7	15.0	17.1	16.9	17.2	17.0	60	71	53	52	71
PLA/A/B1		2.5	17.0	18.2	17.5	18.3	17.8	58	63	58	55	63
PLA/A/B2		2.6	18.0	19.9	17.8	18.9	18.1	52	57	61	47	50
PLA	90	2.4	21.1	20.0	21.4	22.2	23.3	64	41	41	37	44
PLA/A		3.2	18.5	21.4	21.3	23.1	22.8	49	43	43	36	37
PLA/A/B1		3.0	18.4	22.9	20.3	21.5	22.1	45	44	47	41	39
PLA/A/B2		3.0	20.2	19.8	19.0	21.8	21.9	46	45	57	37	49
PLA	100	2.7	23.8	23.4	24.9	23.8	23.4	40	32	35	37	31
PLA/A		3.5	23.1	24.1	23.1	25.2	23.7	36	35	42	38	31
PLA/A/B1		3.4	22.9	22.5	21.9	22.5	23.1	38	36	35	31	28
PLA/A/B2		3.5	20.2	23.4	22.9	24.4	25.9	33	38	38	32	37
PLA	105	3.0	25.4	25.2	25.8	25.4	26.4	32	26	26	26	26
PLA/A		3.5	19.7	22.3	23.0	24.8	24.3	36	38	36	40	41
PLA/A/B1		3.6	20.5	24.8	24.4	23.6	25.7	35	33	32	31	29
PLA/A/B2		3.3	19.4	23.3	24.7	24.7	24.1	36	41	36	37	35

Pure PLA fibres as well as modified PLA fibres were drawn after spinning to the maximum drawing ratio at different temperatures in the range of 80-105°C. The influence of fibre composition as well as the conditions of their preparation, specifically drawing temperature, on the mechanical properties of PLA fibres was studied. At the same time, the effect of aging time on these fibres during three months after fibre preparation was monitored. The measured values of tenacity and elongation at break of drawn fibres are given in Table 2 and showed on Figures 2-5.

In the case of drawn PLA fibres, the influence of the drawing temperature dominates over the influence of the content of additives in the fibres. The effect of fibre's composition varies depending on the specific drawing temperature.

At the lowest drawing temperature 80°C, the effect of the fibre composition is clear, additives improve the tenacity of PLA fibres. The higher the additive content, the higher the fibres' tenacity (Figure 2).

At higher drawing temperatures (90-105°C) the unambiguous influence of the additives is lost and the tenacity values of pure as well as modified PLA fibres are similar within the measurement error (Figures 2a, 2b).

The drawing temperature is a very important factor influencing the mechanical properties of the drawn PLA fibres. From the graphical dependencies on the Figure 3, we can see that with increasing drawing temperature, the tenacity of the fibres increases. This is the case for pure PLA fibres as well as modified PLA fibres with additives.

The highest tenacity value of pure PLA fibres (26.4 cN/tex) was measured at drawing temperature of 105°C, 90 days after fibre preparation (Figure 3b).

The tenacity of PLA/A fibres reached the highest values at the drawing temperature of 100°C during the whole measurement period, while the largest increase in tenacity for PLA/A fibres was recorded 60 days after spinning (25.2 cN/tex).

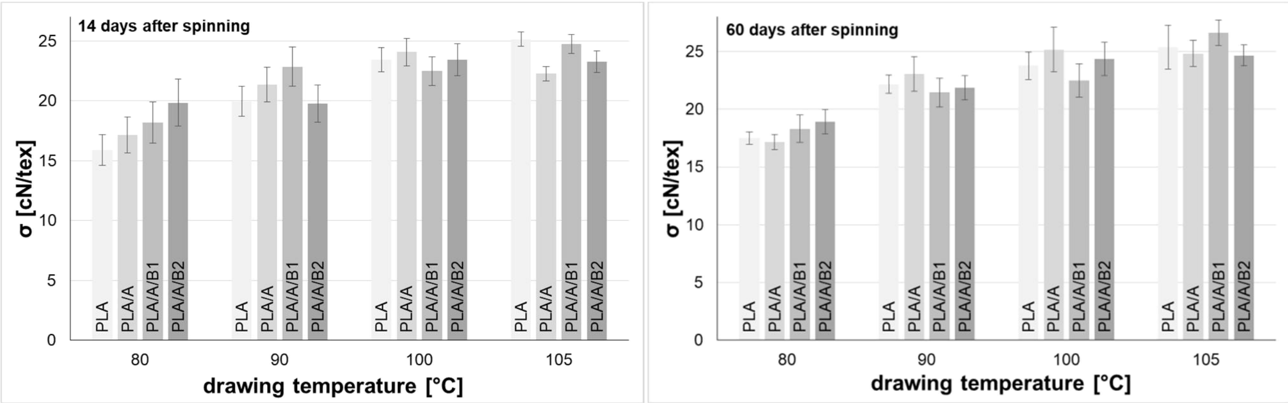

a) b)

Figure 2 Tenacity of PLA and modified PLA fibres in dependence of various drawing temperature, measured a) 14 days and b) 60 days after spinning

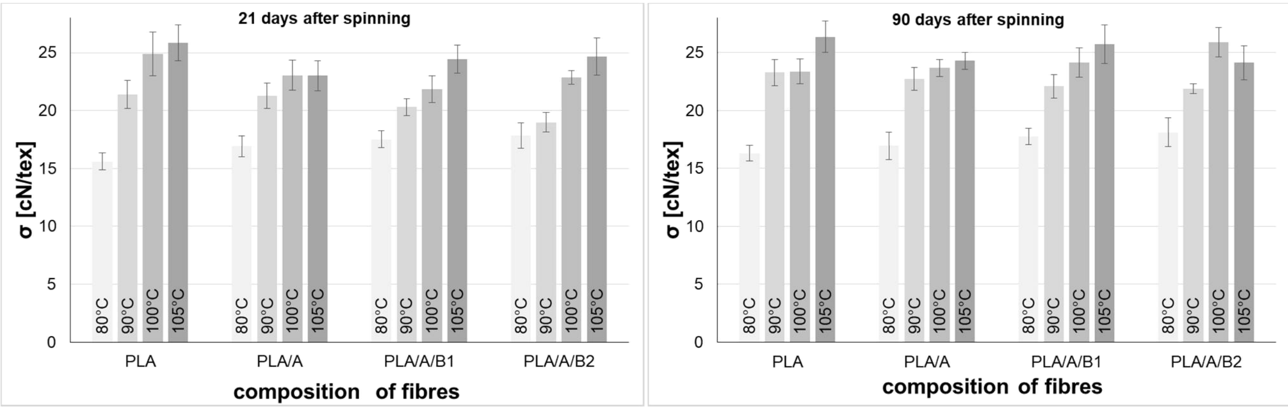

a) b)

Figure 3 Tenacity in dependence of composition of PLA and modified PLA fibres, measured a) 21 days and b) 90 days after spinning

Fibres with a lower content of additive B generally show the best tenacity at drawing temperature of 105°C. The highest tenacity values were measured after 14 days (24.8 cN/tex) and 90 days (25.7 cN/tex) from fibre preparation. The tenacity of fibres with a higher concentration of additive B also increase with increasing drawing temperature and reach the highest value at 100°C after 90 days (25.9 cN/tex) and at 105°C after 21 days (24.7 cN/tex).

From the evaluation of these measurements, we cannot accurately determine one specific drawing temperature for all types of fibres, but based on the results, we can state that to achieve higher tenacity, PLA fibres must be drawn at a higher temperature 100-105°C.

During the whole period (1-90 days), when the mechanical properties of pure and modified PLA fibres were evaluated, no significant decrease in the tenacity of these fibres was recorded, even at any of the drawing temperatures.

The tenacity values practically did not change during the period of 90 days from the preparation of the fibres, or there was a slight increase. This suggests that no fibres degradation occurs over a period of 90 days. Likely, there is a gradual crystallization of the fibres, which results in an increase in the tenacity of the PLA fibres.

Elongation at break for pure PLA fibres as well as modified PLA fibres has a decreasing character depending on the drawing temperature (Table 2, Figure 4). At a drawing temperature of 80°C, all fibres, regardless of their composition, reach significantly higher values of elongation at break (47-71%) than at other drawing temperatures of 90°C (36-63%), 100°C (30-42%) and 105°C (26-41%). This shows to the fact that temperature of 80°C, in relation to the lowest achieved values of fibres' tenacity, is low and unsatisfactory for drawing of PLA fibres.

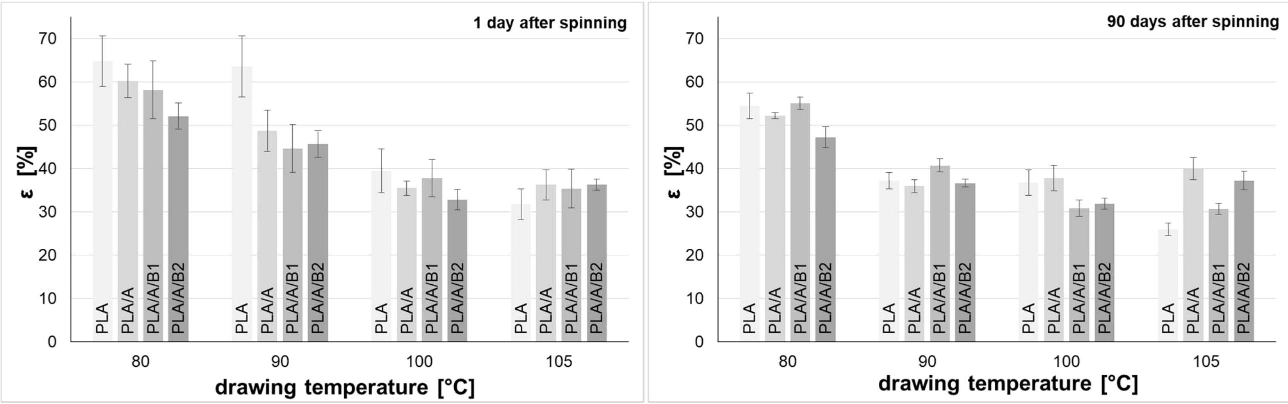

a) b)

Figure 4 Elongation at break of PLA and modified PLA fibres in dependence of various drawing temperature, measured a) 1 day and b) 90 days after spinning

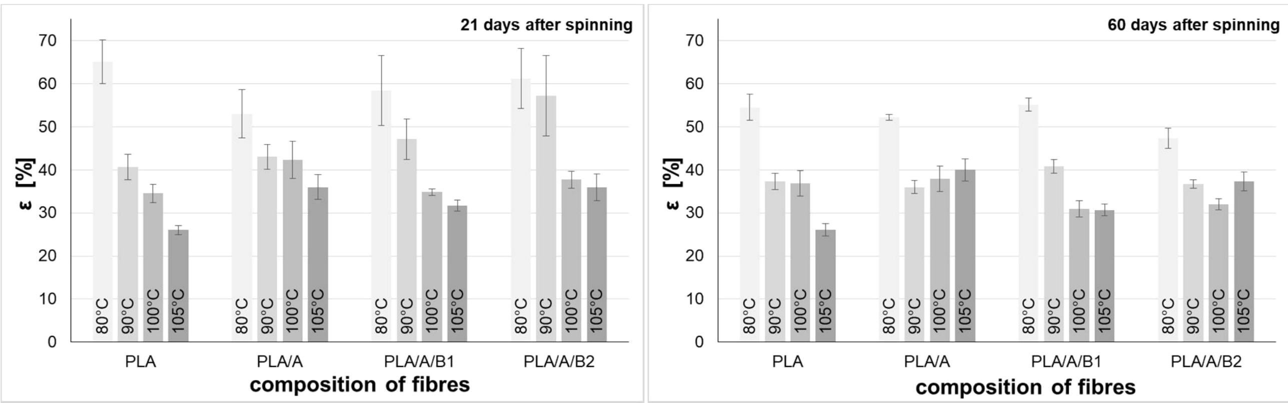

a) b)

Figure 5 Elongation at break in dependence on composition of PLA and modified PLA fibres, measured a) 21 days and b) 60 days after spinning

The effect of the composition of individual types of PLA fibres is not clear. While at lower drawing temperatures of 80 and 90°C the difference in elongation values for individual fibres is more pronounced, at higher temperatures of 100 and 105°C it is lost and the elongation reaches similar values. This trend is especially visible in the first days after spinning (Figures 4a and 5a). After 60 days from the preparation of the fibres, their mechanical properties seem to have stabilized. There was a decrease in the elongation's values for the fibres drawn at 80 and 90°C, while the elongation's values for the PLA fibres drawn at 100 and 105°C remained at the same level (Figures 4b and 5b).

4 CONCLUSIONS

This work was focused on the preparation of polylactic acid fibres, which due to their properties could be a potential replacement for non-degradable petroleum-based polymers. The main goal of the experimental part was to observe and evaluate the influence of fibre preparation conditions (drawing temperature) and the content of additives on the mechanical properties of PLA fibres. Based on the obtained data, the results can be formulated into the following conclusions:

- Pure PLA fibres and modified PLA fibres with content of additives were prepared and then drawn to a maximum drawing ratio at four different drawing temperatures of 80; 90; 100 and 105°C. The spinning and drawing of the fibres proceeded without any problems.
- In the case of undrawn fibres, the content of additives decreased the tenacity and increased the elongation at break of modified fibres in comparison with pure PLA fibres.
- The greater effect of drawing temperature than the effect of content of additives was found for drawn PLA fibres. The tenacity of drawn fibres increased with increasing of drawing temperature, in the case of pure PLA fibres as well as modified PLA fibres containing additives.

- No significant decrease in the tenacity of prepared PLA fibres was noticed (at any of the drawing temperatures) during the period (1-90 days), when the mechanical properties of pure and modified PLA fibres were evaluated,
- The elongation at break for pure PLA fibres as well as for modified PLA fibres has a decreasing character depending on the drawing temperature. A clear effect of the composition of individual types of PLA fibres and the concentration of additives on the elongation at break was not found.

Acknowledgement: *This work was supported by the Slovak Research and Development Agency under the contract No. APVV-17-0078.*

5 REFERENCES

1. Sin L., Tueen B.S.: Polylactic Acid, A Practical Guide for the Processing, Manufacturing, and Applications of PLA, (2nd Ed.), William Andrew, Oxford, UK, 2019, ISBN: 978-0-12-814472-5
2. Avinc O., Khoddami A.: Overview of poly(lactic acid) (PLA) fibre, Part I: Production, properties, performance, environmental impact, and end-use applications of poly(lactic acid) fibres, Fibre Chemistry 41(6), 2009, pp. 391-401, https://doi.org/10.1007/s10692-010-9213-z
3. Sin T.L., et al: Polylactic Acid; PLA Biopolymer Technology and Applications, William Andrew, Oxford, UK, 2013, ISBN: 978-1-4377-4459-0
4. Martin O., Avérous L.: Poly(lactic acid): plasticization and properties of biodegradable multiphase systems, Polymer 42(14), 2001, pp. 6209-6219, https://doi.org/10.1016/S0032-3861(01)00086-6
5. Drumright R.E., Gruber P.R., Henton D.E.: Polylactic Acid Technology, Advanced Materials, 12(23), 2000, pp. 1841-1846, https://doi.org/10.1002/1521-4095(200012)12:23<1841::AID-ADMA1841>3.0.CO;2-E
6. Dugan J.S.: Novel Properties of PLA fibres, International Nonwovens Journal 10(3), 2001, pp. 29-33, https://doi.org/10.1177/1558925001OS-01000308
7. Henton D.E., et al: Polylactic Acid Technology, In Natural Fibres, Biopolymers and Biocomposites, Chapter 16, CRC Press Taylor & Francis Group, USA, 2005, pp. 527-577
8. Gao C., et al: Effects of thermal treatment on the microstructure and thermal and mechanical properties of poly(lactic acid) fibres, Polymer Engineering & Science 53(5), 2013, pp. 976-981, https://doi.org/10.1002/pen.23347
9. Liu Q., et al: Structure and mechanical property of polylactide fibres manufactured by air drawing, Textile Research Journal 86(9), 2015, pp. 948-959, https://doi.org/10.1177/0040517515599743
10. Avérous L.: Polylactic Acid: Synthesis, Properties and Applications, In Monomers, Polymers and Composites from Renewable Resources, Chapter 21, Elsevier, Oxford, UK, 2008, pp. 433-450, ISBN 978-0-08-045316-3

FORMATION OF FASHION SYSTEM IN THE XX - THE BEGINNING OF THE XXI CENTURY

N.V. Chuprina[1], T.F. Krotova[1], K.L. Pashkevich[1], T.V. Kara-Vasylieva[2] and M.V. Kolosnichenko[1]

[1]*Faculty of Design, Kyiv National University of Technologies and Design, Nemirovicha-Danchenka str. 2, 01011 Kyiv, Ukraine*
[2]*Department of Fine Arts and Decorative Arts, Rylsky Institute for Art Studies, Folklore and Ethnology, National Academy of Sciences of Ukraine, Hrushevskoho str. 4, 01001 Kyiv, Ukraine*
chouprina@ukr.net

Abstract. *The factors that influence the functioning of the fashion system, as well as the formation and realization of fashion trends as a result of design activities, are identified and characterized. Dependences of formation of fashion system on factors of design activity are revealed. The transformation of fashion standards in costume design from artistic and stylistic standards to fashion products in the context of aesthetic criteria of modern culture is characterized. Ethnic style, retrospectivity, eclecticism and artistic kitsch as the basis of project practices and tendencies of anti-globalization and individualization in the fashion of the XXI century are studied. The interconnections in the structure of fashion as a cyclically closed system of formation, production, distribution and consumption of fashion standards and fashion products have been revealed. The structural interaction of the subjects of the fashion system in the process of their activity on the creation of the range of fashionable clothes and the implementation of fashionable innovations is revealed. The conceptual principles of design activity in the fashion system, which influence the formation of the actual design image in the costume design, are studied. The design activity of the subjects of the fashion system is determined as a factor of realization of fashion innovations and standards in the contemporary art and cultural space. The specifics of formation of fashionable project images in activity of design brands in the context of the general globalization of mass culture are defined.*

Keywords: *fashion system, design-activity, design brand, costume design, fashion design, fashion standard, objects and subjects of fashion system, fashion innovations, integrated concept of fashion behavior, fashion trend, design practice, fashion product.*

1 INTRODUCTION

Modern fashion is a multifactorial sphere of practical activity in which there is still no unified comprehensive classification of all aspects of functioning. Some researchers attempt to systematize specific areas of its development according to socio-cultural and economic activities. The explanation of fashion as a phenomenon and processes of introduction of fashion innovations in society is conditioned by comparison of results of researches of scientists of many spheres of knowledge. Theoretical searches in the field of fashion have been repeatedly joined by art critics and cultural scientists, sociologists and political scientists, philosophers and psychologists, economists and historians. Particular attention was paid to the interrelation of socio-cultural and individual-psychological aspects of fashion processes, as well as to attempts to explain the factors of materialization of fashion innovations through the creation of objects of material culture, in particular fashion clothing, and to determine their quantitative characteristics. But never once the designers of clothing, who are actually engaged in creating new trends, were systematically involved in this issue, though they know all the problems and specifics of the design of fashionable clothing, as well as the complexity of its promotion in the fashion market.

Contemporary fashion is an organic component of the European art space and design processes. However, the specifics of its development cannot be determined without characterizing all the causal features of the culture in which it operates and the substantiation of the role that fashion plays in national characteristics forming. Accordingly, the experience gained by scientists and designers-practitioners requires the systematization and generalization, as well as the study of the tendencies of development and factors of functioning of modern fashion as a system. On the basis of the analysis of the European leading trends in the fashionable clothes design, as well as on the basis of the study of the authors' creations of domestic designers and design brands, the specificity and tendencies of the development of the fashion system are revealed. Defining fashionable clothing as an object of design activity in the fashion system, it is necessary to concentrate on its properties, which provide the realization of fashion innovations and are fundamental in the artistic design of fashionable clothes [1-3].

Since the 1950s, the Kyiv National University of Technologies and Design (KNUTD) has been conducting research related to the design and decoration of various-purpose apparel, as well as working closely with Fashion Model Houses of Ukraine and the experimental production of relevant enterprises to implement the topical range of clothes. It is worth pointing out that the versatility and constant dynamism of the phenomenon of fashion leads to its study from different angles of view using different methodological approaches, since fashion as a social phenomenon is introduced in all spheres of life. Only a comprehensive approach to the study of fashion and all its manifestations, the introduction of an integrated concept of the fashion system will make possible to provide a scientific description of its characteristics.

Its application will allow to take into account various aspects of the functioning and development of fashion in order to define it as a system and an integrated phenomenon. The spread of fashion trends in modern society has also been strengthened by the globalization of the information sphere and intercultural contacts. Accordingly, the solution of the question of the aesthetics of a modern costume in order to form the aesthetic taste of consumers belongs to the sphere of artistic design, which forms the basis of fashion as a system. Comparison of various aspects of design activities that form a unified process of rational design in the fashion system creates in this complex process a fashionable product, filling it with social meaning and aesthetic value.

2 ANALYSIS OF PREVIOUS RESEARCHES AND SOURCES OF INVESTIGATION

The theoretical basis and information support of the research are the many works of domestic and foreign scientists, who considered the problems of the theory of fashion and design; history of development of costume forms; aesthetic, art and socio-cultural foundations of fashion formation and the process of dissemination of fashion innovations in post-industrial consumption society [4-7].

In the course of the analysis of the state of research of the phenomenon of fashion, existing works on the topic scientists were studied, and methodological foundations of the investigation are outlined. The present state of the art and scientific component of the development of costume and fashion is analyzed, as well as the formation of material and cultural approach to the study of the trends of costume design development in the fashion system is characterized. The analysis of fashion research conducted within the social sciences is performed; the results and methods of the analysis of the fashion or design of the applied clothes are considered. Key areas in which art principles have directly influenced the study of fashion history in recent decades have been identified. It is substantiated that an interdisciplinary approach plays an important role in the study of the influence of design and fashion processes. Therefore, the main directions of the research are: the chronology of the development of fashionable clothing of the late XIX - early XXI centuries; basic prerequisites for forming a fashion system; historical excursion of becoming a mass consumer society in the field of fashion apparel design and consumption; high fashion as a prototype of the fashion system.

The source base for the study of fashion as a system is represented by several groups. The first group of sources - scientific studies of the phenomenon of fashion by scientists in different fields - philosophy, sociology, psychology, cultural studies, marketing, art. The second group of sources - historical and contemporary information on the design activities of European Fashion Houses and design brands: P. Cardin, Chanel, P. Poiret, Dior, S. Rykiel, E. Schiaparelli, Yves Saint Laurent (France), Armani, Gucci, Missoni, Moschino, Roberto Cavalli, Valentino, Versace (Italy), Burberry, V. Becham, A. McQueen, M. Quant, V. Westwood (UK), Bershka, Mango, Zara (Spain), Andre Tan, D. Dorozhkina, Frolov, Varenyky Fashion, Zemskova&Vorozhbit (Ukraine), etc. The third group of sources - collections and models of fashion clothing of European and Ukrainian designers: T. Ford, J. Galiano, J.-P. Gaultier, S. McCartney, Yo. Yamamoto, R. Bohutska, O. Burenina, L. Pustovit, J. Hrytsfeld, O. Karavanska, I. Karavay, M. Reva and others. Information about the design activities of these brands was obtained from official sources and the media: official websites, print, video and internet sources of professional orientation, exhibitions of world museums, internet platforms for the implementation of design projects and the formation of design brands in national segments of the fashion market, etc. The fourth group - European and Ukrainian fashion editions (Collezioni, Elle, Harper's Bazar, L'Officielle, Vogue, Atelier, Fashion industry, Krasa & Moda (Beauty and fashion), Sezony Mody (Fashion Seasons), Styler.ua etc.); examples of European Fashion Houses fashionable clothing from the world's leading museums: Fashion and Textile Museum (London, UK), Victoria & Albert Museum (London, UK), Les Arts Décoratifs (Paris, France), Musée De La Mode De La Ville De Paris (Paris, France), Musee de la Mode et du Textile (Paris, France), Palais Galliera (Paris, France), Costume Moda Immagine (Milan, Italy), Galleria del Costume – Palazzo Pitti (Florence, Italy), Gucci Museo (Florence, Italy), Arizona Costume Institute (Phoenix, USA), The Metropolitan Museum Of Art (New York, USA) [8-18]; analysis of interviews with top designers in Europe and Ukraine (M. Jackobs, M. Kors, S. McCartney, T. Zemskova, S. Smolin, I. Frolov, T. Ford and others). Of particular interest for the study is the fifth group of sources of information - visual materials presented in catalogs, brochures and other printed products of international exhibitions, held by various subjects of fashion - textile companies and factory brands. The most up-to-date and decomposing information for determining the main interrelationships between fashion subjects is provided by print visuals of such worldwide exhibitions, such as Premiere Vision (France), Pitti Filati (Italy), KievFashion (Ukraine), Collection Premiere Dusseldorf (Germany), HKTDC World Boutique (Hong Kong), Milano Unica (Italy), TextileExpo and ExpoFur (Ukraine).

The history of the costume from the point of view of definition the criteria of cultural identification, functions of fashion and fashionable costume is analyzed; a number of issues that need further study in the context of their importance for the development of the fashion system are outlined.

3 OBSERVATION AND DISCUSSION

So, this investigation is devoted to characteristics of main factors and parameters of formation of fashion innovations in design-activity, as well as to definition of functional categories of fashion system. The backgrounds of formation, stages and criteria of evolution, factors of functioning and tendencies of fashion system development were revealed. The history of costume forms' modeling of the late XIX – early XXI centuries is divided into two stages, which played a fundamental role in the formation of the fashion system. The first half of the XX century up until the 1960s was defined by the dominance of so-called “haute couture”, which promoted luxuriance, elegance and selectness, thereby playing an aesthetic and social function in society. The luxury industry, which is another name for this evolutionary stage in the development of fashionable clothes, was self-sufficient and focused solely on self-improvement, and not on the implementation of fashion standards among wide layers of society.

System study of fashion of the XX – the beginning of XXI century was caused by the necessity of a thorough study of art and design processes in modern design of clothes. The development of this topic as an important component of contemporary design is an important factor of design-activity in the field of fashion integration into the European artistic and design culture [19].

The discovery of the principles of interaction of design-activities' aspects, which form a unified process of rational design development in the fashion system, makes it possible to form a wholesome view of the state of modern fashion, and allowes to understand more deeply the general principles, directions and tendencies of its development in the national and European context, as well as to classify the features of design practices in modern fashion system. So, it defines the possibilities of further fashion design development in the context of world and European design practices.

The history of costume from the point of view of identifying the criteria of cultural identification, functions of fashion and fashionable costume substantiate that material-cultural approach to the study of trends in costume design in the fashion system plays an important role in the study of influence of fashion and fashion processes (Table 1).

The criteria and factors for the development of the fashion system from the luxury industry at the turn of XIX – XX centuries to the prosperity of mass-market at the beginning of the XXI century determine the factors of formation of priorities of use of fashion products in the structure of consumer demand of the fashion system were substantiated, as well as the basic concepts of consumption formed in the XX century.

Table 1 Compliance of the concept of cultural identification criteria, the functions of fashion and fashionable costume

The essence of the cultural identification of costume or material culture complexes	Function of a fashionable costume through which the essence of cultural identification is realized	A function of fashion through which the essence of the level of cultural identification is realized
1	2	3
Selection of certain artifacts from a series of similar and their primary use	– utilitarian	– utilitarian
Assimilation of selected costume items (artifacts) in the system of communicative values of both verbal and visual	– individually-symbolic – aesthetic	– creating and maintaining uniformity and diversity in cultural designs – social regulation
Socio-psychological incorporation during which already adapted items of costume (as objects of material culture) are given the characteristics inherent in fashionable products	– emotionally-psychological – socially-symbolic	– recreational – social prestige
Transformation of individual objects and costume complexes as artifacts of material culture into artistic and aesthetic objects that represent a certain cultural value in society	– ideological – artistic	– socialization – communication

So, consumer priorities in the use of fashion system products are, as a rule, limited by the stereotypical, but socially and aesthetically stable frameworks of fashion behavior of the stratification class, to which an individual belongs. Considering this, it can be stated that the evolution of aesthetic tastes, fashion standards and the fashion system itself in the XX – at the beginning of the XXI century are directly dependent on the development and modification of the system of needs of each person and certain segments of society as a whole. The investigation emphasized that such motivation is a constant basis for consumer society globalization and active development of the fashion system, designed to meet different needs of this society in fashion products and standards.

So, the criteria of transformation of fashionable costume and accessories into the system of development, distribution and consumption of fashionable clothes can be characterized from the theoretical point of view. Formation of the origins of fashion system at the turn of the XIX – XX centuries contributed not only to the creation and production of fashionable designs and products, but also to the evolution of aesthetic ideals and artistic trends that determine design-activity in the XXI century. The change of socio-economic conditions for the formation of a consumer society in the middle of the XX century caused the evolution of Fashion houses of the early XX century into design brands as subjects of the fashion system. Under the pressure of the fashion demand industry of mass-market, the couture fashion, which was previously a priority direction of the fashion system, has become one of the spheres of its functioning. Representatives of society elite, who were previously the sole carriers and consumers of fashion designs and cultural innovations, were involved in the process of mass consumption, because they are forced to constantly find and apply various fashion innovations to emphasize their status and social position.

Development of information sphere in the middle of the XX century also affected the functioning of the fashion system and the extension of its influence on a wide range of consumers. The characteristic of basic vectors of the modern fashion system development and the factors of formation of mass fashion make possible to determine the criteria of mass and high fashion assimilation in the context of new standards of forming a fashionable design image in costume design [19].

The development of costume modeling in the XX century and its formation as a sphere of design activity was inspired by national cultural traditions, European experience and hard work of local craftsmen, tailors, fashion designers, creative teams and researchers of ethnic traditions and folk art. Later, rejection of domination of cosmetic display of ethno-artistic traditions became the strategic tendency. Folklore trends of fashion have encouraged fashion designers to use expressive form plasticity, decorative restrictions, clear proportions, with an emphasis on traditional colors.

The main direction of design-activity of costume artists and fashion designers in the XX century was a combination of modern functional silhouette of clothes with the decor and accessories of folk clothes.

a) ethnic embroidery

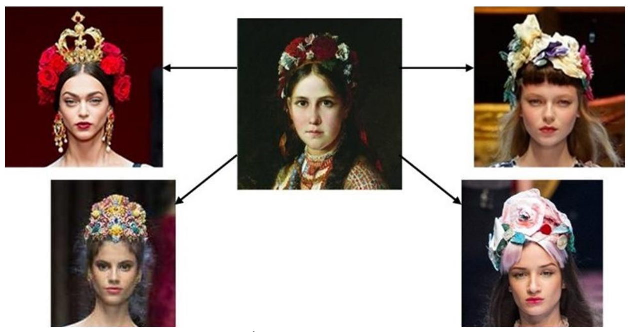

b) ethnic wreath

Figure 1 Transformation of ethnic elements in fashion garment

At the same time, the development of fashionable clothes, that met both European fashion standards and artistic traditions of people, is culturally and politically important, as it facilitate the integration into the pan-European artistic and cultural space, and preserve the national identity of certain nation. So, during the XX century, the folk costume became a priority factor in the formation of national identity and a creative source for the creation of modern fashionable clothes as a product of the European fashion system.

At the same time, the form of clothes reflects the world trends taking into account the peculiarities of the folk costume. The notions of consumers on the functionality, individuality and aesthetics of fashion products are reflected in the desire for European comfort and multifunctionality of fashionable clothes on the one hand, and ethno-artistic manifestations of individuality on the other hand. The fundamental influence on the formation of the project image is the creative elaboration of the artistic image, which provides the individuality of fashion design against the coordination of social inquiries, aesthetic priorities, stylistic selection of fashion trends [20, 21].

So, the issue of formation of criteria for evaluation of aesthetic distinctiveness of fashionable clothes in ethnic style with the view to improving architectonical integrity and both compositional and decorative perfection in the formation of design fashion image through the lens of ethnic design became well timed and urgent. A number of elements, which are most common and are features of the introduction of ethnic style in fashionable clothes, are deduced on the basis of the system analysis of the collections designed in he folk traditions (on the example of the Ukrainian folk suit), (Figure 1, 2). Means of transformation and synthesis of artistic and compositional elements of ethnic style in the formation of the project image in the fashion system reveal the reasons for widespread appeal to national ethno-artistic traditions in contemporary design of clothes.

Thus, the modern design of fashionable clothes of mass-market as a fashion product changes the focus from unified-typed to individually-targeted, based on the use of perspective trends of fashion development and satisfaction of mass consumer's personal needs in self-identification.

A retrospective analysis of the characteristics of the development of design images in the fashion of the XX century defines the main features of their formation in the long term (in the context of long-term and short-term fashion trends). The most effective opposition to the mass unification of modern fashion standards and fashion products is the formation of retrospective and vintage trends in the modern fashion system, which have transformed into a democratic system of fashion standards and fashion products (Figure 3). Varieties of vintage themes as retrospective demonstration while creating modern fashion products are boundless.

The principles and means of eclecticism as a basis of design practices in the formation of artistic images in the modern fashion system were also analyzed during the study. Eclecticism and kitsch were characterized as an assimilation of dissimilar style elements borrowed from self-contained cultural (including subcultural) systems, historical styles, areas of art and architecture, that have different meaning and purpose, with subsequent coordination of compositional and stylistic nature of fashion. In modern fashion trends, artistic kitsch plays the role of kitsch-design and acquires the characteristics of a professional tool for finding new forms and aesthetics, as well as alternatives for traditional views.

a) b) c) d)

Figure 2 Present samples of functional fashionable clothes combined with ethnic decoration (Ukrainian fashion brends Varenyky Fashion (a), Svitlo (b), Yu. Magdych (c) and Kozzachka (d) [26]

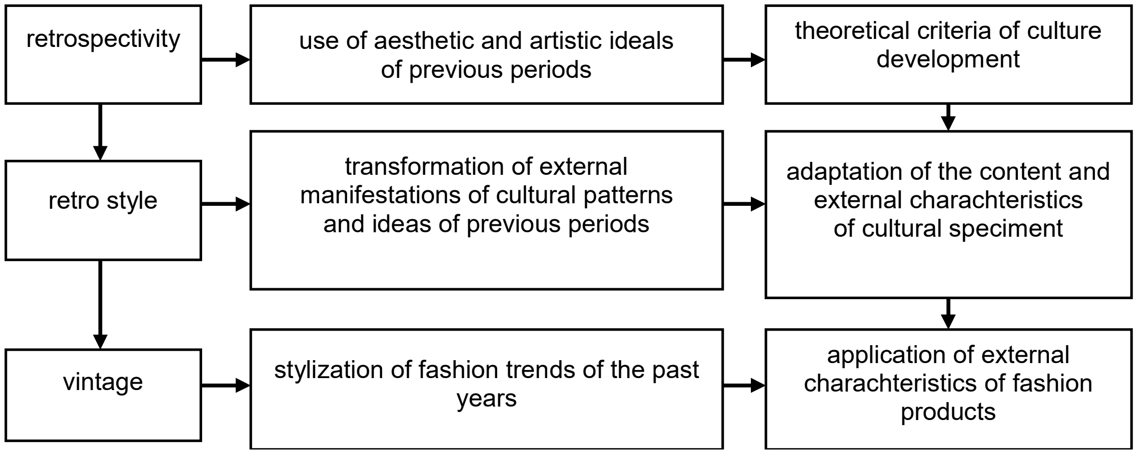

Figure 3 Links of retrospective trends in modern fashion system

Design practices of anti-globalization and individualization in the fashion system of XXI century substantiate that by applying principles of ethno style, eclecticism, retrospective and artistic kitsch to costume design, an individual and unique image that creates preferences for identification of its owner and extends the possibilities of designing clothes as fashion product and further combinational accessories can be designed under consumption conditions. The cause-and-effect relations of the processes of development, distribution and consumption of fashion products in the context of the modern fashion system define the main factors of designing modern fashion products that correspond to fashion trends. The introduction of eclecticism and retrospective means as design practices for fashion trends development and fashion products, especially in the context of consumer crisis, substantiate the behavior of the participants of the fashion process under modern fashion system conditions [22].

In modern fashion system "haute couture" collections can be characterized as a form of representation of the leading artistic images in design-activity. The presentation of fashionable clothes collections for the mass media is a well developed advertising and exhibition technology of propaganda of fashion standards and fashion products. Design brands or Fashion houses can become commercially successful if they combine various aspects in their activities – from creating "haute couture" fashion standards and cultural models to forming design-concepts for advertising their own fashion products and promoting their brand.

The rise of level of success of a brand and rise of the level of sales of a fashion product is due to the mass production of clothes of "prét-a-porte" and "bridge" classes, depending on a segment the designer brand occupies in the fashion market. The most designers locate their activity in several segments of the fashion market, creating fashionable clothes of "pret-a-porter de lux", "pret-a-porter", "bridge" classes. In addition, the cooperation of young fashion designers with the brands of mass-market fashionable clothes development becomes popular, which promotes the development of modern mass fashion.

Structural-logical connections make for structuring of the segments of the fashion system was classified based on the analysis of their interaction in the formation of fashion trends and in the creation of a fashion product (Figure 4).

So, the criteria of the formation of design brands depend on the target consumer audience, on which their design and commercial activities are focused, was carried out. It was substantiated that composite or diffuse lines of fashionable clothes design are created at the boundary of the influence area intercrossing, which combine design and marketing priorities within a single brand portfolio. In the context of globalization of the modern fashion system, the complex designer brands as means of attracting a lot of different types of consumers and increasing the level of success of the brand became the priority for the Fashion Houses. Such collaborations are also actively developing in the European fashion market, overtaking the design-activity of leading designers and textile companies or factory brands. The most design brands of mass-market are holding on the generalized algorithm of the process of creation of fashionable clothes for mass-market. Such algorithm corresponds to the work of different world design brands and textile corporations.

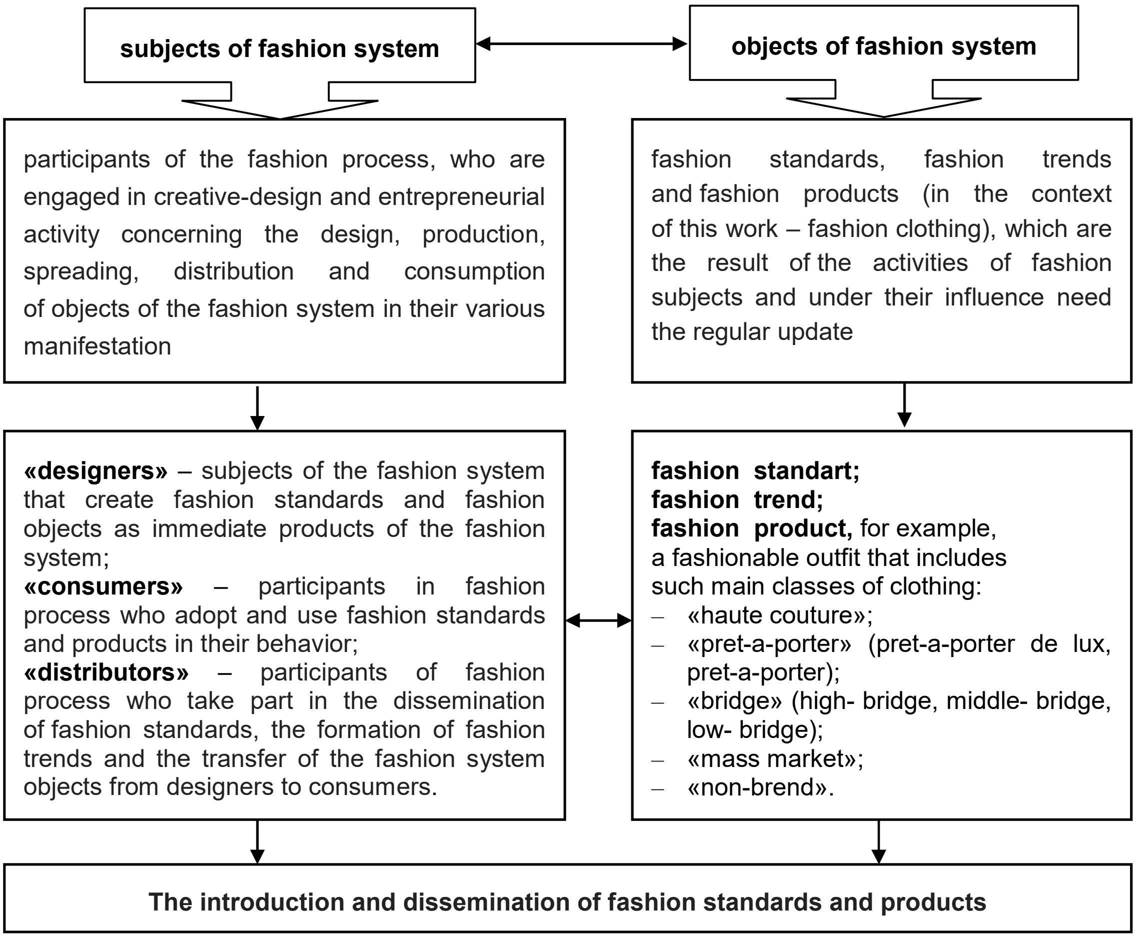

Figure 4 Structuring of generalized categories of the fashion system

The specificity of the concept of prompt response "fast-fashion" as a design practice of the modern fashion system in the segment of mass-market clothes was substantiated. So, the concepts of prompt response "fast-fashion" and "just in time" shape the design-activity of factory and retail brands that specialize in the development and distribution of fashionable mass clothes of a certain product range. Accordingly, the consolidation of creative ideas of designers and stylists of High fashion houses with brands and factory brands operating in the "fast-fashion" segment was defined as the most successful. This tendency of development of such collaborations in the fashion system is progressing so actively and differently, that in the future it may become the basis for a new concept of extension of fashion innovations in society [23].

The total globalization of society is increasing each day, and contributes not only to the direct effect of culture on the trends of the modern fashion system and the formation and extension of fashion standards, but also takes part in production of fashion products, which are universal for various segments of the fashion market, including regional. The decrease of prime cost of popular fashion products because of industrial production of the latter has attracted all social layers of society into consumption. On the other hand, the introduction of industrialization into the production of affordable fashion goods has caused their mass consumption. It is about consumers who form different social or regional segments of fashion goods market, have access to similar or comparable fashion products. At the beginning of the formation of mass consumption society, in the late XIX – early XX century this has led to the transformation of a sustainable system of social and cultural values, and subsequently to a change in consumer behavior and a shift towards fashion and fashion products.

The success of the subjects of modern system of fashion depends on the optimal combination of original design of a fashion product and technologies of its promotion into consumer market. The sources of information influence the formation and extension of fashion trends in modern society and form the methods of forecasting the development of trends in fashionable clothes design were described.

A comparative analysis of the basic concepts of appearance and development of fashion innovations in society determined the principles of classification of the basic fashion theories influencing the specificity of fashion behavior in the modern consumption society. Various factors of functioning and approaches to the study of fashion processes that are of interest for the modern fashion system substantiate that the change of society structure and information sphere of society improvement led to the development of a system of various sources, both verbal and visual. Sources of fashion innovation are becoming more diverse, and street fashion is giving birth to an increasing number of young designers seeking recognition from a specific target audience. However, such a shift does not cancel the basic principle: only the recognition by the official authorities and legislators of the fashion system can give new objects and products the status of fashionable. The recognition by wide layers of society can be gained only through the process of public approval by the fashion system subjects, involved in the development, distribution, extension and consumption of fashion standards. With the modern multi-vector nature of the fashion system, it was substantiated that these fashion innovation trends are interacting equally important for the development of the fashion system and modern consumer society as a whole [24].

The basics in characterization of the fashion system are its characteristic as a complex concept of fashion behavior and extension of fashionable innovations and standards. Accordingly, the fashion system has interdependent cause-and-effect relationships and may be modeled as an integrated concept that contains characterized functional factors of design-activity in contemporary artistic and cultural space. Given the complex integrative structure, it was determined that they can ensure the balanced functioning of the fashion system as a concept of fashion behavior in society only by interacting with each other (Figure 5).

The newly created model of the fashion system as an integrated concept of the extension of fashion innovations presentes the connection of its structural components in order to influence the result and evaluate the efficiency of functioning. It defines the structural configuration of the fashion system as a cyclically closed model of establishment, production, distribution and consumption of fashion standards and fashion products, made from the standpoint of refining the principles of segmentation of the fashion system and articulation of criteria of their interinfluence for the most effective system functioning [25].

So, the design of new models of fashionable clothes will always have the features of innovation, and the process of creating such models will always be creative at its core. All of this allows to adjust main characteristics of the process of creating a new range of fashionable clothes, with the aim of optimizing its artistic and aesthetic properties and functional and design factors of implementation and introduction on European fashion market.

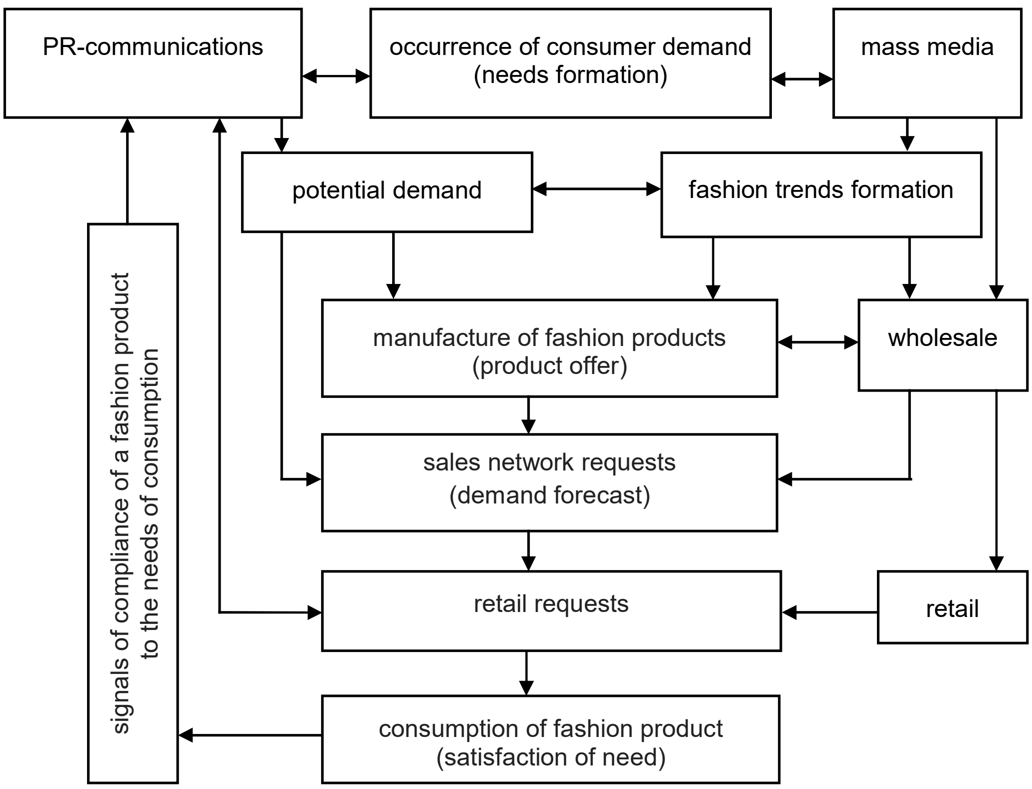

Figure 5 Model of interaction of subjects of the fashion system

4 CONCLUSIONS

The complex researches that were undertaken, became the basis for the formation and practical realization of the range of fashionable clothes by means of harmonizing the conceptual correspondence of descriptive expressiveness and functional relevance of the project image in clothes.

The main objective and judgmental factors that influence the formation and extension of fashion innovations were identified and classified in this investigation. The degree of influence of information sources on fashion trends development and behavior of participants of the fashion process was determined. It is formulated that the fashion system is an integrated sphere of design activity and a structured model of fashion innovations. The criteria and factors of its existence, which influence the formation of the actual project image in the costume design, are revealed. The generalized criteria of realization of fashionable innovations in the conditions of modern system of fashion are formed. The principles of fashion system segmentation and their mutual influence for the most effective functioning are specified.

The structure of development of fashionable clothes classes was developed, which influences the self-presentation of designer brands on the fashion market; the specifics of the organization of development and production, as well as the segmentation of mass consumers of fashionable clothes were determined as criteria for the division of fashionable clothes into classes. The generalized algorithm of fashion innovations' implementation under the conditions of the modern fashion system was formed based on generalization of empirical data of the research, characteristics of the cause-and-effect sequence of stages of fashionable clothes design, and classification of criteria of implementation of innovations in the fashion system.

Accordingly, the algorithm for formation of fashion trends and introduction of current models of fashionable clothes, presented in this study, can be adapted and applied in the design of fashion products in various areas of designactivity.

5 REFERENCES

1. Lahoda O.: Search for Uniqueness and Identification Using Fashion; Space and Culture, Indian 6(4), 2018, pp. 1-4, https://doi.org/10.20896/saci.v6i4.410
2. Yezhova O., Pashkevich K., Kolosnichenko M., Abramova O. and Nazarchuk L.: Provision of the quality of decoration of semi-finished fashionable clothes, made of suiting fabrics with cotton content (denim type), Vlákna a textil (Fibres and Textiles) 25 (4), 2018, pp. 94-102, http://vat.ft.tul.cz/2018/4/VaT_2018_4_17.pdf
3. Pashkevich K., Kolosnichenko M., Yezhova O., Kolosnichenko O., Ostapenko N.: Study of properties of overcoating fabrics during design of women's clothes in different forms, Tekstilec 61(4), 2018, pp. 224-234, https://doi.org/10.14502/Tekstilec2018.61.224-234
4. White N., Griffiths I.: The fashion business: theory, practice, image, Minsk: Grevcov Publisher, 2008 (in Russian)
5. Lynch A., Strauss M.D.: Changing fashion. A critical introduction to trend analysis and meaning, Minsk: Grevcov Publisher, 2009 (in Russian)
6. Kawamura Yu.: Fashionology. An introduction to fashion studies, Minsk: Grevcov Publisher, 2009 (in Russian)
7. Ricchetti M., Khurana K.: Shifting perspectives on sustainable supply chain management in the fashion business, in Part 2: Fashion in the making, in: Fashion Tales: Feeding the Imaginary, 2017, pp. 155-168, https://doi.org/10.3726/b11234
8. The fashion costume collection of the Fashion and Textile Museum (London, UK), https://www.ftmlondon.org/
9. The fashion costume collection of the Victoria & Albert Museum (London, UK), https://www.vam.ac.uk/
10. The fashion costume collection of the Les Arts Décoratifs (Paris, France), https://madparis.fr/
11. The fashion costume collection of the Musée De La Mode De La Ville De Paris (Paris, France), http://www.palaisgalliera.paris.fr/
12. The fashion costume collection of the Palais Galliera (Paris, France), http://www.palaisgalliera.paris.fr/
13. The fashion costume collection of the Musee de la Mode et du Textile (Paris, France), https://madparis.fr/
14. The fashion costume collection of the Costume Moda Immagine (Milan, Italy), http://www.costumemodaimmagine.mi.it/
15. The fashion costume collection of the Galleria del Costume – Palazzo Pitti (Florence, Italy), https://www.uffizi.it/palazzo-pitti/museo-della-moda-e-del-costume
16. The fashion costume collection of the Gucci Museo (Florence, Italy), http://www.florencemuseumguide.com/gucci-museum/
17. The fashion costume collection of the Arizona Costume Institute (Phoenix, USA), http://www.arizonacostumeinstitute.org/
18. The fashion costume collection of the The Metropolitan Museum Of Art (New York, USA), https://www.metmuseum.org/
19. Chuprina N.V.: Fashion system of the XX – the beginning of the XXI century: design practices and factors of functioning (European and Ukrainian contexts): a monograph, Kyiv: KNUTD, 2019 (in Ukrainian)
20. Kolosnichenko O.V., Pryhodko-Kononenko I.O., Ostapenko N.V.: Design of new articles of clothing using principles of contemporary style directions in architecture and art, Vlakna a textil (Fibres and Textiles) 23(1), 2016, pp. 38-44

21. Laurell C.: Fashion spheres - from a systemic to a sphereological perspective of fashion, Journal of Fashion Marketing and Management: An International Journal 20(4), 2016, pp. 520-530, https://doi.org/10.1108/JFMM-04-2016-0033
22. Martinez Barreiro A.: Towards a new system for the fashion industry - The Zara model, Revista Internacional de Sociologia 66(51), pp.105-122, https://doi.org/10.3989/ris.2008.i51.111 (in Spanish)
23. Chuprina N.V.: Characteristics of “FAST FASHION” concept in fashion industry, Vlakna a textil (Fibres and Textiles) 21(1), 2014, pp. 31-36
24. Gofman A.B.: New theory of fashion and fashionable behavior, 3rd ed., SPb: Piter, 2004 (in Russian)
25. Chuprina N.V.: Principles of forming and realization of fashion trends in fashion industry, Yzvestyia VUZov. Tekhnolohyia Tekstylnoi Promyshlennosty (News of higher Institutes. Technology of textile industry*)*, 2(356), 2015, pp. 123-127 (in Russian)
26. Fashionable ethno: 12 Ukrainian brands of folk clothing that are impressive (in Ukrainian), https://kiev.zagranitsa.com/article/5050/modnoe-etno-12-ukrainskikh-brendov-narodnoi-odezhdy-kotorye-vpechatliaiut

TOPOLOGICAL ANALYSIS AND SYNTHESIS OF MACHINE CHAIN STITCHES

Oleksandr Manoilenko

Kyiv National University of Technology and Design, Nemirovich-Danchenko st. 2, 01011 Kyiv, Ukraine
manojlenko.op@knutd.com.ua

Abstract: *The topological analysis of chain stitches of classes 100, 400, 500, 600 and 800 is performed in the work; the general regularities of their formation are established by dividing them into typical structural elements. Also provide recommendations for creating new and potentially possible types of stitches with the development of graphs and calculation of thread consumption for stitches. The method was used in the work, which includes the main stages of topological analysis and synthesis, namely: formation of problems, division of objects (stitches) into elements, construction of models (morphological matrices), synthesis of object variants, and selection of the most rational variants, application of the method of graphs. The result is a generalized hierarchy of the structure of chain stitches of different classes, which are formed by structural elements (loops, broaches and applying thread or sketches [1]) and possible combinations of stitch types. A code record of the structure of stitch elements in the form of routes of 3D-graphs that determine the geometric length of each thread (excluding the properties of the material and threads) is also obtained. Matrixes of stitch configurations are obtained, regularities of formation of new types of stitches of different classes are revealed and the graph-generator of new types of stitches is offered. Regularities of formation of structures of chain stitches of different classes on the basis of development of the hierarchical scheme of structural elements of chain stitches of different classes, morphological matrices and graphs of formation of chain stitches are also revealed. The method of structural analysis and synthesis of new types of stitches is offered. The obtained results can be used for the synthesis of new or potentially possible types of stitches, determining the cost of sewing threads in the stitch depending on the technological parameters of the stitch and materials (stitch length, thickness of materials under the presser foot of the sewing machine, width of overlock stitch, etc.) stitch quality forecasting and the use of initial data for the design and adjustment of sewing machine mechanisms.*

Keywords: *structures of chain stitches, structural analysis, determination of thread length in stitch, 3D stitch graph, stitch intensity matrix, morphological matrix of stitches, chain stitch, chain stitch generator.*

1 INTRODUCTION

Chain stitches of classes 100, 400, 500, 600 and 800 are sold in a wide range of sewing machines, which are manufactured by a number of foreign companies and are designed for processing and stitching fabrics and knitwear. Each class of stitches includes several types of stitches in accordance with 100 class includes 7 types, 400 class - 17 types, 500 class - 16 types, 600 class - 9 types, 800 class - 6 types, which are formed by a combination of individual types of stitches 300 - 600 classes [2]. In addition to the standard types of stitches, there are many other types of stitches that are not included in the general classification and are known from other sources and patents [3-12] and so on. Each type of stitch differs not only in the number of threads, but also in the position of their elements in its structure. The structure of stitches is described in the literature quite fully. Among the elements of the stitch are: loop, broach, applying thread (sketches) [13-15]. The cost of the number of threads per unit stitch is determined by known methods [16-19]. Thus, in [16, 17] thread costs are defined as the sum of individual stitch elements for a certain stitch length, which allows to determine the costs of upper and lower threads, as well as its total value, in the literature [18] thread costs in stitch type 504 are determined by using geometric modeling, at the same time in the literature [19] the algorithm for determining the length of the thread for different types of stitches without explaining the essence of the method of determination.

The difficulty of calculating the costs in one stitch, as a discrete element of the stitch, is that when determining the total cost in the stitch, the error of the length of the thread of each stitch accumulates in arithmetic progression according to the number of stitches, so in such cases deformation of materials by stitch compression [16]. The leading German companies Amann Saba, Gutermann and Epic Coats (UK) offer thread consumption calculations for the main types of stitches, which take into account the properties of the threads, the number of threads and needles, and so on.

The description of the processes of chain stitch formation in the available literature [15, 20] is given only for a few types, and in [15] the author presents in the form of graphs and matrices of adjacency the process of forming the main types of overedge, multi-thred and blind chain stitches, them to analyze the structure and process of formation of any type of stitch.

Issues of synthesis and regulation of the main mechanisms (needles, loops, expanders, top cover spreader, rack and knives) in the literature are covered quite fully. At the same time, there is no general recommendation for the synthesis and selection of the structure of the thread feed mechanisms for a particular stitch type. There are also no recommendations for their adjustment in accordance with the type of thread, materials, stitch structure, its parameters, etc.

2 STATEMENT OF THE TASK

Within the limits of research to carry out the morphological analysis of structures of chain stitches of 100, 400, 500, 600 and 800 classes as a result of which to receive morphological matrices and structural formulas of stitches in the form of routes of 3D-graphs. Obtain formulas for summarizing the routes of 3D-graphs depending on the parameters of the stitch (number of needle threads, the position of the thread weaves on the material and its thickness, zigzag width, etc.), which will obtain generalized formulas for determining the cost of each thread per stitch and graphical computer structure modeling new types of stitches.

It is necessary to establish the logical sequence of formation and hierarchical subordination of each element of a stitch and to reveal new communications between them that will allow to receive new types of stitches with new opportunities. The main task of this work is to develop the basics of the theory of synthesis of new structures and types of chain machine stitches with given geometric properties and design of equipment for their implementation.

3 RESEARCH RESULTS

Class 100 combines single-thread chain stitches (101, 103, 104, 105, 107, 108 types) and double-thread (102 type), which are formed by a needle (straight or arcuate) and an expander [2].

Class 400 combines many thread chain stitches, which are formed by two threads (needle thread and loop thread - 401, 404, 409, 411-417 types), three threads (two needle threads and one loop thread - 402, 405, 406 types), four threads (three needle and one thread of the looper - 403, 407 types) and five threads (two needle, two threads of the looper and cover thread - 408 type), four needle and one thread of the looper - 410 type.

Class 500 combines overedge chain stitches, which are formed by a single thread or groups of threads: single-thread (501, 513 types - formed only by a needle thread); double-threaded (502, 503 types - formed by the threads of the needle and the lower loop); three-thread (504, 505 types - formed by a needle thread and two threads of the lower and upper loops and multi-line in the process of their formation involved two needle threads - 510, 511 types, two needle and two threads of the lower loop - 508, 509, 521 types) , two needle threads and two looper threads (506, 507, 512, 514 types).

Class 600 combines cover chain stitches, which as a result of grinding cover both surfaces of materials with a cover thread (top cover spreader), which are formed by three threads (two needle and one loop thread - type 601), four threads (two needle, one and one loop thread and cover thread - 602 type), five threads (two needle, one loop of thread and two cover threads - 603 type; three needle and one loop of thread and cover thread 605 type), six threads (three needle, one thread of loop and two cover threads – 604; four needle, one thread of loop and one cover thread - 607, 609 threads; needle, one loop of thread and two cover threads - 608 type) and nine threads (four needle threads, four threads of loopholes and one cover thread - 606 type).

Class 800 - combines different types of chain and shuttle stitches 801 (515) formed by a combination of 401 and 503 stitch types; 802 (516) - 401 and 504 types; 803 (517) - 301 and 504; 804 (518) - 301 and 503, 805 (519) - 401 and 602 types; 806 (520) is formed by two stitches type 401 and type 602.

The analysis of stitch types of class 800 shows that they are obtained by combining individual types of stitches and complement the class 500 stitches [20]. Since the 800th class of stitches belongs to the highest hierarchy of stitches, many of its elements will be covered when considering the stitch types of other classes.

Presence of broaches, sketches, loops of threads (needle, threads of loopers, top cover spreader), or the report of a zigzag of a stitch allow to allocate characteristic elemental contours of a thread. In general, in the structure of each type of stitch, you can select the characteristic contours of each thread, which are part of the stitches (Figure 1) determining the rational parameters of the mechanism.

The designation of the contours corresponds to [2], the contours of the thread 1…18 (loops) are formed by a needle thread, the contours of the thread are denoted by lowercase letters ai and bi (broaches) are formed by threads, respectively lower and upper loop, the contours are denoted by letters *Z, Yi* (sketches), correspond to the threads of the decomposer, here are also the contours *a3, c3* and *a4, c4* of the proposed types of stitches [3-11].

For multi-row (multi-needle) stitches as the identifier of interweaving of needle threads of the main element "1" (Figure 1) with other threads, the designation of the number of pairs of inter-loop needle rows is introduced: $i = 0, 1, 2, 3…n$, $j = 0, 1, 2, 3…p$ with the distance h between the i-th and j-th needle rows and the parameter corresponds to the broach formed by the branches of the loop, which is covered by the top of the loop of the thread. Accordingly, the j parameter corresponds to the outline (interlooping connection) of branches that cover with their vertices the branches of the loops of other threads. Interweaving rows correspond to the interweaving of the number of loops $i + 1$ and $j + 1$ needle threads.

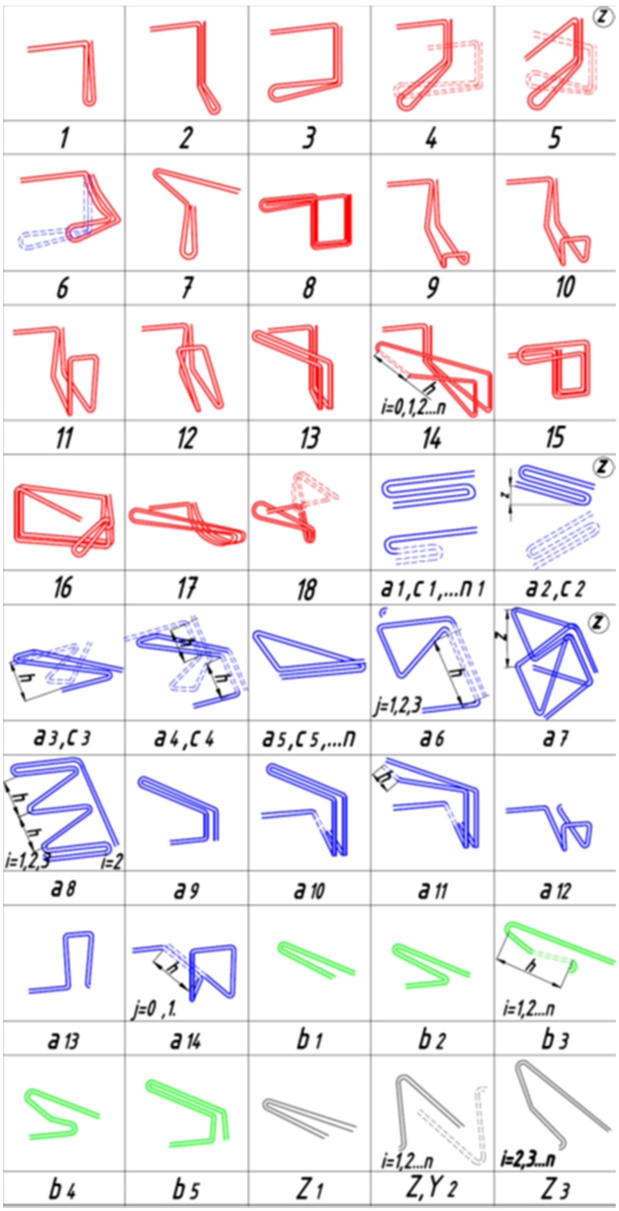

Figure 1 Structural elements of chain stitches of types 100, 400, 500, 600, 800: *1…18* - needle thread (loop); *a1-14* - threads of the lower loop (broaches); *b1-5* - threads of the upper loop (broaches), *Z1-3* - threads of the top cover spreader (sketches)

Based on the analysis of contour elements, the classification of heredity of their formation from elementary to complex is proposed, respectively for needle thread, lower loop thread, upper loop thread and top cover spreader (Figures 2-4) here are also block diagrams with coded notation of structural elements.

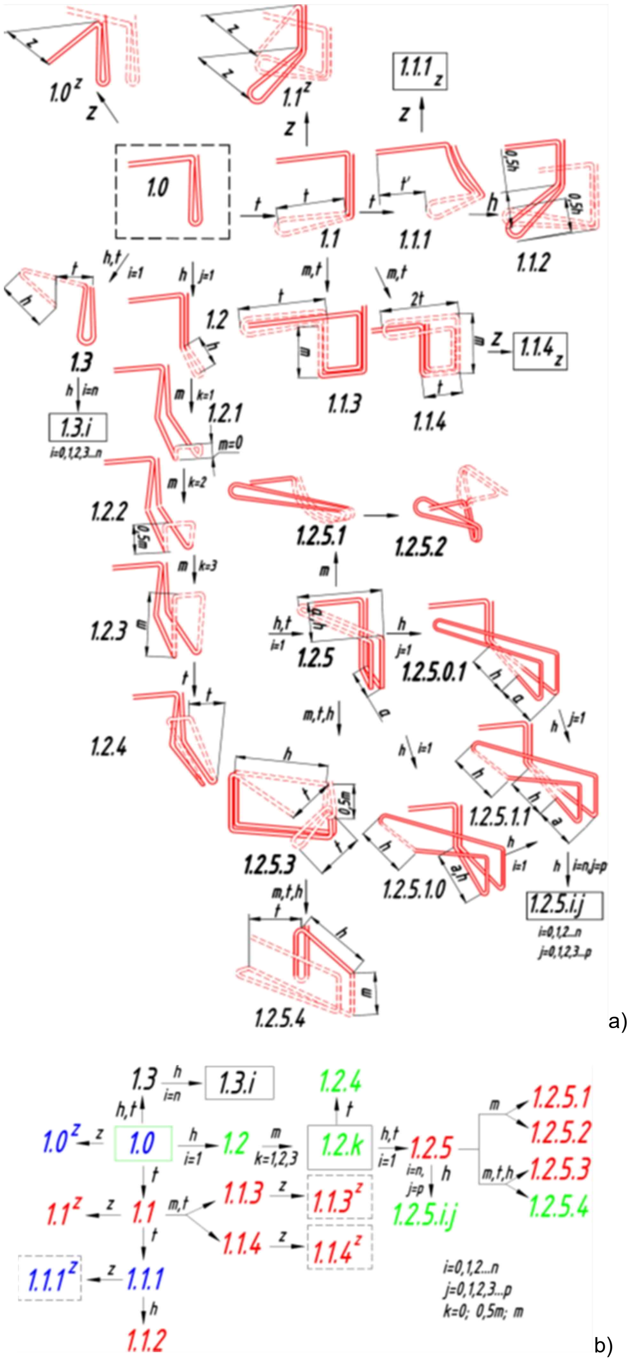

Figure 2 Hierarchical scheme of formation of the elements of the contour of the needle thread of chain stitches: a) graphical - structural representation of the elements; b) is a block diagram of the stitch element

The hierarchical and structural diagrams above the expansion route (indicated by the arrow) show the modifiers (h is the distance between adjacent needle rows, *m* is the thickness of the materials, *t* is the stitch length, *z* is the width of the zigzag), below it is the quantitative characteristic of the modifier. In addition, for several elements of the stitch found structural formulas that reduce the complex contour of the element into a simple (basic) by reducing the *i-th, j-th* parameter to zero (in the diagrams of Figures 2-4 are surrounded by rectangles with a solid line). In turn, the increase of the *i-th, j-th* parameter, leads to the formation of new types of stitches.

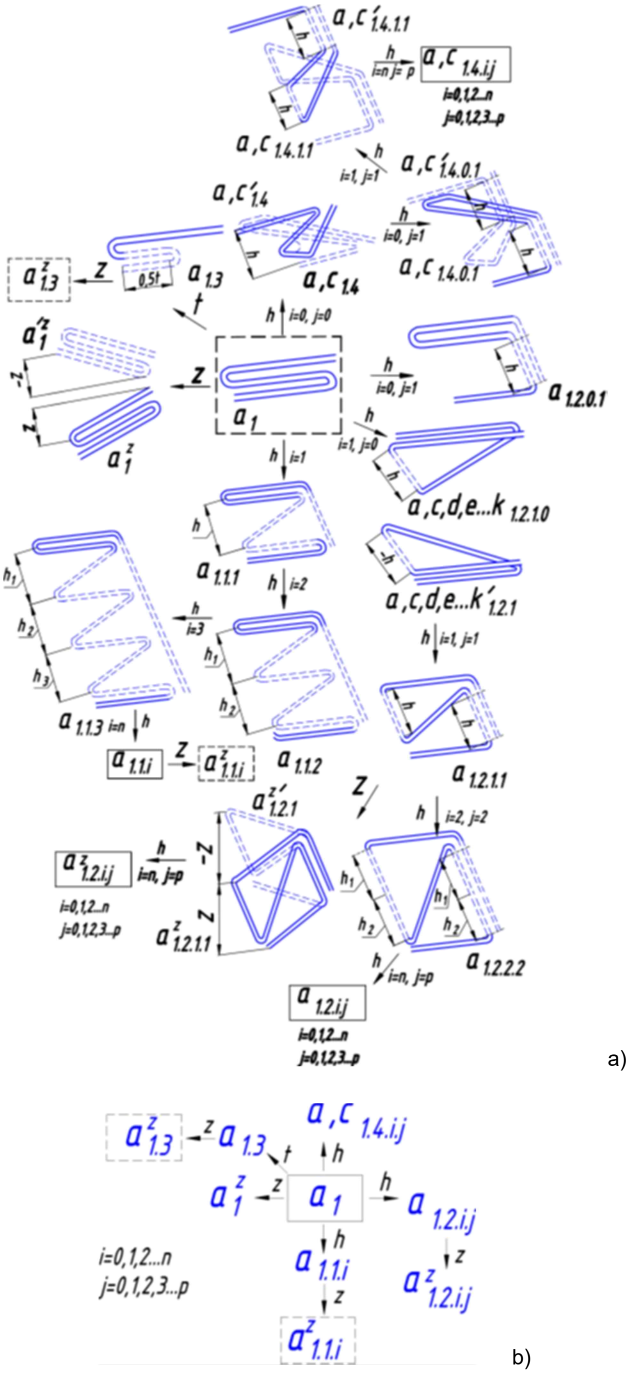

Figure 3 Hierarchical scheme of formation of elements of the contour of the thread of the lower loop of chain stitches: a) graphical - structural representation of the elements; b) block diagram of stitch elements

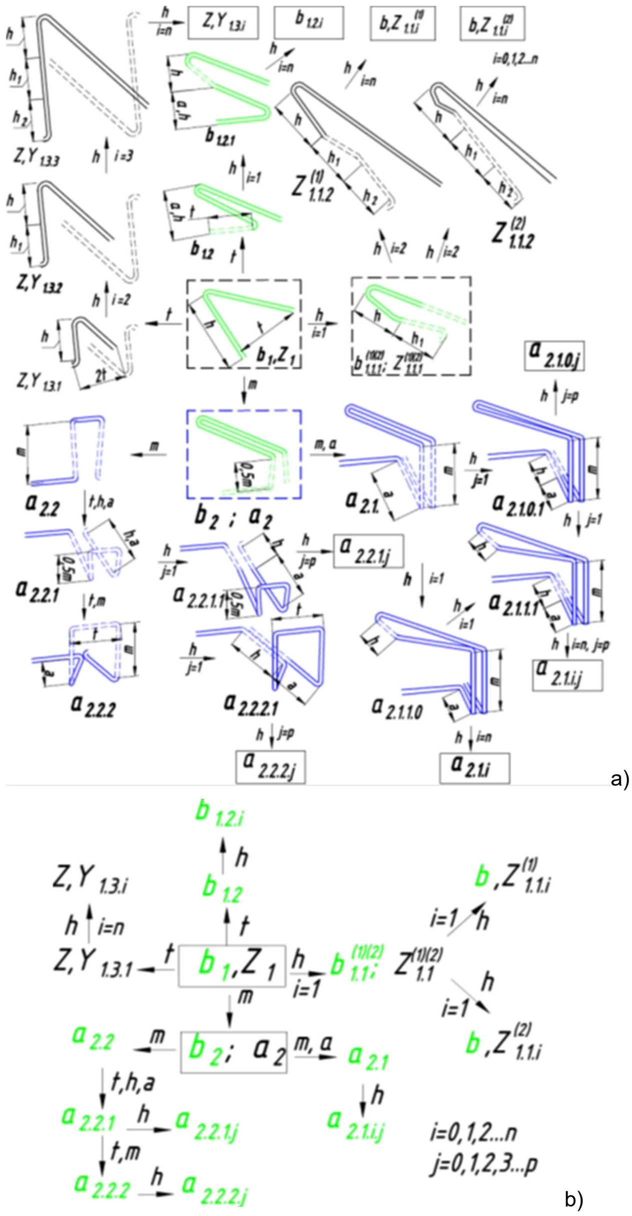

Figure 4 Hierarchical diagram of the elements of the contour of the threads of the lower and upper loop and the top cover spreader of chain stitches: a) graphically - structured representation of the elements; b) block diagram of stitch elements

The contour elements of the needle thread (Figure 2) do not have repeatability among the elements of other stitch threads due to the fact that the thread is passed through a material that is characteristic only of the needle thread. Element *1.2.i.j* is obtained by modifying from element *1.2.5* parameter *h* with the possibility of combining both modifiers of the *i-th, j-th* parameter. In turn, the element *1.2.i* also forms a series of new stitches with a covering thread (600 class) formed by sketching the loop of the extreme needle thread while increasing the number of interneedle rows, ie the parameter *h, i = 2, 3...n*. It is established that some elements of the needle thread contour can be modified due to zigzag *z - 1.1.1Z* and *1.1.3Z 1.1.4Z*, which allows the formation of a zigzag stitch, respectively, stitches of 400 and 100 classes (new elements are surrounded by rectangles with a dashed line Figure 2). At the same time, the element *a1* (Figure 3) of the contour of the thread of the lower loop in the formation of derived elements forms a number of elements that are easily folded into the base (*a1*) by resetting the parameters *i* and *j*. Elements *1.1.1 - 1.1.3* formed by the structural formula of summary *1.1.i at i = 1, 2, 3* are used in stitches of the corresponding types 406, 407, and 410. The formation of new types of stitches is possible by increasing the number of loops of needle threads of the base element *1.0* and the *i-th* parameter. In turn, the elements *1.2.1.1, 1.2.2.2* formed by the structural formula of summary 1*.2.ij* when *i = j* are used in stitches of the corresponding types 402, 403. However, technologically it is possible to form stitches by increasing these parameters, as well as changing their different number (ie. *i ≠ j*). This confirmation is the element *1.2.1.0*, which is formed only by the *i-th* parameter (*i = 1, j = 0*) and applied in a stitch of type 606. The new element *1.2.0.1* can be formed by the inverse combination *i = 0, j = 1* and can form new types of stitches. The elements formed by *1.4.ij* were used in a number of stitches proposed by the authors (Figure 5) [3-11], the peculiarity of the process of formation of these stitches is that the process of capturing loops of needle threads ("loop loops") occurs simultaneously on both sides of the loop a number of needle threads. The introduction of loops of needle threads occurs in opposite loops formed by the threads of the looper, this allows you to significantly increase the width of the stitch and increase its elasticity.

New elements of the lower loop loop contour can be achieved with the zigzag modifier *z - aZ1.1.i* and *aZ1.3* (new elements are surrounded by rectangles with a dashed line Figure 3), which allows the formation of zigzag stitches in accordance with elements *1.0Z* and *1.1.1Z* 400 class.

Instead, the element *b1* of the upper loop thread in terms of location and size and shape corresponds to the element *Z1* of the unfolding thread, the same pattern is observed for derived elements *b1.1.1* (*Z1.1.1*). The elements are formed by a structural formula *b, Z (1) 1.1.i* and *b, Z (2) 1.1.i* differ in the position of the loop branch relative to the loops of the needle row (Figure 4). The possibility of creating new derivative elements due to the positions of the branch branch with increasing *i-th* element and >3 can also be said about the structure of *Y, Z1.3.i*. The creation of new types of stitches can be achieved by increasing the *i-th* parameter in the structure *b1.2.i* at *i >1*.

Element *b2* is identical to element *a2* - the contour of the thread of the lower loop, which in turn forms an additional 6 derivative elements of the same thread, respectively [2].

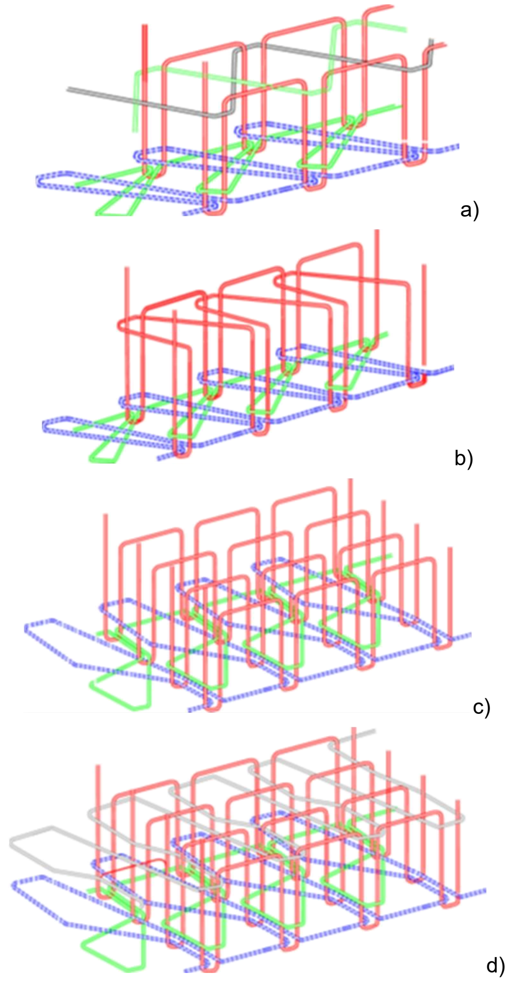

Figure 5 Structures of chain stitches based on the element *1.4.i.j*: a) six-thread cover [6]; b) four-thread cover [7]; c) six-thread flat [8]; d) semi-threaded cover [9]

The structural formula of the summary *a2.1i.j* forms elements *a2.1.0.1*, and *a2.1.1.1*, which corresponds to the elements of the thread stitch of the lower loop of types 508 and 509, the element *a2.1.1.0* is a new element that can be applied to create new types of stitches of class 500 or 800 class. When *i = 0, j = 0* is folded into the circuit *a2.1*, which is used in type 502.

In turn, the structural formulas of the reduction of the contour elements of the thread of the lower loop *a2.2.1.j* and *a2.2.2.j* at *j = 1* form derivative elements *a2.2.1.1* and *a2.2.2.1*, which are used, respectively, in the stitches of types 504 and 512. When *j = 0*, elements *a2.2.1.j* and *a2.2.2.j* are folded into elements *a2.2.1* and *a2.2.2*, which are used, respectively, in types 504 and 506. Thus, the number of elements of the needle thread - 19, the thread of the lower loop - 18, the thread of the upper loop - 5 and the thread of the unfolder - 5. Duplication of thread contour elements for these stitches is observed only in three cases - elements: *b1≡Z1, b1.2.≡ Z1.2, b1≡a2*.

In addition to changing the parameter of modifiers, as well as their number of formation of new types of stitches of the nodal structure [10-12] due to the modification of some elements of needle threads (Figure 6). The nodal structure of the stitch allows to simplify the process of formation of some stitches and the mechanisms of the lower loop, to reduce the loosening of the stitch.

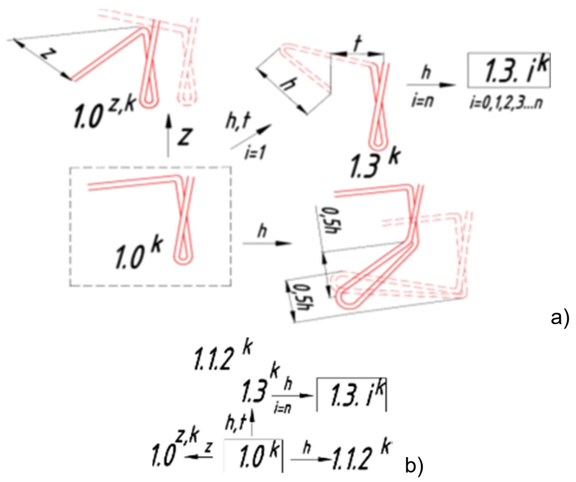

Figure 6 Hierarchical scheme of formation of contour elements of loops of a needle thread of chain stitches of knot structure: a) graphically - structural representation of elements; b) block diagram of stitch elements

Thus, increasing the number of rows of needle threads allows you to significantly expand the range of types of stitches, and the use of the knot structure of some needle threads to form new stitches knot structure. A limitation for the creation of all derived stitches is the possibility of implementing the technological process of stitch formation, ie. the possibility of reliable interaction of needles with loops.

Based on the analysis of the stitch contour element and the structure of chain stitches of classes 100, 400-600, morphological matrices of stitches are proposed, which show from which elements each stitch is formed (Tables 1-5).

From the analysis of morphological matrices it follows a possible combination of stitch elements, which is presented in the form of algorithms (Figure 7).

In turn, many combinations of thread connections of stitch elements form new types of stitches. Thus, using the basic expressions of combinatorics [21], we determine the possible number of chain stitches of each class by placing them (A_m^n).

$$A = \frac{n!}{(n-m)!} = n \cdot (n-m+1) \tag{1}$$

Assuming *i* = *p* = *0, 1, 2, 3* we obtain for elements *a1.2 ij* and *a1.4 ij* the number of placements, the number of types of stitches 400 class, formed with the main elements of needle threads *1.0* and *1.1.1*, is 118, in its turn, zigzag - 62.

Regarding chain stitches with cover thread, taking into account the possibility of implementing the process of stitch formation and *i* = *j* = *1, 2, 3* *a1.2Zi.j* the number of placements, the number of types of stitches 600 class, formed with the main elements of needle threads *1.0*, is 192, elements *1.1.1* and *a1.3 - 3*, and element *1.3.i* - 192, ie. the total number of stitches 600 type may be 387.

Table 1 Morphological matrix of class 100 stitches

Working bodies	Stitch type						
	101	**102**	**103**	**104**	**105**	**107**	**108**
The first needle	1.1	1.1.2	1.2.5.1	1.1.3	1.2.5.2	1.1^z	1.1.4
The second needle	-	1.1.2	-	-	-	-	-

Note: z index corresponds to zigzag stitches

Table 2 Morphological matrix of stitches of class 400

Working bodies	Stitch type										
	401	**402**	**403**	**404**	**405**	**406**	**407**	**408**	**409**	**410**	**411-417**
The first needle	1.0	1.0	1.0	1.1^z	1.1^z	1.0	1.0	1.0	1.1.1	1.0	1.1^z; $(1.0)^*$
The second needle	-	1.0	1.0	-	1.1^z	1.0	1.0	1.0	-	1.0	-
The third needle	-	-	1.0	-	-	-	1.0	-	-	1.0	-
The fourth needle	-	-	-	-	-	-	-	-	-	1.0	-
Lower looper	a1	a1.2.1.1	a1.2.2.2	a^z1	$a^z1.2.1.1$	a1.1.1	a1.1.2	a1; c1	a1.3	a1.1.3	a^z1; $(a1)^*$
Roofing thread	-	-	-	-	-	-	-	Z1	-	-	-

Note: * element code, which is used in conjunction with the main element of the threads to form stitches of types 413 and 415

Table 3 Morphological matrix of stitches of class 500

Working bodies	Stitch type															
	501	**502**	**503**	**504**	**505**	**506**	**507**	**508**	**509**	**510**	**511**	**512**	**513**	**514**	**521**	**522**
The first needle	1.2.5	1.0	1.2.2	1.0	1.2.1	1.2	1.2	1.0	1.0	1.2.5.01	1.2.5.1.1	1.0	1.2.5.3	1.0	1.2.3	1.2.5.4
The second needle	-	-	-	-	-	1.0	1.0	1.0	1.0	1.2.5	1.2.5.1.0	1.0	-	1.0	1.2.4	-
Lower looper	-	a2.1	a2	a2.2.1	a2.2	a2.2.2	a2.2.2	a2.1.01	a2.1.1.1	-	-	a2.2.2.1	-	a2.2.2.1	-	a1.3
The upper loop	-	-	-	b2	b1.2	b1.1	b1	-	-	-	-	b1	-	b1.1	b1.2.1	-

Table 4 Morphological matrix of stitches of class 600

Working bodies	Stitch type								
	601	602	603	604	605	606	607	608	609
The first needle	1.0	1.0	1.0	1.0	1.0	1.0	1.0	1.0	1.0
The second needle	1.3	1.0	1.0	1.0	1.0	1.0	1.0	1.0	1.0
The third needle	-	-	-	1.0	1.0	1.0	1.0	1.0	1.0
The fourth needle	-	-	-	-	-	1.0	1.0	1.0	1.0
Lower looper	a1.1.1	a1.1.1	a1.1.1	a1.1.2	a1.1.2	a,c1.2 d,e1.2´	a1.1.3	a1.1.3	a1.1.3
Roofing thread	-	Z1	Z,Y1.1.3	Z,Y1.3.1	Z1.1	$Z^{(1)}$1.1.2	$Z^{(1)}$1.1.2	Z,Y1.3.2	$Z^{(2)}$1.1.2

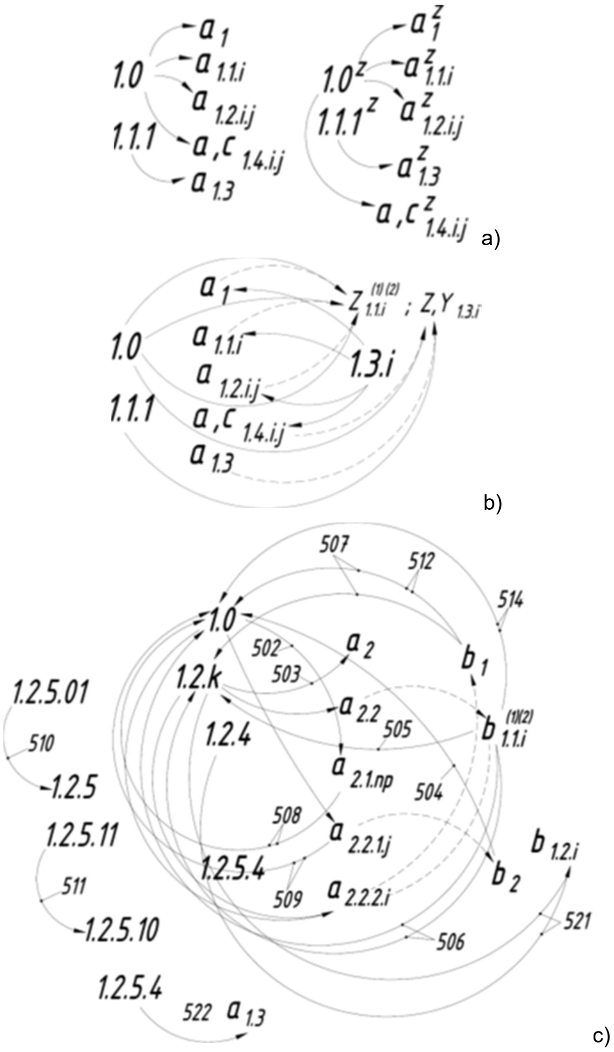

Figure 7 Graph-generator of chain stitches: a) 400 class; b) 600 class, c) 500 class

To determine the length of the stitch and the graphical representation, it is proposed to rearrange the elements of the stitch in the form of a spatial - "3D graph", its base elements and structure are presented in Figure 8. Vertices *11, 12, 13…* and *a1, a2, a3…* reflect the place of needle punctures at the distance of the stitch length *t*, above and below the materials; *11, 21* corresponds to the row spacing between two adjacent needles (*h*), m is the thickness of the materials (depending on the type of stitch may differ and depends on the trajectory of the needle during puncture), *l1,2* - lengths that determine the position of weave threads on the edges of materials and are determined by the structure of the stitch.

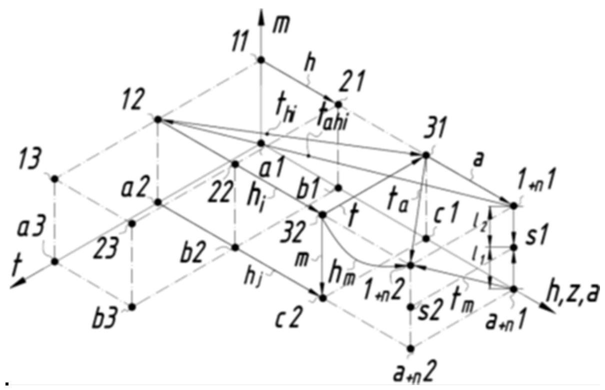

Figure 8 Base of vertices and edges of the "3D-graph" stitch

The "3D subgraphs" of each stitch element in the Table 5 show the sequence of connecting vertices (base points) with edges (elementary sections of the stitch). The length of the "3D subgraph" of the route corresponds to the cost of each thread to form a stitch element, which can be used to automatically determine the length of the stitch thread, as well as to determine the tension of threads when stretching materials, or predict the conditions of stitch tightening.

The lengths of the edges of the "3D graph" (elementary sections of the stitch elements) are determined by the expressions:

$$m' = \frac{m}{\cos\alpha}$$

$$h_i = h \cdot i \,, \ \ h_j = h \cdot j \,, \ \ h_{ia} = h \cdot i + a$$

$$t_{hi} = \sqrt{t^2 + (h \cdot i)^2} \,, \ \ t_{hj} = \sqrt{t^2 + (h \cdot j)^2}$$

$$t_{hia} = \sqrt{t^2 + (h \cdot i + a)^2}$$

$$t_a = \sqrt{t^2 + a^2} \,, \ \ t_m = \sqrt{t^2 + m^2} \,, \ \ t_z = \sqrt{t^2 + z^2}$$

$$i = 0, 1, 2, 3 \ldots n \,, \ \ j = 0, 1, 2, 3 \ldots p$$

where: m - is the thickness of the materials [mm]; m' - the thickness of the materials is equal to the stroke of the needle in the material at an angle (α) in overlocker machines when performing stitches of class 500 [mm]; h_m - is the thickness of the material when holding the loop of the thread of secret sewing machines with an arcuate needle when making stitches of type 103, 105; t - stitch length [mm]; z - is the width of the zigzag [mm]; α is the angle of the needle in the overlocker machines [°]; h - is the length of the broach (distance) between the rows of two adjacent needle threads; h_i, h_j - the length of the broach (branch) of the loops of the threads between the *i-th, j-x* needle rows, respectively, which cover the branches of the loop of the needle thread (main element 1.0) and which are covered by the vertices of their loops [mm]; n - is the number of *i-x, j-x* needle rows (*h = 0, 1, 2 i. i = 0* we have one needle row); a - width of the edging edge of the materials (distance from the edge of the materials to the near needle) [mm]; l_1, l_2 - position of weave loops of threads on the edge of the material (determined by the type of stitch) [mm]; h_{ia} - broach between the *i-th* row and the edge of the materials; t_{hi}, t_{hj}, t_z - is the diagonal broach of the loop branch, respectively, between the *i-th, j-th* rows of needle punctures along the stitch length t; t_a - is the diagonal extension of the loop branch from the edge of the material to the near needle.

Table 5 Routes of 3D graphs of stitch elements

№ p/p	Code of element	The structural formula of the stitch element	Modifier
		Routes of elements of linear stitches	
1	1.0	11(m)a1(m)11(t)12	-
2	1.1	11(m)a1(t)a2(t)a1(m)11(t)12	t
3	1.1.1.	$11(m)a1(t')a2(t')a1(m)11(t)12$	$t' \approx 0.5t$
4	1.1.2	$11(m)a1(t_h)b2(t_h)a1(m)11(t)12$	$t_h \approx 0.5h$
5	1.1.3	11(m)a1(t)a2(m)12(t)13(t)12(m)a2(t)a1(m)11(2t)13	m, t
6	1.1.4	12(m)a2(t)a1(m)11(2t)13(2t)11(m)a1(t)a2(m)12(t)13	m, t
7	1.2	11(m)a1(h)b1(h)a1(m)11(t)12	h
8	1.2.k	$11(m)a1(h_i)b1(m_k)s1(m_k)b1(h_i)a1(m)11(t)12$	m_k =0; 0,5m; k=3
9	1.2.4	$11(m)a1(h)b1(t_m)22(t_m)b1(h)a1(m)11(t)12$	h=a; t
10	1.2.5	$11(m)a1(h)b1(m)21(t_h)12(t_h)21(m)b1(h)a1(m)11(t)12$	h=a; t, h
11	1.2.5.i.j	$11(m)\ a1(h_{j+1})a_{+j+1}1(m)1_{+j+1}1(t_{hi})1_{j-i+1}2(h_i)1_{+j+1}2(t_{hj-i+1})1_{+j+1}1(m)\ a_{+j+1}1(h_{j+1})a1(m)11(t)22$	h; i=0,1, 2…n; j=0,1,2...p
12	1.2.5.1	$11(h_m)21(t_h)12(t_h)21(t_m)11(t)12$	
13	1.2.5.2	$21(t_h)12(t_m)22(t_m)12(t_h)21(t)22(t_m)32\ (t_h)23(t_h)\ 32(t_m)22(t)23$	h; t; t_m;
14	1.2.5.3	$21(l_1)s1(l_1)21(h)11(m)a1(h)b1(l_2)s1(t)s2(t)s1(l_2)b1(h)a1(m)11(t_h)22$	$l_1=l_2$=0,5m; t; h
15	1.2.5.4	$11(m)a1(m)11(h)21(m)b1(t_{hi})a2(t_{hi})b1(m)21(t_{hj})12$	m; t; h
16	1.3.	$21(m)b1(m)21(t_h)12(h)22$	h
17	1.3.i	$1_{+i}1(m)a_{+i}1(m)1_{+i}1(t_{hi})12(h_i)\ 1_{+i}2$	i=0,1,2…n
18	a1	a1(t)a2(t)a1(t)a2	
19	a1.1.i	$a_{+i}1(h_i)a1(t)a2(t)a1(t_h)a_{+1}2(t)a_{+1}1(t_h)\ a_{+2}2(t)\ a_{+2}1(t_h)\ldots\ a_{+i}2(t)\ a_{+i}1(t)a_{+i}2$	i=0,1,2...n
20	a1.2	$a1(t)a2(h)b2(t_h)a1(t)a2$	h
21	a1.2.i.j	$a_{+j}1(h_j)a1(t)a2(h_i)a_{+i}2(t_{hi})a1(h_j)a_{+j}1(t)a_{+j}2$	h; i=0,1, 2…n; j=0,1,2...p
22	a1.3	$a1(t)a2(t')s(t')a1$	$t' \approx 0.5t$
23	a1.4	$a1(t_h)b2(t_h)a1(t)a2$	h
24	a1.4.i.j	$a1(h_j)a_{+j}1(t_{hi})a_{+i+j}2(h_i)a_{+j}2(t_{hi})a_{+j}1(h_j)a1(t)a2$	h; i=0,1, 2…n; j=0,1,2...p
25	b1≡Z1	$b1(t_h)a2(t_h)b1$	h
26	$b,Z^{(1)(2)}1.1.i$	$a_{+i}1(t_{hi})a2(h_i)\ a_{+i}2$	i=0,1,2…n
27	b1.2	$b1(t_h)a2(t_h)b1(t)b2$	t
28	b1.2.i	$a_{+i}1(t_{hi})a2(t_h)b1(t)b2k1(t_{hj})a2(h_i)k1(t)k2$	j=1,2,3…p
29	$Z,Y^{(1)}1.3.i$	$a_{+i}1(t_{hi})a2(t_{hi})\ a_{+i}3$	i=0,1,2…n; t_2=2t
30	a2≡b2	$s1(l2)b1(t_h)a2(t_h)\ b1(l2)s1(t)s2$	l2=0.5m
31	a2.1	$a1(h)b1(m)21(t_h)12(t_h)21(m)b1(h)a1(t)a2$	h=a
32	a2.1.i.j	$a1(h_{j+1})a_{+j+1}1(m)1_{+j+1}1(t_{hi})1_{+j-i+1}2(h_i)1_{+j+1}2(t_{hj-i+1})1_{+j+1}1(m)\ a_{+j+1}1(h_{j+1})a1(t)a2$	h; i=0,1, 2…n; j=0,1,2...p
33	a2.2	a1(m)11(m)a1(t)a2	m
34	a2.2.1	a1(h)b1(l1)s1(l1)b1(h)a1(t)a2	h=a, l1=0.5m
35	a2.2.1.j	$a1(h_{j+1})\ a_{+j+1}1(l1)s1(l1)\ a_{+j+1}1(h_{j+1})a1(t)a2$	l1=0.5m, j=1,2,3…p
36	a2.2.2	$a1(h)b1(m)21(t)22(m)b2(t_h)a1(t)a2$	h=a; t
37	a2.2.2.j	$a1(h_{j+1})a_{+j+1}1(m)1_{+j+1}1(t)1_{+j+1}2(h_{j+1})a1(t)a2$	h; j=0,1,2...p
		Routes of elements of zigzag stitches	
38	1.0^z	$11(m)a1(m)11(t_z)22$	z; $t_{z\equiv}t_h$
39	1.1^z	$11(m)a1(t_z)b2(t_z)a1(m)11(t_z)22$	z
40	$1.1.1^z$	$11(m)a1(t'_z)b2(t'_z)a1(m)11(t_z)22$	z; $t' \approx 0.5t$
41	$1.1.3^z$	$11(m)a1(t_z)b2(m)22(t_z)33(t_z)22(m)b2(t_z)a1(m)11(2t_z)33$	z
42	$1.1.4^z$	$22(m)b2(t_z)a1(m)11(2t_z)33(2t_z)11(m)a1(t_z)b2(m)22(t_z)33$	z
38	1.0^z	$11(m)a1(m)11(t_z)22$	z; $t_{z\equiv}t_h$
43	$a1^z$	a1(t)b2(t)a1(t)b2	z
44	$a1.1.i^z$	$a_{+i}1(h_i)a1(t_z)a_{+1}2(t_z)a1(t_{z+1})a_{+2}2(t_z)a_{+1}1(t_{z+1})\ a_{+3}2(t_h)\ a_{+2}1\ldots(t_{z+1})a_{+i+1}2(t_z)\ a_{+i}1(t_z)a_{+i}2$	z; i=0,1,2...n
45	$a1.2.i.j^z$	$a_{+j}1(h_j)a1(t_z)a_{+j-j}1(h_i)a_{+i+1}2(t_{hi+1})a1(h_j)a_{+j}1(t_z)a_{+j}2$	z; i=0,1, 2…n;
46	$a1.3^z$	$a1(t_z)b2(t_z')s(t_z')a2$	$t_z' \approx 0.5\ t_z$

A certain combination of stitch elements in turn forms the stitch structure, and the total length of the contours of the elements reflects the number of specific threads that are earned in one stitch, and can be determined geometrically and adjusted by factors that take into account the properties of materials and threads. It should be noted that the actual length of the thread in the stitch depends on certain factors (deformation of materials, thread stiffness, twisting, etc.), geometries of thread guides, laws of motion of thread feeders, coordinated interaction of loop-forming bodies, etc.

Also, the "3D graph" of each stitch element (Table 5) can be represented by the incidence matrix Gi [22] in which the coordinate axis (X, Y, Z) are represented by edges along the ordinates (*t, h, m*), which allows not only to show the incidence of vertices, and the direction of the contour of a particular thread in the stitch element, which can be used to determine the flow of threads in the stitch, the force of their tension, etc.

$$G_i = (V, X),\quad V = \{v_1, \dots v_n\},\quad X = \{x_1, \dots x_k\} \tag{2}$$

$$G_i = \begin{pmatrix} a_{11} & a_{12} & \cdots & a_{1k} \\ a_{21} & a_{22} & \cdots & a_{2k} \\ \cdots & \cdots & \cdots & \cdots \\ a_{n1} & a_{n2} & \cdots & a_{nk} \end{pmatrix}$$

$$a_{ij} = \begin{cases} 1, \mathit{if}\ x_j\ \mathit{then\ i з}\ v_i \\ -1, \mathit{if}\ x_j\ \mathit{then\ in}\ v_i \\ 0, \mathit{if}\ x_j \text{not incidental}\, v_i \end{cases}$$

where: G_i - incident matrix of the element of the *i-th* stitch, *V* - vertices of the graph (*11, 12, 1.3 … n1, n2, n3… a1, a2, … s1, s2… n+1, a+p* - depending on the structure of the stitch element (Figure 7)); *X* - the edges of the graph (*m, m´, t, l, h*).

A full description of the stitch structure by the incidence matrix *G* "3D graph" can be found by combining the incidence matrices of 3D/2D subgraphs, which express certain elements of the stitch:

$$G = G_1 \ldots \cup G_n \cup G_A \ldots \cup G_n \cup G_B \cup G_Z \cup G_Y \tag{3}$$

where: $G_1 \ldots G_n$ - incident matrix 3D subgraph of the *i-th* needle thread; $G_A \ldots G_n$ - incidental matrix 3D/2D subgraph of the *i-th* element of the lower loop thread; G_B - incident matrix 3D/2D subgraph of the *i-th* element of the thread of the upper loop; G_Z, G_Y - incident matrix of 2D subgraph of the *i-th* element of threads *Z* and *Y* of the top cover spreader.

The general incident matrix in accordance with the vertices *V* and edges *N* will look like:

$$G = \begin{pmatrix} & 11 & 12 & \ldots & n1 & n2 & a1 & a2 & \ldots & n1 & n2 & \ldots & s1 & s2 & \ldots \\ t & \cdot & \cdot & \cdot & \cdot & \cdot & \cdot & \cdot & \cdot & \cdot & \cdot & \cdot & \cdot & \cdot & \cdot \\ m, m', m'' & \cdot & \cdot & \cdot & \cdot & \cdot & \cdot & \cdot & \cdot & \cdot & \cdot & \cdot & \cdot & \cdot & \cdot \\ h, z, a & \cdot & \cdot & \cdot & \cdot & \cdot & \cdot & \cdot & \cdot & \cdot & \cdot & \cdot & \cdot & \cdot & \cdot \\ t_{h_i}, t_{h_j}, t_a & \cdot & \cdot & \cdot & \cdot & \cdot & \cdot & \cdot & \cdot & \cdot & \cdot & \cdot & \cdot & \cdot & \cdot \\ l_1 & \cdot & \cdot & \cdot & \cdot & \cdot & \cdot & \cdot & \cdot & \cdot & \cdot & \cdot & \cdot & \cdot & \cdot \\ l_2 & \cdot & \cdot & \cdot & \cdot & \cdot & \cdot & \cdot & \cdot & \cdot & \cdot & \cdot & \cdot & \cdot & \cdot \end{pmatrix} \tag{4}$$

Consider similar structures of stitches of type 402 and 403 (Figures. 9 and 10), which differ only in the presence in the stitch of type 403 of the third needle thread and loop thread - *a1.1.2*.

Then the incidence matrices (correct all terms) for stitch elements of type 402 and 403 using (2) for the needle thread of the loop we get:

$$G^{402}_{1;2} = \begin{pmatrix} & 11 & 12 & 21 & 22 & a1 & a2 & b1 & b2 \\ t & 1 & -1 & 1 & -1 & 0 & 0 & 0 & 0 \\ m & 1;-1 & 1;-1 & 1;-1 & 1;-1 & -1;1 & -1;1 & -1;1 & -1;1 \end{pmatrix}$$

$$G^{402}_{a1.1.2} = \begin{pmatrix} & a1 & a2 & b1 & b2 \\ t & 1 & -1 & 1 & -1 \\ h & -1,1 & 1 & 1,-1 & -1 \\ t_{h,i=1} & -1 & 0 & 0 & 1 \end{pmatrix}$$

$$G^{403}_{1;2;3} = \begin{pmatrix} & 11 & 12 & 21 & 22 & 31 & 32 & a1 & a2 & b1 & b2 & c1 & c2 \\ t & 1 & -1 & 1 & -1 & 1 & -1 & 0 & 0 & 0 & 0 & 0 & 0 \\ m & 1;-1 & 1;-1 & 1;-1 & 1;-1 & 1;-1 & 1;-1 & -1;1 & -1;1 & -1;1 & -1;1 & -1;1 & -1;1 \end{pmatrix}$$

$$G^{403}_{a1.1.2} = \begin{pmatrix} & a1 & a2 & b1 & b2 & c1 & c2 \\ t & 1 & -1 & 0 & 0 & 1 & -1 \\ h & -1,1 & 1 & 1,-1 & -1,1 & 1,-1 & -1 \\ t_{h,i=2} & -1 & 0 & 0 & 0 & 0 & 1 \end{pmatrix}$$

By expression (3) we obtain the intensity matrices (4) for stitches of type 402 and 403:

$$G^{402} = G^{402}_{1;2} \cup G^{402}_{a1.1.2},\qquad G^{403} = G^{403}_{1;2;3} \cup G^{403}_{a1.1.2}$$

$$G^{402} = \begin{pmatrix} & 11 & 12 & 21 & 22 & a1 & a2 & b1 & b2 \\ t & 1 & -1 & 1 & -1 & 1 & -1 & 1 & -1 \\ m & 1;-1 & 1;-1 & 1;-1 & 1;-1 & -1;1 & -1;1 & -1;1 & -1;1 \\ h & 0 & 0 & 0 & 0 & -1,1 & 1 & 1,-1 & -1 \\ t_{h,i=1} & 0 & 0 & 0 & 0 & -1 & 0 & 0 & 1 \end{pmatrix}$$

$$G^{403} = \begin{pmatrix} & 11 & 12 & 21 & 22 & 13 & 32 & a1 & a2 & b1 & b2 & c1 & c2 \\ t & 1 & -1 & 1 & -1 & 1 & -1 & 1 & -1 & 0 & 0 & 1 & -1 \\ m & 1;-1 & 1;-1 & 1;-1 & 1;-1 & 1;-1 & 1;-1 & -1;1 & -1;1 & -1;1 & -1;1 & -1;1 & -1;1 \\ h & 0 & 0 & 0 & 0 & 0 & 0 & -1;1 & 1 & 1;-1 & -1;1 & 1;-1 & -1 \\ t_{h,i=2} & 0 & 0 & 0 & 0 & 0 & 0 & -1 & 0 & 0 & 0 & 0 & 1 \end{pmatrix}$$

For analogy of the intensity matrix for stitches of type 504 and 606 (Figures 11 and 12).

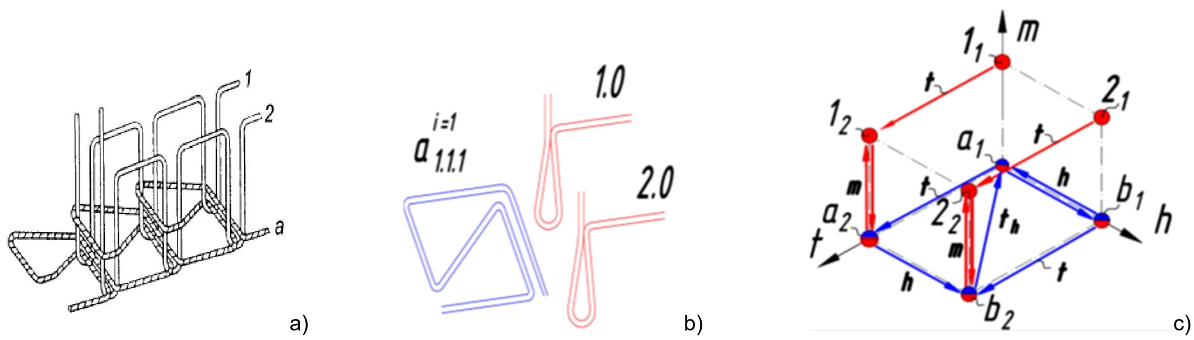

Figure 9 Topological analysis of stitch type 402: a) stitch structure; b) stitch elements; c) "3D-graph" stitch

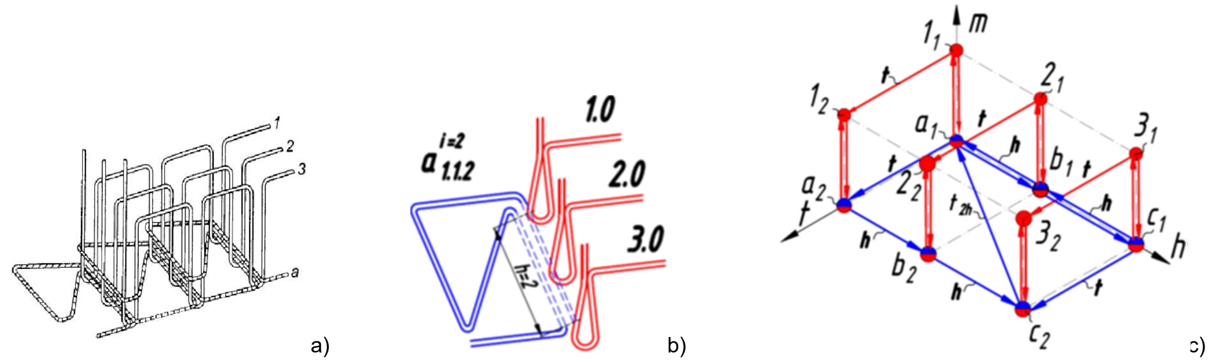

Figure 10 Topological analysis of stitch type 403: a) stitch structure, b) stitch elements, c) "3D graph" stitch

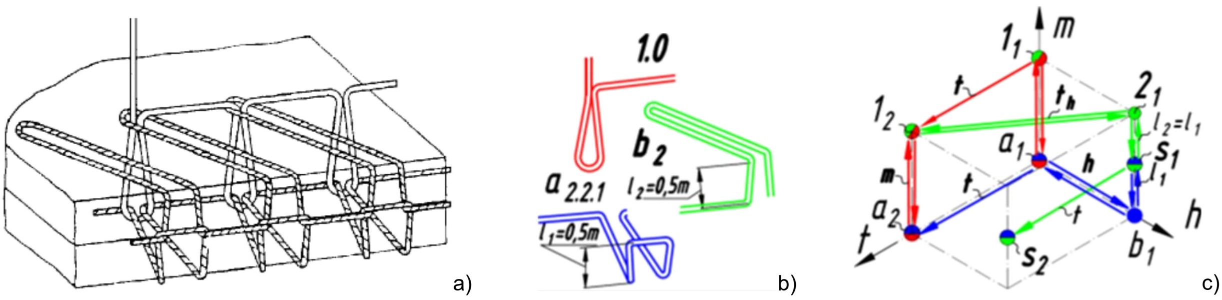

Figure 11 Topological analysis of the stitch type 504: a) stitch structure, b) stitch elements, c) "3D - graph" stitch

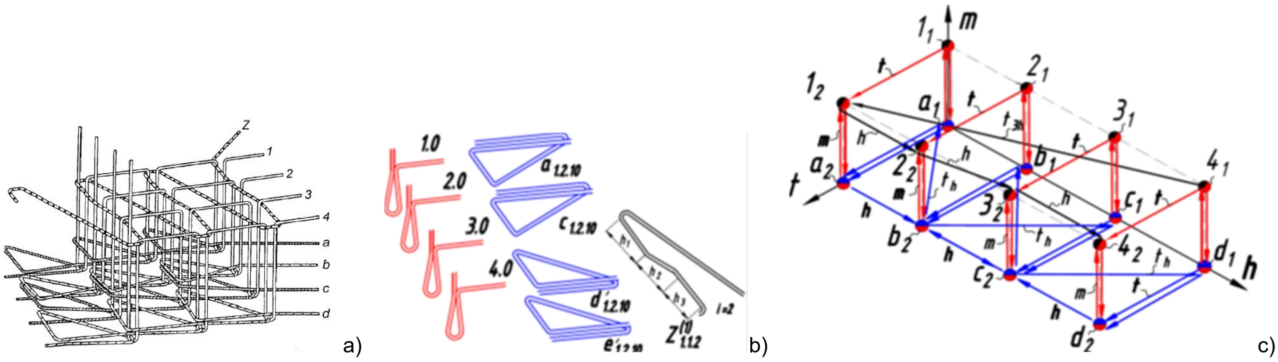

Figure 12 Topological analysis of the stitch type 606: a) stitch structure; b) stitch elements; c) "3D - graph" stitch

Then the intensity matrices for stitch elements of type 504 and 606, similarly applying (2) to the needle thread of loops and cover thread we get:

$$G^{504}_{1} = \begin{array}{c@{}c} & \begin{matrix} 11 & 12 & a1 & a2 \end{matrix} \\ \begin{matrix} t \\ m \end{matrix} & \begin{pmatrix} 1 & -1 & 0 & 0 \\ 1;-1 & 1;-1 & -1;1 & -1;1 \end{pmatrix} \end{array} \qquad G^{504}_{b_2} = \begin{array}{c@{}c} & \begin{matrix} s1 & 21 & 12 & s2 \end{matrix} \\ \begin{matrix} l2 \\ t_{h,j=1} \\ t \end{matrix} & \begin{pmatrix} 1;-1 & -1;1 & 0 & 0 \\ 0 & 1;-1 & -1,1 & 0 \\ 1 & 0 & 0 & -1 \end{pmatrix} \end{array} \qquad G^{504}_{a2.2.1} = \begin{array}{c@{}c} & \begin{matrix} a1 & b1 & s1 & a2 \end{matrix} \\ \begin{matrix} a=h \\ l_1 \\ t \end{matrix} & \begin{pmatrix} 1;-1 & -1;1 & 0 & 0 \\ 0 & 1;-1 & -1,1 & 0 \\ 1 & 0 & 0 & -1 \end{pmatrix} \end{array}$$

$$G^{606}_{1;2;3;4} = \begin{array}{c@{}c} & \begin{matrix} 11 & 12 & 21 & 22 & 31 & 32 & 41 & 42 & a1 & a2 & b1 & b2 & c1 & c2 & d1 & d2 \end{matrix} \\ \begin{matrix} t \\ m \end{matrix} & \begin{pmatrix} 1 & -1 & 1 & -1 & 1 & -1 & 1 & -1 & 0 & 0 & 0 & 0 & 0 & 0 & 0 & 0 \\ 1;-1 & 1;-1 & 1;-1 & 1;-1 & 1;-1 & 1;-1 & 1;-1 & 1;-1 & -1;1 & -1;1 & -1;1 & -1;1 & -1;1 & -1;1 & -1;1 & -1;1 \end{pmatrix} \end{array}$$

$$G^{606}_{\substack{a1.2.10 \\ c1.2.10 \\ d1.2.10 \\ e1.2.10}} = \begin{array}{c@{}c} & \begin{matrix} 11 & 12 & 21 & 22 & 31 & 32 & 41 & 42 & a1 & a2 & b1 & b2 & c1 & c2 & d1 & d2 \end{matrix} \\ \begin{matrix} t \\ m \\ h \\ t_{h,i=1} \end{matrix} & \begin{pmatrix} 0 & 0 & 0 & 0 & 0 & 0 & 0 & 0 & 2 & -2 & 2 & -2 & 2 & -2 & 2 & -2 \\ 0 & 0 & 0 & 0 & 0 & 0 & 0 & 0 & 0 & 0 & 0 & 0 & 0 & 0 & 0 & 0 \\ 0 & 0 & 0 & 0 & 0 & 0 & 0 & 0 & 0 & 1 & 0 & -2;1 & 0 & -2;1 & 0 & 1 \\ 0 & 0 & 0 & 0 & 0 & 0 & 0 & 0 & -1 & 0 & -1 & 2 & -1 & 2 & -1 & 0 \end{pmatrix} \end{array}$$

$$G^{606}_{Z^{(1)}_{1.1.2}} = \begin{array}{c@{}c} & \begin{matrix} 11 & 12 & 21 & 22 & 31 & 32 & 41 & 42 \end{matrix} \\ \begin{matrix} h \\ t_{h,i=3} \end{matrix} & \begin{pmatrix} 0 & 1 & 0 & 1;-1 & 0 & 1;-1 & 0 & -1 \\ 0 & -1 & 0 & 0 & 0 & 0 & 0 & 1 \end{pmatrix} \end{array}$$

Then the intensity matrices for stitches of types 504 and 606:

$$G^{504} = G^{504}_{1} \cup G^{504}_{a2.2.1} \qquad G^{606} = G^{606}_{1;2;3;4} \cup G^{606}_{\substack{a1.2.10 \\ c1.2.10 \\ d1.2.10 \\ e1.2.10}} \cup G^{606}_{Z^{(1)}_{1.1.2}}$$

$$G^{504} = \begin{array}{c@{}c} & \begin{matrix} 11 & 12 & 21 & 22 & a1 & a2 & b1 & b2 & s1 & s2 \end{matrix} \\ \begin{matrix} t \\ m \\ a \\ t_{h,i=1} \\ l_1 \\ l_2 \end{matrix} & \begin{pmatrix} 1 & -1 & 0 & 0 & 1 & -1 & 0 & 0 & 1 & -1 \\ 0 & 1;-1 & 0 & 0 & 0 & -1;1 & 0 & 0 & 0 & 0 \\ 0 & 0 & 0 & 0 & 1;-1 & 0 & -1;1 & 0\ 0 & 0 & 0 \\ 0 & -1;1 & 1;-1 & 0 & 0 & 0 & 0 & 0 & 0 & 0 \\ 0 & 0 & 0 & 0 & 0 & 0 & 1;-1 & 0 & -1;1 & 0 \\ 0 & 0 & -1;1 & 0 & 0 & 0 & 0 & 0 & 1;-1 & 0 \end{pmatrix} \end{array}$$

$$G^{606} = \begin{array}{c@{}c} & \begin{matrix} 11 & 12 & 21 & 22 & 31 & 32 & 41 & 42 & a1 & a2 & b1 & b2 & c1 & c2 & d1 & d2 \end{matrix} \\ \begin{matrix} t \\ m \\ h \\ t_{h,i=1} \\ t_{h,i=3} \end{matrix} & \begin{pmatrix} 1 & -1 & 1 & -1 & 1 & -1 & 1 & -1 & 2 & -2 & 2 & -2 & 2 & -2 & 2 & -2 \\ 0 & 1;-1 & 0 & 1;-1 & 0 & 1;-1 & 0 & 1;-1 & 0 & -1;1 & 0 & -1;1 & 0 & -1;1 & 0 & -1;1 \\ 0 & 1 & 0 & -1;1 & 0 & -1;1 & 0 & -1 & 0 & 1 & 0 & -2;1 & 0 & -2;1 & 0 & -1 \\ 0 & 0 & 0 & 0 & 0 & 0 & 0 & 0 & -1 & 0 & -1 & 2 & -1 & 2 & -1 & 0 \\ 0 & -1 & 0 & 0 & 0 & 0 & 1 & 0 & 0 & 0 & 0 & 0 & 0 & 0 & 0 & 0 \end{pmatrix} \end{array}$$

4 CONCLUSIONS

The performed topological analysis of chain stitch structures of classes 100, 400, 500, 600, 800 provides an opportunity to determine the hierarchical heredity of stitch elements origin and their formation, which can be used to establish patterns of stitch structure formation, its classification, etc.

The obtained morphological matrices of stitch structure allow to reveal the affiliation of the application of certain elements to a particular stitch, which can be used to build a relational database of chain stitches, system analysis of stitches and additions and extensions DSTU ISO 4915: 2015.

The obtained combinations of possible relationships of stitch elements allow to form a generator of possible stitch structures, which allows the formation of new stitch structures of different classes and properties.

The obtained "3D-graphs" and structural formulas of stitch types of classes 100, 400-600 and 800 allow to determine the length of each thread in the stitch, and, accordingly, the cost of threads per stitch. In addition, the results can be used to graphically interpret a particular stitch structure using computer technology, as well as to model dynamic parameters such as stitch and yarn deformation, yarn strength, stitch formation conditions, and so on.

5 REFERENCES

1. Shalov I.I., Dalidovich A.S., Kudryavin L.A.: Knitwear technology, Legprombytizdat, 1986, 376 p. (in Russian)
2. DSTU ISO 4915: 2015 Textile materials. Types of seams
3. Pat. 110547 of Ukraine, IPC D05B 1/08 (2006.01). Method of formation of four-thread flat chain stitch, O.P. Manoilenko, V.A. Gorobets, u201604692; publ. 10.10.2016, Bull. № 19
4. Pat. 120041 of Ukraine, IPC D05B 1/08 (2006.01). The method of formation of a three-threaded chain zigzag stitch, O.P. Manoilenko, V.A. Gorobets, V.M. Dvorzhak, O.O. Samsonenko, u201702623; publ. 10.25.2017, Bull. № 20
5. Pat. 140286 of Ukraine, IPC D05B 93/00, D05B 1/08 (2006.01). The method of formation of a multi-threaded cover chain stitch, O.P. Manoilenko, V.A. Gorobets, A.V. Evdokimenko, I.M. Fedko, V.D. Katselivsky, u201908331; publ. 10.02.2020, Bull. № 3
6. Pat. 139313 of Ukraine, IPC D05B 1/08 (2006.01). The method of formation of a six-threaded cover chain stitch, O.P. Manoilenko, V.A. Gorobets, A.V. Romanchenko, u201907149; publ. 12.26.2019, Bull. № 24
7. Pat. 139944 of Ukraine, IPC D05B 93/00, D05B 1/08 (2006.01). The method of formation of a multi-threaded cover chain stitch, O.P. Manoilenko, V.A. Gorobets, A.H. Hudym, K.A. Bylyk, V.V. Kolisnyk, u201908328; publ. 27.01.2020, Bull. № 2
8. Pat. 140443 of Ukraine, IPC D05B 93/00, D05B 1/08 (2006.01). The method of formation of a multi-threaded cover chain stitch, O.P. Manoilenko, V.A. Gorobet, V.Yu. Shcherban, H.V. Koshel, D.V. Vladymyrchuk, u201908541; publ. 25.02.2020, Bull. № 4
9. Pat. 140430 of Ukraine, IPC D05B 93/00, D05B 1/08 (2006.01). The method of formation of a multi-threaded cover chain stitch, O.P. Manoilenko, V.A. Gorobets, D.Yu. Waldowski, u201908332; publ. 25.02.2020, Bull. № 4
10. Pat. 114319 of Ukraine, IPC D05B 1/00 (2006.01). Method of formation of two-thread flat chain stitch, .V.A Gorobets, O.P. Manoilenko, S.A. Popovichenko, D.V. Logvinov, u201607976; publ. 10.03.2017, Bull. № 5
11. Pat. 139314 of Ukraine, IPC D05B 1/08 (2006.01). Method of formation of four-thread covering chain stitch, O.P. Manoilenko, V.A. Gorobets V.Yu. Shcherban, L.M. Berezin, A.A. Khandriko, u201907153; publ. 26.12.2019, Bull. № 24
12. Pat. 139627 of Ukraine, IPC D05B 1/08 (2006.01). Method of formation of double-threaded flat chain stitch, O.P. Manoilenko, V.A. Gorobet, and others, u201907158; publ. 10.01.2020, Bull. № 1
13. Nayak R., Padhye R. (Eds.): Garment manufacturing technology, Woodhead Publishing, Cambridge, 2015, 498 p., https://doi.org/10.1016/C2013-0-16494-X
14. Ermakov A.S.: Design of mechanisms of edge-marking machines of service enterprises, Monograph, FGOUVPO "RGUTiS", 2009, 290 p. (in Russian)
15. Ermakov A.S., Ermakov S.: Design of flexible sewing technological systems, LAP LAMBERT Academic Publishing, 2012, 308 p. (in Russian)
16. Koketkin P.P., Kochegura T.N., Baryshikova V.I., et al.: Industrial clothing technology, Right 640chnik, Legprombytizdat, 1988, 640 p. (in Russian)
17. Savostitsky A.V., Melichov E.H.: Technology of Garments: a Textbook for Universities, Light and Food Industry, 1982, 440 p. (in Russian)
18. Rasheed A., Ahmad S., Ali N., ur Rehman A., Ramzan M.B.: Geometrical model to calculate the consumption of sewing thread for 504 over-edge stitch, Journal of the Textile Institute 109(11), 2018, pp. 1418-1423, https://doi.org/10.1080/00405000.2018.1423902
19. Glushkova T.V. Automated calculation of thread consumption per product, Sewing Industry № 6., 2001, pp. 35-36, ISSN 0132-0955 (in Russian)
20. Polukhin V.P., Reibarh L.B.: Sewing machines of a chain stitch, Moscow: Light industry, 1976, 352 p. (in Russian)
21. Anderson J.: Discrete Mathematics with Combinatorics, Prentice Hall, US, 2003, 784 p., ISBN: 9780130457912
22. Wilson R.: Introduction to Graph Theory, 5th ed., Dialectics, 2019, 240 p. (in Russian)

THE EFFECTS OF DIFFERENT FIBER TYPES ON THE PERFORMANCE PROPERTIES OF THE LINING FABRIC

Okşan Oral and Esra Dirgar

Ege University, Bergama Technical and Business College, Bergama 35700, Izmir, Turkey
oksan.kansoy@ege.edu.tr; esra.dirgar@ege.edu.tr

Abstract: *In this study, the effects of different fiber types (regenerated cellulose fibers and synthetic fibers) on the properties of the lining fabric to be produced were investigated. Weight, seam slippage, strength, friction, drape properties of fabrics to be produced from different fibers (PES, PES/Lycra, Acetate, Rayon and Cupro) were examined. In addition to the important strength properties of the linings made of synthetic fibers, there are disadvantages such as draping and seam slippage. The lining made of Cupro fiber used in this research eliminates these disadvantages and offers an important alternative.*

Keywords: *Lining fabric, tensile strength, tearing strength, fabric drape, friction coefficient, seam slippage.*

1 INTRODUCTION

Lining has an important role in auxiliary materials and accessories in clothing. Lining is a fabric that has a weight and a handle suitable for the type and usage characteristics of the upper fabric and covers some or all of the inside of the garment.The lining is a separate piece of fabric that is attached to the garment from all edges (such as men's suits, coats, jackets) or combined freely (such as skirts) in accordance with the model of the garment [1].

Performance characteristics expected from the lining vary depending on the product type and end use. For example, the properties expected from a lining used in a jacket are different from those expected from a lining used in a swimsuit.

The main factors affecting the quality and performance of lining fabrics are as follows:

- fabric properties,
- pattern,
- compatibility with upper fabric and other materials, and
- suitability for end use [2].

The lining also provides suitability for clothing and thermal comfort. As they are smooth, moisture absorbent and soft, they provide handle comfort.

Kawabata examined the effects of lining properties of skirts upon comfort and movement. The comfort of lining fabrics and real skirts with and without lining was rated by sensory tests on the basis of sensorial comfort on the skin and body movement. Actual body movements were investigated by motion analysis while the skirts were being worn. Cuprammonium rayon (Cupro) and polyester fiber lining results are compared [3].

Ünal has investigated the fabrics commonly used for lining children's clothing. By obtaining these fabrics, their physical properties and comfort properties were evaluated with various tests. As a result, the most comfortable lining fabric recommendation has been made [4].

Özdil determined tear strength which one of the most important strength property of the fabrics were determined by using plain, twill, satin and ribs fabrics, produced with 100% cotton and 50/50% cotton/PES yarns. The results of tear strength testing were compared according to the fabric structure, material and measurement method statistically [5].

Can examined the yarn characteristics affecting the tear strength of plain fabrics. For this purpose, tear strengths of 17 different plain fabrics were measured. According to the results, yarn count, twist and strength affect the fabric tear strength. Approximately 80% of the change in tear strength can be explained by the change in yarn characteristics [6].

Öztürk examined the effect of weave type and weft density parameters on the surface roughness and friction coefficient [7].

Plattürk aimed to summarize the recent studies and investigate the fabric drape and its relation with the bending rigidity and stated innovations in the measurement of these parameters [8]

Kuyucu examined the effects of sewing parameters on seam strength in 100% polyester lining fabric. Eight different sewing threads, two stitch needles with different thickness, two different stitch tightness and three different fabric directions have been used at the fabric sewing moment [9].

Dirgar investigated performance properties of single jersey knitted fabrics made from viscose, modal, lyocell and cupro. Performance properties of the fabrics such as fabric weight per unit area, thickness, bursting strength, abrasion resistance, fabric stretch, porosity, air permeability and pilling were evaluated statistically and the importance levels of the relationship between the measured parameters were determined [10].

In this study weight, seam slippage, strength, friction, drape properties of fabrics to be produced from different fibers (PES, PES/Lycra, Acetate, Rayon and Cupro) were examined. In addition to the important strength properties of the linings made of synthetic fibers, there are disadvantages such as draping and seam slippage. The lining made of Cupro fiber used in this research eliminates these disadvantages and offers an important alternative.

2 MATERIALS AND METHODS

The aim of the study is to examine classical lining fabrics that are available in the market and widely used in the garments. For this purpose, lining fabrics produced from PES, PES/Lycra (97/3%), Acetate and Rayon fibers were examined. In addition, Cupro lining fabric, which is used today as an alternative to these fabrics, but which is not widespread due to its high price, was also examined.

Before testing, all fabric samples were conditioned for 24 hours under the standard atmospheric conditions (20±2°C temperatures, 65±5% relative humidity).

Firstly, the values (yarn count, types of fabric weave, weight, weft and warp density) of the lining fabrics obtained from the market were determined. Than, the fabric properties (tensile strength, tearing strength, fabric drape, friction coefficient, seam slippage) that will affect the performance characteristics of the lining fabric were examined.

Weft and warp yarn number determination in yarns taken out of the fabric was made according to TS EN 14970 standard.

Type of fabric weave was determined using a suitable magnifying glass.

The weight (g/m²) of the fabrics was made according to TS 251 standard.

The fabrics were cut with a grams per square meter cutter of 100 cm² and weighed on a precision digital scale. The weft and warp yarn count of the fabric was made according to TS 250 EN 1049-2. A loupe of 1 cm² is used for this procedure.

According to the TS EN ISO 13934-2 - Grap test, the tensile strength tests were carried out separately in the direction of weft and warp.

Tearing strength of fabrics was performed according to TS EN ISO 13937-1 standard on Jeames Heal trademark Model Elmatear instrument by ballistic pendulum method.

In the research, the fabric drap was measured according to the TS 9693 standard. Image analysis method was used to measure the fabric drape of lining fabrics.

In this research, the friction coefficient was determined with the Frictorq Device used in the determination of dynamic friction coefficient.

In the study, the seam slippage test was performed according to the TS EN ISO 13936-1 seam slippage method. The analysis of the test results were evaluated in the SPSS 25.0 statistical program at 0.05 significance level and the performance characteristics of lining fabrics produced from different fiber types were investigated.

3 RESULTS

The properties of the lining fabrics used are shown in Table 1. The tensile and tearing strength values of the lining fabrics used in the study in the weft and warp directions are given in Table 2.

Table 1 Characteristics of lining fabrics

Fabrics	Yarn count [Nm]		Type of fabric weave	Weight [g/m²]	Density	
	weft	warp			weft [picks/cm]	warp [ends/cm]
PES	111	109	1/1 Plain	54.42	26	34
PES/LYCRA	156	168	2/1 Twill	72.7	39	66
ACETATE	111	109	2/1 Twill	80.5	27.5	61.5
RAYON	67	75	2/1 Twill	92.4	25	46
CUPRO	116	113	1/1 Plain	72.18	35.5	50

Table 2 Tensile and tearing strength of lining fabrics

Fabrics	Tensile strength [N]		Tearing strength [N]	
	warp	weft	warp	weft
PES	438.42	354.89	31.16	40.70
PES/LYCRA	432.84	277.24	11.01	15.47
ACETATE	133.38	77.18	4.71	6.73
RAYON	239.50	129.28	18.21	23.67
CUPRO	103.41	101.71	8.96	12.33

When Table 2 is examined; considering the tensile strength values, it was observed that the weft and warp tensile strengths of the fabrics woven from PES and PES/LYCRA fibers were the highest. When the tearing strength values were examined, it was found that the fabric woven from PES fibers was the highest (Figures 1 and 2).

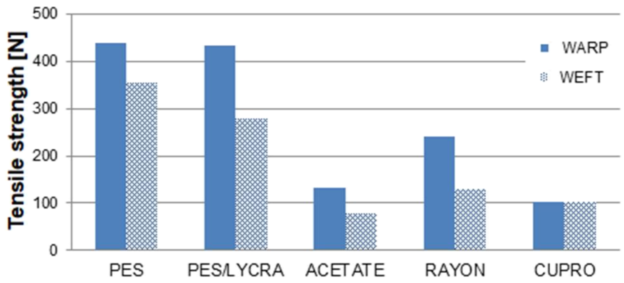

Figure 1 Tensile strength of lining fabric

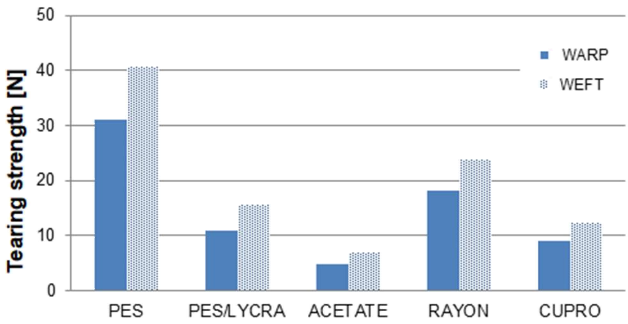

Figure 2 Tearing strength of lining fabric

In Table 3, the fabric drape and friction coefficient values of the lining fabrics used in the study are shown.

Table 3 Fabric drape and friction coefficient values of lining fabrics

Fabrics	Drape coefficient [%]	Friction coefficient [μ kinetic]
PES	52	0.222
PES/LYCRA	38	0.213
ACETATE	33	0.151
RAYON	34	0.160
CUPRO	27	0.155

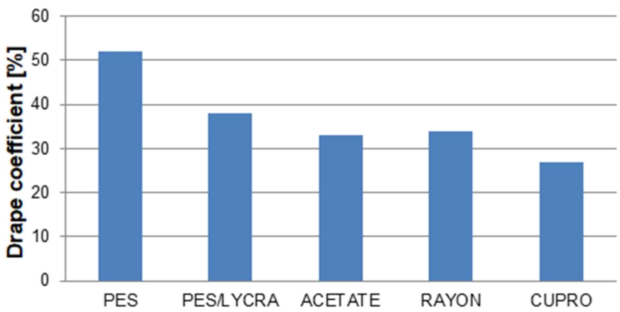

Figure 3 Drape of lining fabric

When Table 3 is examined, the fabric with the lowest drape coefficient is the fabric made of Cupro fibers. The lower the drape coefficient, the higher the drape of the fabric. Cupro has the best drape lining fabric feature (Figure 3).

One of the most important parameters affecting the drape is weight. Correlation analysis was performed to determine the direction and strength of the relationship between Cupro lining fabric and weight. When Table 4 is examined, it was determined that there was a “high” (r = 0.867), positive and significant relationship between fabric drape and weight. (According to the Pearson Correlation scale: r = 0-0.25 very weak, 0.26-0.49 weak, 0.50-0.69 medium, 0.7-0.89 high, 0.9-1.0 very high).

Table 4 Correlation analysis of Cupro lining fabric

Fabric drape	Weight
Pearson correlation (r)	0.867

Correlation is significant at the 0.05 level (2-tailed).

When the friction coefficient values were analyzed, it was observed that the fabrics with the lowest value were fabrics made of Acetate, Cupro and Rayon fiber. This result shows that the Acetate, Cupro and Rayon fabrics surfaces are smoother (Figure 4).

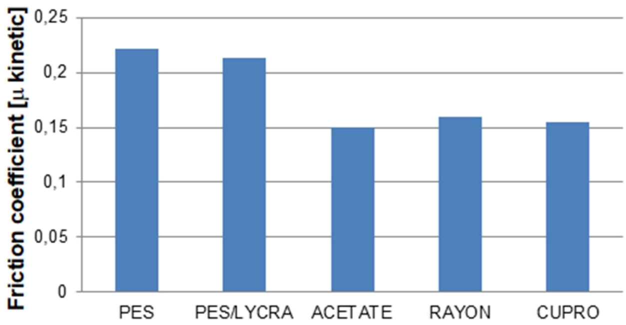

Figure 4 Friction coefficient of lining fabric

Correlation analysis was performed to determine whether there is a relationship between friction coefficient and tearing strength. The lining fabric with the highest friction coefficient is PES (Figure 4). It was determined that there is a "very weak" (r = -0.246) negative relationship between the friction coefficient of PES and the weft tearing strength. It was determined that there is a “high” (r = 0.869) positive relationship between the friction coefficient of PES and the warp tearing strength (Table 5).

Table 5 Correlation analysis of PES lining fabric

Friction coefficient	Weft tearing strength	Warp tearing strength
Pearson correlation (r)	-0.246	0.869

Seam slippage often occurs on fabrics containing slippery threads or on low density fabrics. Therefore, it is seen that in this type of fabrics, a group of threads in the fabric structure can be easily pulled over the other. Parameters such as seam allowance, stitch type and stitch density also affect this problem. These parameters are kept constant in seam slippage tests.

When Table 6 is examined, it is seen that the seam slippage strength of fabrics made of PES/LYCRA and Cupro fibers is the highest. The higher the seam slippage value, the more resistant the fabric is in terms of seam slippage. This makes PES/LYCRA and Cupro fabrics a great advantage in terms of seam slippage during use (Figure 5).

Table 6 Seam slippage values of lining fabrics

Fabrics	Seam slippage [N]	
	warp	weft
PES	29.3	65.3
PES/LYCRA	>200	>200
ACETATE	87.3	174
RAYON	62	148.5
CUPRO	158.7	>200

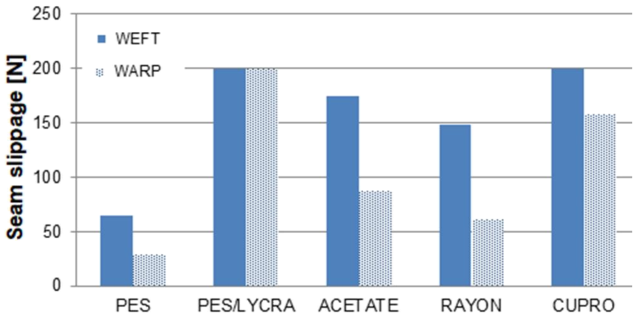

Figure 5 Seam slippage of lining fabric

4 CONCLUSIONS

Lining fabrics are one of the auxiliary materials that complement the garment. Lining fabrics affect the usage, properties, mobility and duration of use of the garment. They provide comfort to the user like a second garment inside the main fabric. Lining fabrics are woven from different yarns, in different types of weaving and are made suitable for final consumption with different finishing processes.

The wrong choice of lining causes huge problems in clothes. Lining fabrics act as a whole with the garment in which they are used. The correct determination of weft and warp densities and weaving type in lining fabrics are the most important factors that determine the durability of the fabric and the behavior of the fabric against the forces in practice.

The more dencity in the weft and warp direction of the fabric, the greater the tensile strength. The tensile strength of the fabric is higher than the sum of the strength value of the yarns that compose the fabric. This is because the weft threads are bonded to the warp threads to increase the strength. Another factor affecting fabric strength is weaving. The more the binding points of the yarns in the fabric, the higher the resistance against the tensile. According to the results of the research, the tensile strength in the direction of weft and warp of the lining fabric produced from PES/Lycra is the highest. In this case, the tensile strength of the fabric produced from PES/Lycra was highest. Fabrics made of synthetic fibers such as PES or high tensile strength fibers have high tensile strength. Since PES and PES/Lycra are synthetic, Acetate, Rayon, and Cupro regenerated cellulose fiber in the research, the tensile strength of PES and PES/Lycra is highest.

Fabrics with low weft and warp density have high tear strength. In a loose fabric structure, the friction forces between the yarns decrease, and in this case the tearing strength increases. In the research, the tearing strength of the lining fabric produced from PES yarns was the highest, since the weft and warp density was the lowest.

When evaluated in terms of fabric comfort, the drape feature is the main parameter affecting the selection, design and appearance of the textile material. Fabric drape in lining fabrics is closely related to the weight of the fabric. As the weight of the fabric decreases, its drape increases. In the research, the weight of the Cupro fabric is low and the drape coefficient is low. Thus, the most drape fabric lining fabrics used in the research is Cupro fabric with 27% drape coefficient.

Surface roughness is a very important parameter that affects the attitude of the fabric. If two fabrics will be used together with each other, as in lining fabrics, due to friction the surfaces will be deformed and strength losses can be seen in the fabrics. In order for these to occur at a minimum, it is desirable that the fabrics have a smooth surface. For this reason, surface roughness is very important in the lining fabrics. The surface roughness is evaluated with the fabric friction coefficient value. Among the lining fabrics used in the research, the fabrics with the lowest friction coefficient are Acetate, Cupro and Rayon (μ kinetic: 0.151-0.156-0.160). Since the tearing strength is affected by the friction property, when the relationship of the two properties is examined, it is seen that there is no relation in the weft direction but there is a strong relationship between the warp tearing strength and the friction coefficient.

Another point to be considered when sewing lining fabrics is to seam slippage. The higher the seam slippage value, the more resistant the fabric in terms of seam slipage. For this reason, especially the end-use is important in terms of quality performance.

In the research, PES/Lycra and Cupro lining fabrics are the most resistant lining fabrics in terms of seam slippage with a strength value of over 200 Newtons. PES/Lycra and Cupro lining fabrics have the highest weft and warp density. For this reason, it is very resistant in terms of seam slippage.

Regenerated fibers can be considered as an alternative to synthetic fibers in lining fabrics. This alternative regenerated fiber should have the advantages of synthetic fibers as well as eliminate the disadvantages. The lining made of Cupro fiber used in the research can be considered as an important alternative to the lining produced from the most widely used PES fiber in the market, especially in terms of draping and seam slippage properties.

ACKNOWLEDGEMENT: *This study was supported by Ege University Scientific Research Projects Coordination Unit, Project Number: 2017/BMYO/001.*

5 REFERENCES

1. Yakartepe Z., Yakartepe M.: From Apparel Technology Fabric to Ready-to-Wear (Konfeksiyon Teknolojisi Kumaştan Hazır Giyime), İstanbul, Vol. 9, Publication number 63, 1995, (in Turkish)
2. Kurumer G.: Garment Production and Technology (Konfeksiyon Üretimi ve Teknolojisi), İzmir, 446 p., 2007, ISBN: 978-9944-0869-0-5 (in Turkish)
3. Kawabata H., Obara K., Komiyama H., Narumi T.: The effects of skirt linning properties on comfort and movement, International Journal of Consumer Studies 25(4), 2001, pp. 271-278, https://doi.org/10.1046/j.1470-6431.2001.00194.x
4. Ünal Z.B., Acar E., Yıldırım F.: Evaluatıng performance characterıstıcs of lınıng fabrıcs used for chıldren dresses, Tekstil ve Konfeksiyon 25[4], 2015, pp. 323-328
5. Özdil N., Özçelik G.: A study on comparıson of tearıng strength test methods of fabrıcs, Tekstil ve Konfeksiyon16(3), 2006, pp. 174-179
6. Can Y., Kırtay E.: Yarn characterıstıc's effects on tear resıstance of cotton plaın fabrıcs, Afyon Kocatepe University, Journal of Science 7(2), 2009, pp. 65-78
7. Öztürk Ş.: A study of the relatıonshıp between surface roughness and structural propertıes of woven fabrıcs, MSc. Thesis, Namık Kemal University, Institute of Science, Department of Textile Engineering, 2016, 167 p.
8. Plattürtk G.G., Kılıç M.: Measurement of fabric drape by the methods based on ımage analysis, Journal of Textiles and Engineer 94(2), 2014, pp. 31-45, DOI:10.7216/130075992014219404
9. Kuyucu Y.: The examınatıon of stıtch parameter effects to the stıtch strength on lınıng fabrıcs, MSc. Thesis, Marmara University, İstanbul, 2009, 105 p.
10. Dirgar E.: The performance properties of the fabrics produced from cupro and some other regenerated cellulose fibers, Tekstil ve Konfeksiyon 27(2), 2017, pp:139-144

DEVELOPMENT AND RESEARCH OF EQUIPMENT FOR PROCESSING OF GRANULATED POLYMERIC MATERIALS VIA 3D PRINTING FOR THE NEEDS OF LIGHT INDUSTRY

Oleh Polishchuk, Petro Zozulia, Andrii Polishchuk, Pavlo Maidan, Mykola Skyba, Nazar Kostyuk, Andrii Kravchuk and Olha Kravchuk

Khmelnytskyi National University, Instytuts'ka str. 11, Khmelnytskyi, Ukraine
opolishchuk71@gmail.com

Abstract: *Current state of 3D printing in various industries and prospects of its application in light industry have been analyzed. It has been revealed that pressure and productivity at the outlet of the extruder, as well as quality of melt preparation in 3D equipment for processing polymeric materials in the form of granules depends on the geometric dimensions of the extruder and auger's working tool. Mathematical modeling of heating process of the polymeric material in the extruder has been done, thermal diagrams have been obtained, which allow to predict the temperature distribution in its different sections. A 3D printer with FMD technology for printing with polymer granules as a raw material has been developed. Resistance to destruction by a wedge-shaped blade of sewing materials with polymeric coatings applied to them by the method of 3D-printing has been researched.*

Keywords: *3D printer, 3D print, polymeric materials, waste, installation, auger, heating mode, sewing and footwear materials.*

1 INTRODUCTION

Additive technologies are one of the main world trends mentioned in the context of the new industrial revolution. Market of goods manufactured with use of such technologies has practically not been yet formed, has no clear boundaries, varies between 20-30% and tends to grow rapidly [1, 2].

It is a known fact that there are several methods of 3D printing, but they are all derivatives of additive technology for manufacturing [3]. Regardless of what 3D printer is used, the product is manufactured via layer-by-layer application of a thin reel of molten material extruded from the extruder on the working platform. The task of the printer is to move the extruder in exact accordance with the digital model. Therefore, the printed physical object totally corresponds to its virtual prototype, created with the help of graphic editors for 3D computer design. The output is details of a complex geometric shape produced in a short time [1, 4].

Modern products are characterized by complexity of construction, a large number of parts and components. For instance, footwear, especially sports type, has a complex geometric shape, may include active elements in the form of tubes, rods, plates, springs and other parts that increase its performance. Such parts are designed to absorb shock loads that occur during various physical exercises, running, jumping, as well as to promote repulsion, which improves performance of athletes in various sports. These elements can be constructively made as a single unit with a sole or in the form of various inserts: polymer or metal ones [5]. In addition to the issues related to the design of polymer products of complex geometric shapes, there are also issues related to their production. To make complex shapes of product parts, new methods of their manufacturing need to be created. Therefore, one of the modern ways to resolve this problem is 3D printing. Having analyzed the use of 3D printers in various industries, we can conclude that the greatest potential of 3D equipment lies in production of industrial goods. Light industry, in particular sewing and footwear, is no exception to this [5, 6]. Some existing consumables for 3D printing are quite suitable for production of clothing, footwear and their elements. Moreover, their range constantly increases. Materials with the required technical parameters appear [6]. All this contributes to the introduction of 3D printing in light industry. Nowadays, the use of 3D printers in mass production is limited due to relatively high cost of equipment and duration of the manufacturing process itself. The technology of 3D printing can be successfully used in production of small-scale and individual products, as production of high-value equipment in this case becomes unreasonable [5].

In paper [1], modern 3D-printing and 3D-printers technologies have been analyzed and systematized. A generalized classification of 3D printers has been developed, which gives a complete idea and characteristics of each type, purpose, etc.

Moreover, a new type of 3D printing was listed in this classification for the first time, namely 3D printing with polymer granules, which will become competitive in a rapidly developing industry along with other types of 3D printing and consumables. This type of printer is under development. One of the main advantages of this type of printer is the ability to reprint parts with granules from waste that was obtained during previous printing. Therefore, the cost of filament can be reduced through the use of secondary raw materials. Thus, it is unreal to obtain a rod equal in diameter from secondary raw materials, simply due to properties of the melt being inhomogeneous in mass; hence it leads to uneven pressure in the industrial extruder, uneven plasticity of the melt and its shrinkage. Respectively, during printing, such rod will behave completely unpredictably. During the first stage of processing of the output polymer and the first service life of the polymer chain there are irreversible changes caused by chemical effects, thermal, heat and photooxidative destruction, which leads to the appearance of active groups. These groups in subsequent processing are able to trigger oxidation reactions. Respectively, the smaller the number of processing, the better the material is, which, as a result, will affect quality of the future part or product. However, in the case of polymers processing, it is possible to create a new material with new properties by adding to their composition various admixtures, dyes, plasticizers to improve elasticity, plastic deformation, frost resistance, impact strength, decrease viscosity to improve their further processing and exploitation [5].

Primary raw material for powering 3D printer extruders is a rod made of polymeric material of a certain diameter. Polymer granules are used as raw materials to produce the rod. This process is long, which is unacceptable in today's competitive environment.

One of the main disadvantages of 3D-rod printing is that at the production stage the polymer is already subjected to temperature heating, which leads to loss of its physical and mechanical properties. Therefore, 3D printing using granules of the material is relevant. Printing using granular material is ideal in cases where additive and subtractive (rapid prototyping) methods of parts production can be combined. This will enable to quickly print the part on a 3D printer.

Growth of production using polymeric materials steadily leads to increase in their share in waste and the issue of recycling becomes integral for the issue of disposal of other wastes of human life. Modern polymeric materials based on various plastics, fibers and elastomers are used in various fields. Light industry is no exception to this [7, 8]. Therefore, the issue of polymer recycling and their subsequent use in light industry is an urgent task.

2 EXPERIMENTAL PART

2.1 Research equipment

To process polymers with different properties, equipment that would meet the necessary requirements, i.e. has optimal geometric parameters and thermal modes, is required. In order to conduct experimental research, a device was developed that allows printing 3D parts with granular or crushed polymeric materials obtained from waste garment and footwear production. Principle of operation of such equipment is as follows. The crushed polymer granules are placed into hopper 2 (Figure 1) or the loading area. After that, the raw material is fed by a rotating auger 4 in the heating zone for melting and subsequent extrusion. The polymer is melted and extruded in the form of a thin reel on the working platform. Further on, by layering the molten polymer material, a physical object is formed, i.e. a previously modeled part.

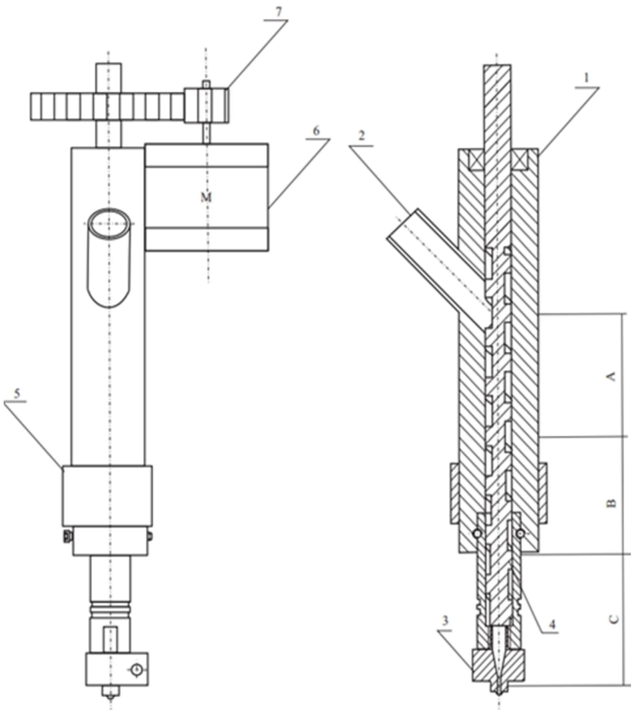

Figure 1 General scheme of the experimental device for processing of polymeric masses: 1 - body; 2 - loading hole; 3 - unloading hole; 4 - auger; 5 - heating element; 6 - stepper motor; 7 - gear; A - loading zone; B - melting zone, C - homogenization zone

To ensure the necessary movement of the material, the conditions for moving the solid material from the loading zone to other zones of the extruder and filling the interturn space in the auger are of great importance. A complete analysis of the movement of solid particles in a traditional single-auger extruder was done in paper [9] for the first time. In order to determine the conditions for the movement of polymeric material from the loading zone to the extrusion zone, experimental studies were conducted, which made it possible to understand how the interturn space in the auger is filled with polymeric material (Figure 2).

This enabled to establish the stages of transformation of solid-crystalline-state polymer particles into a viscous state of the finished material for layering by 3D printing to obtain a physical object (Figure 3).

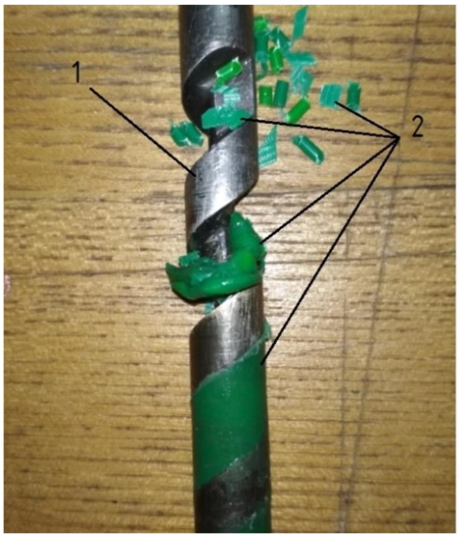

Figure 2 Photo of auger's interturn space filling with polymeric material

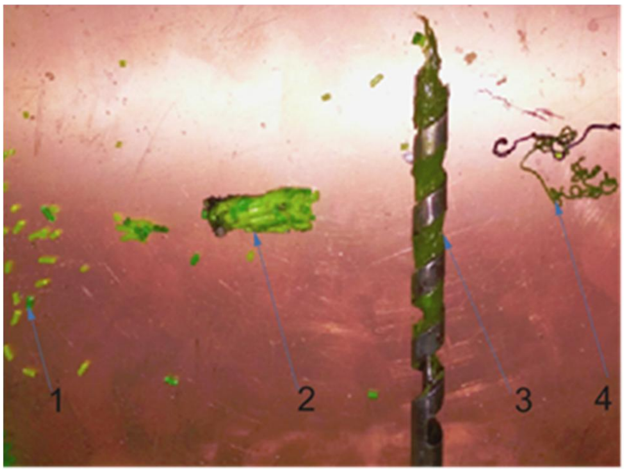

Figure 3 Stages of polymeric parts transformation: 1 - polymeric parts, 2 - start of adhesion stage melting of polymeric particles into a single unit, 3 - working auger's interturn space filling during operation, stage of polymeric parts homogenization into a single unit, 4 - output material after extrusion

The analysis of the obtained samples allowed us to reveal that at first, at normal temperature, a long polymeric plug is formed, which is pushed through the auger channel. The length of the plug must be large enough so that the pushing force resulting from the longitudinal movement allows the polymer to move into the melting zone. Transportation of polymeric materials of different shapes and sizes (crushed waste) or powders with poor flowability and low flow weight in the supply area is quite a difficult task. Therefore, when designing equipment for 3D printing with polymer granules, it is necessary to take into account all the forces that affect the printing process of parts. This, in turn, will allow to calculate optimal parameters of the device for processing polymer masses (Figure 1) and ensure uninterrupted operation of the 3D printer [10].

The defining parameters in the extrusion of polymers are the pressure and productivity at the outlet of the extruder as well as the quality of melt preparation. These parameters significantly depend on the design and geometry of the auger.

Productivity of process Q and melt pressure P from auger diameter D, length of auger working zone L from productivity of process Q, melt pressure P from length of auger working zone L, melt pressure P from density (shear rate) of material, auger productivity Q_w from parameters of density (shear rate) of the polymer [8, 9] has been calculated. On the basis of the received data the corresponding dependences of certain sizes have been constructed. For example, Figure 4 shows graphs of the dependence of productivity of the process Q and the melt pressure P on the diameter of the screw D. The calculations made it possible to determine optimal geometric parameters of the device to process polymer masses on the basis of which it was manufactured.

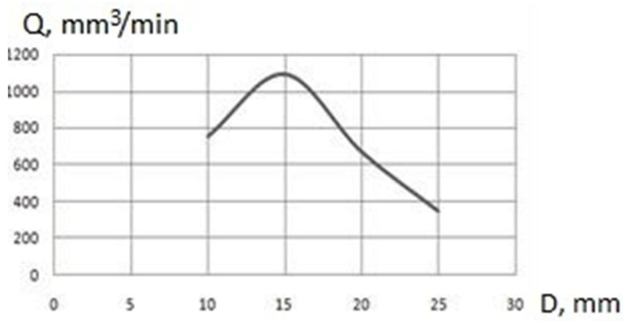

a)

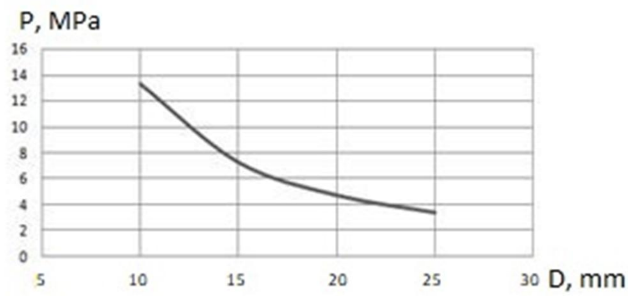

b)

Figure 4 Dependency graph: a) process Q productivity on diameter of auger D; b) melt pressure in extruder P on diameter D

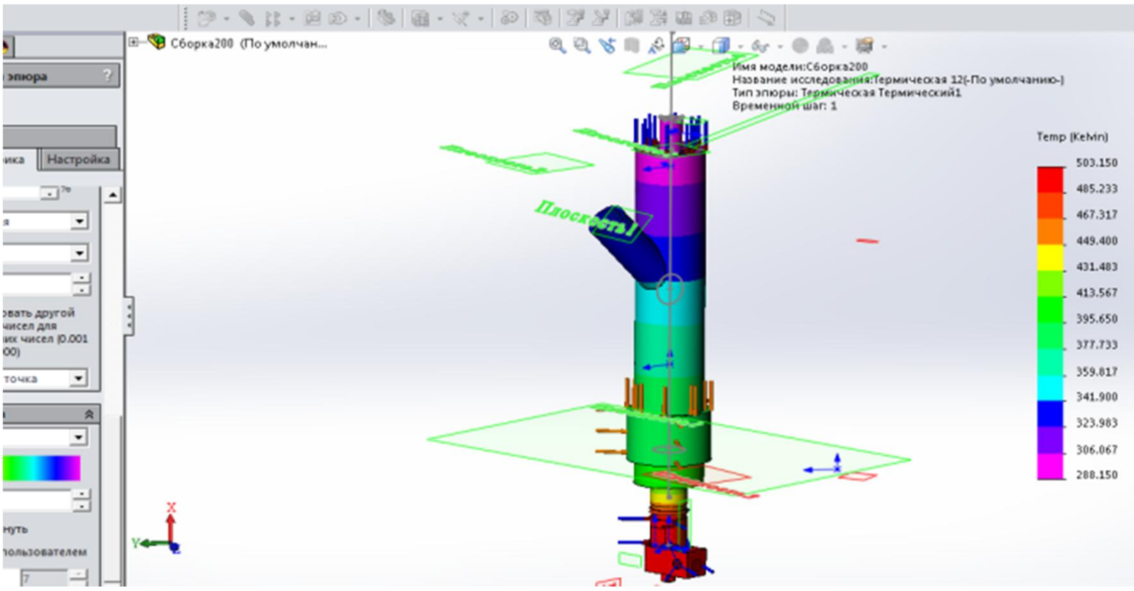

Figure 5 Distribution of temperatures along the device

An important step in the introduction of energy-saving (energy-saving) equipment for processing filaments by extrusion is modeling of the heating process, which would allow to control heating modes of the extruder in its working areas [11].

In this regard, there is a need for mathematical modeling of heating modes of the extruder before the stage of the direct process of production and the study of temperature distribution in the installation depending on the power of the heaters in different areas.

For this purpose, mathematical modeling of the heating process of polymeric material in the extruder was performed; a system of equations and a thermal diagram (Figure 5) of the temperature distribution along the entire length of the extruder were obtained.

This approach allows to predict the temperature distribution in different parts of the real device and selects optimal temperature modes when performing the process.

Based on the thermal diagram, it can be concluded that the physical object, i.e. the part to be printed, will have sufficient and uniform heating at the specified temperatures.

Therefore, the necessary plasticization and homogenization of polymeric materials in different areas of the extruder will be provided.

Installation for experimental research was developed on the basis of an inkjet 3D-printer with FMD-printing technology (Figure 6).

In this installation, the print head for polymer-rod printing was dismantled and a developed device for processing polymer masses entering the extruder in the form of granules was installed (Figure 7).

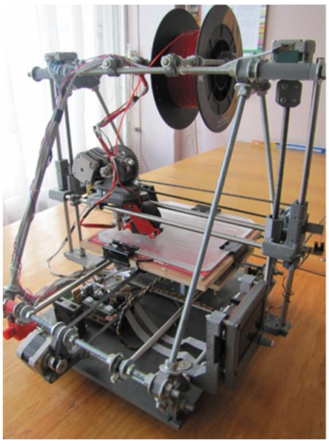

Figure 6 Basic model of 3D printer with FMD printing technology

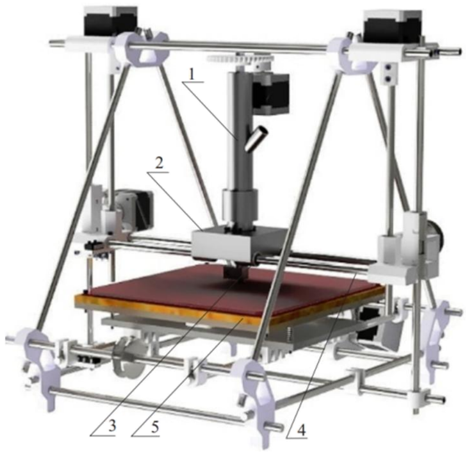

Figure 7 General scheme of the installation with a device for processing of polymeric masses: 1 - extruder; 2 - extruder installation fastening; 3 - linear motion bearing; 4 - device motion shaft; 5 - working surface for cooling of output material

2.2 Methodology

Experimental studies of the application of polymeric material by extrusion on materials used in the garment industry were carried out using the developed and manufactured installation [13, 14]. Samples of various sewing materials were selected, in particular denim, cashmere and synthetic fabrics [12]. To obtain a 3D coating, as a feed source for the extruder, waste from ABS plastic was used. Technical characteristics of materials are given in Table.1. Figure 8 shows the obtained samples of sewing materials.

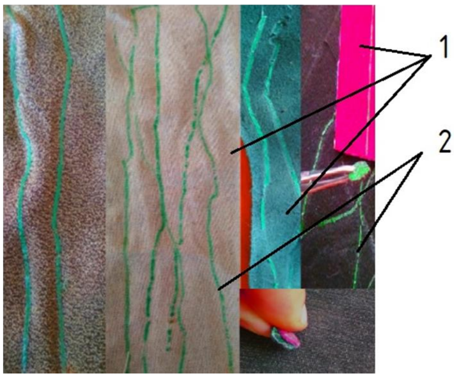

Figure 8 Samples of sewing materials with applied polymer layer: 1 - material; 2 - polymer coating

The obtained samples of materials with a polymer coating have been studied in regards to resistance to destruction by a wedge-shaped blade. For this purpose, an experimental setup was developed, which is presented in Figure 9. The principle of operation of the installation is as follows. Beforehand, a punch 2 was screwed into the rod 1 of the press, and a stand located on a strain gauge was placed in the lower part of the press. This strain gauge allows to measure the cutting force of the material. Another strain gauge connected to the punch allows to determine the volume of a dip of the punch into the material. The material, in its turn, is placed on the stand. The effort required for cutting the material is created via means of the handle of the press. The analog signals generated in the strain gauges are amplified, fed to an analog-to-digital converter, converted to a digital signal and fed to a computer. With the help of the installed software the signals are processed and graphs of dependences of technological efforts of cutting F_{cut} of material on depth of the dip of the punch Δ are constructed.

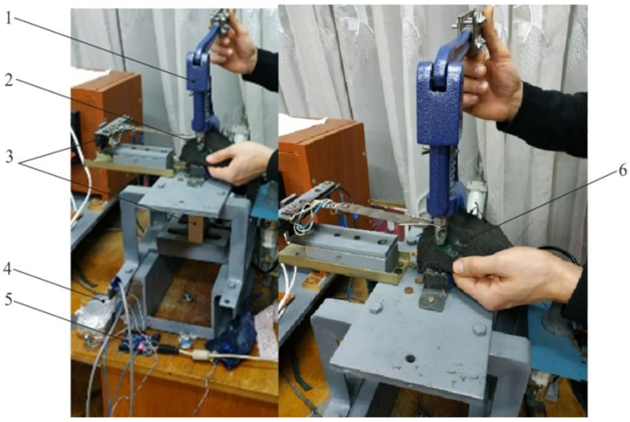

Figure 9 Experimental installation for the research of materials resistance at destruction with a wedge-shaped blade: 1 - cutting press; 2 - working organs (punch and stand); 3 - strain gauge; 4 - amplifier; 5 - analog-digital converter; 6 - material sample

3 RESULTS AND DISCUSSION

The results of the research on resistance of sewing materials to destruction by a wedge-shaped blade are shown in Figure 10. The graphs show the dependence of the technological cutting forces F_{cut} for different materials studied without and with coated coatings on the depth of the dip of the punch in the material Δ.

From the obtained diagrams it is seen that the technological effort at cutting the material with a punch reaches its maximum value at full dip of the punch in the material to a thickness Δ.

Analysis of the obtained experimental data showed that after applying the polymer layer on the material, its resistance to destruction increases, as shown by the results given in Table 2.

Table 1 Types of sewing materials fabrics used in the experiment

№	Type of material	Application material	Material thickness prior to application of polymer layer [mm]	Material thickness after application of polymer layer [mm]
1	Cashmere	ABS	2.17	2.27
2	Synthetic fabric (with interfacing)	ABS	1.20	1.69
3	Denim	ABS	1.69	1.93

Table 2 Value of material destruction maximum efforts

№	Sewing material	Coating material	Destruction effort prior to coating F_{cut} [H]	Destruction effort after coating F_{cut} [H]
1	Cashmere	ABS	294.79	342.48
2	Synthetic material	ABS	301.10	326.57
3	Denim	ABS	366.35	414.13

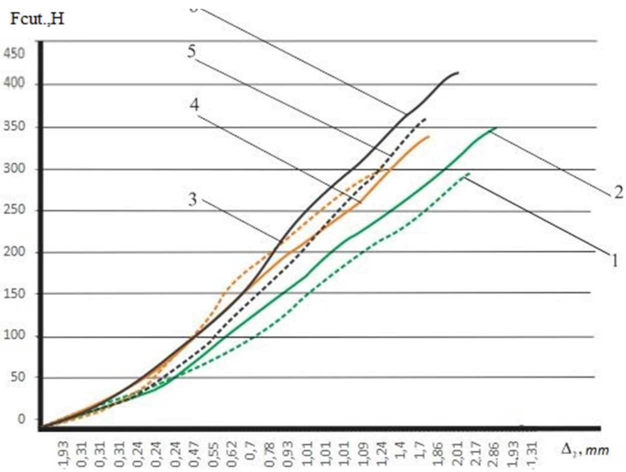

Figure 10 Graphs of F_{cut} technological effort dependencies for various materials on depth of plunger's dip into the material *Δ*: 1 - cashmere with no polymer layer; 2 - cashmere with polymer layer; 3 - synthetic material with no polymer layer; 4 - synthetic material with polymer layer; 5 - denim with no polymer layer; 6 - denim with polymer layer

4 CONCLUSIONS

The use of 3D printing technology can solve a number of problems in light industry, in particular in clothing and footwear industries. Introduction of this technology in mass production of clothing and footwear is an urgent task.

The defining parameters in the extrusion of polymers are pressure and productivity at the outlet of the extruder, as well as quality of melt preparation. The dependences of the process productivity *Q* and the melt pressure *P* on the screw diameter *D* have been obtained.

Mathematical modeling of heating process of the polymeric material in the extruder and the obtained thermal diagrams allow to predict temperature distribution in different parts of the device and selects optimal temperature modes when performing the process.

On the basis of theoretical and experimental research, a 3D printer with FMD technology for printing with polymer granules as a raw material has been developed, which allows the use of crushed polymer waste generated in production of clothing and footwear.

The obtained results of research on resistance of sewing materials to destruction by a wedge-shaped blade showed that after applying a surface layer of polymer on material, resistance of materials to destruction, their durability, and wear resistance increase.

5 REFERENCES

1. Zozulia P., Pyshcheniuk N., Skyba M., Polishchuk O., Malec M.: General classification of 3D printing. Analytical study of a device for loading of PET bottles in rotary crushers. Actual problem of modern science. Monograph, edited by Musial J., Polishchuk O., Sorokatyi R., Bydgoszcz, Poland, 2017, pp. 413-421 (in Poland)
2. Androschuk H.O.: Additive technologies: perspectives and issues of 3D printing (Part I), Science, Technology, Innovation 1, 2017, pp. 68-77 (in Ukrainian)
3. Strutynska O.V.: Modern state and development of the 3D modeling and 3D printing technologies, Scientific journal of NPU named after MP Drahomanova, Series 2. Computer-based learning systems 20(27), 2018, pp. 88-94, https://doi.org/10.31392/NPU-nc.series2.2018.20(27).15 (in Ukrainian)
4. Ozhga M.M.: Systems of three-dimensional computer design for training of future engineers-teachers, Issues of engineering and pedagogical education, 2013, pp. 105-114 (in Ukrainian)
5. Zozulya P.F., Polishchuk O.S., Neimak V.S., Polishchuk A.O.: Application of 3D-printing technology in footwear industry, Scientific Notes of Lutsk National University 67, 2019, pp. 48-52 (in Ukrainian)
6. Zozulya P.F., Polishchuk O.S., Polishchuk A.O.: Prospects for the use of 3D printing in light industry, Academic Notes of Khmelnytsky National University 4, 2017, pp. 102-104 (in Ukrainian)
7. Polishchuk O.S., Zozulya P.F., Polishchuk A.O.: Generalized classification of filaments for 3D printing, Academic Notes of Khmelnytsky National University 6, pp. 51-59 (in Ukrainian)
8. Sporyagin E.A., Varlan E.O.: Theoretical fundamentals and technology of production of polymer composite materials, DNU Publishing House, 2012, 188 p. (in Ukrainian)
9. Basov N.I.: Calculation and design of equipment for production and processing of polymeric materials, Chemistry, 1986, 488 p. (in Russian)
10. Zozulia P.F., Kostyuk N.O., Polishchuk O.S.: The influence of geometric parameters of an extruder screw on the process of treatment of thermoplastic materials, Colloquium-journal 3(2), 2020, pp. 45-49 (in Poland)
11. Turner B.N,, Strong R., Gold S.A.: A review of melt extrusion additive manufacturing processes: I. Process design and modeling, Rapid Prototyping Journal 20(3), 2014, pp. 192-204 https://doi.org/10.1108/RPJ-01-2013-0012
12. Patlashenko O.A.: Materials studies of clothing production, Aristei, 2007, 288 p. (in Ukrainian)
13. Ivitsky I.I., Solovey V.V., Sokolsky O.L., Oleksishen V.O.: Influence of parameters of three-dimensional printing on physical and mechanical properties of thermoplastic products, Academic Notes of National Technical University of Ukraine "Kyiv Polytechnic Institute", series "Chemical Engineering, Ecology and Resource Conservation" 1(17), 2018, pp. 17-23 (in Ukrainian)
14. Zhang Y., Shapiro V.: Linear-time thermal simulation of as-manufactured fused deposition modeling components, Journal of Manufacturing Science and Engineering 140(7), 2018, pp. 1-11, https://doi.org/10.1115/1.4039556

SMART MATTRESS TOPPER WITH ENHANCED HYGIENIC PROPERTIES FOR ECG MEASUREMENT AND DETECTION OF POSITION

Dana Rástočná Illová[1], Ľudmila Balogová[1], Katarína Ščasníková[1], Michal Gála[2], Branko Babušiak[2] and Štefan Borik[2]

[1]*Research Institute for Textile Chemistry (VÚTCH) - CHEMITEX, spol. s r.o., Rybníky 954, 011 68 Žilina, Slovakia*
[2]*Department of Electromagnetic and Biomedical Engineering, Faculty of Electrical Engineering and Information Technology, University of Žilina, Univerzitná 1, 010 26 Žilina, Slovakia*
rastocna-illova@vutch.sk; michal.gala@fel.uniza.sk

Abstract: *The contribution focuses on technical solution and confirmation of functionality of a prototype of a smart mattress topper with enhanced hygienic properties, designed for monitoring of human bio-medicinal data in real time. It involves integration of progressive technologies in a form of low-temperature atmospheric-pressure plasma, application of nanotechnologies in a form of an antimicrobial nanosol and integrated sensing system for monitoring electrical activity of the heart (ECG) and position of a lying person. The sensing system consists of a set of active ECG capacitive textile electrodes with incorporated microelectronics, capacitive sensors for detection of presence and position of a lying person, passive DRL electrode, data, control and communication elements integrated into construction of the mattress topper with an own mobile application. Functionality of prototype of the mattress topper will be demonstrated by measurement of ECG and position of a lying person by means of a patient simulator as well as a real person.*

Keywords: *smart topper, antimicrobial nanosol, low-temperature plasma, ECG, position detection.*

1 INTRODUCTION

Cardiovascular diseases belong among leading causes of death in Europe and they are responsible for more than 50 % of all deaths [1]. The cardiovascular diseases can be indicated, but mainly reduced by a soon diagnostics, suitable disease management, rehabilitation and prevention [2]. Electrocardiogram (ECG) sensing represents a traditional diagnostic method often used to monitor human health and diagnose potential cardiovascular diseases. The conventional method of ECG sensing uses electrodes and electro-conductive gel in direct contact with skin surface of an examined person. A special feature of this type of measurement is high quality of measured signal due to low transfer resistance between the electrode and the skin (when using an electro-conductive gel). On the other hand, long-term measurement is uncomfortable and can cause allergic skin reaction in some cases. In recent years, capacitive sensing of ECG signal avoiding direct conductive contact between the electrode and the skin of an examined person is being developed. This unconventional method of capacitive sensing has been successfully integrated e.g. into office arm-chairs, car seats or beds [3, 4]. Decubital ulcers (bed sores) arise frequently in immobile, usually older, long-term lying patients and/or patients with a diagnose requiring monitoring of their health condition in a bed. This primarily concerns the lesions caused by circulatory insufficiency due to pressure applied on the affected place between a bone and a base, when insufficient congestion takes place. Therefore, prevention of genesis of decubital ulcers is identification of position and regular displacement of a lying patient.

The developed original proposal of a prototype of smart mattress topper „ECG-SmartSheet“ with enhanced hygienic properties designed for monitoring of human biomedical data in real time constitutes a system of unobtrusive long-term monitoring electric activity of the heart (ECG) and position of a lying person over the day and/or during sleep. An efficient and advanced design of a smart mattress system is involved. Progressive technologies used on elaboration of the project included:

- plasma finish: activation of the surface by low-temperature plasma under atmospheric pressure aimed at achievement of improved adhesion of the functional nano-coating on the textile material used as basic material for development of the mattress topper;
- nanotechnologies: application of antimicrobial nanosol with incorporated nano-particles on the plasma activated textile surface aimed at creation of nano-structured surface with high adhesion to achieve functional hygienic properties of the mattress topper;

- smart technologies: integration of a system of active textile capacitive ECG electrodes with incorporated microelectronics, power, data, control and communication components into construction layers of the mattress topper using innovative antimicrobial (AMB) nano-coated textile material, customized algorithms and mobile application.

2 TECHNOLOGIES AND MATERIALS

The mattress topper consists of a protective removable shell and a core consisting of several internal layers on which functional components of the sensing system are placed. The sensory part of the mattress topper consists of active textile ECG capacitive electrodes with incorporated microelectronics, designed to monitor electric activity of the heart (ECG) and textile sensors designed to detect presence and position of a lying person, made on a base of electro-conductive textiles. A customized application developed for readily available imaging equipment allows assessment of the sensed data in real time.

2.1 Construction of the mattress topper

Shell of the mattress topper consists of an upholstery fabric pre-finished by activation of its surface structure using low-temperature atmospheric-pressure plasma and subsequently finished by an antimicrobial nanosol imparting hygienic properties to the mattress topper during its long-term use. Permanency of the antimicrobial nanofinish on the surface of the upholstery fabric has been evaluated after 20 washing cycles performed using 4N process according to STN EN ISO 6330 and its antibacterial efficiency has been evaluated according to AATCC TM 100 and expressed as a percentage of bacterial reduction of Staphylococcus aureus. The achieved bacterial reduction after 20 washing cycles was on a level of 50% (bacteriostatic efficiency). A positive influence of the pretreatment by activation of the surface of the upholstery fabric using low-temperature plasma on enhancement of affinity of the antimicrobial coating to the surface of the upholstery fabric has been demonstrated by bacterial reduction, which was higher by about 35% in comparison with an upholstery fabric finished by the antimicrobial nanosol under the same conditions without activation of the textile surface by low-temperature plasma.

On a face side of the surface of the shell of the mattress topper there is a set of active ECG capacitive textile electrodes with incorporated microelectronics and a reference active ECG capacitive textile electrode for monitoring heart activity, creating an eight-lead system of ECG measurement. On the shell of the topper there is also a passive textile DRL electrode to repress technical artefacts, primary interference from the electrical network. Electronics of the ECG electrodes is placed on a flexible circuit board and it is conductively connected with the textile sensor. Connection of the electrodes is terminated by a power take-off connector, connected to the control unit.

In construction of the core of the mattress topper there are pressure capacitive textile sensors for detection of presence and position of a lying person. The pressure sensors are connected by an electro-conductive sewing thread. Between the pressure sensors there is a dielectric, which on change of the pressure changes its thickness and this way capacity of the pressure sensors changes as well. The pressure sensors allow to monitor not only presence of a patient in the bed, but also distribution of pressure on the topper and monitor this way the most vulnerable places of human body for the purpose of positioning a long-term lying patient. The pressure sensors are connected with the circuit board by a connector connecting the conductors conducting signal further to the sensing unit which passes the information to the control unit.

The control unit captures signals from the electrodes, performs their further analog processing, digitizing of the data and their transfer to a computer by means of universal serial bus (USB). A basic element of the control unit is an eight-canal integrated circuit, analog-digital (AD) convertor with internal reference and adjustable amplification, sampling frequency and microcontroller ensuring communication with a personal computer. A prototype mobile application has been developed for analysis, evaluation, display and storage of the sensed data as well as for display of a position. It monitors actual state of the patent in real time.

The active ECG capacitive textile electrodes and passive pressure capacitive textile sensors have been made from electro-conductive fabrics with electric resistivity of 1.5 Ω/10 cm, creating their sensing part. An advantage of the textile electrodes is a pleasant feel, elasticity and ability to adapt to contours of a human body what enhances comfort of a man during his stay in bed and ECG measurement. The electrical conductivity of the fabrics used to prepare the textile sensors and electrodes ensures functionality of the whole sensing system integrated into construction of the mattress topper. Influence of washing and mechanical abrasion on change of the surface electric resistance and electric conductivity of the electro-conductive textiles has been evaluated after 20 washing cycles using 4N process. Functionality of the fabrics designed for sensing of ECG and position of a person has been confirmed. The electric resistance of the fabrics increased after 50 000 abrasions to a level of 19 Ω/10 cm, whereby the fabrics preserved their appearance without significant changes. Tests for human-ecological properties of the applied electro-conductive textile materials have been performed according to test methods of the international association OEKO-TEX® to confirm health safety and health protection of a consumer: determination of forbidden disperse dyestuffs classified as allergenic, carcinogenic and other forbidden dyestuffs, determination of extractable heavy metals, determination of total quantity of lead (Pb) and cadmium (Cd), determination of total quantity of silver, determination of polycyclic aromatic hydrocarbons (PAH), determination of phenol, chlorinated phenols and orthophenylphenol (OPP) and determination of pH of water extract. No presence of health harmful substance has been determined in the applied electro-conductive textiles. The determined quantities have been under detect limit and they meet the required limit concentrations of harmful substances for textiles and clothing products for children up to 3 years of age, for direct and indirect contact with the skin according to the technical requirements of the standard STN 80 0055 and the international OEKO-TEX® Standard 201.

2.2 Capacitive measurement of ECG

The principle of capacitive ECG sensing is that the active ECG textile electrode constitutes one plate of a plate condenser and surface of human skin constitutes the second plate of the plate condenser. A dielectric layer is placed between these two plates; the most frequently this layer is a layer of cotton clothing in which a lying person is dressed during measurement. Capacity of such a condenser is calculated according to the formula 1:

$$C = \varepsilon_0 \varepsilon_r \frac{S}{d} \tag{1}$$

where *S* is surface of condenser plate, *d* is distance between the condenser plates, ε_0 is permittivity of vacuum and ε_r is dielectric permittivity.

If surface of an electrode is 25 cm^2, dielectric material is a cotton fabric with 0,5 mm thickness and 2.077 permittivity [5], capacity of the plate condenser will be approximately 92 pF. The active ECG electrode incorporates a low-noise operational amplifier in connection of a voltage tracker. Static charge of the condenser is discharged by means of R resistor. Combination of C condenser with R resistor creates a filter whose limit frequency is calculated according to the formula 2:

$$f_c = \frac{1}{2\pi RC} \tag{2}$$

If value of the resistor will be 2 GΩ, then the cut off frequency of the filter will be 0.87 Hz. Such a filter will enable to remove unacceptable biological artefact caused by breathing.

2.3 Position sensing

Hardware and software modules have been developed to detect presence and position of a lying person. Result of sensing presence of a person in a bed using a method of measurement capacity between two pressure capacitive sensors can be shown in two ways:

a) curve representing sensed capacity in real time for a pushed sensor (Figure 1b) and/or a non-pushed sensor (Figure 1a).

b) using a color map (color squares), representing a more sophisticated method to display change of pressure by presence of a person lying in a bed.

Data obtained by measurement can be transformed to „pictures“ where the individual cells will represent pressure intensity. Innovative algorithms known from recognition of a picture and software developed for the purpose of data monitoring and data capture from the sensors in real time are used in the developed module. After starting the measurement the measured values are recorded and at the same time level of pressing the sensor is shown in graphical form by means of colors. Each square in the map represents one sensor and capacity is represented by coloring the square. Unloaded (non-pushed) sensor is represented by blue color and pushed sensor by yellow color. Such a color map displays position of a patient in a bed. Pressure sensors of matrix 2x2 sensors in „quiescent“ condition are shown in Figure 2a, from which is can be seen on the base of the color map, that the sensors are not loaded. In Figure 2b one square is yellow; it means that the sensor in left upper corner was pressed. In Figure 2c it can be seen a case when the right lower sensor was pressed. After completion of the measurement it is possible to store the data for subsequent use when training the innovative algorithms for detection of position of a man.

a) b)

Figure 1 Capacitive curves: a) non-pushed sensor, capacity about 12.4 pF; b) pushed sensor, capacity about 15.1 pF

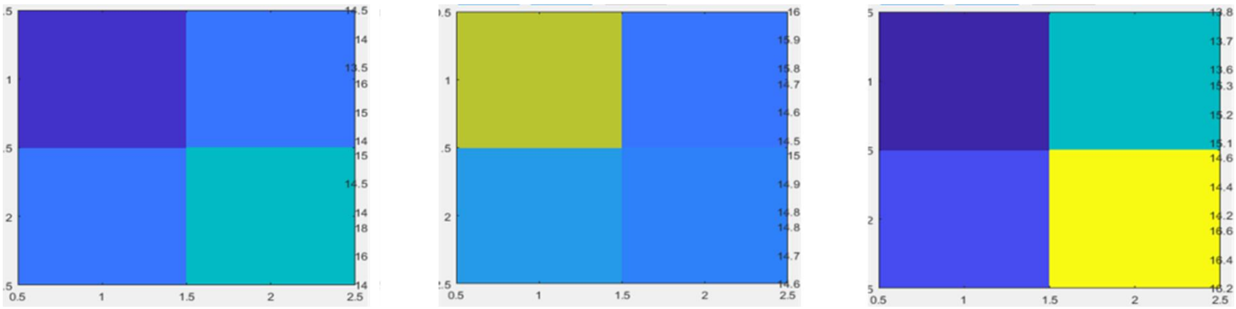

a) b) c)

Figure 2 Color map representing: a) non-pushed sensors; b) pushed left upper sensor; c) loaded right down sensor

3 RESULTS AND DISCUSSION

Functionality of the cover of the mattress topper has been evaluated on a person lying on his back for 1 hour (Figure 3).

Figure 3 A proband lying on the developed mattress topper

The subject wore nightdress made from cotton fiber. Sampling frequency was adjusted to 250 Hz. Amplification was adjusted to value 6 for all channels with the exception of channel No. 2 and No. 3. Signal in these channels exceeded the range on amplification 6 and therefore amplification in these channels was reduced to 4. DRL circuit was active and signal for DRL circuit was derived from all input channels. Raw ECG record is shown in Figure 4. The channels are arranged in lines, i.e. channels No. 1 and No. 2 are shown in the first line. It is obvious from the figure that signals in the channels are influenced by noise differently and show also different offset. This phenomenon is caused by local differences in distribution of electrical potential on the skin, accumulation of static charge and different pressure of the electrodes.

Although DRL circuit has been used and electronics of the active electrodes have been shielded, the output signals comprise considerable noise on the frequency of 50 Hz as it is evident from the power spectral density (PSD) in Figure 5. A narrow band notch filter for 50 Hz, applied to all channels, has been proposed to reduce the noise. ECG record after application of the filter is shown in Figure 4b. The main problem is electrostatic charge and movement artefacts. The movement artefact causes saturation of the operational amplifier inputs and it can take even several seconds until the signal has been stabilized again. Solution of this problem consists in application of a special electronic circuit grounding temporarily inputs of the operational amplifier as soon as a signal gets outside the measuring range [6].

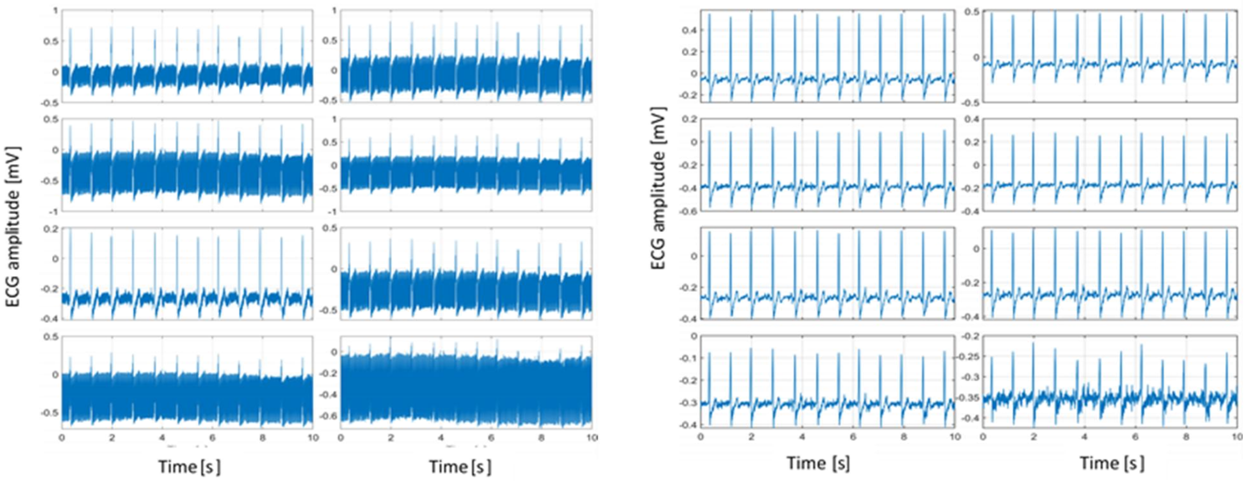

a) b)

Figure 4 Eight-channel ECG record measured from the cover of the mattress topper: a) raw, b) filtered

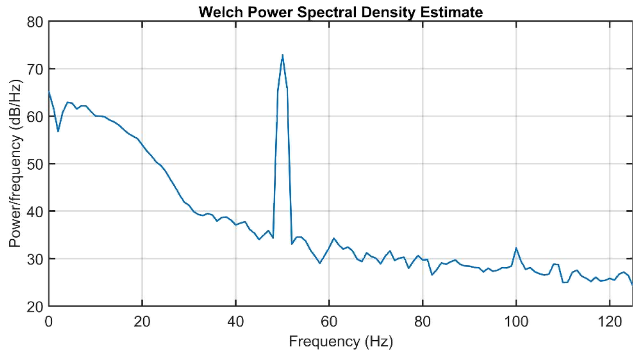

Figure 5 Power spectral density (PSD) of the channel No. 1

The measured signals clearly show visible course of the ECG signal, suitable for subsequent analysis. Although not all canals are without disturbing arfefacts, incidence of these artefacts in some canals does not represent any risk from a viewpoint of determination of diagnosis as the applied algorithm selects for the needs of diagnosis only the canal with the best signal quality.

A graphical display of results from measurement of capacity using colour map (colour squares) was selected to measure position of a lying person on a prototype of the mattress topper (Figure 6).

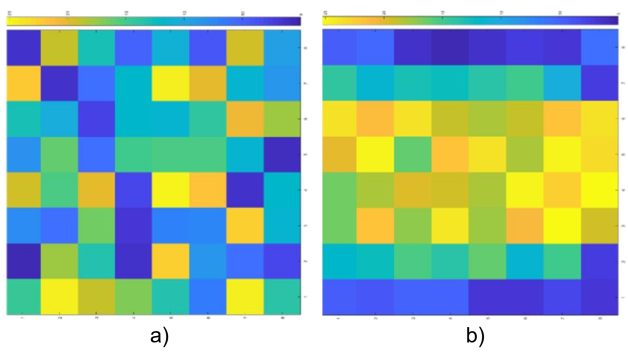

Figure 6 Detail of colour map of the matrix of sensors of position: a) without shielding; b) with shielding

From a viewpoint of monitoring position of a patient it is not necessary to know concrete value of capacity but only its change. Each square in the map represents one sensor and capacity is represented by colouring the square. Unloaded (unpushed) sensor is represented by blue colour and loaded sensor by yellow colour. Influence of shielding on measurement and values of capacities sensed using the sensors is shown in Figure 6a, when measurement was performed without shielding and in Figure 6b, where measurement was performed with an applied shielding layer. Shielding layer of the electroconductive fabric has been inserted between shell of the mattress topper and the passive pressure capacitive textile sensors. While from results measured without shielding it is not possible to identify unambiguously a lying person (influence of spurious capacities), after introduction of a shielding layer to the construction of the mattress significant improvement is visible which allows identification of area of a lying person and distribution of pressure cause by weight of a body on the topper.

4 CONCLUSION

The matter of prevention of cardiovascular diseases is very actual, important and necessary not only in the Slovak Republic but world-wide at present. The proposed prototype of smart mattress topper “ECG-SmartSheet“ with enhanced hygienic properties, designed for monitoring of bio-medicinal human data in real time ensures ECG monitoring of a patient on capacitive principle in lying position as well as detection of presence and position of a lying patient in a bed. It is a conjunction of progressive technologies for textile finishing such as plasma treatment and nanotechnologies with application of smart technologies such as smart systems for biodata collection with subsequent positive impact on socio-health aspects of social and demographic development. The smart topper „EKG-SmartSheet“ is a functional system of contactless and unobtrusive long-term monitoring of human vital functions in health service establishments or in the domestic environment. Sensing bio-potentials using textile electrodes prepared from electro-conductive textiles is a progressive solution of measurement of ECG signal without direct contact with human skin. The method of contactless measurement of ECG signal becomes an alternative of common Ag/AgCl electrodes used at present in health service establishments. The textile electrodes act as dry electrodes allowing measurement of ECG signal without electrolyte gel or adhesives. Besides, application of textile material with antimicrobial nano-coating with plasma application ensures permanently enhanced functional hygienic properties during the long-term use even after 20 washing cycles and/or after multiple abrasion of the surface of electro-conductive textiles in the form of textile sensors and/or ECG electrodes. Besides, from a viewpoint of materials used in the construction of mattress topper, health safety and maximal protection of consumer health has been confirmed according to the test methods of the international association OEKO-TEX® Standard and technical requirements of the standard STN 80 0055.

***Acknowledgement**: This work was supported by the Slovak Research and Development Agency under the contracts No. APW-14-0190, No. APW-16-0190 and No. APW-18-0167.*

5 REFERENCES

1. Šestáková A., Šestáková Z., Matejka P.: Active prevention of cardiovascular diseases in the conditions of a public pharmac (Aktívna prevencia kardiovaskulárnych ochorení v podmienkach verejnej lekárne), PharmINFO spol. s r. o., Bratislava, (in Slovak)
2. Nichols M., Townsend N., Scarborough P., Rayner M.: Cardiovascular disease in Europe 2014: epidemiological update; Published on behalf of the European Society of Cardiology, European Heart Journal, 2014, http://www.oxfordjournals.org/our_journals/eurheartj/press_releases/freepdf/prpaper.pdf
3. Lim Y.G., Hong K.H., Kim K.K., et al: Monitoring physiological signals using nonintrusive sensors installed in daily life equipment, Biomedical Engineering Letters 1, 2011, pp. 11-20, https://doi.org/10.1007/s13534-011-0012-0
4. Lim Y.G., Lee J.S., Lee S.M., et al.: Capacitive measurement of ECG for ubiquitous healthcare, Annals of Biomedical Engineering 42(11), 2014, pp. 2218-2227, https://doi.org/10.1007/s10439-014-1069-6
5. Lesnikowski, J.: Dielectric permittivity measurement methods of textile substrate of textile transmission lines, Przeglad Elektrotechniczny 88(3A), 2012, pp. 148-151
6. Spinelli E., Haberman M., Garcia P., Guerrero F.: A capacitive electrode with fast recovery feature, Physiological Measurement 33(8), 2012, pp. 1277, DOI: 10.1088/0967-3334/33/8/1277

DETERMINING TENSION OF YARNS WHEN INTERACTING WITH GUIDES AND OPERATIVE PARTS OF TEXTILE MACHINERY HAVING THE TORUS FORM

Volodymyr Shcherban'[1], Oksana Kolysko[1], Gennadiy Melnyk[1], Marijna Sholudko[1], Yuriiy Shcherban'[2] and Ganna Shchutska[2]

[1]Kyiv National University of Technologies and Design, 2 Nemirovicha-Danchenko Str., 01011 Kyiv, Ukraine
[2]Department of Light Industry Technologies State Higher Educational Establishment «Kyiv College of Light Industry», Ivana Kudri str. 29, 01601 Kyiv, Ukraine
melnik2000@ukr.net

Abstract: *The research related to determining of the yarns tension when interacting with guide and operative parts of weaving looms and knitting machines having the form of torus in the area of contact with yarn established the mechanism of yarn tension increase behind the guide having the torus form due to change in geometrical dimensions and friction forces within contact area. It was proved that yarn tension increase behind the guide is effected by ratio of radius of internal circumference of torus to radius of working circumference; contact angle between yarn and working circumference of torus; radial contact angle between the yarn and internal surface of torus; physico-mechanical and structural properties of yarn. For multifilament and spun yarn, the actual contact angle is more than nominal one due to yarn diameter distortion in the contact area with surface of torus. Values of contact angles between yarns and working circumference and values of radial contact angles between yarns and internal torus surface shall be determined according to geometrical dimensions and design of guide and operative parts of weaving looms and knitting machines. The paper includes experimental research of interaction between different by its nature yarns and spun yarn (natural, synthetic, and man-made) and surfaces having the torus form imitating guide and operative parts of weaving looms and knitting machines. Based on experimental research the regression relationships between tension values behind the guide and ratio of radius of internal circumference of torus to working circumference radius, yarn tension prior it goes to guide and nominal value of contact angle were obtained for cotton, woolen, linen spun yarn, and polyamide multifilament. The analysis of the regression relationships made it possible to establish ultimate values of geometrical dimensions for guide having the form of torus when tension has its minimum value. This will enable minimization of the yarn tension during its processing on the weaving looms and knitting machines. This leads to a decrease in yarn breakages, an increase in the production equipment performance by reducing its downtime, improving the quality of the fabric and knitted garments produced. This suggests a practical value of the proposed technology solutions. These latter are related, in particular, to determining optimal geometric dimensions of guides and operative parts of weaving looms and knitting machines having the form of torus in the area of contact with yarn, at which the output tension will have the minimal required degree. Therefore, there is a good reason to claim the possibility of guided management of the process of changing the yarn tension in weaving looms and knitting machines by choosing geometrical dimensions of high-curved guide for specific yarn types.*

Keywords: *tension, yarn, guide surface having the torus form, contact angle.*

1 INTRODUCTION

Improvement of technological processes for weaving and knitting production shall mean optimization of technological efforts based on minimization of yarn tension in the area of fabric and knit formation [1, 8, 9, 20]. Determining of yarn tension degree in the working area of technological machine when rewinding spun yarn [2-4], of weaving loom [5, 6, 20], knitting machine [7, 9] makes it possible to evaluate intensity of running technological process. Main characteristic property of most technological processes in textile industry is interaction between yarns and guide and operative parts, when guide's surface curvature radius in the area of contact is comparable to the yarn or spun yarn diameter [8, 14, 20]. Figure 1a represents cases of interaction between the yarn and guide and operative parts of knitting machines. Figure 1b represents cases of interaction between the yarn and operative parts of weaving looms. Figure 1c represents designed diagram of interaction between a yarn and guide surface having the form of torus when guide's curve radius and yarn diameter radius are comparable with each other.

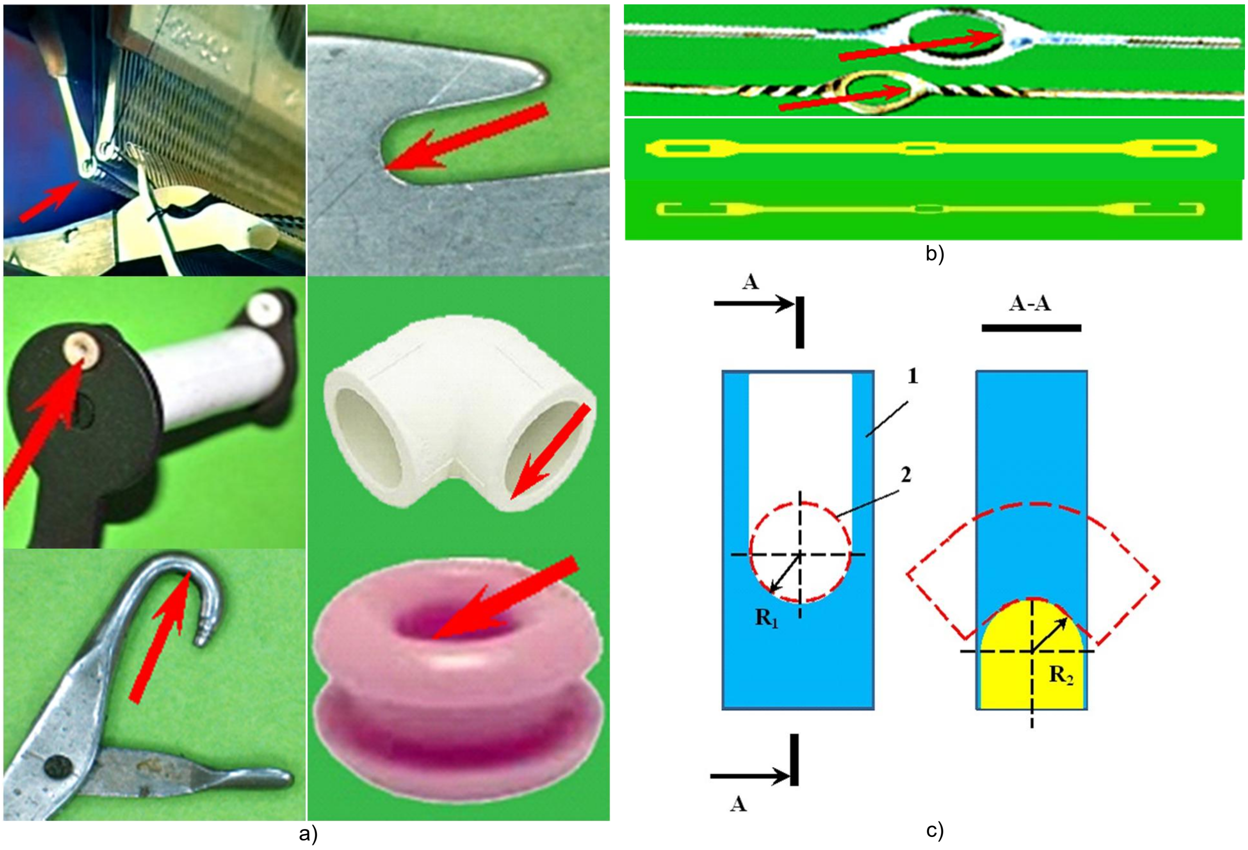

Figure 1 Interaction of yarn with high-curved guides at the textile machinery: a) with guides and operative parts of knitting machines; b) with operative parts of weaving looms; c) designed diagram of interaction between yarn and guide having the form of torus; 1 - fragment of guide surface; 2 - yarn; R_1 - radius of internal circumference of torus; R_2 - radius of working circumference of torus

Analysis of interaction diagram shows that ratio of the radius of internal circumference of torus R_1 to the radius of the working circumference R_2, contact angle between the yarn and the working surface of torus' circumference, radial contact angle between the yarn and internal surface of torus [9] are of great significance. Interaction between the yarn and guide surface, if there exists a radial contact with that surface, occur during fabric element and new course of knitted fabric formation [10]. Such a complex type of interaction requires taking into account the direction of the yarn's friction surfaces and guide surface [11], as well as relative motion of moved material [12]. In our paper [13] we underline the necessity to take into account twists of multifilament and spun yarn and value of its bending modulus. Bending modulus has significant effect on the value of the actual contact angle between the yarn and the guide surface. The above has been proved in our paper [14] during research of conditions of interaction between polyamide multifilament or polyamide monofilament and guide surface. The mentioned papers consider cases of interaction between the yarn and high curved guide surfaces regardless of radial contact with the yarn surface in the contact area. Our papers show the results of experimental determining of the yarn tension with a help of special units [15, 16]. It is impossible to use the obtained results when performing research of interaction between the yarn and high-curved guide, in case there is a radial contact with the yarn surface in the contact area. To contribute to increase accuracy of dimensions and possibilities to ensure metrological self-control in is better to use the redundant measurements method, which makes the measurements result independent of conversion function parameters and their deviation from nominal values [17]. Design of experimental unit determines the accuracy of results receives when determining the yarn tension. The paper [18] shows the diagram for determination of the yarn tension, which uses cylinders with big radii as guides. The mentioned diagram has its disadvantages. Using this diagram, it is impossible to simulate actual conditions of interaction between the yarn and guide and operative parts of weaving looms and knitting machines. The experimental unit with rotating cylinder has similar disadvantages [19]. The paper [20] represents results of determining tension value for wide spectrum of guide surfaces having the form of cylinder. During the experiment, however, there was no radial contact between the yarn and guide surface. Absence of such contact limits the use of obtained results in terms of analysis of conditions pf interaction between the yarn and the actual guide and operative parts of weaving looms and knitting machines.

2 MATERIALS

Four types of yarn have been chosen for experiment.

SN1 series: carded cotton spun yarn 29x2 tex. It is used as warp yarns for production of tartan (spring-autumn twill fabric), and knitted fabric (for outer garments and body linen).

SN2 series: woolen spun yarn 31x2 tex. It is used as warp yarns to produce pure-wool twill suiting (for knitted outer garments, small part also for winter and sports hosiery, as well as hand-wear).

SN3 series: linen wet-spun yarn made of bleached roving 41 tex, obtained from dressed flax. It is used as warp yarns to produce sindon, knitted fabric LN-1 and LN-2 for outer garment.

SSA series: polyamide multifilament 29x2 tex. It is used as warp yarns of outer protective layers of multilayer technical fabrics (MTF) for laying yard-coated pipes, as well as for knitting of outer knitwear and sportswear.

3 EXPERIMENT

For four series SN1, SN2, SN3 and SSA an orthogonal second-order plan for three factors was designed and implemented in the paper [9, 20]. The general view of the regression equation to determine the joint effect of the yarn tension prior it goes to the guide having the form of torus P_0, ratios of radius of internal circumference of torus R_1 to working circumference radius R_2, and the nominal value of the contact angle φ_p on the yarn tension behind the guide having the form of torus P, is as follows:

$$P = b_0 + b_1x_1 + b_2x_2 + b_3x_3 + b_{12}x_1x_2 + b_{13}x_1x_3 + b_{23}x_2x_3 + \\ + b_{11}x_1^2 + b_{22}x_2^2 + b_{33}x_3^2. \quad (1)$$

The range of factor variation in the equation (1) was determined by the actual yarn processing conditions. In the blinded values: yarn tension before it goes to the guide having the form of torus P_0 was indicated as x_1; ratio of the radius of internal circumference of torus R_1 to working circumference radius R_2 was indicated as x_2; the nominal value of the contact angle φ_p was indicated as x_3.

While determining ratio of radius of internal circumference of torus R_{1S1} to working circumference radius R_{2S1} the diameter of carded cotton spun yarn 29x2 tex, which is 0.31 mm is taken into account. Therefore, in the middle of the experiment, radius of working circumference of torus R_{2S1} takes on the value of 0.35 mm. Radius of internal circumference of torus R_{1S1} is determined by geometrical dimensions of the operative parts of weaving looms, knitting machines, and textile looms (needles and sinkers of knitting machines, heddles of the textile looms). Radii values were determined using USB Digital microscope Sigeta (Figure 2). In the middle of the experiment, to exclude the yarn jamming the R_{1S1} takes on the value of 0.6 mm. Table 1 shows values of ratio of radius of internal circumference of torus R_{1S1} to radius of working circumference R_{1S1} in the blinded values.

Factor x_3 is a nominal value of contact angle for knitting machines when producing knitted fabric for outer garments and body linen, for needles and sinkers it changes within the range from φ_{pS1} = 60° to φ_{pS1} = 180°. When producing tartan (spring-autumn twill fabric) the maximum nominal value of contact angle (heddle eye) for shuttle looms is φ_{pS1} = 29° in case of open shed. The same for shuttleless looms will be φ_{pS1} = 22°; and pneumatic type rapier looms it will be φ_{pS1} = 41°. Taking into account the above values it takes up in the middle of the experiment the value of nominal contact angle of guide surface having the form of torus 95°.

Table 1 Second-order orthogonal matrix for series SN1 for carded cotton spun yarn 29x2 tex

№	Factors					
	Input tension		Torus radii ratio		Contact angle	
	x_1	P_{0S1} [cN]	x_2	R_{1S1}/R_{2S1}	x_3	φ_{pS1} [°]
1	+1	27	+1	2	+1	105
2	-1	23	+1	2	+1	105
3	+1	27	-1	1.4	+1	105
4	-1	23	-1	1.4	+1	105
5	+1	27	+1	2	-1	85
6	-1	23	+1	2	-1	85
7	+1	27	-1	1.4	-1	85
8	-1	23	-1	1.4	-1	85
9	-1.215	22.6	0	1.7	0	95
10	+1.215	27.4	0	1.7	0	95
11	0	25	-1.215	1.3	0	95
12	0	25	+1.215	2.1	0	95
13	0	25	0	1.7	-1.215	83
14	0	25	0	1.7	+1.215	107
15	0	25	0	1.7	0	95

The correlation between the open-label and blinded values of series SN1 for carded cotton spun yarn 29x2 tex is as follows:

$$x1 = \frac{P_{0S1} - 25}{2}, \quad x2 = \frac{R_{1S1} / R_{2S1} - 1.7}{0.3}, \quad x3 = \frac{\phi_{PS1} - 95}{10} \quad (2)$$

Table 2 shows a second-order orthogonal matrix for series SN2. Factor x_1 is a yarn tension prior the yarn goes to the guide having the form of torus, in the middle of the experiment for woolen spun yarn 31x2 tex it is taken up as relatively equal to filling tension of warp yarns. During production of pure-wool twill suiting, outer knitted garments, hosiery of winter and spots assortment, as well as handwear this value will be P_{0S2} = 22 cN.

When determining ratio of radius of internal circumference of torus R_{1S2} to radius of working circumference R_{2S2} the diameter of woolen spun yarn 31x2 tex, which is 0.34 mm shall be taken into account. Therefore, in the middle of the experiment, the radius of working circumference of torus R_{2S2} is taken up as equal to 0.35 mm. The radius of internal circumference of torus R_{1S2} is determined by geometrical dimensions of operative parts of knitting machines and textile looms. Values of radii were determined using USB Digital microscope Sigeta (Figure 2). In the middle of the experiment, to exclude yarn jamming the value of R_{1S2} was taken up as equal to 0.8 mm. Table 2 shows values of ratio of radius of internal circumference of torus R_{1S2} to the radius of working circumference R_{2S2} in blinded values.

Table 2 Orthogonal matrix for series SN2 for woolen spun yarn 31x2 tex

№	Factors					
	Input tension		Torus radii ratio		Contact angle	
	x_1	P_{0S2} [cN]	x_2	R_{1S2}/R_{2S2}	x_3	φ_{pS2} [°]
1	+1	24	+1	2.9	+1	105
2	-1	20	+1	2.9	+1	105
3	+1	24	-1	1.7	+1	105
4	-1	20	-1	1.7	+1	105
5	+1	24	+1	2.9	-1	85
6	-1	20	+1	2.9	-1	85
7	+1	24	-1	1.7	-1	85
8	-1	20	-1	1.7	-1	85
9	-1.215	19.6	0	2.3	0	95
10	+1.215	24.4	0	2.3	0	95
11	0	22	-1.215	1.6	0	95
12	0	22	+1.215	3	0	95
13	0	22	0	2.3	-1.215	83
14	0	22	0	2.3	+1.215	107
15	0	22	0	2.3	0	95

The correlation between the open-label and blinded values of series SN2 for woolen spun yarn 31x2 tex is as follows:

$$x1 = \frac{P_{0S2} - 22}{2}, \quad x2 = \frac{R_{1S2} / R_{2S2} - 2.3}{0.6}, \quad x3 = \frac{\phi_{PS2} - 95}{10} \tag{3}$$

Table 3 shows a second-order orthogonal matrix for series SN3. Factor x_1 is yarn tension prior the yarn goes to the guide having the form of torus, in the middle of the experiment for linen wet-spun yarn made of bleached roving 41 tex it is taken up as relatively equal to filling tension of warp yarns. During production of sindon, knitted fabric LN-1 and LN-2 for outer garments this value will be equal to P_{0S3} = 28 cN.

When determining the ratio of radius of internal circumference of torus R_{1S3} to radius of working circumference R_{2S3} the diameter of linen wet-spun yarn made of bleached roving 41 tex which equals 0.28 mm is taken into account. Therefore, in the middle of experiment, radius of working circumference of torus R_{2S3} is taken up as 0.35 mm. The radius of internal circumference of torus R_{1S3} is determined due to geometrical dimensions of operative parts of knitting machines and textile looms. In the middle of experiment, to exclude yarn jamming the value of R_{1S3} is taken up as 0.5 mm. Table 3 shows the ratios of radius of internal circumference of torus R_{1S3} to radius of working circumference R_{2S3} in blinded values.

Table 3 Orthogonal matrix for series SN3 for linen wet-spun yarn made of bleached roving 41 tex

№	Factors					
	Input tension		Torus radii ratio		Contact angle	
	x_1	$P_{0S3,}$ [cN]	x_2	R_{1S3}/R_{2S3}	x_3	φ_{pS3} [°]
1	+1	30	+1	1.7	+1	105
2	-1	26	+1	1.7	+1	105
3	+1	30	-1	1.1	+1	105
4	-1	26	-1	1.1	+1	105
5	+1	30	+1	1.7	-1	85
6	-1	26	+1	1.7	-1	85
7	+1	30	-1	1.1	-1	85
8	-1	26	-1	1.1	-1	85
9	-1.215	25.6	0	1.4	0	95
10	+1.215	30.4	0	1.4	0	95
11	0	28	-1.215	1	0	95
12	0	28	+1.215	1.8	0	95
13	0	28	0	1.4	-1.215	83
14	0	28	0	1.4	+1.215	107
15	0	28	0	1.4	0	95

The correlation between the open-label and blinded values of series SN3 for linen wet-spun yarn made of bleached roving 41 tex is as follows:

$$x1 = \frac{P_{0S3} - 28}{2}, \quad x2 = \frac{R_{1S3} / R_{2S3} - 1.4}{0.3}, \quad x3 = \frac{\phi_{PS3} - 95}{10} \tag{4}$$

Table 4 shows a second-order orthogonal matrix for series SSA. Factor x_1 is yarn tension prior the yarn goes to the guide having the form of torus, in the middle of the experiment for polyamide multifilament 29x2 tex it is taken up as relatively equal to filling tension of warp yarns. When producing multilayer technical fiber MTF for laying yard-coated pipes, knitting outer knitted and sports garments this value will be P_{0SA} = 35 cN.

When determining the ratio of radius of internal circumference of torus R_{1SA} to radius of working circumference R_{2SA} the diameter of polyamide multifilament 29x2 tex, which is 0.29 mm, is taken into account. Therefore, in the middle of experiment, the radius of working circumference R_{2SA} is taken up as 0.35 mm. The radius of internal circumference of torus R_{1SA} shall be determined based on geometrical dimensions of operative parts of knitting machines and textile looms. Values of radii were determined using USB Digital microscope Sigeta (Figure 2). In the middle of the experiment, to exclude yarn jamming, the value R_{1SA} is taken up as 0.55 mm. Table 4 shows values of ratio of radius of internal circumference of torus R_{1SA} to radius of working circumference R_{2SA} in blinded values.

Table 4 Orthogonal matrix for series SSA for polyamide multifilament 29x2 tex

№	Factors					
	Input tension		Torus radii ratio		Contact angle	
	x_1	P_{0SA} [cN]	x_2	R_{1SA}/R_{2SA}	x_3	φ_{pSA} [°]
1	+1	37	+1	1.9	+1	105
2	-1	33	+1	1.9	+1	105
3	+1	37	-1	1.3	+1	105
4	-1	33	-1	1.3	+1	105
5	+1	37	+1	1.9	-1	85
6	-1	33	+1	1.9	-1	85
7	+1	37	-1	1.3	-1	85
8	-1	33	-1	1.3	-1	85
9	-1.215	32.6	0	1.6	0	95
10	+1.215	37.4	0	1.6	0	95
11	0	35	-1.215	1.2	0	95
12	0	35	+1.215	2	0	95
13	0	35	0	1.6	-1.215	83
14	0	35	0	1.6	+1.215	107
15	0	35	0	1.6	0	95

The correlation between the open-label and blinded values of series SSA for polyamide multifilament 29x2 tex is as follows:

$$x1=\frac{P_{0SA}-35}{2},\quad x2=\frac{R_{1SA}/R_{2SA}-1.6}{0.3},\quad x3=\frac{\phi_{PSA}-95}{10}. \quad (5)$$

Values of radii of guide having the form of torus were determined using USB Digital microscope Sigeta (Figure 2).

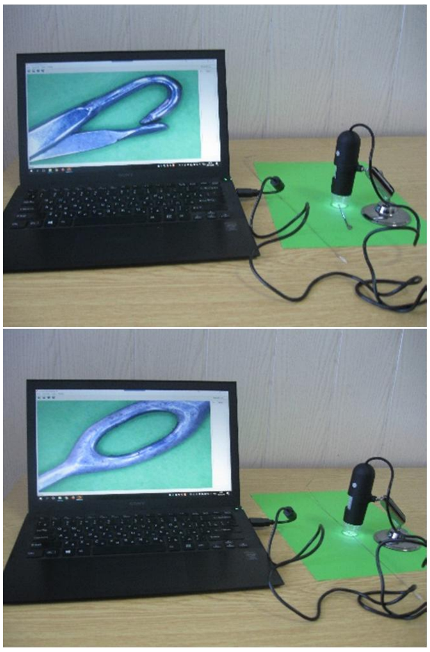

Figure 2 Installation to determine radii of guide having the form of torus yarns/decimetre); 5 - MTF - 9 (density of weft yarns 140 yarns/decimetre)

Figure 3 shows the diagram of experimental unit. Its set-up is described in detail in the paper [9, 20]. The distinction is that unit 4 of modelling the conditions of interaction between guides and operative parts of textile looms and knitting machines, which have the form of torus in the contact area with a yarn, includes a set of needles and sinkers, and heddles of knitting loom. The diameter of the working surface of torus is commensurate with diameter of the processed yarns.

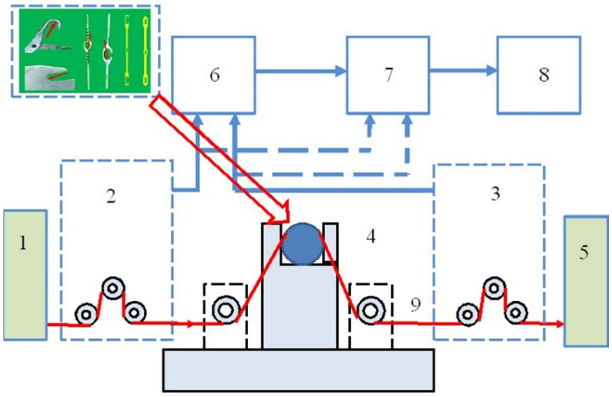

Figure 3 Installation to determine radii of guide having the form of torus yarns/decimetre); 5 - MTF - 9 (density of weft yarns 140 yarns/decimetre). The diagram of the experimental unit: 1 - yarn feeder unit; 2 - unit for measuring the yarn tension's slack side; 3 - unit for measuring the yarn tension's slack side; 4 - unit for modelling the conditions of interaction with guides and operative parts of textile machines; 5 - yarn receiver unit; 6 - driver; 7 - analog-to-digital converter ADC; 8 - personal computer; 9 - yarn

4 RESULTS AND DISCUSSION

As a result of implementation of second-order orthogonal designs for three factors (Tables 1-4) for series SN1-SN3 and SSA about 10 parallel measurements were performed. Its mean values are shown in Table 5.

Table 5 Results of the series of the experimental research to determine the joint effect of the yarn tension prior it goes to the guide having the form of torus P_0, the ratios of radius of internal circumference of torus R_1 to the radius of working circumference R_2, and nominal values of the contact angle φ_P to the yarn tension P behind the guide having the form of torus (series SN1-SN3 and SSA)

№	Factors			P_1 [cN]	P_2 [cN]	P_3 [cN]	P_{SA} [cN]
	x_1	x_2	x_3				
1	+1	+1	+1	49.6	36.3	31.9	70.5
2	-1	+1	+1	40.5	29.4	27.7	60.8
3	+1	-1	+1	50.3	36.8	32.1	71.7
4	-1	-1	+1	41.1	29.8	27.8	61.8
5	+1	+1	-1	44.8	33.8	31.6	63.6
6	-1	+1	-1	36.9	27.4	27.4	55.1
7	+1	-1	-1	45.4	34.2	31.7	64.5
8	-1	-1	-1	37.3	27.8	27.4	55.9
9	-1.215	0	0	38.1	27.9	27.1	57.5
10	+1.215	0	0	48.3	35.9	32.2	68.4
11	0	-1.215	0	43.6	32.1	29.9	63.7
12	0	+1.215	0	42.8	31.6	29.6	62.3
13	0	0	-1.215	40.6	30.5	29.5	59.1
14	0	0	+1.215	45.7	33.2	29.9	66.8
15	0	0	0	43.1	31.8	29.7	62.9

Using the known method of determining the coefficients in the regression equation (1) for the second-order orthogonal plan [10, 14], taking into account the relationships (2-5), the following regression relationships were determined.

Table 6 shows the values of the coefficients and the range of error in the regression equation (1) for the coded values of the factors, the error of the values of which, using the Student's test, with 95% probability allows to determine their value.

Table 6 Coefficient values and range of error in the regression equation

Series SN1		Series SN2	
	value		value
b0	43.1054+/-0.359364	b0	31.8135+/-0.347293
b1	8.3844+/-0.368791	b1	6.46958+/-0.356404
b2	-0.588622+/-0.368791	b2	-0.343582+/-0.356404
b3	4.18336+/-0.368791	b3	2,29375+/-0,356404
b11	0.109283+/-0.529399	b11	0.0923636+/-0.511618
b12	-0.075+/ 0.438569	b12	0.075+/-0.423839
b13	0.575+/-0.438569	b13	0.375+/-0.423839
b22	0.109283+/-0.529399	b22	0.0320084+/-0.511618
b23	-0.075+/-0.438569	b23	-0.125+/-0.423839
b33	0.0489278+/-0.529399	b33	0.0320084+/-0.511618
Series SN3		Series SNA	
	value		value
b0	29.7+/-0.339485	b0	62.9135+/-0.36778
b1	4.16568+/-0.348391	b1	8.96794+/-0.377428
b2	-0.138974+/-0.348391	b2	-1.00799+/-0.377428
b3	0.338505+/-0.348391	b3	6.29525+/-0.377428
b11	-0.0603552+/-0.50011	b11	0.0320084+/-0.541797
b12	-0.05+/-0.414309	b12	-0.075+/-0.44884
b13	0.0+/-0.414309	b13	0.625+/-0.44884
b22	0.0603552+/-0.500114	b22	0.0923636+/-0.541797
b23	-0.05+/-0.414309	b23	-0.125+/-0.44884
b33	0.0+/-0.500114	b33	0.0320084+/-0.541797

Series SN1, for carded cotton spun yarn 29x2 tex, the range of change in input tension *22.6 cN* ≤ P_{0S1} ≤ *27.4:*

$$P_{S1}=15.07+0.081P_{0S1}-0.3Z1-0.17\varphi_{PS1}+0.02P_{0S1}\varphi_{PS1}-0.07P_{0S1}Z1- \\ -0.01Z1\varphi_{PS1}+0.02P_{0S1}^2+0.7Z1^2+0.0002\varphi_{PS1}^2,\quad Z1=R_{1S1}/R_{2S1}. \tag{6}$$

Series SN2, for woolen spun yarn 31x2 tex, the range of change in input tension *19.6 cN* ≤ P_{0S2} ≤ *24.4 cN*:

$$P_{S2}=12.6+0.22P_{0S2}-0.52Z2-0.12\varphi_{PS2}+0.007P_{0S2}\varphi_{PS2}-0.01P_{0S2}Z2- \\ -0.002Z2\varphi_{PS2}+0.02P_{0S2}^2+0.1Z2^2-0.0004\varphi_{PS2}^2,\quad Z2=R_{1S2}/R_{2S2}. \tag{7}$$

Series SN3, for linen wet-spun yarn made of bleached roving 41 tex, the range of change in input tension *25.6 cN* ≤ P_{0S3} ≤ *30.4 cN*:

$$P_{S3}=1.52P_{0S3}+0.79Z3+0.029\varphi_{PS3}-0.04P_{0S3}Z3- \\ -0.008Z3\varphi_{PS3}-0.007P_{0S3}^2+0.3Z3^2-8.68,\quad Z3=R_{1S3}/R_{2S3} \tag{8}$$

Series SSA, for polyamide multifilament 29x2 tex, the range of change in input tension *32.6 cN* ≤ P_{0SA} ≤ *37.4 cN*:

$$P_{SA}=9.69+0.57P_{0SA}+0.79Z_{SA}-0.22\varphi_{PSA}+0.015P_{0SA}\varphi_{PSA}-0.07P_{0S2}Z_{SA}- \\ -0.02Z_{SA}\varphi_{PSA}+0.01P_{0SA}^2+0.56Z_{SA}{}^2+0.0002\varphi_{PSA}^2,\quad Z_{SA}=R_{1SA}/R_{2SA}. \tag{9}$$

For nominal value of contact angle in the middle of experiment φ_P = 95°, when determining changes in yarn tension behind the guide surface having the form of torus, the equations (6-9) are converted as follows:

- series SN1, for carded cotton spun yarn 29x2 tex, the range of change in input tension *22.6 cN* ≤ P_{0S1} ≤ *27.4*:

$$P_{S1}=0.73+1.98P_{0S1}-1.25Z1-0.07P_{0S1}Z1+0.02P_{0S1}^2+0.7Z1^2; \\ Z1=R_{1S1}/R_{2S1}, \tag{10}$$

- series SN2, for woolen spun yarn 31x2 tex, the range of change in input tension *19.6 cN* ≤ P_{0S2} ≤ *24.4*:

$$P_{S2}=4.81+0.89P_{0S2}-0.71Z2-0.01P_{0S2}Z2+0.02P_{0S2}^2+0.1Z2^2 \\ Z2=R_{1S2}/R_{2S2}, \tag{11}$$

- series SN3, for linen wet-spun yarn made of bleached roving 41 tex, the range of change in input tension *25.6 cN* ≤ P_{0S3} ≤ *30.4*:

$$P_{S3}=1.52P_{0S3}+0.03Z3-0.04P_{0S3}Z3-0.0075P_{0S3}^2+0.3Z3^2-5.93 \\ Z3=R_{1S3}/R_{2S3}, \tag{12}$$

- series SSA, for polyamide multifilament 29x2 tex, the range of change in input tension *32.6 cN* ≤ P_{0SA} ≤ *37.4*:

$$P_{SA}=1.99P_{0SA}-1.11Z_{SA}-0.067P_{0S2}Z_{SA}+0.005P_{0SA}^2+0.56Z_{SA}{}^2-9.03; \\ Z_{SA}=R_{1SA}/R_{2SA}. \tag{13}$$

Figure 4 shows the response surfaces for series SN1-SN3 and SSA. Yarn tension behind the guide surface having the form of torus is represented by functions, which take into account joint effect of yarn tension before the yarn goes to the guide having the form of torus P_0, ratios Z of radius of internal circumference of torus R_1 to radius of working circumference R_2. Nominal value of the contact angle φ_p was fixed value. Such value corresponded to the middle of the experiment (Tables 1-4). Adequacy of the obtained regression relationships was tested using SPSS program for statistical processing of experimental data [8, 9, 14, 20].

For nominal value of contact angle φ_P = 95°, having fixed value of the input tension, the equations (10-13) are converted as follows:

- series SN1, for carded cotton spun yarn 29x2 tex, with the value of input tension in the middle of experiment P_{0S1} = 25 cN:

$$P_{S1}=62.75-3Z1+0.7Z1^2,\quad Z1=R_{1S1}/R_{2S1} \tag{14}$$

- series SN2, for woolen spun yarn 31x2 tex, with the value of input tension in the middle of experiment P_{0S2} = 22 cN:

$$P_{S2}=33.96-0.93Z2+0.1Z2^2,\quad Z2=R_{1S2}/R_{2S2} \tag{15}$$

- series SN3, for linen wet-spun yarn made of bleached roving 41 tex, with the value of input tension in the middle of experiment P_{0S3} = 28 cN:

$$P_{S3}=30.76-1.09Z3+0.3Z3^2,\quad Z3=R_{1S3}/R_{2S3} \tag{16}$$

- series SSA, for polyamide multifilament 29x2 tex, with the value of input tension in the middle of experiment P_{0SA} = 35 cN:

$$P_{SA} = 66.93 - 3.46 Z_{SA} + 0.56 Z_{SA}^{2}, \quad Z_{SA} = R_{1SA} / R_{2SA}. \quad (17)$$

Equations (14-17) were used to obtain values for yarn tension behind guide surface having the form of torus depending upon ratio Z of radius of internal circumference of torus R_1 to radius of working circumference R_2, which are represented in Table 7. Figure 5 shows curves reflecting the changes in yarn tension behind guide surface having the form of torus depending on ratio Z of radius of internal circumference of torus R_1 to radius of working circumference R_2. These curves were fitted according to the data from Table 6. Analysis of the curves on Figures 5a and 5b shows that value of tension behind the guide surface having the form of torus decreases with the value of ratio Z of radius of internal circumference of torus R_1 to radius of working circumference R_2 (Figure 1c) increase. It can be explained by decrease of value of contact angle of the lateral surface of yarn in the contact are with guide surface having the form of.

Obtained results may be used for optimization of technological processes in weaving and knitting productions with relation to minimization of the yarn tension in the working area, where knitted fabric and fabric are formed.

Table 7 Values of yarn tension behind the guide surface having the form of torus depending on ratio Z of radius of internal circumference of torus R_1 to radius of working circumference R_2

Z	Yarn tension values behind the guide surface having the form of torus			
	SN1	SN2	SN3	SSA
1	60.45	33.13	29.97	64.03
1.1	60.29	33.05	29.92	63.80
1.2	60.15	32.98	29.88	63.58
1.3	60.03	32.92	29.85	63.37
1.4	59.92	32.85	29.82	63.18
1.5	59.82	32.79	29.80	63.00
1.6	59.74	32.72	29.78	62.82
1.7	59.67	32.66	29.79	62.67
1.8	59.61	32.61	29.75	62.51
1.9	59.57	32.55	29.76	62.37
2.0	59.55	32.50	29.78	62.25

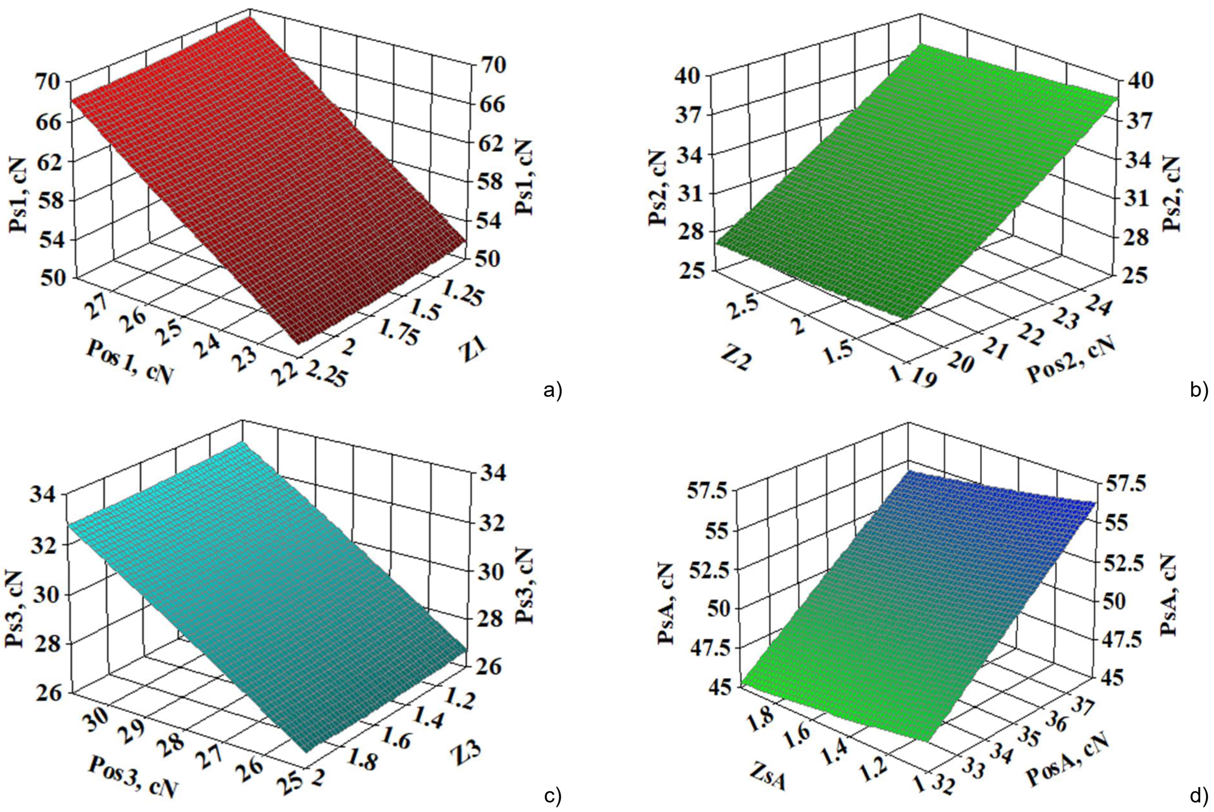

Figure 4 response surfaces for series SN1-SN3 and SSA: a) for cotton carded spun 29x2 tex (series SN1); b) for woolen spun yarn 31x2 tex (series SN2); c) for linen wet-spun yarn made of bleached roving 41 tex (series SN3); d) for polyamide multifilament 29x2 tex (series SSA)

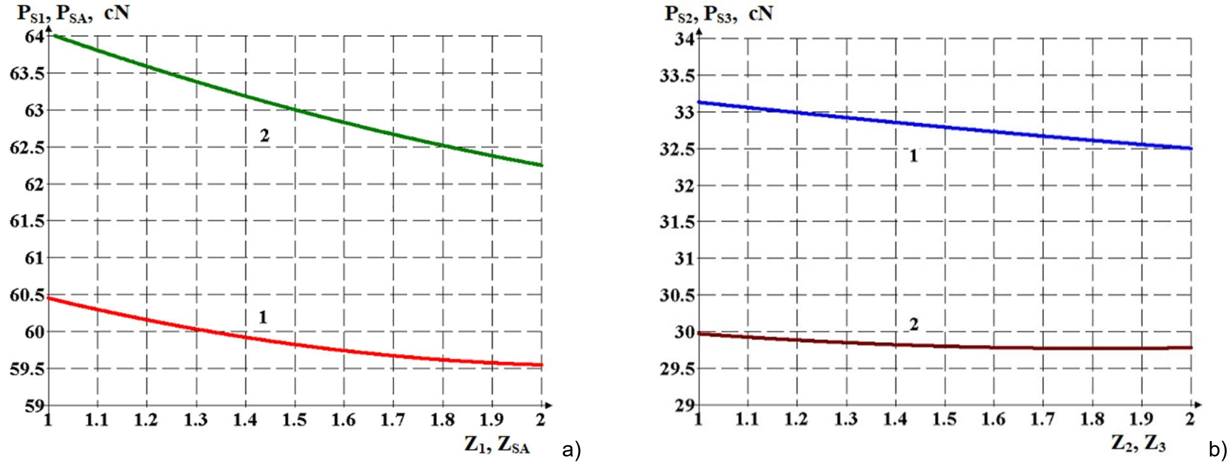

Figure 5 curves reflecting the changes in yarn tension behind guide surface having the form of torus depending on ratio of radius of internal circumference of torus to radius of working circumference: a) series SN1(1), series SSA(2); b) series SN2(1), series SN3(2)

5 CONCLUSIONS

Improvement of a technological process in weaving and knitting production means optimization of technological efforts based on minimizing of yarn tension in the fabric and knitted fabric formation area. The research related to determining of the yarns tension when interacting with guide and operative parts of weaving looms and knitting machines having the form of torus in the area of contact with yarn established the mechanism of yarn tension increase behind the guide having the torus form due to change in geometrical dimensions and friction forces within contact area.

The regression relationships were obtained resulting from delivery of series of experimental researches to determine joint effect of yarn tension prior it goes to guide having the form of torus P_0, ratio of radius of internal circumference of torus R_1 to radius of working circumference R_2, and nominal value of contact angle φ_P on yarn tension P behind the guide having the form of torus for carded cotton spun yarn 29x2 tex (input tension variation range $22.6\ cN \leq P_{0S1} \leq 27.4$ - series SN1), for woolen spun yarn 31x2 tex (input tension variation range $19.6\ cN \leq P_{0S2} \leq 24.4\ cN$ - series SN2), for linen wet-spun yarn made of bleached roving 41 tex (input tension variation range $25.6\ cN \leq P_{0S3} \leq 30.4\ cN$ - series SN3), for polyamide multifilament 29x2 tex (input tension variation range $32.6\ cN \leq P_{0SA} \leq 37.4$ - series SSA). It was established that tension degree behind the guide surface having the form of torus becomes less while value of ratio Z of radius of internal circumference of torus R_1 to radius of working circumference R_2 increases. It can be explained by decrease of contact angle value for lateral surface of yarn in the area of contact with guide surface having the form of torus.

Obtained results and their usage make it possible to optimize yarn manufacturing process at the technological equipment in view of minimization of yarn tension in the working area, where fabric and knitted fabric are formed, to reduce yarn breakage, and to improve performance of weaving and knitting machines.

Obtained results can be used to improve technological processes in the fabric and knitted fabric production.

Acknowledgement: *We would like to express our gratitude to management of Danish Textiles for raw materials provided to carry out experiments and for possibility to test research results in working environment.*

6 REFERENCES

1. Vasconcelos F.B., Marcicano J.P.P., Sanches R.A.: Influence of yarn tension variations before the positive feed on the characteristics of knitted fabrics, Textile Research Journal 85(17), 2015, pp. 1864-1871, https://doi.org/10.1177/0040517515576327
2. Koo Y., Kim H.: Friction of cotton yarn in relation to fluff formation on circular knitting machines, Textile Research Journal 72(1), 2002, pp. 17-20, https://doi.org/10.1177/004051750207200103
3. Yakubitskaya I.A., Chugin V.V., Shcherban' V.Yu.: Dynamic analysis of the traversing conditions at the end sections of the groove in a winding drum, Izvestiya Vysshikh Uchebnykh Zavedenii (Technology of Textile Industry) 5, 1997, pp. 33-36 (in Russian)
4. Yakubitskaya I.A., Chugin V.V., Shcherban' V.Yu.: Differential equations for relative yarn movement in the end sections of the channel in the winding drum, Izvestiya Vysshikh Uchebnykh Zavedenii. (Technology of Textile Industry) 6, 1997, pp. 50-54 (in Russian)
5. Shcherban' V.Yu.: Interaction of stiff yarns with the working parts of knitting and sewing machines, Textile industry 10, 1988, pp. 53 (in Russian)

6. Shcherban' V.Yu.: Determining the technological forces during beating-up in the production of multilayer industrial fabrics, Izvestiya Vysshikh Uchebnykh Zavedenii (Technology of Textile Industry) 3, 1990, pp.44-47 (in Russian)
7. Weber M.O., Ehrmann A.: Necessary modification of the Euler-Eytelwein formula for knitting machines, The Journal of The Textile Institute 103(6), 2012, pp. 687-690, https://doi.org/10.1080/00405000.2011.598665
8. Shcherban' V., Makarenko J., Petko A., Melnyk G., Shcherban' Yu., Shchutska G.: Computer implementation of a recursion algorithm for determining the tension of a thread on technological equipment based on the derived mathematical dependences, Eastern-European Journal of Enterprise Texnologies 2(1), 2020, pp. 41-50, DOI: 10.15587/1729-4061.2020.198286
9. Shcherban' V., Melnyk G., Sholudko M., Kolysko O., Kalashnyk V.: Yarn tension while knitting textile fabric, Vlákna a textil (Fibres and Textiles) 25(3), 2018, pp. 74-83
10. Shcherban' V., Melnyk G., Sholudko M., Kolysko O., Kalashnyk V.: Improvement of structure and technology of manufacture of multilayer technical fabric, Vlákna a textil (Fibres and Textiles) 26(2), 2019, pp. 54-63
11. Kovar R.: Impact of directions on frictional properties of a knitted fabric, Vlákna a textil (Fibres and Textiles) 14(2), 2007, pp. 15-20
12. Vasil'chenko V.N., Shcherban' V.Yu., Apokin Ts.V.: Attachment for holding multilayer fabrics in the clamps of a universal tensile tester, Textile Industry 8, 1987, pp. 62 (in Russian)
13. Vasilchenko V.N., Shcherban' V.Yu.: Effect of the twist of Kapron filament yarn on its bending rigidity, Izvestiya Vysshikh Uchebnykh Zavedenii. (Technology of Textile Industry) 4, 1986, pp. 8-9 (in Russian)
14. Shcherban' V., Makarenko J., Melnyk G., Shcherban' Y., Petko A., Kirichenko A.: Effect of the yarn structure on the tension degree when interacting with high-curved guides, Vlákna a textil (Fibres and Textiles) 26(4), 2019, pp. 59-68
15. Döonmez S., Marmarali A.: A model for predicting a yarn's knittability, Textile Research Journal 74(12), 2004, pp. 1049-1054, https://doi.org/10.1177/004051750407401204
16. Liu X., Chen N., Feng X.: Effect of yarn parameters on the knittability of glass ply yam, Fibres & Textiles in Eastern Europe 16(5), 2008, pp. 90-93
17. Shcherban' V., Korogod G., Chaban V., Kolysko O., Shcherban' Yu., Shchutska G.: Computer simulation methods of redundant measurements with the nonlinear transformation function, Eastern-European Journal of Enterprise Technologies 2(5), 2019, pp. 16-22, https://doi.org/10.15587/1729-4061.2019.160830
18. Hammersley M.J.: 7-A simple yarn-friction tester for use with knitting yarns, The Journal of The Textile Institute 64(2), 1973, pp. 108-111, https://doi.org/10.1080/00405007308630420
19. Sodomka L., Chrpová E.: Method of determination of Euler friction coefficients of textiles, Vlákna a textil (Fibres and Textiles) 15(2-3), 2008, pp. 28-33
20. Shcherban' V., Melnyk G., Sholudko M., Kalashnyk V.: Warp yarn tension during fabric formation, Vlákna a textil (Fibres and Textiles) 25(2), 2018, pp. 97-104

PERFORMANCE OF TEXTILE MATERIALS FOR THE NEEDS OF CHILDREN WITH SKIN PROBLEMS

Marcela Skodova[1], Viera Glombikova[2], Petra Komarkova[2] and Antonin Havelka[2]

[1]The Institute for Nanomaterials, Advanced Technologies and Innovation, Technical University of Liberec, Czech Republic
[2]Department of Clothing Technology, Faculty of Textile Engineering, Technical University of Liberec, Czech Republic
marcela.skodova@tul.cz, viera.glombikova@tul.cz, petra.komarkova@tul.cz, antonin.havelka@tul.cz

Abstract: *This study focuses on the experimental investigation of the efficiency of knitted fabric for the needs of children with skin problems. The aim of this study was to compare the end-use properties of commonly available cotton knitted fabrics with other knitted fabrics from fibres mixtures such as Tencel, Viloft, Micromodal, Crabyon, polypropylene with Ag+ and linen. The physiological and sensory comfort of knitted fabrics was determined by laboratory measurements. The following parameters were tested on selected knitted fabrics: pilling, total hand value, air permeability, thermal effusivity and water vapour permeability. The results suggest that knitted fabrics made from viscose fibre or linen have been shown to be better or comparable as cotton. In addition, some viscose materials (with chitosan) and linen are antibacterial, antistatic and thermoregulatory. Clothes made of mixtures of viscose fibres or linen can substitute for cotton fabrics for clothing intended for children with skin problems.*

Keywords: *Physiological and sensory comfort, skin problems, Tencel, Viloft, Micromodal, Crabyon, polypropylene, linen.*

1 INTRODUCTION

Expertise studies show that for people with skin problems is important option appropriate clothing, especially when the fabric comes into direct contact with the skin [1]. Until now, cotton materials have been used as the most suitable for this purpose. Recent studies have reconsidered this view [2]. Short cotton fibres can irritate the skin and high moisture absorption cotton creates conditions for bacterial growth. Rapid development in the field of materials research offers enormous opportunities to improve the functionality of the clothing and textile products [3]. Conditions can be created that will increase the comfort of children in the event of skin problems and optimize the skin environment [4]. Modern technologies and innovative possibilities are offered by a new generation of chemical fibres. They represent a significant potential for improving health care and preventing the health problems of the population [5].

1.1 Clothing requirements for children with skin problems

When caring for human skin, it is important to:

- keep its basic functions in balance,
- protect it from exposure to adverse environmental influences,
- maintain optimal hydration,
- prevent excessive overheating or drying.

These requirements can be met by appropriate clothing, modification of the external and internal environment, the use of appropriate cosmetic and medical care products [6].

It is necessary to increase the immunity of the skin, keeping the skin supple due to appropriate hydration, prevent inflammatory infections and soothe itching for children with skin diseases [7].

The first step is the choose the right clothes in caring for children's skin. Such clothing does not seal, does not irritate the skin, is breathable, does not lead to overheating or to increased sweating, especially in the skin folds, where the skin touches each other [1].

Children's skin differs from adult skin by morphological and functional peculiarities [8]. The structure of children's skin changes with the age of the child and each stage of childhood requires a specific approach - different is the care of the skin of a newborn, different is the skin of a school-age child [9]. Excessive sweating, unsuitable materials and the wrong size of clothes are not good for children's skin. Child's organism is constantly growing and evolving and is equipped with a less sophisticated system of thermal regulation [10].

Children's skin requires attention and individual care 24 hours a day, 365 days a year [6]. This means a different seasonal approach to her treatment. It is necessary, especially for the youngest children, protection against the sun's rays (photoprotection) in summer. Summer hats and caps protect children from overheating, sunburn and reduce the radiation that falls on the eyes by up to 50%. Moreover, children tolerate very low temperatures less than adults due to the currency of a perfect system of thermoregulation in winter. Proper dressing and prevention of cold sweat are ones of the most important measures that relate not only to the seasons and the activity of the child but also the appropriate choice of clothing size [4]. There are important pleasant fabric handle (the handle characteristics of fabric), non-irritability, good drain of humidity (sweat) and breathable material for clothes for children with skin problems. Used seams should not be hard, sharp or irritating. The issue of easy maintenance needs to be addressed for all products [11]. Clothes are in direct contact with the skin throughout the day, so it is important to carefully select suitable substances that would not damage the skin. Due to their hygienic properties, fabrics made of natural fibres are preferred. Cotton is the most commonly used fabric for patients with atopic dermatitis. It has good folding resistance, better heat conduction, easy dyeing and excellent moisture absorption. Silk fabrics help to keep body temperature by reducing excessive sweating and moisture loss. A new type of silk fabric made from translucent and slightly elastic woven silk is now commercially available (Microair Dermasilk®) and can be used to care for the skin of children with atopic dermatitis. Silver products (textiles/fibres containing silver) have also been shown to offer two benefits in controlling bacterial infections. The fabrics can be used not only on clothing, but also to prevent mite sensitization in atopic patients [12]. Wool fibres that irritate the skin are not suitable, but wearing of Merino wool clothing did not produce any negative cutaneous effects compared with wearing standard clothing [13]. Other studies [14, 15] show that fine-diameter Merino wool clothing should be considered acceptable for people with eczema and seems to be therapeutic to patients with mild to moderate atopic dermatitis. Functional textiles are gaining in importance in medical applications and play a vital role in inflammatory skin conditions. For example, the benefits of two cellulose-based fabrics, Lyocell and SeaCell®, for patients with dermatitis are reported. The use of Lyocell as a nonwoven fabric with biofunctional properties and the ability of SeaCell® to bind and absorb substances, including antimicrobial substances such as silver, are emphasized [16].

1.2 Properties of fibrous knitted fabrics

Modern technologies and innovative possibilities offered by the new generation of fibres represent a significant potential for improving health care and preventing problems. Highly functional fibres give textiles and clothing products made from them specific properties, such as antibacterial, anti-inflammatory, increased absorbency and breathability, thermal insulation or thermoregulatory ability. Rapid development of materials research offers enormous opportunities to improve the functionality of clothing and textiles. The properties of fibrous materials fundamentally determine the properties complexivity of knitted fabrics which are used for AD patients clothing. Therefore properties of special fibres have been investigated to uncover their benefit for AD patient clothing in this article.

Tencel viscose fibre excels in its softness, it is softer than cotton. It is easy to maintain, breathable, helps with temperature control and is suitable for the production of underwear [17].

Polypropylene fibre has low moisture absorbency, low thermal conductivity, high color fastness, and low weight. Polypropylene fibres have a special profile. The cross-section of the fibre is similar to a five-lobed star, and thanks to this profile, moisture wicking is doubled. Thanks to this construction, the fibre is able to absorb a large amount of air, which acts as an insulating layer when the body is unloaded and cools [18].

The special ***Viloft® viscose fibre*** excels in breathability, exceptional moisture transport ability, antistatic properties, softness, thermal insulation properties and easy maintenance [19].

MicroModal® is a fibre made of beech cellulose. The material of these fibres is light, fine and with a regular structure, compared to silk. It is resistant to mechanical stress, resistant to wrinkling, better wicks moisture away from the skin - greater comfort [20].

Crabyon cellulose fibre is completely biodegradable, has an effective antibacterial function for a long time, excellent coloring, prevents the skin from drying out and is therefore suitable for children with skin problems [21].

Linen fibres have high moisture-wicking abilities and low heat retention abilities. Linen products have a stiffer total hand value, good absorbency and are cool. Thanks to the high strength of linen, the products are durable [22].

Cotton fibres have good tensile and abrasion strength. The products have a good total hand value and high absorbency. The products are easy to squeeze, pilling and only provide limited protection against the cold [23].

2 MATERIALS AND METHODS

2.1 Parameters of tested knitted fabrics

The aim of this study is to compare the end-use properties of fabrics made of both functional fibres and classic fibres (cotton). Textiles and clothes with increased comfort properties for the specific needs of children with skin problems have been produced from the above-mentioned fibres. These fabrics appear to be an essential part of complex measures to increase wearing comfort and support the healing process. The knitted fabrics were produced (K1, K2, K3 and K4 are custom made) and selected (K5 and K6 are commercially available) that meet the requirements of sensory and physiological comfort. Based on this requirement, the selection of the following materials (Table 1) for children's clothing was recommended.

Table 1 Parameters of tested knitted fabric for the production of children's clothing

Sample	Fibre content/commercial name	Structure of knitted fabric	Weight [g/m^2]	Thickness [mm]	Stitch density [cm^{-2}]
K1	Viscose (Tencel) 50% / Polypropylene with Ag+ 50%	jersey fabric	161	0.64	240
K2	Viscose (Viloft) 60% / Viscose (Micromodal) 40%	jersey fabric	116	0.45	234
K3	Viscose (Micromodal) 48% / Cotton 40% / Viscose with chitosan(Crabyon) 12%	double jersey	143	0.93	374
K4	Linen 100%	jersey fabric	149	0.53	224
K5	Cotton 100%	interlock	210	0.90	330
K6	Organic cotton 100%	jersey fabric	154	0.64	323

Note: Organic cotton refers to naturally cultivated cotton without the use of any synthetic agricultural chemicals such as fertilizers or pesticides or transgenic technology [24].

2.2 *Methods of testing*

Selected end-use properties and their evaluation methods that are associated with physiological comfort will now be presented. It is important to testing of pilling, total hand value, air permeability, thermal effusivity and water vapour permeability for the physiological and sensory properties of knitted fabrics for children with skin problems. The measurement was applied on brand-new samples (without maintenance).

Pilling / Abrasion resistance - appearance change - determination of the pilling / abrasion resistance of tested samples was carried out by the Martindale method EN ISO 12945-1 / EN ISO 12947-4. The degree of appearance change AP [-] of tested samples was determined in range 1-5. The degree 1 means the biggest appearance change and the degree 5 the smallest one.

Total Hand Value - determination of the total hand value of tested samples was being executed by Kawabata system by Internal regulation IP KOD 01_2004 [25]. Properties that allow objective evaluation of total hand value are measured. The measuring system is able to test the tensile, shear, bending and surface properties in a standard load. The measurement of the fabric is called the Total Hand Value and takes values from 1 to 5 (excellent THV has a value of 5).

Air permeability - the rate of air flow passing perpendicularly through a known area of fabric is adjusted to obtain a prescribed air pressure differential between the two fabric surfaces [26]. From this rate of air flow, the permeability of the fabric is determined by the standard EN ISO 9237 “Determination of the permeability of fabrics to air”.

Heat transport - thermal transport properties were measured using C-Therm Thermal Conductivity Analyzer TCi. The TCi employs the Modified Transient Plane Source (MTPS) technique in characterizing the thermal conductivity TC [W/m.K] and thermal effusivity TE [W.s^{½}/m^{2}K] of materials. The standard test method EN 61326-2-4:2006 was used for this testing by TCi.

Water vapour permeability - the FX 3180 Cup Master was used for measurement of water vapour permeability. This equipment determines parameter the Water Vapour Transmission Rate WVTR [g/m²/24 h] using the gravimetric measuring principle. The measurement was carried out according to standard JIS L 1099 (2012).

3 RESULTS AND DISCUSSION

As shown in Figure 1, the samples K1, K2 and K4 achieve very good resistance to pilling. This is due to the structure of knitted fabric and stitch density. Cotton samples K5, K6 have a lower resistance to pilling because of the character of used fibres.

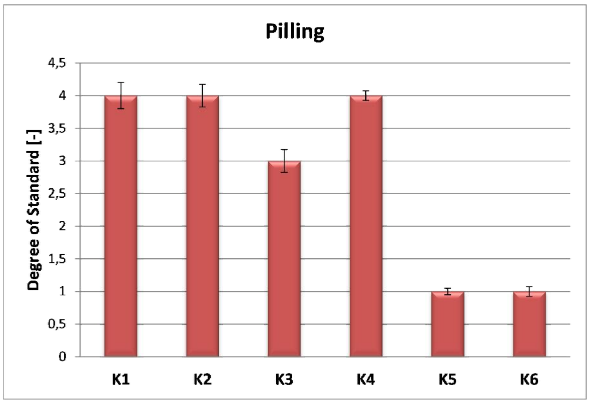

Figure 1 Test results of pilling

On the contrary to the pilling results, samples containing cotton K3, K5 and K6 achieve excellent total hand value. These samples have below-average stiffness, above-average smoothness, fullness of hand value and softness as measured. These properties are given mainly by fabric structure (pattern, density, thickness, etc.) in combination with material raw of tested samples. In the above-average total hand value of the samples are K1 and K4. Below-average stiffness, good smoothness and softness were found here. Surprisingly, the sample K2 (Viloft/Micromodal) has been shown the lowest total hand value, because of a limited low stiffness, above-average smoothness and fullness of the hand value. What is interesting about this fact is that sample K2 has the lowest thickness, weight and density from all tested samples and there is a positive structure condition to pleasant to touch.

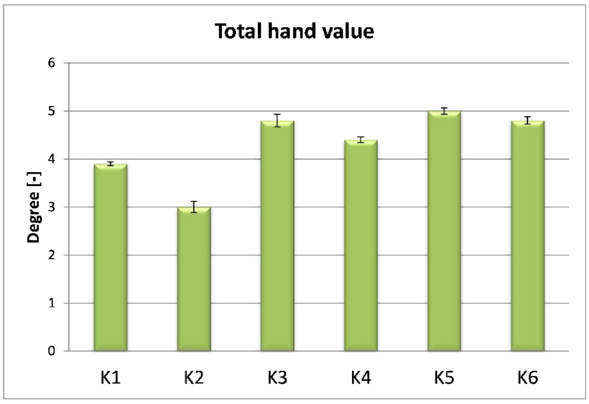

Figure 2 Test results of Total Hand Value

Figure 2 provides the test results of the total hand value.

Air permeability is significantly influenced by a fabric´s material and structural properties too. The results of the air permeability test are presented in Figure 3. Very good air permeability is achieved by samples K1, K2 and K4, which have a lower stitch density and a smaller thickness. In contrast, samples containing cotton K3, K5 and K6 have lower air permeability values due to higher stitch density and higher thickness.

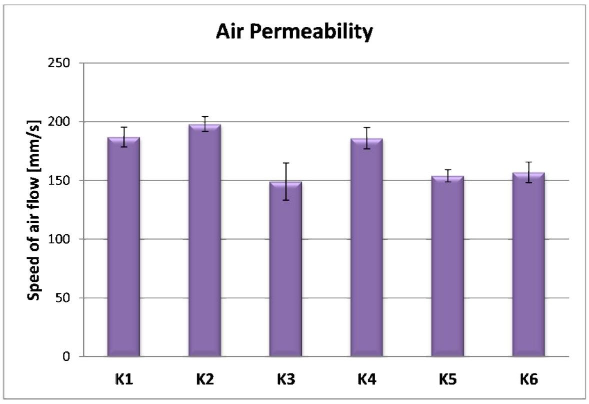

Figure 3 Test results of air permeability

When determining the water vapour permeability, the tested samples are compared with a reference water sample, where Water Vapour Transmission Rate WVTR = 17.000 g/m^2/24 h. Figure 4 presents the value of testing water vapour permeability. The samples K1, K2 and K4 with a smaller thickness and a smaller stitch density have very good water vapour permeability. The samples K3, K5 and K6 containing cotton fibres show lower values of water vapour permeability due to a higher thickness and higher stitch density.

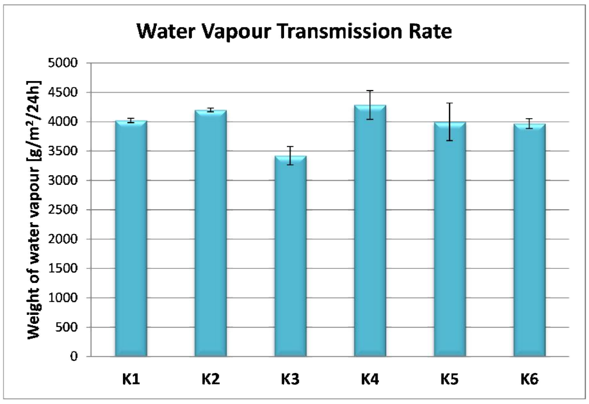

Figure 4 Test results of WVTR

Thermal effusivity is a parameter that characterises the transient thermal feeling during the first contact of the body skin with clothes. From the point of view of thermal effusivity, the samples K1, K2 and K4 have lower values, which is related to the high thermal conductivity and it represents the cold character of the knitted fabric. In contrast, samples K3, K5 and K6 containing cotton show a warm feeling, as shown in Figure 5.

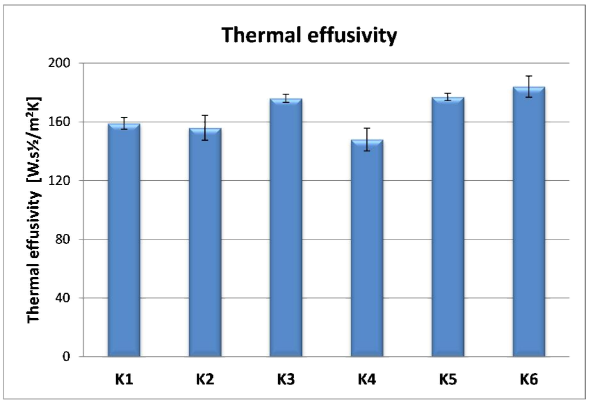

Figure 5 Test results of thermal effusivity

The Figure 6 presents parameter TLWC [%] (Total Level of Wearing Comfort) that is given by sum of percentage contributions (PC) of each tested properties to total performance of tested samples. These percentage contributions were calculated for each tested parameter on the basis of the measured value of the best sample (e.g., value PC of WVTR for sample K4 was considered such as 100%). PC values of WVTR for rest of samples were proportionally related to this "the best" value. The same procedure was applied for each measured parameter. Tested samples can achieve maximum value of TLWC equals 500%.

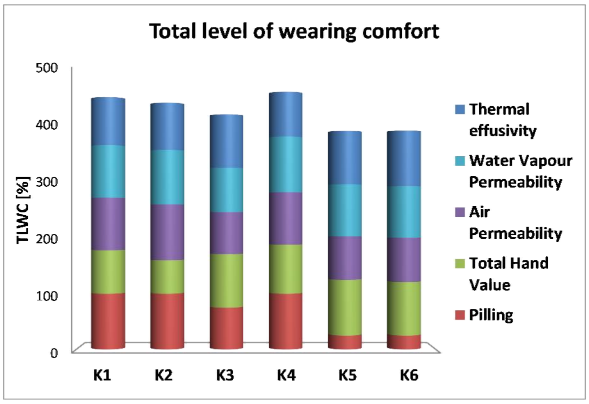

Figure 6 Comparison tested samples from point of view of TLWC

Parameter TLWC can be considered to simplified and moreover rough tool for appraisal of tested samples performance. Nevertheless, the Figure 6 shows clear differences between efficiency of tested samples. The most obvious finding to emerge from this analysis is that sample K4 (linen) achieved the best value of TLWC, moreover the distribution of PC for individual tested parameters of sample K4 are nearly uniform. In the present study, comparing cotton fabrics with others functional samples including linen showed that is possible to substitute commonly used cotton material for these special materials in order to support heath for AD illness. It is question, if this fact is acceptable by customer manners.

4 CONCLUSIONS

The aim of this study was to test the end-use properties of selected knitted fabrics intended for clothing of children with skin problems. Methods for evaluating the performance of knitted fabrics from mixtures of viscose, polypropylene and linen yarns and their comparison with knitted fabrics containing cotton were selected and described. The following the end-use properties were tested - pilling, total hand value, air permeability, water vapour permeability and thermal effusivity. The purpose of this study was to select a suitable material with better both physiological and sensorial properties for clothing for children with skin problems. This research has shown that all selected knitted fabrics achieve good value in terms of performance, but some knitted fabrics are more suitable for children with skin problems. In the evaluated parameters, sample K1 from a mixture of viscose and polypropylene fibres with silver performed best and K4 from 100% linen yarns. The problem with linen material is the difficult workability and durability of the material due to the brittleness of the fibres in use. Sample K2, which is composed of a mixture of Viloft and Micromodal viscose fibres, also shows very good values of the tested parameters.

The research has shown that, from the point of view of the evaluation of thermal effusivity, these knitted fabrics can be divided into use for summer and winter periods. Samples K1, K2 and K4 have a cooling character and are suitable for summer. On the contrary, samples K3, K5 and K6 show a warm feeling and are suitable for cold conditions. Taken together, these results suggest that fabrics made from mixtures with viscose fiber or made from linen can fully substitute cotton fabric to support and even increase in health for AD patients.

A natural progression of this work is to complete the objective laboratory evaluation of end-use properties of knitted fabrics by subjective practical test. The selected set of probands will record the course and conditions of using clothes made from samples K1 and K2. The evaluation will be performed using standards and questionnaires. Clothes made of tested materials for children with skin problems will significantly contribute to increased comfort in case of skin diseases, support the healing process and help optimize the skin environment.

Several questions still remain to be answered. Therefore future research should be focus on determining of effect of fabric maintenance (namely by washing) to clothing comfort performance of tested samples.

ACKNOWLEDGEMENT: *This research work is supported by Project MPO FV20287 – TEXDERM.*

5 REFERENCES

1 Glombikova V., Nemcokova R., Komarkova P., Kus Z.: Evaluation of liquid moisture transport in textile structures, Indian Journal of Fibre and Textile Research 43(1), 2018, pp.74-82

2 Gu J., Yuan L., Zhang Z., et al.: Non-leaching bactericidal cotton fabrics with well-preserved physical properties, no skin irritation and no toxicity, Cellulose 25, 2018, pp. 5415-5426, https://doi.org/10.1007/s10570-018-1943-8

3 Tomanova L.: The dress of the future as a second cyborg skin (Šaty budoucnosti jako druhá kůže kyborgova), 2014, available 11.09.2020 from: https://www.materialtimes.com/tema-tydne/saty-budoucnosti-jako-druha-kuze-kyborgova.html (in Czech)

4 Horakova M.: Pediatric dermatovenerology (Dětská dermatovenerologie), Avicenum, Praha, 1985 (in Czech)

5 Nelson G.: Application of microencapsulation in textiles, International Journal of Pharmaceutics 242(1-2), 2002, pp. 55-62, https://doi.org/10.1016/S0378-5173(02)00141-2

6 Vocilkova A.: Principles of skin care (Zásady péče o pokožku), available 11.09.2020 from: http://vyzivadeti.cz/wp-content/uploads/2013/05/Skripta_Pece-o-pokozku.doc (in Czech)

7 Wollenberg A, Feichtner K.: Atopic dermatitis and skin allergies - update and outlook, Allergy 68(12), 2013, pp. 1509-1519, https://doi.org/10.1111/all.12324

8 Štork J. et al.: Dermatovenerology (Dermatovenerologie), Praha: coedition Galén - Karolinum, 2008 (in Czech)

9 Shekariah T., Kalavala M., Alfaham M.: Atopic dermatitis in children: a practical approach, Paediatrics and Child Health 21(3), 2011, pp. 112-118, https://doi.org/10.1016/j.paed.2010.08.018

10 Havenith G.: Clothing and thermoregulation, Elsner P., Hatch K., Wigger-Alberti W. (Eds): Textiles and the Skin, Curr Probl Dermatol. Basel, Karger vol. 31, 2003, pp 35-49, https://doi.org/10.1159/000072236

11 Deljova R.A., Afanasjevova R.F., Cubarovova Z.S.: Clothing hygiene (Hygiena odívani), SNTL, Praha 1984 (in Czech)

12 Hipler U.-C., Elsner P. (Eds.): Biofunctional Textiles and the Skin, Karger, Current Problems in Dermatology Vol. 33, 2006, pp. 127-143, ISBN: 978-3-8055-8121-9, DOI: 10.1159/isbn.978-3-318-01349-8

13 Fowler J.F., Fowler L.M., Lorenz D.: Effects of merino wool on atopic dermatitis using clinical, quality of life, and physiological outcome measures, Dermatitis 30(3), 2019, pp. 198-206, DOI: 10.1097/DER.0000000000000449

14 Su J.C., Dailey R., Zallmann M., et al.: determining effects of superfine sheep wool in Infantile Eczema (DESSINE): a randomized paediatric crossover study, British Journal of Dermatology 177(1), 2017, pp. 125-133, https://doi.org/10.1111/bjd.15376

15 Spelman L.J., Supranowicz M.J., Davidson K.A., et al.: An investigator blinded, clinical trial assessing the efficacy of superfine merino wool base layer garments (SMWBG) in children with atopic dermatitis (AD) measuring SCORAD, EASI, POEM and DSA scores, Biomedical Journal of Scientific & Technical Research 7(1), 2018, pp. 5687-5603, DOI: 10.26717/BJSTR.2018.07.001450

16 Hipler U.C., Wiegand C.: Biofunctional textiles based on cellulose and their approaches for therapy and prevention of atopic eczema, chapter 12 in Handbook of Medical Textiles, Woodhead Publishing Series in Textiles, 2011, pp. 280-294, https://doi.org/10.1533/9780857093691.2.280

17 Tencel General - feel right with a natural touch. Lenzing, 2020, available 11.09.2020 from: https://www.tencel.com/b2b/branded-offers/general

18 The Definitive Guide to Polypropylene (PP), Omnexus, 2020, available 11.09.2020 from: https://omnexus.specialchem.com/selection-guide/polypropylene-pp-plastic

19 VILOFT a sustainable viscose fibre, Kelheim Fibres, 2020, available 11.09.2020 from: http://www.viloft.com/

20 What is Micromodal? Your Top Questions Answered about Micromodal vs Cotton Clothes, 2019, available 11.09.2020 from: https://www.ejisinc.com/blogs/news/what-is-micromodal

21 Crabyon fibers for anti-bacteria textile products, Swicofil, 2020, available11.09.2020 from: https://www.swicofil.com/commerce/brands/various/crabyon

22 Hodake B.: What is linen fabric: properties, how it's made and where, Sewport, 2020, available 11.09.2020 from: https://sewport.com/fabrics-directory/linen-fabric

23 Weigmann H.-D.H.: Cotton, Encyclopedia Britannica, 2020, available 11.09.2020 from: https://www.britannica.com/topic/cotton-fibre-and-plant

24 Yu C.: Chapter 2 - Natural Textile Fibres: Vegetable Fibres, Textiles and Fashion, Woodhead Publishing, 2015, pp. 29-56, ISBN 9781845699314

25 Kolinova M., Koldinska M.: Evaluation of sensory comfort of functional knitwear. Fine mechanics and optics (Hodnocení senzorického komfortu funkčních pletenin, Jemná mechanika a optika), No. 10/2015, pp. 296-298, ISSN 0447-6441 (in Czech)

26 Glombikova V., Komarkova P., Havelka A., Kolinova M.: Approach to evaluation of car seats fabrics performance, Industria Textila 69(2), 2018, pp. 96-103

ANALYSIS OF FORCE INTERACTION BETWEEN PUNCHEON'S WORKING TOOL AND METAL FITTINGS AT THE STAGE OF DEFORMATION OF PUNCHEON'S LAST CONIC PART

Mykola Skyba, Oleh Polishchuk, Vitalii Neimak, Taras Romanets, Andrii Polishchuk, Svitlana Lisevych and Maksym Luchynskyi

Khmelnytskyi National University, Instytuts'ka str. 11, Khmelnytskyi, Ukraine
opolishchuk71@gmail.com

Abstract: *The article deals with force interaction between puncheon working tool and metal fittings at the stage of deformation of puncheon's last conic part. Eyelet's deformation stages have been studied, components of eyelet's stress-strain state have been analyzed, and eyelet's deformation effort with puncheon's conic surfaces has been calculated. A series of experiments to prove validity of the obtained mathematical model has been conducted. The obtained dependencies can be used to achieve approximate calculation of maximum efforts of metal eyelet's deformation with puncheon's conic surfaces.*

Keywords: *eyelet, fitting, deformation effort, puncheon.*

1 INTRODUCTION

Calculation of deformation force parameters is rather useful when tackling a number of practical tasks. It allows to predict tool's solidity, equipment's capacity and wear resistance. Information about force parameters enables to define the final effort of eyelet's pressing to the base, which totally defines quality of the device. Analysis of previous research showed that calculation of stress-strain state of such constructions has been studied partially [1, 2]. Tackling of the task of metal fittings deformation with puncheon's shape-generating surfaces has not been previously studied. This is why it is rather urgent to define eyelet's deformation effort in the function of puncheon's motion. Tackling of this task is the content of further research. Obtaining of analytical correlations of this dependency will allow to study the influence of puncheon's geometrics and, as a result, to control deformation force mode.

2 THEORETICAL PART

2.1 Stages of eyelet's deformation

Analysis of geometrical forma of puncheon's shape-generating surface will allow to define three stages of deformation with various character of interaction between puncheon and eyelet, each of which requires respective calculation algorithm. Schematically, these stages are shown in Figure 1 [1, 3].

The first stage is deformation with puncheon's curvilinear surface, which is arch-shaped having the radius of r = 0.0022 m (Figure 1a). Eyelet deformation is done with a part of this surface from the section of initial contact with the eyelet, which has the radius of r_3 to upper point of the surface. Given the fact that the length of the surface, on which deformation takes place, is small, the surface can be construed as a cone.

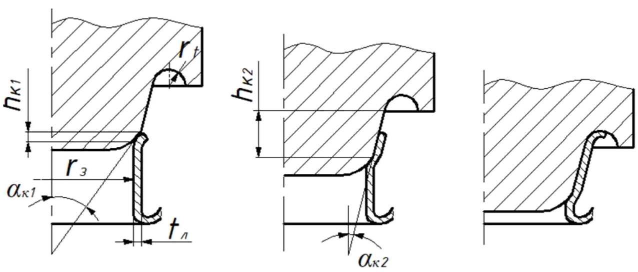

Figure 1 Diagram of characteristic stages of eyelet's deformation: a) first; b) second; c) third; r_3 - eyelet's internal radius; $t_л$ - eyelet's thickness; r_t - radius of puncheon's toroidal part

The height of this part of the puncheon is marked as $h_{к1}$, while angle of inclination towards the axis is $\alpha_{к1}$. The surface at the second stage of deformation is also conic having the length of $h_{к2}$ and angle of inclination towards the axis $\alpha_{к2}$ (Figure 1b). The third stage if eyelet deformation with toroidal part of puncheon's surface. The radius of this surface is marked as r_t (Figure 1c). The surface is continuation of the conic part; however, angles on inclination of adjacent surfaces differ.

This article deals with force interaction between working tool and metal fitting at the first two stages.

2.2 Analysis of components of eyelet's stress-strain state

Radius of internal surface of this element is marked as ρ, while external one as $\rho+\partial\rho$ (Figure 2b), on horizontal planes of which normal meridional tensions are in effect σ_ρ, $\sigma_\rho+\partial\sigma_\rho$, which are distributed over its upper and lower verges, are changeable in height, and are tangential or circumferential σ_θ, which do not change along the circle. The element receives meridional ξ_ρ and circumferential ξ_θ deformations. Thickness of the element that has been cut out is marked as $t_п$. We shall consider it as small. This means that movable and normal in regards to surface tension is unavailable, while areas, on which they are in effect σ_ρ, σ_θ, are primary.

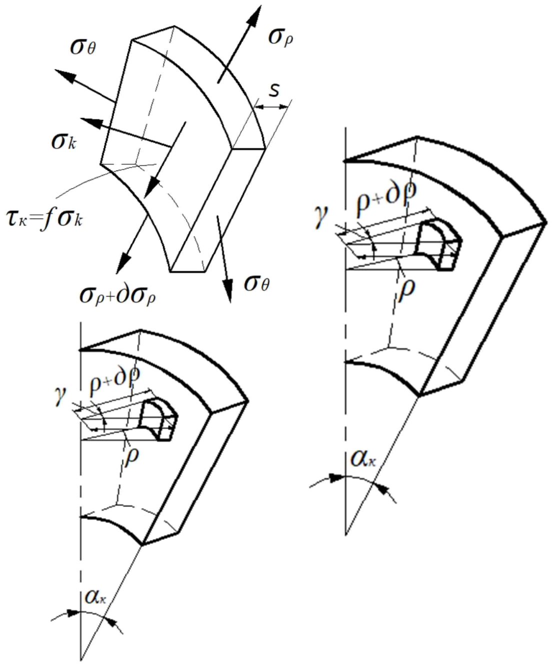

Figure 2 Components of stress-strain state: a) cut out element; b) elements geometrical dimensions; γ - angle between meridional planes turned to each other

For this case (small thickness of the element), contact load σ_k, which is in effect along the internal surface, is considered as pressed to element's middle plane. Tangent friction tensions τ_k will be in effect there, volume of which shall be defined by Coulomb's law:

$$\tau_K = f \cdot \sigma_K \tag{1}$$

in which f - friction coefficient.

Conic surface, from which the element has been cut out, is inclined towards the axis at an angle that is marked as α_κ. Based on these assumptions we will reveal distribution of tensions along eyelet's height depending on puncheon's motion, which will allow to solve the given task [1].

2.3 Calculation of eyelet's deformation effort with puncheon's conic surfaces

Solution will be obtained on the basis of differential equilibrium equation given in the paper [4]. It is as follows:

$$\rho \cdot \frac{d\sigma_\rho}{d\rho} + \sigma_\rho - \sigma_\theta \cdot (1 + f \cdot ctg\alpha_K) = 0 \tag{2}$$

Solution of this equitation along with plasticity condition:

$$\sigma_\theta - \sigma_\rho = \sigma_S \tag{3}$$

in which σ_s - fluctuation tension at a single-axis trained state, gives the following correlation

$$\rho \cdot \frac{d\sigma_\rho}{d\rho} - \sigma_\rho \cdot f \cdot ctg\alpha_K - \sigma_S \cdot (1 + f \cdot ctg\alpha_K) = 0 \tag{4}$$

After integration the equation is brought to the following:

$$\frac{\ln\left[\sigma_\rho \cdot f \cdot ctg\alpha_K + \sigma_S \cdot \left(1 + f \cdot ctg\alpha_K\right)\right]}{f \cdot ctg\alpha_K} = \ln\rho + c \tag{5}$$

Integration constant c can be defined if meridional tensions σ_ρ equal 0 on eyelet's upper edge, the radius of which is marked as R_k (Figure 3) [1]. Given this, integration constant will equal:

$$c = \frac{\ln\left[\sigma_S \cdot \left(1 + f \cdot ctg\alpha_K\right)\right]}{f \cdot ctg\alpha_K} - \ln R_K \tag{6}$$

After substitution of the obtained value into the previous equation, we receive the following:

$$\sigma_\rho = -\sigma_S \cdot \left(1 + \frac{tg\alpha_K}{f}\right) \cdot \left[1 - \left(\frac{\rho}{R_K}\right)^{\frac{f}{tg\alpha_\kappa}}\right] \tag{7}$$

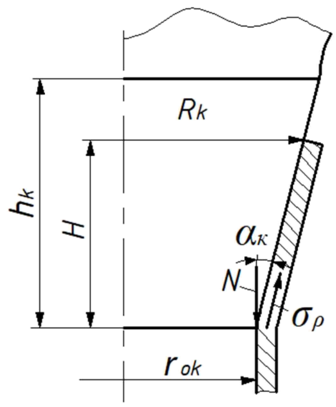

Figure 3 Generalized diagram of cylindrical workpiece deformation with puncheon's conic surface

Now, we will find value of radius R_k as puncheon's H motion function:

$$R_K = r_{0K} + H \cdot tg\alpha_K \tag{8}$$

in which r_{0k} is radius of conic surface in lower section.

Given this, (7) is as follows:

$$\sigma_\rho = -\sigma_S \cdot \left(1+\frac{tg\alpha_K}{f}\right) \cdot \left[1-\left(\frac{\rho}{r_{0k}+H\cdot tg\alpha_K}\right)^{\frac{f}{tg\alpha_K}}\right] \tag{9}$$

Resultant of these tensions N_ρ will equal:

$$N_\rho = 6{,}28\sigma_\rho \cdot \rho \cdot t_п \tag{10}$$

Analyzing equation (9), it can be seen that the value of meridional tensions increases with decreasing radius ρ (Figure 3). In this case, they gain biggest values in cone's lower part at $\rho = r_{0k}$:

$$\sigma_{\rho_{k0}} = -\sigma_S \cdot \left(1+\frac{tg\alpha_K}{f}\right) \cdot \left[1-\left(\frac{r_{0k}}{r_{0k}+H\cdot tg\alpha_K}\right)^{\frac{f}{tg\alpha_K}}\right] \tag{11}$$

Respective value of resultant of these tensions equals:

$$N_{k\rho} = -\sigma_S \cdot \left(1+\frac{tg\alpha_K}{f}\right) \cdot \left[1-\left(\frac{r_{0k}}{r_{0k}+H\cdot tg\alpha_K}\right)^{\frac{f}{tg\alpha}}\right] \cdot 6{,}28 \cdot r_{0k} \cdot t_п \tag{12}$$

Given the fact that the value of this resultant is a projection of cone's N_k deformation projection we see that deformation effort equals:

$$N_k = \frac{-\sigma_S \cdot \left(1+\frac{tg\alpha_K}{f}\right) \cdot \left[1-\left(\frac{r_{0k}}{r_{0k}+H\cdot tg\alpha_K}\right)^{\frac{f}{tg\alpha_K}}\right] \cdot 6{,}28 \cdot r_{0k} \cdot t_п}{\cos\alpha_K} \tag{13}$$

The biggest deformation on the cone is gained at contact with the puncheon along the entire conic surface, i.e. at $H = h_k$ [1]:

$$N_{kH} = \frac{-\sigma_S \cdot \left(1+\frac{tg\alpha_K}{f}\right) \cdot \left[1-\left(\frac{r_{0k}}{r_{0k}+h_k\cdot tg\alpha_K}\right)^{\frac{f}{tg\alpha_K}}\right] \cdot 6{,}28 \cdot r_{0k} \cdot t_п}{\cos\alpha_K} \tag{14}$$

In this case, puncheon's eyelet deformation has two conic surfaces with different angles of inclination and radiuses of lower butt (Figure 4).

These values will be marked the following way: angles of inclination of lower and upper cones as α_{k1}, α_{k2}, smallest radiuses as r_{0k1} and r_{0k2}. We will calculate these values in a specific case. For lower cone $r_{0k1} = r_3$, while the value of angle of inclination in radians will be defined according to puncheon's drawings α_{k1}*=arctg(0.0008/*h_{k1}*)=0.8 rad*. By analogy, for the second cone r_{0k2}*=0.003+0.0022=0.0052 m*, while angle α_{k2}*=26°=0.47 rad*.

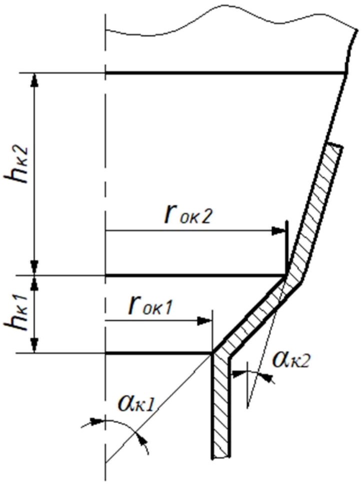

Figure 4 Diagram of eyelet deformation with puncheon's conic surfaces

Given the revealed parameters of correlation, (13, 14) for the first and second cone will be as follows.

For the first cone:

$$N_{k1} = \frac{-\sigma_S \cdot \left(1+\frac{tg\alpha_{K1}}{f}\right) \cdot \left[1-\left(\frac{r_3}{r_3+H\cdot tg\alpha_{K1}}\right)^{\frac{f}{tg\alpha_{K1}}}\right] \cdot 6{,}28 \cdot r_3 \cdot t_п}{\cos\alpha_{K1}} \tag{15}$$

while its biggest value at $H = h_{k1}$

$$N_{Hk1} = \frac{-\sigma_S \cdot \left(1+\frac{tg\alpha_{K1}}{f}\right) \cdot \left[1-\left(\frac{r_3}{r_3+h_{k1}\cdot tg\alpha_{K1}}\right)^{\frac{f}{tg\alpha_{K1}}}\right] \cdot 6{,}28 \cdot r_3 \cdot t_п}{\cos\alpha_{K1}} \tag{16}$$

For the second:

$$N_{k2} = \frac{-\sigma_S \cdot \left(1+\frac{tg\alpha_{K2}}{f}\right) \cdot \left[1-\left(\frac{r_{0k2}}{r_{0k2}+(H-h_{k1})\cdot tg\alpha_{K2}}\right)^{\frac{f}{tg\alpha_{K2}}}\right] \cdot 6{,}28 \cdot r_{0k2} \cdot t_п}{\cos\alpha_{K2}} + \frac{-\sigma_S \cdot \left(1+\frac{tg\alpha_{K1}}{f}\right) \cdot \left[1-\left(\frac{r_3}{r_3+h_{k1}\cdot tg\alpha_{K1}}\right)^{\frac{f}{tg\alpha_{K1}}}\right] \cdot 6{,}28 \cdot r_3 \cdot t_п}{\cos\alpha_{K1}} \tag{17}$$

The biggest effort on the second conic area N_{Hk2} is gained at $H = h_{k2} + h_{k2}$, the value of which equals [1]:

$$N_{Hk2} = \frac{-\sigma_S \cdot \left(1+\frac{tg\alpha_{K2}}{f}\right) \cdot \left[1-\left(\frac{r_{0k2}}{r_{0k2}+h_{k2}\cdot tg\alpha_{K2}}\right)^{\frac{f}{tg\alpha_{K2}}}\right] \cdot 6{,}28 r_{0k2} \cdot t_п}{\cos\alpha_{K2}} + \frac{-\sigma_S \cdot \left(1+\frac{tg\alpha_{K1}}{f}\right) \cdot \left[1-\left(\frac{r_{0k1}}{r_3+h_{k1}\cdot tg\alpha_{K1}}\right)^{\frac{f}{tg\alpha_{K1}}}\right] \cdot 6{,}28 r_3 \cdot t_п}{\cos\alpha_{K1}} \tag{18}$$

It should be noted that the obtained correlations can be applied in certain limits of puncheon's motion. Correlations (15, 16) within $0 \le H \le h_{k1}$, while (17, 18) - at $h_{k1} \le H \le h_{k1} + h_{k2}$.

3 RESULTS AND DISCUSSION

To prove validity of the obtained mathematical model (18) of eyelet's *N* deformation total effort dependency on puncheon's *H* motion, the process of eyelet's deformation with puncheon's conic surfaces has been experimentally studied. With the help of measuring system, diagrams of eyelet's N deformation technological effort dependency and puncheon's *N* motion have been taken.

Comparison of values deformation effort obtained in the same way as experimental results is given in Figure 5.

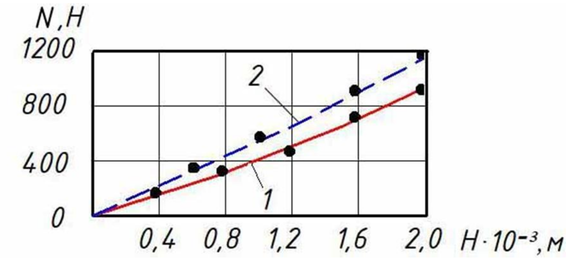

Figure 5 Eyelet's deformation total effort on both conic parts dependency on puncheon's motion: 1) calculation values; 2) experimental

4 CONCLUSION

Having analyzed the obtained results we may conclude that the shape of working surfaces and puncheon's geometrics have significant influence on technological effort *N*. The biggest influence have: conicity angels α_{k1}, α_{k2}, radiuses of conic parts r_{0k1} and r_{0k2} and height of conic part *H*.

The error between calculation and experimental values fastening *N* effort is around 20%, which is permissible. Thus, formula (18) can be used for approximate calculation of maximum effort of metal eyelets deformation with puncheon's *N* conic surfaces [5].

5 REFERENCES

1. Polishchuk O.S.: Electric and mechanical pressing equipment at enterprises of light industry: monograph, Khmelnytskyi. PolyLux Publishers, 2018, 285 p. (in Ukrainian)
2. Komissarov A.I., Zhukov V.V., Nikiforov V.M., Storozhev V.V.: Design and calculation of machines for sewing and footwear production, Mashinostroienie, Moscow, 1978, 431 p. (in Russian)
3. Chumakova S.V.: Analytical review of the methods and equipment for installation of metal fittings into light industry products, Journal of Kyiv National University of Technology and Design 2(5), 2010, pp. 142-148 (in Ukrainian)
4. Popov Ye.A.: Fundamentals of the theory of sheet-metal stamping, Mashinostroienie, Moscow, 1968, 283p. (in Russian)
5. Chumakova S.V.: Study of the process of fixation of metal eyelets in light industry products in quasistatic mode, Journal of National University, Technical Sciences № 2, 2013, pp. 147-153 (in Ukrainian)

DEVELOPMENT OF THE PRODUCTION MODEL OF SCALING UNIFORMITY OF THE ASSORTMENT COMPLEX CLOTHING FAMILY LOOK

A. Slavinska, O. Syrotenko, V. Mytsa and O. Dombrovska

Khmelnitskyi National University, Institutska str. 11, Khmelnitskyi, Ukraine
syrotenko@email.ua

Abstract: *The problem of combining the image system with the image types of social order for a new line of fashion trends has been investigated. A methodology for generating a productive model of systematic database selection using numerical methods for solving scaling problems has been developed. The mechanism of typing of similarity on the basis of compositional homogeneity of models in patterns of consumer demand has been investigated. An algorithm for determining the coefficients of proportionality of the constructions of the range of complexes has been developed, taking into account the gender, age and style features. It has been established that the production model of scale of control measurements provides technical conditions of quality control of design documentation.*

Keywords: *image, product range, production model, scale, similarity types, homogeneity, proportionality factor, control measurements, design documentation.*

1 INTRODUCTION

The priority area for the development of computer technologies in the second decade of the 21st century is the development of methods of complex assessment of the quality of objects based on the theory of "pattern recognition". One of the components of flexible production is to take into account the social status of behavior of the modern consumer of clothing, which eliminates such classification features as assortment, gender, age, place of residence, type of employment in the characteristics of preferences [1, 2]. The technical and economic benefits of automatic resizing according to the morphological classification of figure types include saving development costs in the long run [3]. The influence of marketing on the social dimension of the development of symbolic associations of fashion trends does not take into account the influence of environmental factors. The new line in fashion is often defined by the image types of social order for copyright inspiration in a fundamentally new combination of the image system, in particular, for the promotion of family values. A family-friendly outfit - Family Look is becoming a new trend, which creates a shared family style and shows that this family is one. The usefulness, reliability, benefit of using the tandem of paired clothing of parents and children is manifested in the homogeneity of the morphological structure of products, which corresponds to the characteristics of the classical fixing unification of the main forming parts by means of proportional scaling.

The relevance of the competitive equilibrium of the targeted demand for the functional orientation of the use of "exactly" in the sub-brand of Family Look positions the image level of motivation. This is confirmed by studies in the field of competitive advantages of targeted demand for homogeneity of composite decisions of the family wardrobe [4-7].

The use of the cost-savings method on the principle of "combine what already exists" involves the development of group design documents to regulate the flexibility of production design preparation.

2 DISCUSSING IDEAS

Buying clothes goes from a physical domain into a virtual domain, and mass customization becomes the only way to win and retain a buyer [8, 9]. Virtual fittings for 3D clothing modeling [10] provide the flexibility to use scanned anthropometric data in the automatic design of clothing at a higher level [11, 12]. The role model of consumption, in which children view parents as role models, is based on the transition from qualitative to quantitative methodology [13]. Empirical studies of communications in the competitive advantages of price groups among consumers determine the direction of experimental design in the formation of a hypothetical image of models of the range [14, 15]. A hierarchical regression of the relationship between fashion innovation, consumer's behavior and information sources involves the use of a genetic algorithm to evaluate goods [16]. Fuzzy Clustering methods (FCM) [17] take into account the systematic selection of part of the database by the functional orientation of the Family Look assortment. The methodology for identifying the relationship between the content of the process of designing clothing and its abstract description in the form of context diagrams, presented in [18], does not take into account the gender status in a particular range. The method of forming the capsule of the assortment complex [19] involves the application of relations of geometric similarity on the basis of uniformity of structural belts in the lines of transition of sections of the product, which will ensure the preservation of the compositional properties of the form. It is proposed to perform the transformation of the spatial characteristics of the capsule design objects by the methods of metric transformation. This approach positions in the gender and age standard set the modernized stylization of microstyle "Family Casual", for models of the product group "City Casual" on the basis of duplication of styles, materials, colors and processing.

3 METHODS

The trendy pattern recognition strategy for young, low-budget consumers is aimed at consuming pret-a-porter clothing in virtual domains. The quantitative research methodology is based on the method of statistical analysis of the homogeneity of groups of classification features of consumer demand patterns [20-22].

Initial data for such developments are existing photos of existing in the world wide web of models of clothing of brand “Family Look”.

The homogeneity of self-expression of a person in society is characterized by the assortment group "Basa" (65%), whose hypothetical image does not change for 3-4 years.

The positioning of regular customers and the stability of production for the target audience is characterized by the “Basis” group (55%). It defines the basic range for research. The diversification strategy of the composition of models of the City - Casual product group determines the advantages of the Bestseller group, the types of which are relevant for at least 4-5 years.

From the point of view of consumers who want to impress others and follow the fashion, this group is called "conformists" (65%). The basic values of novelty are the answers to the question "What did I buy?" Thus, the model of the hypothetical image of consumer preferences in the conformists group describes the range of the Bestseller group (80%) with a sufficiently high degree of homogeneity [23]. This corresponds to the creation of identical images with the same Family Look style clothing [24].

The social status of the consumer group is described by tandems: parents - children, father - mother, brother - sister. Gender: father - son, mother - daughter, brothers - sisters. Gender and age differences in body characteristics are subordinated to anthropometric features and affect the identification of the appearance of the product.

The regulatory documents (Table 1) contain the specifications and methods of anthropometric measurements of the size of the human body for the clothing design. The degree of technical perfection of the product design in proportion determines the methods of designing clothes. Calculation and graphical design techniques that determine the contour of a typical product detail with different approximation accuracy are based on the discrete measurements of figures, increases and typical articulations of parts. Numerical methods of calculation in industrial methods, in particular, CRIGI (Central Research Institute of the Garment Industry), UMDC CMEA (unified method of designing clothes of the CMEA) contain analytical substantiation of the use of body measurements for determination of the main structural points of the contour taking into account the tectonic functionality of the part [18].

The range of modern calculation tools, combined with the rapidly increasing computing power of CAD, make it possible not only to calculate any design document, but also to take into account the typing principles of the similarity properties in the target portfolio of Family Look models. To recognize the hypothetical image of the assortment kind, it is advisable to apply the method of typing quantitative indicators of the appearance of the model.

Table 1 Regulatory documentation for the design and manufacture of clothing

Standard number	Application
DSTU 3321: 2003	Terms and definitions of basic concepts in the system of design documentation
DSTU GOST 25294: 2005: 2006	Technical conditions of production of the dress-blouse assortment
DSTU ISO/TR 10652: 2006	Standard dimensioning system
DSTU ISO 8559: 2006	Anthropometric measurement of human body size for clothing design
DSTU GOST 31396: 2011	Means and methods of measurement. Classification of typical women’s figures
DSTU ISO3635: 2004	Determination and removal of measurements by the standard method
GOST 17522-72	Dimensional features of typical women’s figures for designing clothes
GOST 17917-86	Dimensional features of typical boys’ figures for clothing design
GOST 17916-86	Dimensional features of typical girls’ figures for clothing design

DSTU - State standards of Ukraine; GOST - State standard

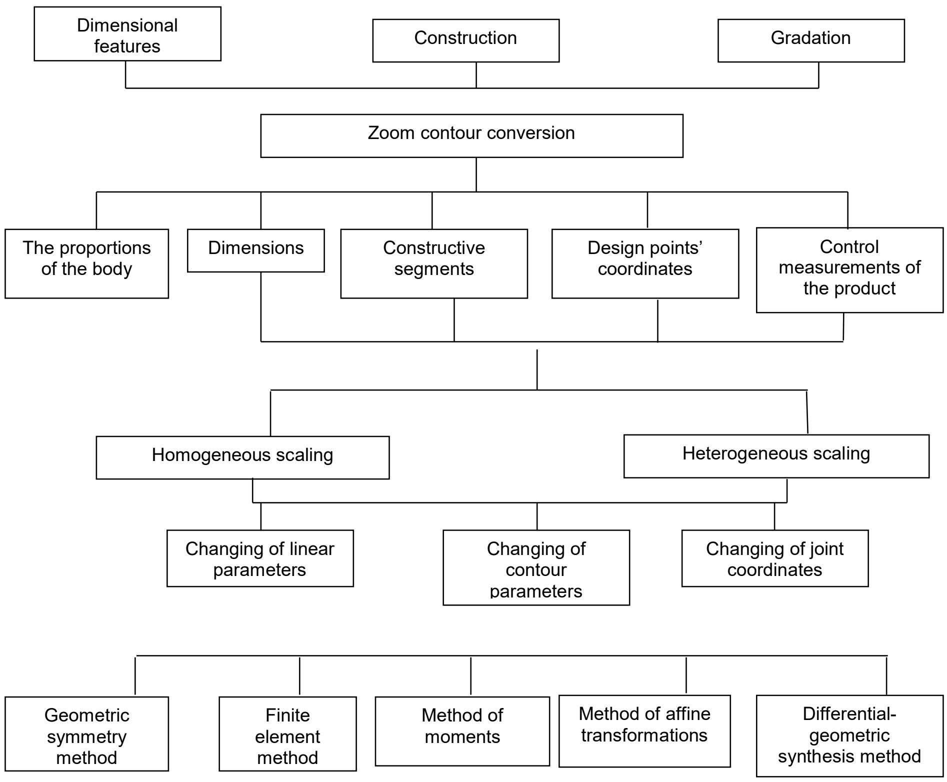

Figure 1 Classification of numerical methods for solving scaling problems

The production model of the generalized characteristic is based on the typing rules in the form "If (condition) then (action)". To select typical compositional features, this figure is equal to more than 45% [23].

The strategy of diversifying the composition of models to positioning of consumer's demand involves the choice of patterns of stylization on the basis of homogeneity. The summer wardrobe of the product group "City - Casual" is characterized by the academic stylization of elements of classical style on the basis of isomerization of many objects of the same composition, but of different structure. Accordingly, the Family - Casual microstyle is manifested in the form of a pattern of modernized stylization [24].

Therefore, design features are dominant for typological analysis of the homogeneity of groups in the matrix of the market-model capabilities on the basis of competitive equilibrium of target demand. Maintaining proportions is a prerequisite for sizing Family Look products which is done by scaling the object.

Scaling is a special case of affine transformations, which in computer graphics is regarded as stretching/contracting along the coordinate axes and described by the following equation (1):

$$x_1=ax, \quad y_1=dy \tag{1}$$

where, *a* and *d* are the scaling factors.

Mathematical models of proportionality are represented by a set of formulas for calculating the coordinates of the structural points of the detail's design and the scaling factors equation (2) [26]:

$$Kx = \frac{\sum_{i=1}^{n} a_i}{n}; \; Ky = \frac{\sum_{i=1}^{m} d_i}{m} \tag{2}$$

where, $a = \frac{x_1}{x_0}$ - is the scaling factor along the X axis for the i-th constructive point; $d = \frac{y_1}{y_0}$ - is the scaling factor along the Y axis for the i-th construct point; *n(m)* - is the number of design points lying in the direction of the scaling axis *X*, (*Y*).

To simplify the mathematical calculations, a Cartesian coordinate system with a center at the intersection of the diagonals of a rectangle constructed according to the control dimensions of the dimensions of the structure of the parts has been chosen. The polar radii are drawn through the main design points of the contour of the detail. The scaling factors along the X and Y axes are calculated as the average of the coefficients of the same name. As a special case of scaling is a way of grading patterns. The gradation of the pattern implies the displacement of the structural points by a value that is determined proportionally. Auto CAD has a built-in zoom feature. The block is a part that is broken down into parts for scaling.

The mathematical formulation of the problem of compliance with the requirements of homogeneity of typing in the system of models of Family Look is provided by the condition *{3n} = C* [18]. Each type of proportionality should include at least two alternatives for the transformation of the spatial structure by the principle of orientation of the proportions of the product. Numerical methods for solving scaling tasks using the proportional guidance method are shown in Figure 1.

$$M_m \supseteq M_{m1} \cup M_{m2} \cup M_{m3} \cup M_{m4} \cup M_{m5} \quad (3)$$

where, M_{m1} is the method of moments for splitting a contour into a finite number of elements in a polar coordinate system; M_{m2} is the geometric symmetry method for maintaining the symmetry of the quadrants of the polar coordinate system of the design points of the detail's contour; M_{m3} is the finite element method for taking into account the variability of dimensional features; M_{m4} is the method of affine transformations for proportional contraction / stretching of coordinates of constructive points of a contour; M_{m1} is a method of differential geometric synthesis for grading design documents.

4 EXPERIMENTAL

The process of developing a model of proportionality to preserve compositional homogeneity on the basis of "exactly the same" in group of design documents describes the algorithm for the study of typing similarity: tectonics' form - contour details - design document [23]. Form tectonics is determined by the stage of introducing anthropometric planes into the scheme, which describe anthropometric features. The contour of the part is characterized by the constructed structure by empirical calculations of the main nodal points. A design document in the form of a gradation characterizes a drawing of parts for the required dimensions of the product. The model of cross-certification of consumer demand is based on the concept of typing the classification features of stylization patterns within the consumer's psychographic portrait (Table 2).

The study of the artistic aspect of the targeting of Family Look models is made on the basis of similarity of the main basis and aesthetic expressiveness of composite decisions for the assortment complex women's dress - dress for girls of preschool group - shirt for a boy of nursery group. The three objectives of the task are defined by age group status, namely, the dominant role of the mother in the behavior of preschool children.

As a general idea for a hypothetical object is accepted characteristic: product group - classic dresses and shirts, consumer type - conformist, shape symbol - rectangle, associative style symbol - "softened" academic stylization City Casual [24].

A mathematical description of the morphological changes of the range in patterns of consumer's demand is represented by the operations of combining and crossing sets of personal and social factors of consumer's behavior to form a generalizing idea:

$$\begin{aligned}
&\text{Zone A} \quad \text{Basis} \subset T \subset K2 \cap K3 \cup C2 \cup M1 \cup B3 \cap B5 \\
&\text{Zone B} \quad \text{Fashion} \subset M \cap C \subset K4 \cup C1 \cap C5 \cup M4 \cup B2 \qquad (4) \\
&\text{Zone C} \quad \text{Bestseller} \subset T \cap C \subset K5 \cup C1 \cap C4 \cup M2 \cup B1
\end{aligned}$$

Statistical studies of descriptions of the figurative solution of models contain four variants of the psychological portrait of the consumer that correspond to the "4C" marketing system: Consumer, Cost of Expectation, Convenience, Communication.

A hierarchical regression of the relationship between age, gender, and environmental factors confirms the presence of brand symbolism impact on children from the age of 2 years and it increases throughout the preschool years [25].

Formation of profiles of structural and compositional characteristics of the hypothetical image of the Family Look product range is accomplished by systematization of quantitative indices of occurrence, in particular, typing, stylization, and similarities of structural modification (Figure 2, Table 3).

Table 2 Cross stratification matrix of consumer demand patterns

Fashion zones		A - conceptual model of competitive properties	B - fashionable range of trends of the season
Type of marketing strategy		I - cost savings for the basic range of the target audience Basis	II - Fashion Microstyle Diversification
Consumer demand pattern	**Type of stylization**	Academic styling	Upgraded styling
	Group novelties	Typical – T	Fashionable - F, Contemporary – C
Psychographic portrait of a consumer	**Class**	Pragmatist - C1; Traditionalist - C2; Materialist - C3;	
	Categories of values	Social status - V1; Material interest - V2; Career Achievements - V3; Personal development - V4; Image - V5	
	The level of motivation	Targeting - M1; Copying - M2; Limited reach - M3 Stylishness - M4	
	Selection criteria	Prestige - S1; Originality - S2; Conceptuality - S3; Availability - S4; Acceptability - S5	

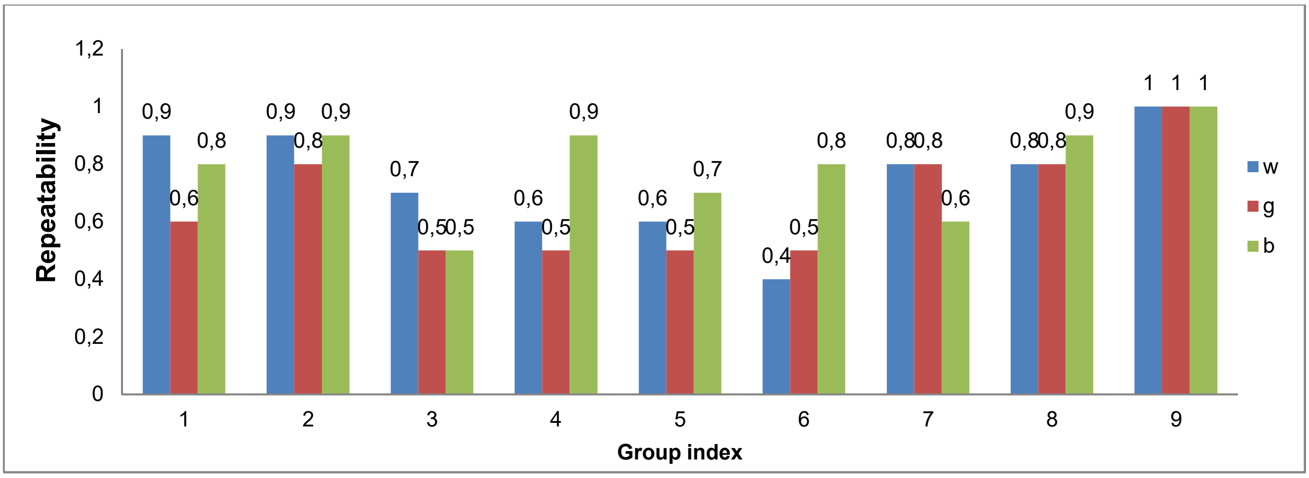

Figure 2 Diagram of the repeatability of typical elements in the range of models

Table 3 Indexing of typical elements of structural and composite solutions of models of assortment complex

Group index	Item name	Kind of element
1	Sleeve	Sewn with length transformation
2	Longitudinal partitioning	Constructive seams
3	Cross partitioning	Structural and decorative seams
4	Clasp	On-Board Buttons
5	Neck	Round with collar
6	Pocket	Attached 1 or 2
7	Nuance	Folded skirt shape
8	Symmetry	Mirror, similarity of elements
9	Scalability	Proportional metric order

The use of a matrix of search of a systematic set of classification features of hypothetical images of an assortment complex by combination 1 (yes), 0 (no) in the automated layout of elements allowed to obtain 24 variants of combinations of group classification features.

The morphological characteristics of consumer figures for Family Look clothing take into account age, proportion type, body type, posture, baseline dimensions. The age of the mother of the family corresponds to the adult first period of 21-35 years, which is included in the younger group. The girl is included in the length of the 3-7 years age, which corresponds to the first period of childhood and to the group of preschool age. The boy is included in the length of the age period of 1-3 years, which corresponds to the period of early childhood and nursery group.

The type of body figure which is female one by B. Scherley is uniform, with a moderate fat accumulation, the type of posture is normal (*Pk* = 6.2 ± 1.0 cm, *VP* = 5.9 ± 0.75 cm).

Type of proportions according to the classification V. Bunaka is mesomorphic with an average ratio of trunk to limb lengths.

Most children under the age of 7 are kept straight because the spine has not yet acquired the usual curvature: forward - lordosis (cervical and lumbar), back - kyphosis (thoracic and sacral). Lordotic type LIII posture is considered normal.

Studies of basic body sizes for model development and clothing design have confirmed an identical degree of compliance with national and international anthropometric standards in Table 1. Female - 164-96-104 (96 MS); girl 110-56-51 (110-56); boy 92-52 (92-54).

To ensure operational comfort, the tectonic integrity of models of the Family Look range has been investigated by scaling by the method of proportional three-dimensional clothing in the light of family-style fashion trends (Figure 3).

The proportional ratio of the shape of the bodice and the skirt has been determined by the ratio of the proportional measurements of heights for the three specified age groups. In particular, the height of the waist line is 7, the height of the knee line is 9, and the height of the base of the neck is 10.

For the bodice, the difference of dimensions (10-7) is taken into account, for the skirt (7-9), which are divided in pairs in the age groups of the basic size: woman - girl (WG), girl - boy (GB).

The proportionality coefficients of the ratios of the upper and lower parts relative to the waist line are calculated by the equation (5):

$$C_{pr} = \frac{B_i}{B_j} \quad (5)$$

where, B_i is the projection measurement of the output height in pairs; B_j is the projection measurement of the second height in a pair.

W-G (bod) Cpr^1 = 1.5;

W-G (skirt) Cpr^2 = 1.58;

G-B (bod) Cpr^3 = 1.16.

The average proportionality factor projection measurements for a pair of W-G is 1.54, which suggests that the approximation to the harmony of the golden section (for women, 1.6).

Typical proportions of body measurements form a stable morphological structure of the body section in typical designs of three products.

The study of maintaining the proportionality of the body in the design of the product has been performed on the structures constructed by the method of the CRIGI, which is used in the industrial production of clothing.

Dimensions of typical figures of the selected group of consumers of clothing for the study of the proportions of horizontal (X) and vertical (Y) measurements (woman 164-96-104, girl 110-56-54, boy 92-52-48) are shown in Table 4.

The proportionality factor calculations are made in pairs of the same numbers by the ratio of larger to smaller by the compression principle: W-G; G-B.

Since the design of the bodice by the type of members is homogeneous for all the designs of the range of the Family Look complex, studies of the changes in the basic structures have been performed with the help of scaling by equation (2). For this purpose, the design of the parts of the body (back and forepart) is introduced into the system of cylindrical coordinates relative to the center of scaling O (Figure 4). The structural points of the contours of the parts for the three investigated structures are the points of intersection with polar radii drawn from the center of scaling and are the origin to determine the coordinates basic the structural points (Figure 5, Table 5).

Figure 3 Family Style fashion trends

Table 4 Anthropometric database for determining the proportionality of figures for Family Look style

Measurement plane	Ti number by size standard	W 164-96-104 GOST 17522–72	G 110-56-54 GOST 17916-86	B 92-52-48 GOST 17917-86	Cpr W-G	Cpr G-B
X	13	18.5	13.3	12.2	1.39	1.09
X	15	50.4	29.25	26.5	1.72	1.10
X	18	38.0	25.5	25.0	1.49	1.02
X	19	52.0	31.75	28.7	1.64	1.10
X	45	17.3	10.9	10.8	1.59	1.01
Y	43	43.3	28.7	26.2	1.51	1.09
Y	40	40.3	26.3	25.0	1.63	1.052
Y	61	44.0	27.2	26.0	1.61	1.038
Y	39	17.9	13.1	12.1	1.37	1.08
Y	41	43.6	28.9	26.1	1.51	1.11
X	47	18.3	12.5	10.3	1.47	1.19
X	31	13.3	9.8	7.0	1.36	1.4
∑	-	399.6	257.2	236.4	1.56	1.088

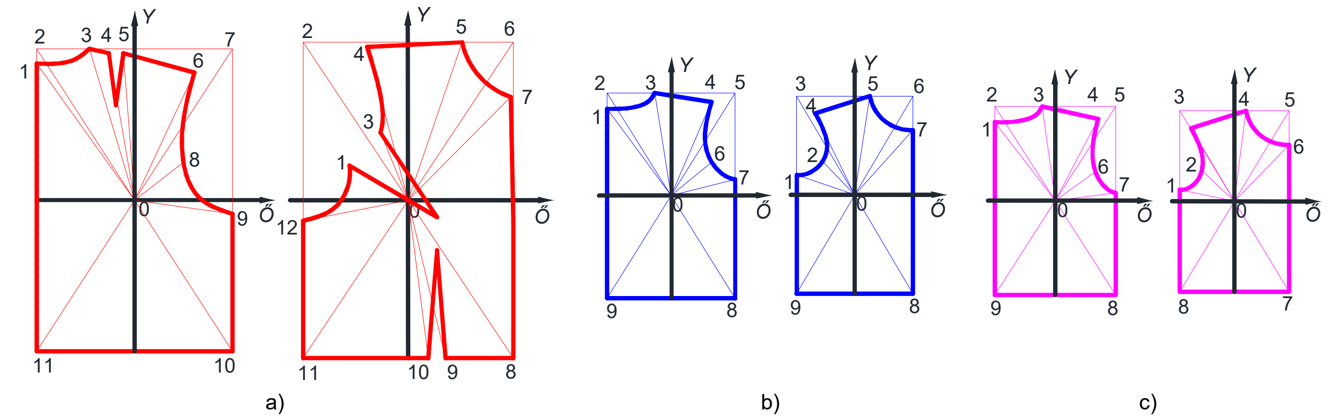

Figure 4 Experimental designs for back and forepart for scaling: a) for women; b) for a girl; c) for a boy

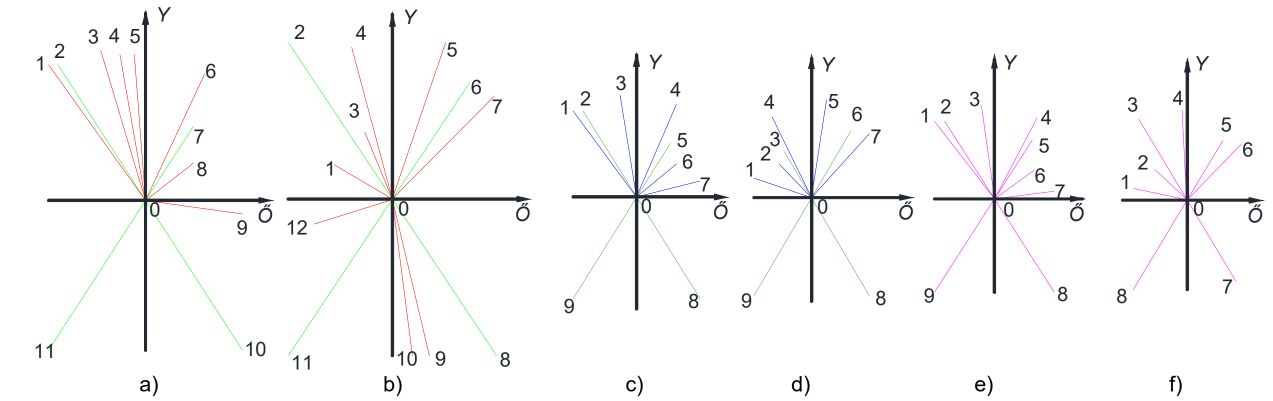

Figure 5 Polar radii of the structural points of the parts of the back and forepart to determine the coordinates X, Y: a) c) e) back (W, G, B); b) d) f) forepart (W, G, B)

Table 5 Coordinate database for determining the proportionality of the major contour points for the Family Look trend [cm]

The contour point number of the detail	Woman				Girl				Boy			
	back		***forepart***		***back***		***forepart***		***back***		***forepart***	
	X	***Y***	***X***	***Y***	***X***	***Y***	***X***	***Y***	***X***	***Y***	***X***	***Y***
1	-13.6	19.0	-8.2	4.8	-8.2	14.1	-7.6	-8.4	8.0	12.0	-8.0	-8.5
2	-12.3	18.9	-14.6	21.9	-8.2	12.5	-5.5	-1.3	8.0	13.0	-4.0	-1.5
3	-6.3	21	-3.9	9.4	-3.5	14.1	8.0	14.4	-4.0	13.0	-6.8	12.5
4	-3.6	20.4	-5.7	21.3	6.8	12.1	3.0	14.5	3.6	11.0	-4.5	10.0
5	-1.6	20.4	7.5	21.9	8.0	14.1	8.0	14.5	8.0	13.0	3.1	12.5
6	8.3	17.7	10.8	16.3	5.2	2.2	8.0	7.8	4.5	1.3	6.9	12.5
7	6.7	10.3	14.3	14.4	8.0	8.4	8.0	14.0	8.0	4.5	6.9	7.1
8	6.8	6.3	14.6	-2.2	8.0	14.7	8.0	14.0	-8.0	-13.5	6.9	-13.0
9	13.6	-1.9	5.2	-2.2	8.0	14.7	-	-	-8.0	-13.5	-6.9	13.0
10	13.6	-21.0	2.8	-22.3	-	-	-	-	-	-	-	-
11	-13.6	-21.0	-14.6	-22.0	-	-	-	-	-	-	-	-
∑|X|, ∑|Y|	100	177.9	102.2	198.3	63.9	106.9	56.1	88.9	60.1	94.3	54.0	90.6

*Note: Absolute values ∑|*X*|, ∑|*Y*| fixes the area bounded by the contour of the detail (see Figure 4)

The contour point numbering captures the sequence of determining the main design points of the experimental design in the polar coordinate system relative to the center of the details' area.

The symmetry of the quadrants of the rectangle of the part relative to the center 0 fixes the coordinates of the polar radii to study the scaling of the details (Figure 5).

Significant differences ∑|X| and ∑|Y| are explained by the presence of the undercuts in the designs of the back and forepart for women: back - points 4.5 (shoulder recess), forepart - points 1.3 (breast recess), points 9.10 (thallium recess). These coordinates can be excluded from proportionality studies because they determine the shape of the detail's surface in the product. For the backrest ∑|X| + ∑|Y| points 4.5 is equal to 46 cm, for the forepart ∑|X| + ∑|Y| points 1, 3, 9, 10 is equal to 78.6 cm.

To typify the space of control measurements of the assortment complex, a study of the proportionality of the leading dimensional features and the system of control measurements of the dimensions of the experimental structures has been performed. The estimated proportionality coefficients of the leading dimensions (height, girth) for the baseline sizes are as following: a woman - 164:96 = 1.71, a girl - 110:56 = 1.96, a boy 92:52 = 1.77, indicating the dominant vertical measurements for body development. For growth, the proportionality coefficients in the studied pairs are: W-G – 164 : 110 = 1.49; G-B – 110 : 92 = 1.19, which, within the margin of error, coincide with the compositional proportionality of the dimensions of the bodice shape.

In the calculations of the coefficients of proportionality (formula 5) pairs of measurements X and Y are involved (Figure 6).

For W-G:

Cpr_X^b = 27.2:16.8 = 1.62; Cpr_Y^b = 40.9:28.7 = 1.43

Cpr_X^f = 29.2:15.2 = 1.92; Cpr_Y^f = 43.9:27.2 = 1.62

For G-B:

Cpr_X^b = 16.8:15.8 = 1.063; Cpr_Y^b = 28.7:26.2 =1.095

Cpr_X^f = 15.2:14.2 = 1.07; Cpr_Y^f = 27.2:26.0 = 1.046

The scheme of control measurements of the dimensions of the experimental designs of the body parts in the assortment complex dress-shirt confirms the possibility of scaling the designs of the girl's waist in the design of the boy's shirt, since the width of the product in the design differs by the amount of indifference interval of 2 cm.

In addition, the calculated proportionality coefficients for the designs of the back and the waist of the pair G-B create the preconditions for scaling by the method of gradation by the magnitudes of increments Δy, Δx at design points.

System of proportionality coefficients, defined according to Table 4 and 5, provides a description the uneven scaling of the details' contours (Table 6).

5 RESULTS

Finding proportional ratios for the Family look range in variations of the design's dimensional features (see Table 6) provides a qualitative assessment of the compositional features of product similarity.

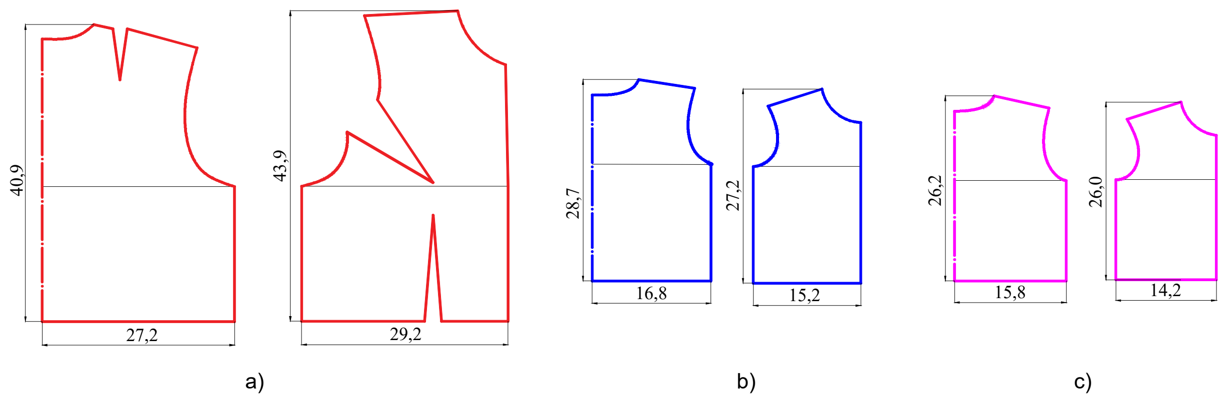

Figure 6 Scheme of control measurements of the dimensions of the experimental designs of the back and forepart of the Family Look range: a) woman; b) girl; c) boy

Table 6 Anthropometric base coefficients for the designs of the Family Look assortment

Scaling option	Anthropometric database					
	1 - dimensional features		*2 - construction*		*3 - gradation*	
	W-G	*G-B*	*W-G*	*G-B*	*W-G*	*G-B*
The proportionality of the body	1.50	1.170	1.50	1.050	1.210	1.150
Product dimensions	1.56	1.088	1.64	1.069	1.078	1.020
Measurements of the basis of construction	1.61	1.072	1.59	1.060	1.098	1.020
Design basis coordinates	1.51	1.020	1.83	1.056	1.075	1.085
Averaged outline	*1.55*	*1.088*	*1.56*	*1.051*	*1.092*	*1.054*

The proportionality coefficients body and dimensions of the product in the pair W-G provide homogeneity of the typical construction of the bodice: $C_{pr_1}^{av} = 1.55$, $C_{pr_2}^{av} = 1.56$ with the property of nuance. The proportionality coefficients averaged outline in the pair G-B $C_{pr}^{av} = 1.088$, $C_{pr_2}^{av} = 1.051$ confirm the uniformity of the structures of the bodice and the property of the identity of the composite means in the design of details. $C_{pr_3}^{av} = 1.92$ та $C_{pr_3}^{av} = 1.054$ in typical schemes of grading patterns have a discrepancy of 2%, which confirms the reliability of the method of proportionality in the procedures of pattern's scaling. Complex drawings of the coordinate system of rectangles of overall dimensions of the back and forepart are shown in Figure 7.

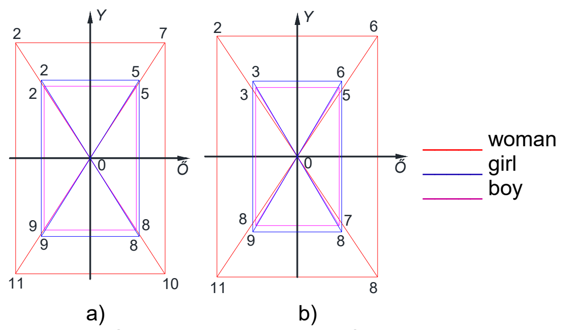

Figure 7 Complex system of polar coordinates of dimensions of products of the assortment complex: a) back; b) forepart

The algorithm for the method of determining the similarity of models of the range of Family Look range contains the following sequence of steps:

- Choosing a prototype of the base structure on the basis of "exactly the same" (see Figure 2).
- Division of the structure into sections in the polar coordinate system (see Figures 6, 7).
- Calculation of proportionality coefficients.
- Validation of the production scaling model.

Comprehensive blueprints for combining the details of back and forepart for W-G and G-B pairs in the polar coordinate system are presented in Figure 8.

To determine the increments in the structural points of the contours of the parts, a diagram of polar radii and angles (rads) relative to the center of scaling (Figure 9) has been created.

The system of transformations in the production model of the use of gender-age and style features of the assortment complex is subject to the proportionality estimation according to the scheme: dimensional features - design - scaling.

A production model for estimating the proportionality of control measurements is presented in Table 7. A graphical interpretation of the proportionality coefficients, depending on the stage of application of the control measurements, is shown in Figure 10 (see Table 6).

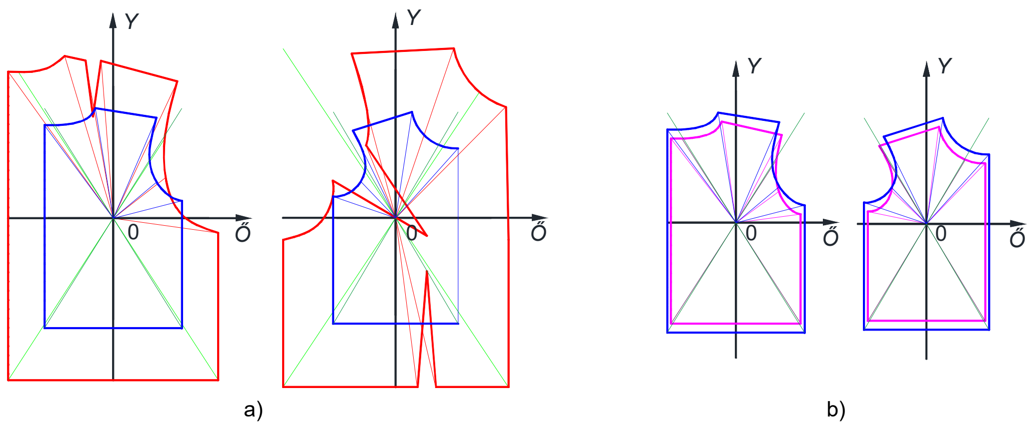

Figure 8 Complex drawings of the main details of the bodice: a) W-G; b) G-B

Table 7 Summary matrix of the production model of the proportionality of the control measurements of the complex drawing of pairs W-G, G-B

Control measurements		W-G				G-B			
		back		*forepart*		*back*		*forepart*	
		X	Y	*X*	Y	*X*	Y	*X*	Y
1	Dimensional features	1.46	1.53	1.59	1.59	1.21	1.052	1.01	1.01
2	Gradation coefficients	1.0	1.0	1.4	1.0	1.0	1.0	1.5	1.3
3	Measurements from the technical description	1.62	1.43	1.92	1.62	1.06	1.095	1.07	1.046
4	Dimensions of the drawing	1.55	1.43	1.54	1.61	1.056	1.095	1.24	1.046
5	Coordinates of diagonal endpoints	1.43	1.27	1.41	1.43	1.006	1.057	1.16	1.105
6	Length of diagonal	-	1.423	-	1.65	-	1.13	-	1.12
7	Polar angle [°]	1.088	-	1.091	-	1.048	-	1.033	-

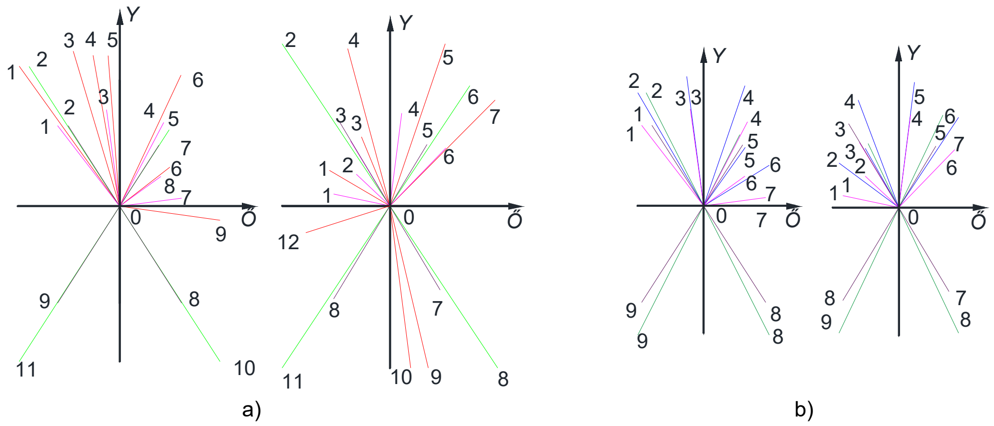

Figure 9 Diagram of the polar radii of the design points of the parts of the back and the forepart: a) W-G; b) G-B

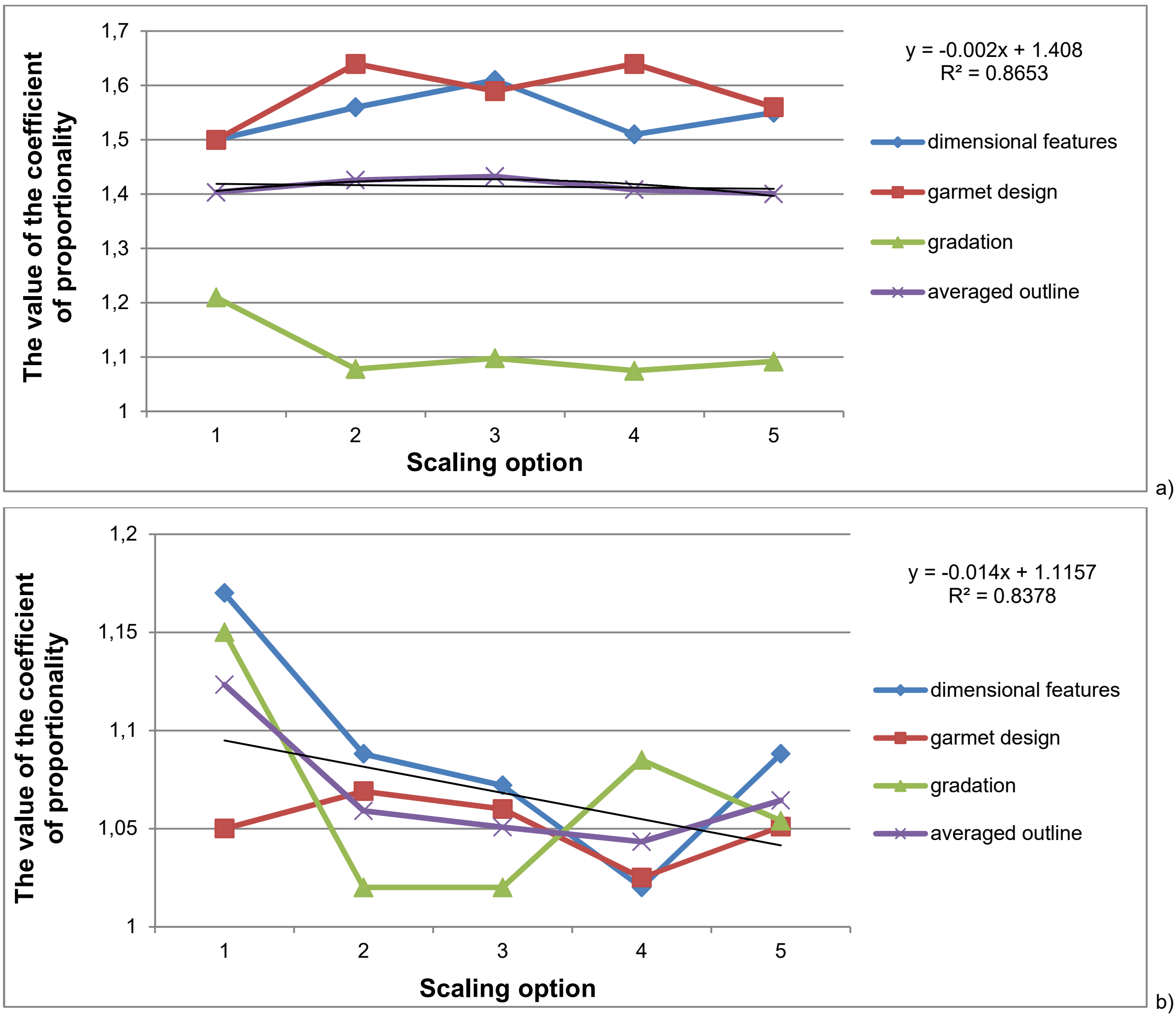

Figure 10 Dependences of Cpr on control measurements from scaling stages a) W-G; b) G-B

The linear regression equations averaged outline (Figure 10) correspond to the unified mathematical models of subordinate control measurements in stepwise quality control of design documentation for compliance with standards (see Table 1). The obtained mathematical models are adequate because $R^2 \rightarrow 1$. Comparative analysis of the proportionality coefficients of measurements from the technical description and the experimental designs shows that the percentage of deviations for the pair of W-G is 7.3%, for the pair G-B is 2.7%. Such a deviation for the pair of W-G confirms that the scaling is performed in close compliance with the proportions of the golden section. Matching the silhouette is achieved by adjusting the waist line level.

6 CONCLUSIONS

In determining the effectiveness of the algorithm for calculating the proportionality of structural measurements, it is natural to use software products of graphic graphics, which follows from the levels of typing numerical methods for solving problems in simulation modeling (Figure 1). It should be noted that graphic editors do not provide a mechanism of similarity in the design of details. In this sense, it is advisable to use the method of control measurements in the scaling stages.

To prove this statement, a method for systematically selecting a database for the functional orientation of cross stratification of consumer demand patterns is proposed (Table 2). This is not at odds with the practical data known from [21, 22], which characterize the structure of the parameterization of design patterns in the comfort of women's clothing. The classification of numerical methods for solving scaling problems (Figure 1), in contrast to the results of studies published [16, 26, 27], allows us to state the following:

- the main regulator of the collection of scaling parameters in the transforms of the contour of the part is not so much the complexity of the composition of the model, but the proportionality of body sizes by the genetic algorithm of preservation of similarity;
- for trendy assortment of complexes, using the example of Family Look it is expedient to use formalization of control measurements in Cartesian coordinate system. This allows you to balance the proportionality of the details in the range of proportional changes, which is important for recognizing the trendy image in the capsule of the range.

Structuring of the outer contour through the heterogeneous scaling of the coordinates of the joints by the method of moments on the principle of affine transformations has a significant influence on the internal filling of a typical structure by affine transformations.

In some polar sections of the contour of the part in the complex drawing (Figure 8) the principle of parallel transfer of lines of control measurements of dimensions is maintained. Such conclusions may be considered practical from the point of view of applying increments of polar radii in the form of a diagram to select a graphical scaling editor.

From a theoretical point of view, using the diagram of the polar radii of the design points, it is possible to estimate the proportionality of the model according to the scheme: dimensional features - design - scaling.

The proposed production model provides for the formation of a matrix of proportionality coefficients of the system of control measurements with the prediction of the assessment of composite features of similarity of products in pairs of gender and age characteristics. This greatly reduces the time required to process primary samples of clothing and ensures the uniformity of standard designs.

However, it should be noted that the principle of similarity in the production model of data depends on the property of identity of the composite means and indicates the ambiguous influence of indicators of proportionality of the body. Such uncertainty imposes certain limitations on the use of scaling software modules, which may be interpreted as a drawback of this research. A potentially interesting direction for further studies may be focused on a critical approach to brand symbolism based on the unification of forms for the scaling design method.

7 REFERENCES

1. Krzywinski S. Siegmund J.: 3D product development for loose-fitting garments based on parametric human models, IOP Conference Series: Materials Science and Engineering 254(15), 2017, pp. 1-5, https://doi.org/10.1088/1757-899X/254/15/152006
2. Kim Y.-K., Sullivan P.: Emotional branding speaks to consumers' heart: the case of fashion brands, Fashion and Textiles 6(2), 2019, pp. 1-16, https://doi.org/10.1186/s40691-018-0164-y
3. Slavinska A., Syrotenko O., Dombrovska O., Mytsa V.: Simulation model of the morphological field of data for constructing a universal design of trousers, Eastern-European Journal of Enterprise Technologies 1(1), 2020, pp. 52-61, https://doi.org/10.15587/1729-4061.2020.192590
4. Family Look Sets (electronic resource), available from http://newsdaily.com.ua/garderob/dlya-zhinok/4855-simejni-komplekti-odyagu-family-look.html, accessed: 2020-02-25
5. Family Look: a Trend that Brings Together (electronic resource), available from http://blog.shafa.ua/family-look-trend-kotoryiy-obedinyaet, accessed: 2020-02-18
6. Yaroshenko D.: Family Look: One for All (electronic resource), available from http://www.cablook.com/fashion/family-look-odin-za-vseh, accessed: 2020-02-12
7. Sagakova E.: 4 Options of How to Dress the Whole Family in the Style of Family Look (electronic resource), available from https://letidor.ru/moda/4-varianta-kak-odetsya-vsey-semey-v-stile-family-look.htm, accessed: 2020-02-22

8. Traumann A., Peets T., Dabolina I., Lapkovska E.: Analysis of 3-D body measurements to determine trousers sizes of military combat clothing, Textile & Leather Review 2(1), 2019, pp. 6-14, https://doi.org/10.31881/TLR.2019.2
9. Nayak R., Padhye R., Wang L., Chatterjee K., Gupta S.: The role of mass customisation in the apparel industry, International Journal of Fashion Design, Technology and Education 8(2), 2015, pp. 162-172, https://doi.org/10.1080/17543266.2015.1045041
10. Porterfield A., Lamar T.A.M.: Examining the effectiveness of virtual fitting with 3D garment simulation, International Journal of Fashion Design, Technology and Education 10(3), 2017, pp. 320-330, https://doi.org/10.1080/17543266.2016.1250290
11. Hong Y., Bruniaux P., Zeng X., Liu K., Curteza A.: Visual-simulation-based personalized garment block design method for physically disabled people with scoliosis (PDPS), AUTEX Research Journal 18(1), 2018, pp. 35-45, https://doi.org/10.1515/aut-2017-0001
12. Hong Y., Curteza A., Zeng X., Bruniaux P., Chen Y.: Sensory evaluation based fuzzy AHP approach for material selection in customized garment design and development process, IOP Conference Series: Materials Science and Engineering Vol. 133, International Conference on Innovative Research - ICIR Euroinvent 2016 19–20 May 2016, Iasi, Romania, pp. 450, https://doi.org/10.1088/1757-899X/133/1/012058
13. Gavish Y., Shoham A., Ruvio A.: A qualitative study of mother-adolescent daughter-vicarious role model consumption interactions, Journal of Consumer Marketing 27(1), 2010, pp. 43-56, https://doi.org/10.1108/07363761011012949
14. Slavinska A.: Model for adjusting the stages of design preparation for the production of garments of different price ranges, Bulletin of the Khmelnytskyi National University 3(261), 2018, pp. 102-108 (in Ukrainian)
15. Clare G., Uddin S.: Corporate image and competitive advantage for apparel companies, Trends in Textile Engineering & Fashion Technology 5(4), 2019, pp. 663-671, DOI: 10.31031/TTEFT.2019. 05.000618
16. Rahman O., Kharb D.: Fashion innovativeness in India: shopping behaviour, clothing evaluation and fashion information sources, International Journal of Fashion Design, Technology and Education 11(3), 2018, pp. 287-298, https://doi.org/10.1080/17543266.2018.1429498
17. Zarezade T., Payvandy P.: 3D garment design using interactive genetic algorithm and clustering, Trends in Textile Engineering & Fashion Technology 5(1), 2019, pp. 594-597, DOI: 10.31031/TTEFT.2019.05.000604
18. Slavinska A.: Method of optimization of structural and technological features of a systematic types of series of models of garments, Bulletin of Khmelnytskyi National University 2(223), 2015, pp. 45-49 (in Ukrainian)
19. Slavinska A.: Technological aspect of the multifunctionality of operation of the transformer product, Bulletin of Khmelnytskyi National University 1(269), 2019, pp. 53-62 (in Ukrainian)
20. Baker R., Yu U.-J., Gam H. J., Banning J.: Identifying tween fashion consumers' profile concerning fashion innovativeness, opinion leadership, internet use for apparel shopping, interest in online co-design involvement, and brand commitment, Fashion and Textiles 6(8), 2019, pp. 1-17, DOI: 10.1186/s40691-018-0158-9
21. Guo M., Kuzmichev V.E., Adolphe D.C.: Human-friendly design of virtual system "female body-dress, Autex Research Journal 15(1), 2015, pp.19-29, https://doi.org/10.2478/aut-2014-0033
22. Saharova N.A., Zang N.: Prediction of three-dimensional shape features of female dresses according to the pattern block design, Technology of Textile Industry 346(4), 2013, pp. 92-99 (in Russian)
23. Slavinskaya A.L.: Design-program for identification of structural-technological modules of products in the structure of the technological process, Bulletin of the Khmelnytskyi National University 5(229), 2015, pp. 134-140 (in Ukrainian)
24. Slavinskaya A.L, Ivanova M.A, Kotsyuk O. Yu.: Verification system of clothing model portfolio according to consumer preferences scenario, Proceedings of International Conference of Young Scientists & Students on Resource-Saving Technologies of Apparel, Textile & Food Industry, Khmelnytskyi, October 2019, Khmelnytskyi National University, Khmelnytsky, 2019, pp. 18-19, accessed: 2020-02-27, available from http://tksv.khnu.km.ua/inetconf/2019/slavinska_ivanova_kocjuk.pdf, (in Ukrainian)
25. Watkins L., Aitken R., Thyne M., Robertson K., Borzekowski D.: Environmental influences on pre-schooler's understanding of brand symbolism, Marketing Intelligence & Planning 35(7), 2017, pp. 907-922, https://doi.org/10.1108/MIP-11-2016-0211
26. Zakharkevich O.V., Kuleshova S.G.: Development of the method of scaling patterns and virtual garments forms, Vlakna a textile (Fibres and Textiles) 24(4), 2017, pp. 34-40
27. Mok P.Y., Xu J., Wu Y.Y.: 9 - Fashion design using evolutionary algorithms and fuzzy set theory - a case to realize skirt design customizations, Woodhead Publishing, 2016, pp. 163-197, https://doi.org/10.1016/B978-0-08-100571-2.00009-9

TEMPORAL EVALUATION OF CUSTOMIZED CLOTHING PATTERNS AND PATTERN DESIGNS

Gökçe Tabaklı[1], Zümrüt Bahadır Ünal[2] and Eda Acar[2]

[1]BR Mağazacılık Tic. A.Ş, Torbalı, İzmir
[2]Ege University, Faculty of Engineering, Textile Engineering Department, İzmir, Turkey
gokce_tabaklı @hotmail.com, zumrut.bahadir.unal@ege.edu.tr , eda.acar@ege.edu.tr

Abstract: *With the development of garment manufacturing, huge amounts of garment production in short time has been possible; which led to an increase in the profitability of companies and meeting customer expectations. But in due course, with the increase of household income, customers started to ask for dressing different than other individuals instead of wearing same clothes with everyone. Therefore, in order to maintain the variety of styles in manufacturing, the production quantities have decreased and the production methods have been evolved in this direction. Accordingly, due to meet these new expectations, customized clothing production concept has been born. The main fact which differentiates this production method from the old style tailoring is that; the design is also personally customized. The fabric, color, design, pattern details of the cloths can be customized according to customer choice. All of above points naturally increase the cost of the product. However in this method, the main importance is the customers who aspire their dream cloth instead of the product price. With this research, the systems which is needed to meet the new high level customer expectations have been analyzed; the production lead time and the effect of this method on the labour has been investigated in a facility which is making customized production.*

Keywords: *Customized clothing design, production time, pattern placement.*

1 INTRODUCTION

Rapid development of technology continuously changes the daily life course, preferences and expectations. For this reason, it is indispensable to develop different marketing strategies. One of them is customized production system. Customized production is supported by new technologies such as virtual merchandising, online shopping, three dimensional systems and body scanners which pioneered revolutionary innovations in textile industry [1, 2]. Companies that favored lesser model and much production strategy in the past have been passed to customer focused production model today. Thanks to possibility provided by digital technology, transition to production model according to demand has become much easier. Suitability of dress to the body is an important criterion for evaluation of a textile product by a customer [3]. Today it is determined that many customers cannot make use of ready-made products from non-compliance of body measurements with the standards. A study in the United States revealed that 62% of consumers could not find fit clothes for themselves, 59% of them found the fitness to body has changed even with the same trademark, 57% of them found that their bodies did not fit to the standards and 85% of them claimed that only reason of a trademark was the fitness of dresses to their bodies [4].

A wide variety of printing methods have been developed for ornament purposes in the garment industry [5]. The increase in digital products has also been effective in the development of the transfer printing method. This method is for considering the demands of the customized production. Customers can provide specification in color and design. This method is applied especially for low quantities. Thanks to the working with transfer printing machine, different types of fabric structures and unlimited colors even the most complex colors can be printed at once [6-8]. Transfer printing technology has high printing quality and enables to achieve expected fabric attitude and to save time [9, 10]. Within the scope of this study the research has been conducted on customized production techniques which have been increasing in importance in recent years that are predicted to provide a significant competitive advantage to the clothing industry of our country. In the study concrete data about the functioning of the system were determined by making sample applications in a plant that designs personalized patterns. The time required for the completion of these processes is calculated by ensuring the customer pattern inside the model molds with customer pattern measurements. At the same time all details such as pattern preference, color selection and pattern size are determined by the customers. After design is completed, the mold can be printed on the fabric with body sizes directly. In this study, it was aimed to evaluate the time spent on the design of the garment, taking into account the preferences and opinions of the customer.

2 EXPERIMENTAL PART

2.1 Materials

Within the scope of the study, design prepared specially for customer studies were conducted in a plant operating according to transfer printing method. The molds in which patterns are placed were prepared in the CAD system. Design dimensions and pattern size magnification and reduction were designed by the designer using Photoshop program. Working in connection with transfer printing machine, designs prepared were transferred to the printing paper machine. In transfer printing, dyestuff is transferred to the printing paper. Designs first printed to paper with heat and steam by dyestuff, were transferred to fabric by transfer printing. In the fabric mixture various fabrics such as PES (polyester), PAC (polyacrylic), EA (elastane) can be printed, In this study printing was applied in pain weave fabric produced from 100%PES. Since printed fabrics were used in transfer printing, they did not go through any finishing process. If requested by customer antistatic finishing may be applied to prevent electrification in the fabric.

2.2 Methods

After the pattern work is set in the reports and colors requested by the customer, a printing attempt on the fabric is made to present it to the customer. At operation conditions first printing of the design is realized on a special printing paper at the printing machine. The fabric quality of the sample printed on the printing machine was determined on special printing paper in the sample transfer hand printing machine so that color test is carried out by providing the transfer of the special printing paper to the fabric (Figure 1).

Figure 1 Fabric after color trial and transferred paper image

If the color is not the same as the color tone suggested by the customer, a color check is made by printing again. If the colors on the fabric comply with the color references requested by the customer, the production phase is started. Roll-shaped pattern paper was printed by special printing machine is mounted under the machine and printing is provided by heat transfer.

3 EXAMPLE OF CUSTOMIZED PATTERN WORK

The steps of placing the design in the garment pattern are explained as below.

Pattern preparation: The original file of the pattern marker layout is taken from the pattern Gerber Accumark v10.3 pattern program (Figure 2).

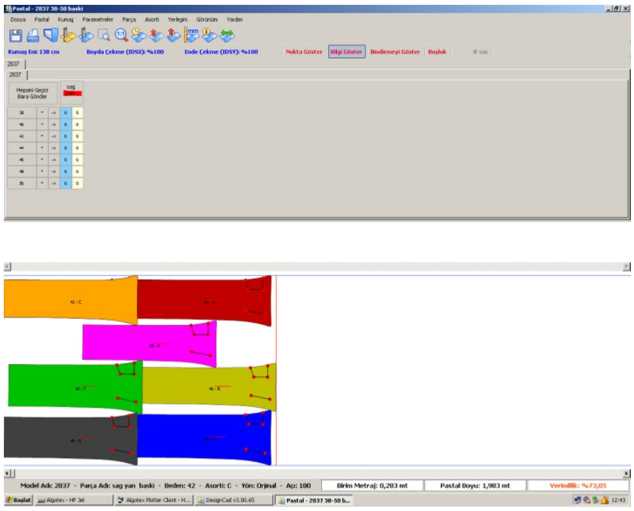

Figure 2 Images of the pattern programme

Pattern placement: The original version of the pattern is enlarged in the pattern program in the original mold size. The requirement of the customer is placed in it as in Figure 3.

Figure 3 Pattern work placed in the mold

The combination of all the parts that make up the related size is ignored. The printing is done in parts in a few sizes. After the pattern work is completed, the original size pattern is printed on the digital paper machine described above and transferred to the fabric in the fabric quality requested by the customer.

4 FINDINGS

Images of 10 different patterns requested by customer are given in Figure 4.

The time spent by the designer to place 10 different patterns designed specifically for customer demands were examined in two stages as pattern preparation and pattern placement. The first stage, the mold preparation time, gives the time to take the screenshots of the molds prepared in the CAD system, transfer them to the Photoshop program and bring the mold back to its original dimensions. The second stage, which is specified as the pattern placement in Table 2, shows the time spent in placing the designated patterns in these patterns brought to their original dimensions. Information about the times and how many parts the patterns consist of are given in Table 1 below.

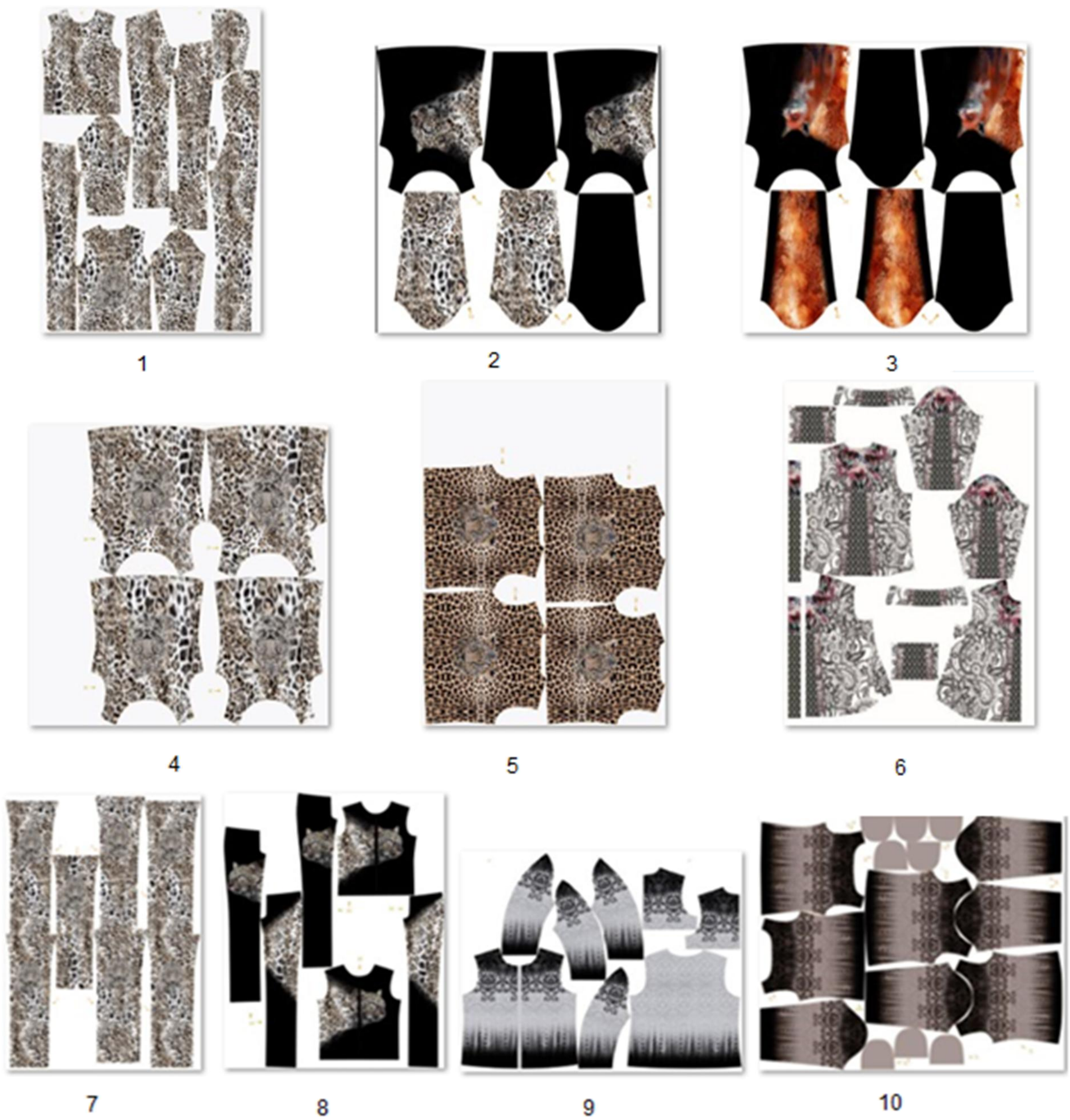

Figure 4 Customized pattern placement images

Table 1 Times spent on pattern creation and pattern placement

Pattern No.	Number of pieces that make up the patterns	1. PHASE	2. PHASE
		Pattern preparation [min]	Pattern placement [min]
1.	11	25	90
2.	6	10	60
3.	6	10	70
4.	4	10	45
5.	4	10	45
6.	11	31	180
7.	7	15	60
8.	6	15	90
9.	9	20	150
10.	16	35	90
Average [min]		**18**	**88**

5 CONCLUSIONS

Some pattern reports are requested specially to be placed on the garment in line with customer demands. The most important factor in demanding this layout is that the pattern is easily placed in the designated places, saving the fabric, cancelling some operations in the workflow and making the layout more standard. When it is desired to place special patterns on different parts of the product, this process should be preferred. Thus, the method of placing a pattern in the mold in the fabric design provides an advantage for the patterns to be positioned at the desired place. Pattern 1 in Table 1 covered the entire surface of the mold. Due to the high number of molds, the durations were found to be longer.

When the 2nd and 3rd pattern periods are examined, it is seen that the patterns and preparation times are the same, but the patterns applied to the sleeves are different. This difference was due to the placement of the 3rd pattern being different on the arms. It took a little more time for pattern placement than it should be left with an equal spacing on the right and left of the arms. Also, the 4th and 5th patterns are very similar. For this reason, mold preparation and pattern placement times were the same. When pattern 7 and pattern 8 are examined, mold preparation times are found equal. Pattern 8 was placed in certain parts of the mold, pattern placement needed more time to position it. Although the 9th and 10th patterns are similar, the pattern preparation and pattern placement times are different. Since the number of molds in the pattern 10 is higher, the mold preparation time is longer. However, since there are no patterns on small molds, pattern placement time is shorter.

Thanks to transfer and digital printing, customers' needs are responded quickly. These technologies have provided great convenience in the production of personalized production. Changes in the design and color determined by the customers can be answered in a short time. Developments in this regard are in a way to support lesser productions. With this method used, the possibility of designing the pattern on the computer and transferring it to the fabric provides designers with many options for obtaining the pattern, color and similar issues.

With all kinds of changes can be made according to the customer requests, it has made the possibility of that the printing pattern can be created and then placed in the mold that the customer wants to use, with different variations. It has reduced the waste rates in the sector. Information in transfer printing can work with computer programs. It is suitable to make the print sizes based on body series. It is possible to adjust the pattern used in printing according to each body size.

With a competitive focus; increasing product diversity, shortening of product life curves, demanding quality products with low prices, has made classic production models obsolete. Innovations made in this field can be organized especially in accordance with the production in low quantities.

6 REFERENCES

1. Vuruşkan A.: Developing a new approach on customized clothing considering fit and design parameters, Dokuz Eylül University, Institute of Science and Technology, PhD thesis, İzmir, 2010, 191 p. (in Turkish)
2. Yıldıran M.: The desing and production by 3D printings in the fashion ındustry, Art-e Art Journal 9(17), 2016, pp. 155-172 (in Turkish)
3. Bye E., LaBat K.: An analysis of apparel industry fit sessions, Journal of Textile and Apparel, Technology and Management 4(3), 2005, pp. 1-5
4. Kurt Salmon Associates, Annual consumer outlook survey, American Apparel and Footwear Association Apparel Research Committee, Orlando, FL, November 2000
5. Akpınarlı F., Bulat F.: Manipulation of textile surfaces and trialling of digital transfer printing, Motif Academy Journal of Folklore 9(17), 2016, pp. 167-186 (in Turkish)
6. Akbostancı İ.: The chaning definition of printed textile design and manufacturing in the 20th and 21st century, Art and Design Journal (5), 2014, pp. 31-41 (in Turkish)
7. Yüksel D.: Printing various feautured textile patterns with today's printing styles, Marmara University, Graduate School of Fine Arts, Master thesis, İstanbul, 2009 (in Turkish)
8. Özpulat F., Yurt D.: Design styles and techniques in current print patterned fabrics, Journal of Mediterranean Art 4(7), 2011 (in Turkish)
9. Miles L.W.C.: Textile printing, 2nd ed., Society of Dyers and Colourists, 2003, 320 p., ISBN: 978-0901956798
10. Yüksel M.: The tests and results of the fabrics that are put in production by printing process through new technologies on woven and non-woven surfaces, Haliç University, Institute of Social Sciences, Textile and Fashion Design, Master Thesis, İstanbul, 2012

STUDY ON VARIOUS DISPERSANTS IN PP MASTERBATCHES AND FIBRES MODIFIED BY PROTECTIVE PHOTOLUMINESCENT PIGMENT

Zita Tomčíková, Štefan Krivoš and Jana Ileninová

Research Institute for Man-Made Fibres a.s., Štúrova 2, 05921 Svit, Slovak Republic
tomcikova@vuchv.sk

Abstract: *Polypropylene (PP) doesn't contain functional groups; therefore dyeing in the mass by pigments is used in the dyeing of PP fibres. Dispersants are used to improve dispergation, increasing the homogeneity of the masterbatches. In this work, the influence of three types of dispersants on the processability and processing properties of protective photoluminescent pigment of PP masterbatches as well as the effect of dispersants on the resulting structural and mechanical properties of modified PP fibres were studied. Dispersants D1 and D2 (polyethylene waxes) weren't significantly demonstrated in the preparation of masterbatches, while dispersant D3 (N, N-bis-stearyl ethylenediamine) affected the melt flow index of the resulting masterbatches. The modified PP fibres with the protective photoluminescent pigment were prepared from masterbatches and PP by the discontinuous process of the spinning and drawing associated with the false-twist texturing of the fibres. The influence of dispersants on the resulting properties of the fibres didn't manifest itself significantly.*

Keywords: *modified PP fibres, masterbatches, properties, photoluminescent pigment, dispersants.*

1 INTRODUCTION

The development of special, modified, mono- and multi-functional active fibres and textiles characterized by their high functionality, flexibility, diversity and environmentally acceptable production is still a topical issue [1-3]. One of the ways to achieve sophisticated properties of fibres and consequently also of textiles is the use of photoluminescent pigments. Photoluminescent pigments belong to the materials where the excitation is caused by light and can be: fluorescent - with a short light response or phosphorescent - with a long light response [4-6].

Polypropylene (PP) fibres having a nonpolar paraffinic character are generally undyeable by the classical bath-dyeing method and therefore the substantial part of the PP fibre production is colored with pigments (mass dyed fibres) thereby obtaining a permanent functional modifications of fibres [7, 8]. The incorporation of an additive into the fibre mass is almost always preceded by the preparation of a functional masterbatch containing - carrier, additive (pigment) and an appropriate dispersing system [9, 10]. Dispersing system ensures a higher dispergation of the pigment in the fibre mass. A masterbatch is added to main PP stream in a pre-defined volume during the spinning process. The mixture is then melted, homogenized and spun into the form of modified fibres.

This article provides results of the three types dispersants influence on the preparation and properties of photoluminescent pigment masterbatches as well as their influence on the result properties of modified PP fibres. The modified PP fibres with protective photoluminescent pigment were prepared by the discontinuous process of spinning and drawing associated with the false-twist texturing of the fibres.

2 EXPERIMENTAL AND METHODS

2.1 Materials

Isotactic polypropylene (PP) produced by Slovnaft Company with MFI = 27.6 g/10 min (230°C/2.16kg), protective organic photoluminescent pigment (FP) of Radiant Color Company were used, and three types of dispersants: D1 - is a polyethylene wax having medium molecular weight, D2 - is a non-polar high density polyethylene with low molecular weight and the last D3 - is an amide wax of type N,N-bis-stearyl ethylenediamine, all produced by Clariant Corporation.

2.2 Preparation of PP masterbatches

The preparation of PP masterbatches of photoluminescent pigment was carried out on a Werner-Pfleiderer ZDSK-28 twin-screw extruder with a screw diameter ∅ = 28 mm, with a vacuum zone and accessories for premix preparation process.

The premixes consisted of a PP carrier, photoluminescent pigment (FP) and a dispersants D1, D2 and D3 (Table 1). The ingredients of PP premixes were compounded, melted and the resulting extrudates were cooled in water and pelletized.

Table 1 Composition of PP masterbatches

Sample	Concentration of additives [wt.%]				
	PP	FP	dispersants		
			D1	D2	D3
PP/1%FP	99.0	1.0	-	-	-
PP/1%FP/D1	98.7	1.0	0.3	-	-
PP/1%FP/D2	98.7	1.0	-	0.3	-
PP/1%FP/D3	98.7	1.0	-	-	0.3
PP/3%FP	97.0	3.0	-	-	-
PP/3%FP/D1	96.5	3.0	0.5	-	-
PP/3%FP/D2	96.5	3.0	-	0.5	-
PP/3%FP/D3	96.5	3.0	-	-	0.5

2.3 Fibres preparation

The modified PP fibres were prepared from mechanical blends of PP granulated polymer and PP masterbatches using the discontinued process of spinning and drawing associated with the false-twist texturing of the fibres. The undrawn PP fibres on the laboratory spinning line with an extruder diameter of D = 32.0 mm and with constant processing conditions - the spinning temperature of 220°C, spinneret 2x25 holes with diameter 0.3 mm and final process speed of 1500 m.min^{-1} were prepared. Subsequently, drawing associated with false-twist texturing of fibres was performed on the Barmag AFK-U-HTI line under process conditions - drawing ratio DR = 1.69, texturing temperature of 225°C, mechanical speed of 350 m.min^{-1} and D/Y ratio of 1.77.

2.4 Methods used

MFR of masterbatches was evaluated using a Dynisco Kayness capillary rheo-viscometer according to EN ISO 1133-1 Plastics: Determination of melt flow mass index (MFR) and melt flow volume index (MVR) of thermoplastics. Part 1: Standard method.

Filterability (filter pressure value) was evaluated using a filtration single-screw extruder with a screw diameter of 25 mm and pore density of the filtration sieve of 16000 pores per cm^2. The filterability of the dispersion (F) is expressed as ratio of an increment of the pressure (Δp) on the filter to a weight unit of the filtrate (m) at the definite filtration conditions.

Fibre´s birefringence: The orientation of the segments of macromolecular chains in fibre expresses the level of anisotropy of oriented polymer system (fibre). The total orientation of prepared modified PP fibres was evaluated using polarization microscope DNP 714BI. The refractive indexes of light in the fibre axis ($n_{//}$) and in the perpendicular direction of fibre ($n_{\perp}$) were determined. From the difference of refractive indexes of light, the fibre birefringence was calculated.

Crystallinity β represents the crystalline portion of fibres. In this work DSC-Q20 apparatus TA Instruments was used. The non-isothermal process of analysis was performed. All samples of PP fibres were heated at temperatures from 60 to 260°C at a rate of 10°C.min^{-1} under a nitrogen flow. From melting endotherm of 1st heating of PP fibres the melting enthalpy (ΔH_m) was determined. This value was used for the calculation of crystallinity in PP fibres using equation 1:

$$\beta = \frac{\Delta H_m}{\Delta H_{m,0}} \cdot 100\% \qquad (1)$$

where $\Delta H_{m,0}$ = 198.11 kJ.kg^{-1} is the melting enthalpy of PP with the 100% crystallinity.

Mechanical properties of fibres were measured in accordance with the EN ISO 2062 and fineness was measured in accordance with the EN ISO 2060. The equipment of Instron 3345 tensile tester for the measurement of mechanical properties (Young´s modulus, tenacity and elongation at the break) was used.

3 RESULTS AND DISCUSSION

3.1 Preparation of masterbatches and determination of their properties

The performed experimental work proved the possibility of preparation of PP masterbatches containing 1 wt.% and 3 wt.% of protective photoluminescent pigment using dispersants D1 - D3. The process of preparing masterbatches (Table 1) was technologically stable without interrupting the strings entering the pelletizer. The uniformity of the granules was satisfactory for all PP masterbatches of the pigment, without undercuts and without an increased proportion of dust particles. It follows that the selected type of polypropylene is a suitable polymeric carrier for the preparation of PP masterbatches. To prevent agglomeration of the pigment particles in the matrix under the preparation of PP masterbatches the dispersants D1 - D3 were used.

In terms of technological stability of the preparation of PP pigment masterbatches, the following twin screw extruder parameters were monitored - melt temperature, screw speed, drive load of the twin screw extruder, output rate and string pelletizing speed (Table 2).

Table 2 Parameters of PP masterbatches preparation

Sample	Melt temperature [°C]	Screw speed [rpm]	Drive load [%]	Output rate [kg/h]	Pelletizing speed [m.min^{-1}]
PP/1%FP	249	270	62	4.2	12
PP/1%FP/D1	249	270	61	4.1	12
PP/1%FP/D2	249	270	63	4.3	12
PP/1%FP/D3	298	270	73	4.3	12
PP/3%FP	274	270	63	4.1	12
PP/3%FP/D1	273	270	58	4.2	12
PP/3%FP/D2	273	270	72	4.4	12
PP/3%FP/D3	268	270	66	4.2	12

It was found that due to the dispersant D3 being at its lower content of 0.3 wt.% in the PP/1%FP/D3 masterbach, the melt temperature and the drive load of extruder increased compared to parameters of remaining masterbatches with a 1% FP content. This is probably due to the formation of agglomerates in the melt. On the other hand, at its higher content of 0.5 wt.% (PP/3%FP/D3 masterbatch) there is a decrease in the melt temperature compared to the melt temperature of remaining 3% FP masterbatches. In this case, the drive load is comparable to other masterbatches. This is partly related to the higher MFR of the masterbatch PP/3%FP/D3 as well as to the lower filter pressure value of mentioned masterbatch (Table 3). The effect of dispersants D1 and D2 did not manifest itself significantly in the preparation of concentrates.

By evaluating the processing properties of PP masterbatches (Table 3), it was found that the addition of dispersant D3 (masterbatches PP/1%FP/D3 and PP/3%FP/D3) causes an increase in melt flow index and a reciprocal decrease in melt viscosity of PP masterbatches compared to masterbatches PP/1%FP and PP/3%FP without dispersant content. If necessary, there is therefore a realistic assumption of the possibility of regulating the melt flow index; resp. melt viscosity of PP concentrates by dispersant type in masterbatch. Dispersants D1 and D2 do not have a significant effect on the processing properties of masterbatches. Low coefficients of variation 1.68%-2.32% demonstrate the high flow uniformity of PP masterbatches of the protective photoluminescent pigment.

For PP masterbatches containing 3 wt.% of photoluminescent pigment, the filter pressure value is significantly lower compared to the FPV of 1% PP masterbatches (Table 3). This is probably due to the higher content of low molecular weight substances (pigment, dispersant) in the polymer matrix of 3% masterbatches, which leads to its dilution, as well as due to the different ratio of photoluminescent pigment (FP): dispersant (D). In the case of 1% masterbatches the FP:D content ratio is 3.3:1.0, while in the case of 3% masterbatches the FP:D ratio is 6.0:1.0, which means that in 1% masterbatches on the same amount of dispersant accounts for a smaller number of pigment particles. This can result in an excess of dispersant, which can lead to agglomeration of the pigment particles in the PP melt and thus to an increase in the filter pressure value of the masterbatches. From the above, it is clear that 3% masterbatches are more suitable for fibre preparation because they have a low filter pressure value, which demonstrates a high degree of pigment dispersion in the PP matrix.

PP masterbatches with 1% content of photoluminescent pigment will be used to prepare fibres containing 0.01 wt.% FP and PP masterbatches with 3% content of FP will be used to prepare fibres containing 0.1 wt.% FP pigment in the PP matrix. The purpose was to minimize the amount of once remelted polymer in the preparation of the fibres.

Table 3 Processing properties: melt flow index (MFR), viscosity (V), filter pressure value (FPV) and associated variation coefficients (CV_X) of prepared PP masterbatches

Sample	MFR[a)] [g/10 min]	CV_{MFR} [%]	Viscosity [Pa.s]	CV_V [%]	FPV [MPa/kg]
PP/1%FP	26.05	1.68	299.5	1.7	< 398
PP/1%FP/D1	27.10	2.31	286.6	2.3	< 401
PP/1%FP/D2	26.88	1.85	288.7	1.8	< 415
PP/1%FP/D3	28.25	2.27	274.7	2.3	< 433
PP/3%FP	27.81	1.91	280.3	1.9	< 128
PP/3%FP/D1	27.60	2.02	281.2	2.0	174
PP/3%FP/D2	26.16	1.81	276.5	1.8	< 140
PP/3%FP/D3	29.79	2.32	255.7	2.3	112

[a)] 230°C/2.16 kg (τ = 19500 Pa)

3.2 *Preparation of modified PP fibres and determination of their properties*

Spinning process of the prepared PP blends was stable in all cases and the prepared fibres corresponded to the quality required for discontinuous shaping and drawing of the fibres. Fibres containing 0.01 wt.% and 0.1 wt.% of the protective photoluminescent pigment were prepared from mechanical blends of 1% and 3% PP masterbatches and polypropylene. The resulting structural parameters and mechanical properties of the false-twist textured PP fibres are shown in Figures 1-3.

The birefringence of the modified PP fibres is in the range of 0.0286 - 0.0312 and remains practically unchanged due to the dispersants (Figure 1a). Crystallinity of the fibre with a dispersant D3 content was increased by 14% compared to the fibre without the dispersant at a photoluminescent pigment content of 0.01 wt.%, indicating that it could partially act as a nucleating agent. At higher FP contents of 0.10 wt.%, the crystallinity of concentrates containing dispersants D2 and D3 is 10% higher compared to the fibre without dispersant content, which may be partly due to the effect of dispersants and partly to measurement error (Figure 1b).

Fineness of the false-twist textured PP fibres with the content of photoluminescent pigment is in the range of 165 - 172 dtex, which means that the dispersants do not affect the fineness and the resulting deviations are caused by a failure of the bursting device (Figure 2a).

Young's modulus of elasticity was decreased by dispersants (max. 20%) in the fibres containing 0.01 wt.% of photoluminescent pigment (Figure 2b). In this case, the diluting effect of the dispersants was manifested too. Fibres with a higher pigment content of 0.10 wt.% did not show this effect; probably all of the dispersant was used to coat the pigment particles.

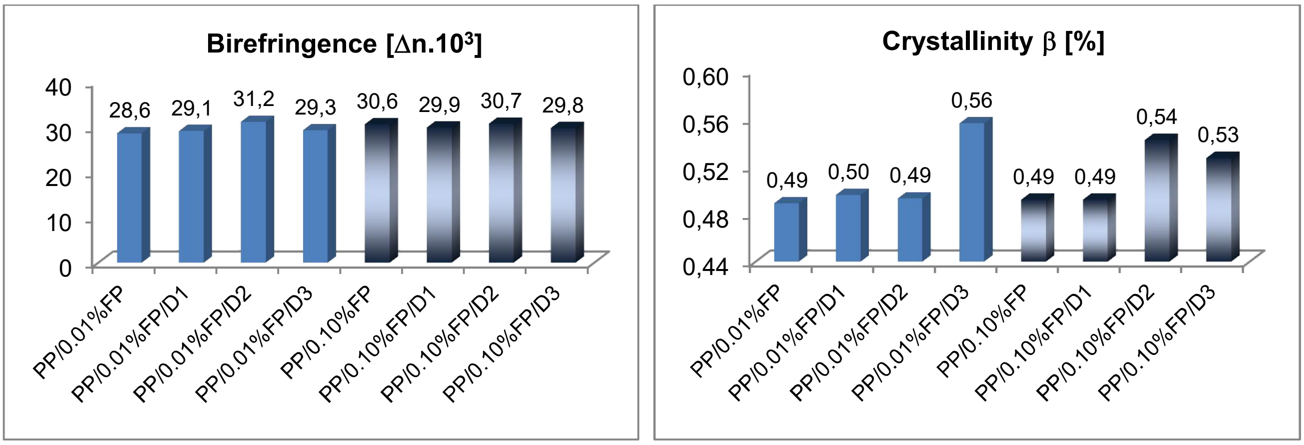

a) b)

Figure 1 Comparison of structure parameters: a) birefringence and b) crystallinity of false-twist textured PP fibres containing photoluminescent pigment (FP) and dispersants D1, D2 and D3 as well as fibres without dispersants

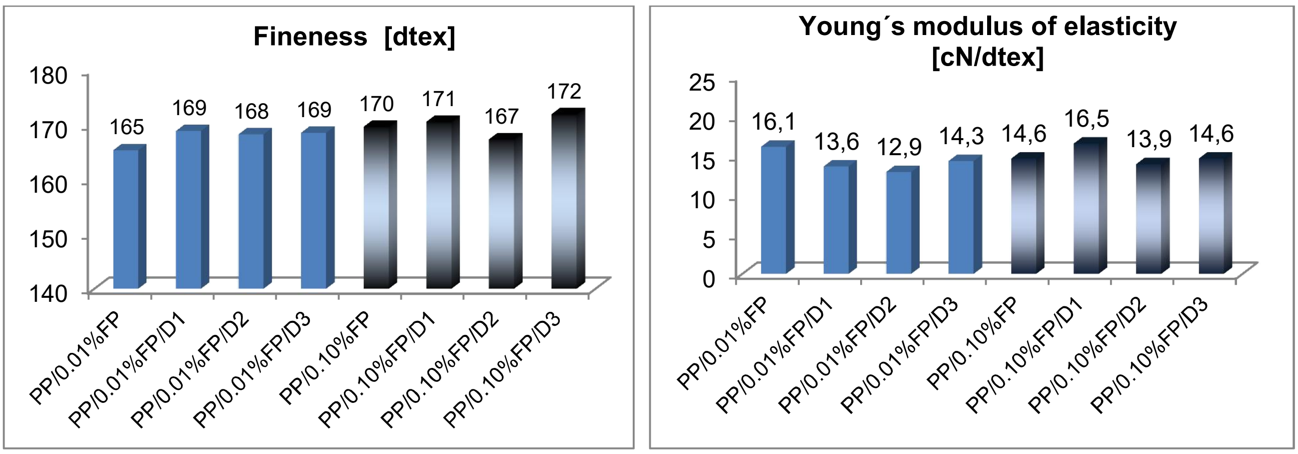

a) b)

Figure 2 Comparison of a) fineness and b) Young's modulus of false-twist textured PP fibres containing photoluminescent pigment (FP) and dispersants D1, D2 and D3 as well as fibres without dispersants

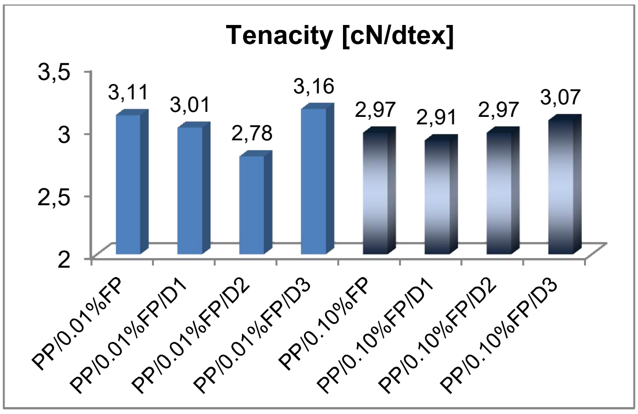

a)

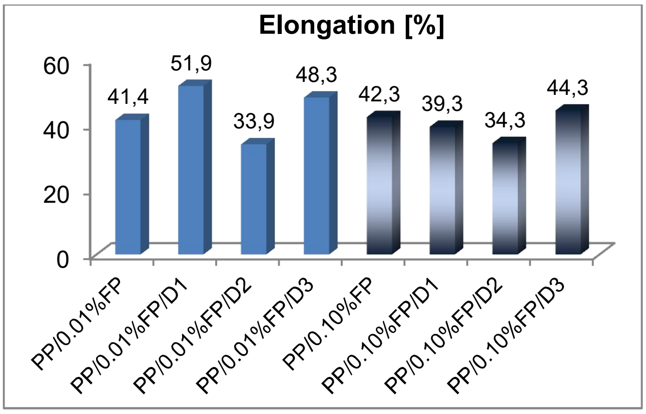

b)

Figure 3 Comparison of mechanical properties: a) tenacity and b) elongation of false-twist textured PP fibres containing photoluminescent pigment (FP) and dispersants D1, D2 and D3 as well as fibres without dispersants

Tenacity of the most modified fibres containing dispersants does not change significantly; the difference compared to fibres without dispersants does not exceed 10%. The lowest mechanical properties were measured for the PP/0.01%FP/D2 fibre (Figure 2b and Figure 3). The decrease in mechanical properties of the PP/0.01%FP/D2 fibre is probably related to the low molecular weight character of the dispersant.

Small differences in the structural parameters and mechanical properties of the fibres are related to the low content of masterbatch in the spinning mixture and the associated low content of pigment and dispersants in the fibres.

4 CONCLUSION

In the first part, the influence of dispersants D1, D2 and D3 on the preparation of masterbatches of protective photoluminescent pigment (FP) was studied. Masterbatches with 1.0 wt.% FP and 0.3 wt.% dispersant and 3 wt.% FP and 0.5 wt.% dispersant as well as masterbatches without dispersants with 1.0 wt.% and 3.0 wt.% FP were prepared. Low coefficients of variation 1.68 - 2.32% of melt flow index and viscosity demonstrate high flow uniformity of PP masterbatches. The effect of dispersants D1 and D2 itself did not prove significantly in the preparation of masterbatches, while the dispersant D3 (N, N-bis-stearyl ethylenediamine) influenced the melt temperature during the preparation of the masterbatches as well as the melt flow index of the resulting masterbatches. The filter pressure value is significantly lower for PP masterbatches containing 3 wt.% of photoluminescent pigment, compared to the filterability of 1% PP masterbatches. This is probably due to the higher content of low molecular weight substances (pigment, dispersant) in the polymer matrix as well as due to the different pigment-dispersant ratio.

In the second part, the influence of dispersants on the preparation of false-twist textured fibres as well as their influence on the structural parameters and mechanical properties of the fibres was studied. The spinning process of the prepared PP blends was stable in all cases. Dispersants have been found not to have a significant effect on the structural parameters and mechanical properties of fibres, what it is probably related to the final low content of pigment and dispersants in the resulting fibres.

ACKNOWLEDGEMENT: *This work was supported by the Slovak Research and Development Agency under the contract No. APVV-18-0187.*

5 REFERENCES

1. Baseri S.: Surface modification of nylon 6 multifilament yarns with 3-aminopropyltriethoxysilane and study of its special properties, Fibres & Textiles in Eastern Europe 28(2), 2020, pp. 29-34, DOI: 10.5604/01.3001.0013.7311
2. Struminska T.V., et al: Designing of special clothing based on experimental researches of material properties, Vlákna a textil (Fibres and Textiles) 26(4), 2019, pp.84-95
3. Aznar N.L.: Improved biobased fibres for clothing applications, bioplastics Magazine13(6), 2018, p. 28
4. Sharma R.; Bairagi N.: The role of photoluminescent pigments in textiles, Trends in Textile, Engineering & Fashion Technology 2(2), 2018, pp. 164-167, DOI: 10.31031/TTEFT.2018.02.000533
5. Campanella B., et al: The shining brightness of daylight fluorescent pigments: Raman and SERS study of a modern class of painting materials, Microchemical Journal 152, 2020, pp. 1-8, https://doi.org/10.1016/j.microc.2019.104292
6. Lusvardi GMalavasi G., Menabue L., Smargiassi M.: Systematic investigation of the parameters that influence the luminescence properties of photoluminescent pigments, Journal of Luminescence 175, 2016, pp. 141-148, https://doi.org/10.1016/j.jlumin.2016.02.038

7. Yu Ch., Zhu M., Shong Y., Chen Y.: Study on dyeable polypropylene fiber and its properties, Journal of Applied Polymer Science 82(13), 2001, pp. 3172-3176, https://doi.org/10.1002/app.2175
8. Marcinčin A.: Dyeing of polypropylene fibers, In: J.Karger-Kocsis (Ed.), Polypropylene: An A-Z Reference, Kluwer Publishers, Dordrecht, 1999, pp. 172-177, DOI: 10.1007/978-94-011-4421-6
9. Buccella M.: Color masterbatches for polyamide 6 fibers. Optimization of compounding and spinning processes. Physical-chemical characterization of industrial products. PhD thesis, Dept. of Industrial Engineering, University of Trento, 2014
10. Benetti F., Buccella M., Caciagli A., et al: Identification of colored-masterbatch process-parameter with greater influence on pigment dispersion and color perception, In: Proceedings of the event IPSP2014, DOI: 10.13140/RG.2.1.1658.0962

THE DRAGON IMAGE AS AN INSPIRATION IN THE DESIGN OF COSTUMES WITH CONSIDERING TECHNICAL ASPECTS

Olena Yakymchuk[1], Mariia Artemenko[1], Olena Chepelyuk[1], Anna Polietaieva[1], Nadiia Myrhorodska[1], Larisa Shpak[2], Sergii Gakhovych[3], Inna Yakovets[4], Oleksandr Luhovskyi[4] and Mykola Blyzniuk[5]

[1]Kherson National Technical University, Berislav highway 24, Kherson, Ukraine
[2]Kherson State University, University Street 27, Kherson, Ukraine
[3]Taras Shevchenko National University of Kyiv, Volodymyrska Street 60, Kyiv, Ukraine
[4]Cherkasy State Technological University, Shevchenko Street 460, Cherkasy, Ukraine
[5]Poltava V.G. Korolenko National Pedagogical University, Ostrogradski Street 2, Poltava, Ukraine
starcon84@gmail.com

Abstract: *The purpose of the study is determining the main characteristics of Dragon in a prototype and a shielded image for the formation of an inspirational perspective basis used in designing a suit. Analysis was performed on the following parameters: nature, outward, the division and graphics lines, colour gamma. A classification of application spheres of snakeskin imitation in a suit and basic technologies for imitation of snakeskin in a suit was created. A three models of a men's and women's suits were created, which provide a visual representation of the proposed solutions. The recommendations for designing a modern costume with a dragon inspiration have been developed. The series of a men's and women's costume have been developed. The research results will allow to develop a visual image's, that can be used in the design of clothing and the development of a game personages, movie personages, thematic costumes, etc. An image of the Dragon in a movies and cartoons was analysed, and their main characteristics have been identified. As a result, the new costumes that reflect a modern vision of such transformation where created.*

Key words: *textile materials, image, dragon, costume design, inspiration.*

1 INTRODUCTION

Today, the use of modern design ensures development of anything, equipment or object. Modern technologies and methods of objects modelling of applied value allow creating them on a technologically new level; especially considering the possibility of 3D printing and modelling. However, there is a problem of matching clothing design with materials and design methods. Very often when designing clothes, designers do not take into account the material of clothes with its general concept. This leads to deterioration of the visual component of the finished product and its imbalance with the surrounding space. For this reason, it is necessary to take into account the specific parameters of future product at the stage of product design, one of which is complex image design. That is applied design. It provides not only correct selection of the image, but also material coordination with manufacturing technology and finished product. This principle is used for most industries. Actual is appeal to the cultural roots and territorial features in the design of interiors, as well as in the process of creating costumes. Applied design in this context is a complex and lengthy process that requires a detailed study of the necessary image in original.

In general, modern designers in search of inspiration often turn to folk traditions, epics, tales or myths. However, in designing costumes for tourism this fact is alone. Although this approach allows to provide a measure of authenticity and originality, stand out among the rest, to offer visitors an additional attraction element.

The result of designer's works who seek for inspiration to folk art is the transformation of folk costume. It should be noted, that when choosing an inspirational image, first of all, be guided by the concept of establishment. It is also advisable to take into account modern fashion trends of the world. So, one of trends that periodically appear in the collections of fashion designer is a Dragon motive. As a rule, this image is used by Asian countries, but European countries also use this image. An actual is combining national-mythological conceptual roots and modern fashion trends. Therefore, development of a modern costume using elements of applied design is actual task that solved in this work.

The inspirational power of art effects on creativity of artists to create beautiful works [1]. In this case, the images displayed in the cinema provide appearance of new ideas and impressions from the viewer.

Today received distribution a new forms of cinema representation of images, aimed at expanding understanding of the effects, operating at present time [2]. The description of new figures of subject knowledge emphasizes the viewer's ability to represent themselves and others as art subjects. Clothes in the era of its technological reproducibility are based on modern technologies which interfere with the everyday life of man [3]. The screen area separates the distance between the viewer and the objects, which perceived.

Considering the two-tier analysis [4] can represent, as a cinematic form serves as an indirect expression of faith. In this case to understand the significance of the described experiences and psychology it is need to be complemented by research at the level which can be called spiritual. With the passage of the time technical cinematic devices transformed the perception of the visual world [5]. The concept of alienation in poetic language became a manifestation of aesthetic experience. An effective associative project of cinematographic realization [6], symbolizes the economic, symbolic and historical imbalances that are characteristic of certain countries. In this case, there are some specific stresses that cover the relationship between cinema and literature as a tandem of imaginative thinking. The film has strongly changed the perception of creative images [7]. The discovery of the art of mechanical recording through the reproduction of motion and images provokes a peculiar "miracle" where the viewer gets new impressions from viewing.

It is known that folk personages such as Grandfather Frost, Snow Maiden, Baba Yaha, Dragon and Koshchiy Bezsmertnyi do not have prototypes that resemble them [8]. This judgment according to the authors is questionable and requires a more detailed examination of the study subject. The origins of the image of Dragon appropriate to trace the mythology of the Eastern Slavs. Therefore, there is a need to consider all the mentioned Dragons in this area. It was investigated in work [9] that the synthesized typing of the image of the fairy-tale Dragon was studied using the results of the predecessors: dragon-kidnapper, dragon-assassin, dragon-guard of the boundaries, dragon-squirrel and dragon-tempter. Sometimes Dragon belongs to the category of thieves / pseudo thieves in the aspect of the development of image toys of cartoons characters [10]. It is known [11], that in the domestic animated cartoons, Dragon belongs to the category of characters, who are endowed with great magic and negative qualities, but they do not interfere in the story of the tale and do not interfere with the protagonist. Recently, this fact has undergone transformation and requires more detailed research. Studies have shown that the majority of respondent's attribute Dragon to negative (evil) tale characters. In addition, the main direct associations with him were determined: three-headed, breath-taking, green, big [12]. From the tale's texts it is determined that the Dragon has the ability to turn around to a good guy or household items such as the broom, etc. [13]. It was investigated that in the representation of respondents about Dragon there is shift of emphasis in the direction of external characteristics.

It is noted in [14] that in Slavic tales there is no specific description of Dragon. From the contents of some tales it follows that the Dragon is multi-headed (preferably having three, six, nine or twelve heads, less than five or seven heads). Sometimes it is mentioned that he breathes fire. An assumption was made in the article [14] that he is some way connected with the mountains or "one, who lives on top", "forest", because "mountain" according to the old Slavic means "top" or "forest". It is noted that the Dragon is associated with fire or lightning [15-17]. His appearance is a mechanical combination of two animals: a bird (image of a distant kingdom) and a dragon (the image of the underground kingdom). Therefore, Dragon is associated with the abduction of souls and is a negative character in traditional Slavic tales.

Considered works exploring the Dragon in mythology and old Slavic tales do not determine the transformational changes of his image in contemporary culture and art. Therefore, they do not take into account the perception of the modern audience stereotype, compiled in cartoons and movies. The study of this question is very relevant in the formation of stereotypical inspiratory characteristics for further use in design of the costume.

The purpose of the study is determining the main characteristics of Dragon in a prototype and a shielded image for the formation of an inspirational perspective basis used in designing a costume. The image, that combines both of these elements (national-mythological conceptual roots and fashion trends) can be Slavic dragons. For today is absolutely new for creation of clothes in post-Slavic and world countries. So it is particular for designing a costume. Therefore, studying the image of Dragon in this context is actual task. Conceptualization of the recreation sphere with each passing day is grows and becomes one of the trend directions. Costume as an element of the decision of interiors and the integral visual image of the institution becomes the simplest means of its adaptation to the new realities of the development of the industry of recreation and tourism. Today it is advisable to speak not just about the costume service staff which in the classical version must correspond to a certain dress code. But about the artistic images of the characters who interact with the rest and immerse it in a new alternative atmosphere. In this key, at the first stage of research it was decided to analyse the characteristics of the images of dragons regarding their original source in the Slavic culture. Dragon image belong to the class of chimeric creatures, which are distinguished in Slavic mythology among other deities and spirits. There are seven such creatures: Aspid, Yusha, Vasilisk, Dragon, Smiulan, Tsmok, Fire dragon (Table 1). The study of external characteristics of chimeric dragon species has identified the following identical features: presence of many heads: Dragon, Tsmok; absence of wings: Smiulan, Fire dragon; eruption of a fire (hot heat) or fire image: Aspid, Vasilisk, Dragon, Fire dragon. Analyzing of their characters (Aspid, Vasilisk, Dragon, Fire dragon) can be attributed to a negative images. Thus, the Dragon can be considered as a complex image of the chimeric beings of Slavic mythology. This confirms its relevance as one of the inspirational prototypes in costume design in recreational and tourist sector. Today, the Dragon popularity in modern Slavic culture and television art is growing. This image inspiration can be translated into other areas of the economy, for example, the costume of workers as a popular character conceptual vector. Therefore, there is a need to study the artistic image of Dragon with an emphasis on its visual component for the further development of recommendations for designing costumes of workers.

Table 1 Analysis of chimeric creatures (dragon images) of Slavic mythology

№	Character	Region	Abilities	Image in mythology	Look	Image
1	Aspid	East, west, south	Able to throw a fire	Evil demon, devastates the earth	Winged dragon with bird's beak	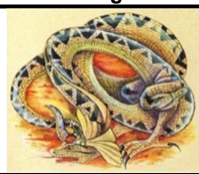
2	Yusha	East, west, south	When he yawns or turns over, the earth shakes	World dragons, holding ground	Huge dragon	
3	Vasilisk	East, west, south	Able to kill with a sight or breath - from his breath the grass dries, rocks break down	Demonic character, unclean spirit in a bird-dragon manner, serpent king	May have a head of a cock, a torso frog, a dragon's tail	
4	Dragon	East, west, south	Breathes fire, can turn into a person	Representative of the evil beginnings, kidnaps young girls	Dragon with 3, 6, 9 or 12 heads (sometimes 5 or 7 heads)	
5	Smiulan	East	Becomes a marital union with a human woman, brings in the house of wealth from those hidden in the earth	The patron saint of dark clouds inhabits the hollow of an ancient oak	Dragon-like demonic creature	
6	Tsmok	East	Brings to his master money, welfare, makes the fields fertile	The spirit that protects the house and the economy of people	A huge dragon, with 3, 6 or 12 heads, wings and claws	
7	Fire dragon	East, west, south	Transforms into humans and animals, flies to the fireplace and visits women, who mourn by men	Incarnation of fire and cunning	Demon in the form of a fireball	–

2 EXPERIMENTAL

To study the screened image of Dragon fourteen cartoons and films were chosen. The collected graphic material of the filmed image of Dragon was arranged in chronological order (Table 2).

As a result of the analysis the basic features of the visual component of Dragon were established: he always has three heads, in most cases large, and in individual ones – low, sometimes Dragon meets with a beak, often has wings and four paws, in rare cases it meets with hair; colour scheme consists of bright colours: red, green, orange, yellow, violet; division and graphic lines are horizontal (on the neck, abdomen, tails) and diagonal (on the wings). With regard to behaviour, in almost all screenplays, he has the role of an evil antagonist, in addition to films of recent years (from 2006 to today), where there is a shift in emphasis from antagonistic to a positive character.

Table 2 Analysis of the filmed image of Dragon

№	Source	Nature	Outward	The division and graphics lines	Colour gamma	Image
1	Film “Vasilisa is beautiful” 1939	Angry, fighter	Great, three heads, a beak, an eagle, a dragon body	Vertical lines on the neck on the abdomen, horizontal on the neck, abdomen and back	–	
2	Film “About an evil stepmother” 1966	Not disclosed	Three heads, a long neck, a mane around the neck, four paws	–	Green, grey	
3	Cartoon movie “The fairy tale affects” 1970	Angry, antagonist	Three heads, beak, hair, wings, four paws	Diagonal on the wings	Dark green, purple, black	
4	Cartoon movie “Baba Yaha against!” 1980	Angry, harmful	Little, three heads, wings, dragon tail, four paws	Diagonal on the wings, vertical on the back	Yellow, orange	
5	Cartoon movie “Ivashka from the Palace of Pioneers” 1981	Angry, antagonist	Three heads, small wings, dragon tail, two paws	Horizontal on the head	Grey, blue	
6	Cartoon movie “Fantasers from the village of Ugry” 1994	Angry, antagonist	Big, three heads, small wings, dragon tail, four paws	Horizontal on the neck, tails, diagonal on the back	Yellow, orange	
7	Cartoon movie “Babka Yezhka and others” 2006	Angry, greedy	Big, thick, three heads, beak, dragon tail	Horizontal on the stomach	Salad, pink, blue-green and violet	

8	Cartoon movie “Dobrynia Nikitich and Dragon” 2006	Good	Big, thick, three heads, long neck, small wings, four paws, claws	Diagonal on the wings	Red	
9	Cartoon movie “Ivan Tsarevich and the Grey Wolf” 2011	First angry, then good	Big, three heads, long neck, middle wings, dragon tail, four paws, claws	Horizontal on the tail, diagonal on the wings	Light green and green	
10	Cartoon movie “Three heroes on the far shores” 2012	Good	Big, thick, three heads, long neck, small wings, four paws, claws	Diagonal on the wings	Red	
11	Cartoon movie “Three heroes and sea king” 2016	Good	Big, thick, three heads, long neck, small wings, four paws, claws	Diagonal on the wings	Red	
12	Cartoon movie “The Heroine” 2016	First angry, then good	Big, three heads, a long neck, large wings, a dragon long tail, four paws, claws	Diagonal on the wings, vertical lines on the back	Light green and green	
13	Cartoon movie “Three heroes and princess of Egypt” 2017	Good	Big, thick, three heads, long neck, small wings, four paws, claws	Diagonal on the wings	Red	
14	Film “The last knight” 2017	Good	Small, three heads, beak, fangs, dragon body, long tail, large wings	Diagonal on the wings	Brown, dark green	

Snakeskin was in fashion at all times. Now this is one of the most popular trends that finds its application in various spheres of design (design of fashion and shoes, manicure and makeup, interior, cars, etc.). Despite this popularity, few people know how to get snake skins and how many snakes are used every year in order for fashionistas from all over the world to buy a new handbag or shoes.

Snakeskin production has its own technology, which consist of different parts. Usually it is a handmade work (Figure 1).

The best snake skins are obtained in Indonesia, where the special snake slaughterhouses and factories are. Every day hundreds meters of snakeskin are sold from such a factory. Snakes are kept alive in slaughterhouses and used in such a way not to damage the skin (a stick is inserted in the snake’s mouth).

Next technology can have two vectors: getting an unfolded snakeskin; getting an unbroken snakeskin. To get the unfolded skin, a snake’s body is cut with scissors. Then it is washed and separated from the skin. The meat of snake is sold to local restaurants. Skins are twisted and sent to the oven for heat treatment. In this way it is dried. There is a variant of getting an unbroken snakeskin without cutting when it is stripped. In this case, it is not twisted and dried in the sun, putting on a stick.

After drying, the snake skins in both versions are transferred to factories for the production of products of snake skin. There they are painted, dried and then clothes, bags and shoes are sewed from them. From unfolded snake skins you can get any product in a constructive way. The unbroken snake skins are used to manufacture the belts, straps and for accessories and shoes.

Regarding the economic aspect, snakeskin goods are quite cheap at the factories (for example, bags cost from 15 to 31 dollars), and in fashion stores, they are tens or hundreds of times more expensive. Such rapid use of snakes is harmful to the environment. An alternative to snakeskin is its imitation, obtained artificially (Figure 2).

Figure 1 Producing technology of natural snakeskin

Modern technologies make it possible to copy snake ornament and texture in the smallest details. In addition, this can be done not only on fabric, but on absolutely any surfaces. Nowadays, imitation of snakeskin is used in the interior (furniture, various surfaces, accessories: photo frames, boxes, pillows, etc.), costumes (clothing, shoes, accessories, manicure and makeup, cars, etc.). Due to the large number of applications, there are many ways to simulate snakeskin. Polymer decorative plaster is used to simulate snakeskin on various surfaces in the interior, wood carvings, decoupage, painting and imitation with the help of various texture matrices are used to decorate various small interior items and decorations.

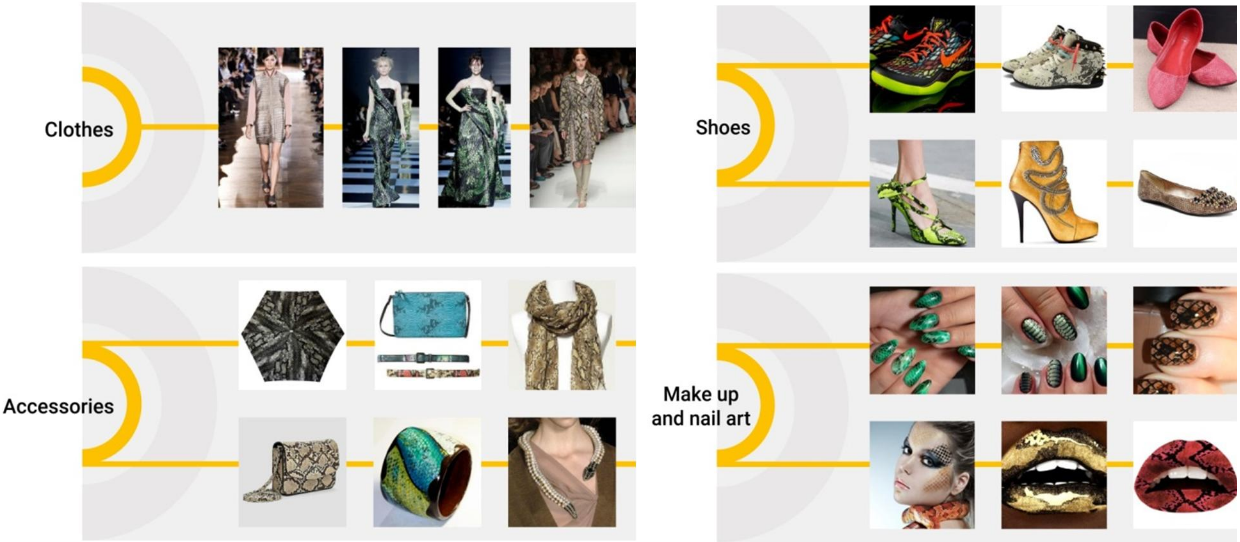

Figure 2 Spheres of application of snakeskin imitation in a suit

Vinyl film, aqua print (immersion printing is a technology for transferring a printed image to volumetric objects with complex surface relief) or the technology of 3D decoration of goods with the water-soluble film are used for car decoration. To create an imitation of snakeskin on shoes, designers use perforation, embossing, printing, embroidery, decoration with stones and rhinestones, applications. Today, snake motifs are also popular in the art of make-up and nail art. To create a "snake" manicure, manicurists use craquelure varnish, stencils made of fabric or paper, and slough. Temporary lip tattoos, painting with cosmetics are used for "snake" makeup.

The more spheres of snakeskin application, the more ways to imitate it. Imitation technologies of snakeskin in a suit can be divided into several types.

Print on fabric is the most popular for imitation in clothing, as at minimal cost we can produce large volumes of fabric and create the most incredible prints. There are several types of printing on fabric: transfer, silk screen printing or silk stencil, sublimation printing. Sublimation printing is the most popular in mass production, because it does not change the properties of the fabric and is the most resistant. Modern fabric printers allow making a 3D print and creating the illusion of texture. Batik painting is used not so often and mainly for small productions or individual orders. We can create a real texture using various embroideries and sequins, beads, rhinestones, and decorated ribbons. The perforation of the fabric is no less popular (slitted ajour burning out).

To create an imitation of snakeskin in jewellery, besides mentioned printing, perforation and painting, jewellers use polymer clay, decoupage, a weaving of beads, threads, ribbons, and painting. It is also possible to use natural stones. For example, opals, which sometimes have a natural snakeskin effect. Tailors use printing, applique, perforation, embossing to imitate a snakeskin on the bags.

Every year technologies are improved and the cost of production is significantly reduced without losing the quality or appearance of the product. Therefore, the use of snakeskin imitation can not only reduce the harm to the ecosystem, but also make goods available to a wide range of consumers.

3 RESULTS AND DISCUSSION

As a result of the analysis of seven dragon images it is determined that Dragon can be considered as a complex image of the chimeric creatures of Slavic mythology. Since he is multi-headed (like Tsmok), has wings (like Aspid, Yusha, Vasilisk, Dragon, Tsmok), extinguishes the fire (like Aspid, Vasilisk, Dragon, Fire dragon) and refers to negative characters (like Aspid, Vasilisk, Fire dragon).

It is established that the stereotypical filmed image of Dragon differs from dragon images of the Slavic mythology by constant presence of three heads and tendency to change character in positive direction, which apriority contradicts the nature of this image.

An inspirational basis for designing costumes in the form of Dragon was developed, which includes recommendations on coloristic, geometry, plastics, mass and form factor, decorative elements and ornamental textures accents.

Taking into account the results of the study dragon images of Slavic mythology and the filmed image of Dragon, it is possible to recommend the following basic inspirational principles for designing a costume that reflect the image of Dragon (Table 3, Figure 3).

Table 3 The inspirational basis for designing the costume of Dragon

Coloristic	**Geometry and form plastic**	**Decorative elements and facture**
Yellow, red, orange, green, light green, brown, grey, blue, purple, blue-green	The silhouette of the costume is curvilinear with smooth and rounded lines. Main mass shifted to the center of gravity with the output thin details	3, 6, 9, 12, 5 or 7 heads claws, eagles, wings, beak, tail
In front of the suit in light tones	The interior of the plastic details of costume is more straightforward or broken aggressive	Ornamental-factures accents: fire motives, scales
The back of the suit in dark tones	Plastic division of costume details: horizontal (head, waist, limbs), vertical (on the middle line of the back), diagonal, radial (side parts)	–

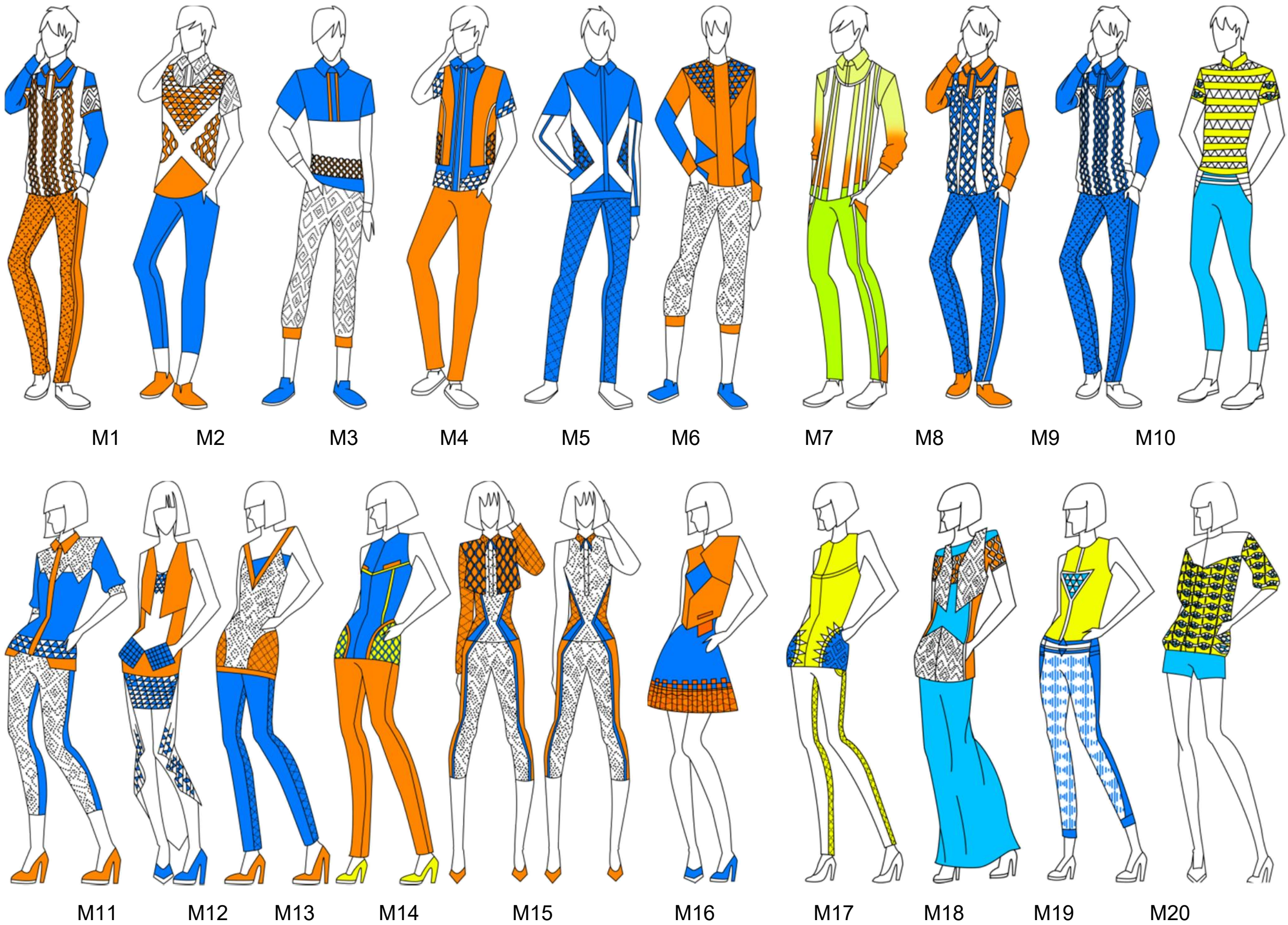

Figure 3 Developed series of costumes (M - model): M1-M10 - men’s costumes; M11-M20 - women’s costumes

Therefore, conducted researches of dragon images of Slavic mythology and filmed image of Dragon allowed to develop basic inspirational principles for designing a costume. This allowed to develop models of men’s and women’s costumes of different series (Figure 3).

Model M6 from men’s costumes series and models M12, M15 from women’s costumes series were made in material. Model constructions were used in their design, which are shown in the Figure 4.

As a practical result were executed a three models in the material (Figure 5).

Thus, taking into account the conducted research, three models of men's and women's suits were created, which provide a visual representation of the proposed solutions. Developed models can be used as everyday clothing. It’s aimed young consumers, who leads an active lifestyle, wants to show his individuality and expresses it through the visual component of his image. These models are synthesizing sports and classic styles of clothing and provide originality through the use of ornamental compositions. The presence of a pockets and pants in most models indicates their utilitarian functionality. Such clothes are optimal for citizens with a fast pace of life.

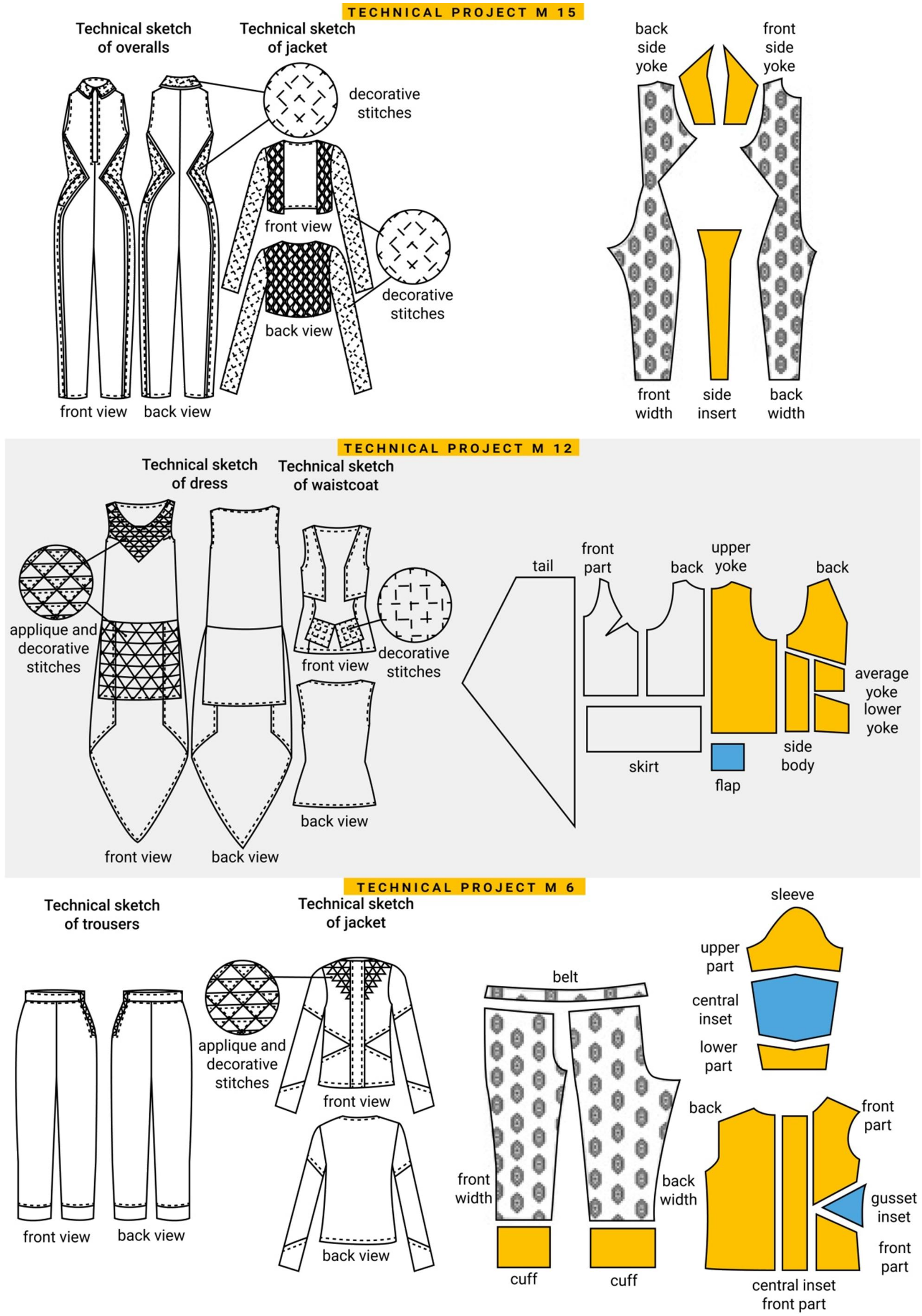

Figure 4 Drawings of basic details of model constructions of designed suits

Figure 5 Developed costumes in material (models M6, M12, M15)

4 CONCLUSIONS

The article is devoted to determining the main characteristics of Dragon in a prototype and a shielded image for the formation of an inspirational perspective basis used in designing a suit.

A classification of application spheres of snakeskin imitation in a suit and basic technologies for imitation of snakeskin in a suit was created.

A three models of a men's and women's suits were created, which provide a visual representation of the proposed solutions.

The recommendations for designing a modern costume with a Dragon inspiration have been developed. The series of a men's and women's costume have been developed.

The research results will allow to develop a visual image's, that can be used in the design of clothing and the development of a game personages, movie personages, thematic costumes etc.

A new costumes that reflect a modern vision of such transformation where created.

5 REFERENCES

1. Donghwy A., Nara Y.: The inspirational power of arts on creativity, Journal of Business Research 85, 2018, pp. 467-475, https://doi.org/10.1016/j.jbusres.2017.10.025
2. Zanoni F.: The genius and the new forms of cinematic representation of the subject of knowledge, Antíteses 9(17), 2016, pp. 157-175 , http://dx.doi.org/10.5433/1984-3356.2016v9n17p157
3. Ahn S.: Cinematic innervation: the intuitive form of perception in the distracted perceptual field, Journal of Aesthetics & Culture 5(1), 2013, pp. 1-16, https://doi.org/10.3402/jac.v5i0.21681
4. Bacon H.: Faith and Form on Screen, London, UK: Religions 7(11), 2016, pp. 1-14, https://doi.org/10.3390/rel7110130
5. Machado I.: Cem anos de estranhamento, Significação: Revista de Cultura Audiovisual 39(38), 2012, pp. 311-322 (in Portuguese), https://doi.org/10.11606/issn.2316-7114.sig.2012.71200
6. Amancio T.: Fronteira, fusão, filme: um toque, Contemporanea: Revista de Comunicação e Cultura 8(2), 2010, pp. 1-10. (in Portuguese)
7. Sobieszczanski M.: Entre l'immersion dans l'image cinématographique et l'immersion totale, Cahiers de Narratologie 19, 2010, pp. 1-8 (in French), https://doi.org/10.4000/narratologie.6184
8. Terenina N., Shustelev K., Illin V.: Ethno-folklore heritage of regions of the north-west and the centre of Russia and the possibility of creating tourist objects on its basis, Pskov Regionological Journal 8, 2009, pp. 84-88 (in Russian)
9. Lyzlova A.: Folklore motif of a woman's abduction by a Dragon in the literary tradition, The Problems of Historical Poetics 8, 2008, pp. 50-62 (in Russian), DOI: 10.15393/j9.art.2008.2593
10. Aleshina I., Ivanova E.: On the relevance of development of the classification figurative toy cartoon characters, Vestnik THU, 2012, 10(114), pp. 229-234 (in Russian)
11. Kuznetsova E.: On the specifics of animation, Scientific Bulletin of BelSU. Series: Philosophy. Sociology. Law 23(166), 2013, pp. 261-264 (in Russian)
12. Elina A.: "Good" and "angry" characters of Russian folk tales: aspect ratio, Diploma, Philological Sciences, Questions of theory and practice 4(II), 2013, pp. 70-74 (in Russian)
13. Elina A.K.: Negative characters of Russian folk-tales in perception of native speakers, The World of Science, Culture and Education 1(32), 2012, pp. 368-370 (in Russian)
14. Shtemberg A.S.: Heroes of the Russian fairy tales: Who are they and why they are behaving as they do? II, Space and Time 1, 2012, pp. 207-214 (In Russian)
15. Zhihui M.: on the folk customs of Huazhao Festival which is a kind of intangible cultural heritage and its modern value, Conservation Science in Cultural Heritage 14(2), 2014, pp. 155-174, https://doi.org/10.6092/issn.1973-9494/5450
16. Lidin K.: Dancing with the Dragon (chaos and order dialectics in the Far East cultures), Project Baikal 3(10), 2006, pp. 8-16 https://doi.org/10.7480/projectbaikal.10.516
17. Casado Presa C.: And they didn't live happily ever after: the rewriting of the fairy tale and the problematization of female subjectivity in Nueva historia de la princesa y el dragón by Carmen Resino, Revistas - Feminismo/s 0(30), 2017, pp. 31-46 (in Spanish), http://dx.doi.org/10.14198/fem.2017.30.02

EXPERIMENTAL INVESTIGATION OF MULTILAYER THERMAL INSULATION MATERIAL PERFORMANCE WITH USING OF DISCRETE HEAT TRANSFER MODEL

Alexander Zasornov[1], Iryna Zasornova[1] and Inna Marynchenko[2]

[1]*Khmelnitskyi National University, 11 Instytutska str., Khmelnitskyi, Ukraine*
[2]*Oleksandr Dovzhenko Hlukhiv National Pedagogical University, 24 Kyiv-Moscow str., Hlukhiv, Ukraine*
izasornova@gmail.com

Abstract: *This paper describes the results of multilayer thermal insulation material performance investigation with using of discrete heat transfer model. The material presented can be used in special clothing for high temperature protection. The thermal insulation efficiency is estimated by the analysis of temperature dependencies at the outer and inner surfaces of the presented material. The analysis is performed with using the technique on the base of heat transfer equations discretization. The proposed technique is realized with numerical differentiation error estimation procedure which allows a significant decrease of thermal insulation behavior prediction error*

Keywords: *thermal protective clothing, multilayer material, heat transfer, discrete model, numerical differentiation error.*

1 INTRODUCTION

Under high temperature conditions the safety of human life strongly depends on the performance of thermal insulation materials [1, 2]. The modern thermal insulation material must meet high requirements to heat transfer characteristics for efficient practical application [3-5]. The known thermal protection problems are described in [1, 6-10] for different heat transfer conditions. The main requirements to thermal insulation materials are formulated in [1-4]. In [9, 11-13] the data about heat impact on human health is presented in dependence with parameters of heat transfer processes.

The modern thermal protective clothing is designed on the base of different types of heat insulation materials [1]. The use of different fibers and fabrics in heat protection applications is described in [1, 8, 14, 15]. The thermal insulation properties of ceramic materials are described in [1, 9]. Composites and some other kinds of thermal insulation materials are considered in [1, 16, 17].

Most of the modern thermal insulation materials have multilayer structure [1, 5, 6]. The separate layers of materials with different physical and chemical properties allow the optimization of thermal insulation characteristics by varying the layers' thickness and order.

Therefore the modeling of heat transfer processes is one of the most important problems in thermal insulation material design. The minimization of heat transfer model approximation errors allows avoiding material destruction and people injury during material exploitation and laboratory testing [7, 18, 19].

The known thermal protective materials' models are based on continuous [20-23], discrete [20, 24, 25] and mixed [26, 27] processing of heat transfer characteristics. The advantage of discrete heat transfer models is the absence of errors caused by fitting of experimental data by analytical functions [25, 28, 29]. But, it should be noted that the discretization of heat transfer equations can cause a significant numerical differentiation errors [30-32]. These errors can be minimized with using of discrete processing such as filtering, smoothing, interpolation and selecting the correct discretization steps [25, 33-38].

This article presents the experimental results of thermal insulation material performance investigation with using of discrete heat transfer model. The discretization error estimation technique is presented for different discretization frequencies.

Margins, column widths, line spacing, and type styles are built-in; examples of the type styles are provided throughout this document and are identified in italic type, within parentheses, following the example. Some components, such as multi-leveled equations, graphics, and tables are not prescribed, although the various table text styles are provided. The formatter will need to create these components, incorporating the applicable criteria that follow.

2 MATERIALS AND METHODS

2.1 The experiment setup

The purpose of presented work is the design of heat insulation material which includes thermal protective layers with different properties. The minimization of thermal conductivity can be achieved by combination of screening materials and heat insulation materials. For obtaining an efficient multilayer thermal protective material the thickness and order of its layers must be defined with using of accurate heat transfer processes' analysis. The most useful methods of thermal insulation material performance estimation are based on the analysis of heat transfer from outer surface to inner surface of the material [7, 20, 23]. The investigation of dependencies between outer and inner surfaces' temperatures allows to meet necessary conditions of multilayer thermal insulation material design.

This article presents the results of experimental investigation of heat transfer processes which were performed with the laboratory equipment shown in Figure 1.

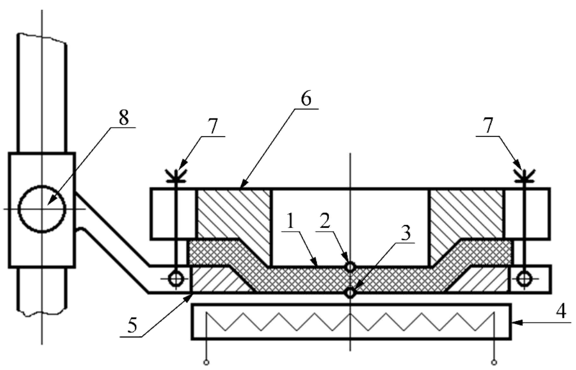

Figure 1 Experiment setup: 1 - material sample; 2 - temperature measurement on inner surface; 3 - temperature measurement on outer surface; 4 - heater; 5 - bracket; 6 - clamping ring; 7 - clamps; 8 - fastening screw

The equipment consists of console 5, clamping ring 6 and clamps 7 that are used for fixing of thermal insulation material sample under the heater 4. The sizes of console and clamping ring are chosen so that the bag materials do not shrink at the points of taking temperature measurement. The material sample 1 is heated and the temperatures are measured on the outer surface (measurement 1) and inner surface (measurement 2). The temperature decreases from outer layer to inner layer of thermal insulation material. For each layer the temperature decrease curve depends on the parameters and characteristics of its material.

2.2 The heat transfer modelling methods

At the present time the known methods of heat transfer modeling could be divided into two main groups. The first group includes the methods which use approximation of heat transfer characteristics by analytical functions [21, 39-42]. The advantage of such methods is the expression and analysis of heat transfer characteristics in the form of analytical functions. If the approximating functions are selected correctly, then analytical form of heat transfer characteristics allows to perform interpolation and extrapolation of heat transfer characteristics with fairly low errors [21]. But if the experimental data is distorted and does not give enough information, then heat transfer characteristics can be approximated with analytical functions which do not correspond to real heat transfer process dynamics. Such approximation can be characterized by significant interpolation and extrapolation errors caused by the difference between the forms of physical processes and approximating functions outside of the time range and space region of the experimental data [21, 41, 42].

The second group includes methods which are built on the base of numerical heat transfer modeling [22-24]. Such models use the information which is given by the experimental data without distortions caused by analytical approximation [20, 33, 34]. The numerical interpolation and extrapolation of heat transfer characteristics are based on experimental data and the laws of discrete mathematics. The accuracy of numerical heat transfer modeling is limited by the discretization and round-off errors [30, 34, 43]. Thus, if the discretization steps are selected correctly, then error of numerical approximation can be acceptably low [31, 35, 38, 44]. The advantage of numerical heat transfer modeling methods is the absence of analytical approximation errors. Also, it should be noted that the complexity of discrete model is defined mainly by the discretization process for different material sample shapes and time-domain characteristics. With regarding to the described advantages, the numerical heat transfer modeling methods were selected for the estimation of thermal insulation material efficiency. The use of discrete heat transfer models gives a relatively simple way to obtain a high reliability of thermal protective clothing performance estimation.

3 THEORY AND CALCULATION

The mathematical model of the process of heat transfer from outer surface to inner surface of the material is based on the heat transfer equations expressed by (1) [20, 21, 43]:

$$\frac{\partial T}{\partial t} = a\frac{\partial^2 T}{\partial x^2} \tag{1}$$

where t is the time, x is the spatial coordinate, T is the absolute temperature, a is the coefficient of temperature conductivity.

The discretized form of equation (1) is given by (2) [20, 25, 28]:

$$\frac{T_{i,k+1} - T_{i,k}}{\Delta t} = a_i \frac{(T_{i+1,k+1} - 2T_{i,k+1} + T_{i-1,k+1})}{\Delta x^2} \tag{2}$$

where k is the index in time domain; i is the index in spatial domain; a_i is the coefficient of temperature conductivity:

$$a_i = \frac{\lambda_{i-1} c_i \rho_i + \lambda_i c_{i-1} \rho_{i-1}}{2 c_{i-1} \rho_{i-1} c_i \rho_i} \tag{3}$$

where λ_i is the thermal conductivity; c_i is the mass specific heat capacity; ρ_i is the volumetric density.

Therefore the discrete model of heat transfer through multilayer material is expressed by the system (4):

$$\begin{cases} \dfrac{T_{1,k+1} - T_{1,k}}{\Delta t} = \dfrac{2\lambda_1 (T_{2,k+1} - T_{1,k+1})}{c_1 \rho_1 \Delta x^2}, \\ \dfrac{T_{2,k+1} - T_{2,k}}{\Delta t} = a_i \dfrac{(T_{3,k+1} - 2T_{2,k+1} + T_{1,k+1})}{\Delta x^2}, \\ \dots \quad \dots \quad \dots \quad \dots \\ \dfrac{T_{i,k+1} - T_{i,k}}{\Delta t} = a_i \dfrac{(T_{i+1,k+1} - 2T_{i,k+1} + T_{i-1,k+1})}{\Delta x^2}, \\ \dots \quad \dots \quad \dots \quad \dots \\ \dfrac{T_{n,k+1} - T_{n,k}}{\Delta t} = \dfrac{2\lambda_{n-1} (T_{n-1,k+1} - T_{n,k+1})}{c_{n-1} \rho_{n-1} \Delta x^2}, \end{cases} \tag{4}$$

where the first and the last equations are define the margin conditions.

The measured temperature can be represented as the sum of true temperature value $T_{0i,k}$ and error $\varepsilon_{i,k}$:

$$T_{i,k} = T_{0i,k} + \varepsilon_{i,k} \tag{5}$$

The heat transfer model (4) includes discrete differentiation operations. Thus if condition (6) is satisfied, then the discrete differentiation error reach great values.

$$T_{i,k+1} - T_{i,k} \approx \varepsilon_{i,k+1} - \varepsilon_{i,k} \tag{6}$$

For minimization of such error the difference between measured temperature values must be much greater than the difference between the corresponding errors:

$$T_{i,k+1} - T_{i,k} >> \varepsilon_{i,k+1} - \varepsilon_{i,k} \tag{7}$$

A robust estimation of absolute discretization error is given by (8) for time domain in accordance with [30, 38].

$$A_i = \frac{1}{\Delta t} \sum_{k=2}^{N-1} \left| T_{i,k+1} - 2T_{i,k} + T_{i,k-1} \right| \tag{8}$$

The relative error in time domain is given by (9):

$$E_t = \frac{1}{M} \sum_{i=1}^{M} \frac{A_i}{q \cdot \overline{T_i}} \tag{9}$$

where $\overline{T}_i$ is the discrete approximation of temperature integral given by (10) for time domain:

$$\overline{T_i} = \sum_{k=1}^{N} \left| T_{i,k} \right| \cdot \Delta t \tag{10}$$

The coefficient q is used for normalization of relative error in (9) and in the next formulae.

In spatial domain the absolute and relative errors are defined by expressions (11) and (12) respectively:

$$B_k = \frac{1}{\Delta x} \sum_{i=2}^{M-1} \left| T_{i+1,k} - 2T_{i,k} + T_{i-1,k} \right| \tag{11}$$

$$E_{x1} = \frac{1}{N} \sum_{k=1}^{N} \frac{B_k}{q \cdot \overline{T_k}} \tag{12}$$

where $\overline{T}_k$ is the discrete approximation of temperature integral given by (13) for spatial domain:

$$\overline{T_k} = \sum_{i=1}^{M} \left| T_{i,k} \right| \cdot \Delta x \tag{13}$$

The absolute error of second-order differentiation in spatial domain is defined by (14):

$$C_k = \frac{1}{\Delta x^2} \sum_{i=2}^{M-2} \left| (T_{i+2,k} - 2T_{i+1,k} + T_{i,k}) - (T_{i+1,k} - 2T_{i,k} + T_{i-1,k}) \right| \tag{14}$$

The corresponding relative error is given by (15):

$$E_{x2} = \frac{1}{N} \sum_{k=1}^{N} \frac{C_k}{q \cdot \overline{\Delta_i T_k}} \tag{15}$$

where $\overline{\Delta_i T_k}$ is the discrete approximation of integral of temperature derivative absolute value given by (16) for spatial domain:

$$\overline{\Delta_i T}_k = \sum_{i=2}^{M} \frac{\left| T_{i,k} - T_{i-1,k} \right|}{\Delta x} \cdot \Delta x \tag{16}$$

For an example, the discretization error estimation with the described technique is presented below for time-domain temperature dependence shown in Figure 2.

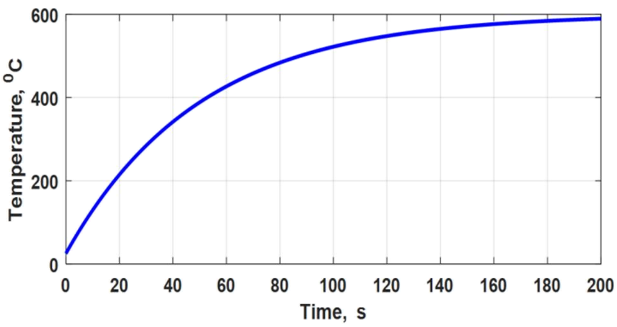

Figure 2 A sample temperature dependence of material layer

The temperature dependence (Figure 2) has the error range within 0.01°C. But Figure 3 shows that at different discretization frequencies such error can cause significant distortions of discrete derivative.

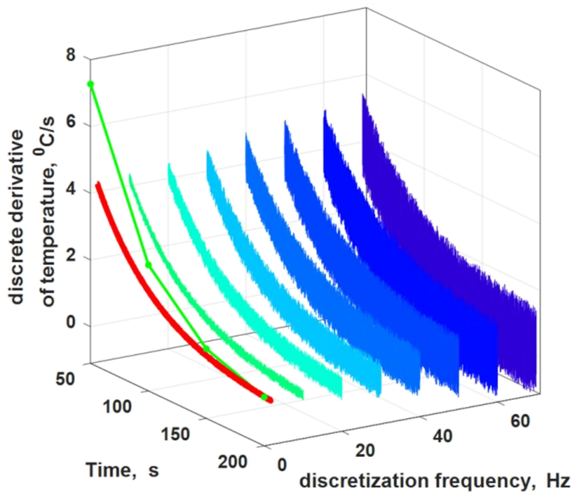

Figure 3 Discrete derivatives of the temperature dependence (Figure 2) at different discretization frequencies

The distortion of approximated temperature derivative curve at low discretization frequencies (first green line) is caused by great value of time step which leads to missing of many significant temperature values. At higher frequencies the error is caused mostly by discrete differentiation operations in accordance with the expression (6). Figure 4 shows the estimation (8) of time-domain absolute error A_i for the temperature dependence shown in Figure 2 at different discretization frequencies. The discrete differentiation error increases almost linearly with the discretization frequency. In accordance with the estimation, discretization error has a minimum near 1.76 Hz. This minimum corresponds to the red curve in Figure 3, which demonstrates the best accuracy of discrete temperature derivative fitting.

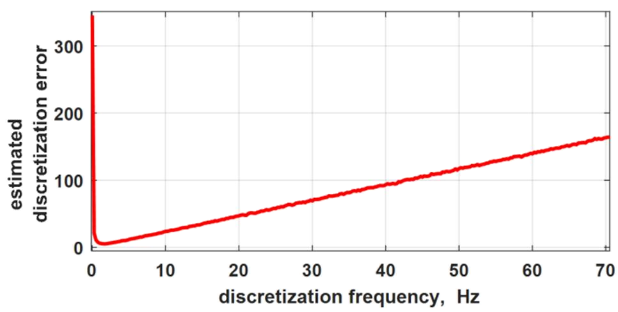

Figure 4 Estimation of discretization error

4 RESULTS

The estimation of thermal protection performance was performed for multilayer material with parameters presented in Table 1. The structure of presented multilayer material is shown in Figure 5 in accordance with Table 1.

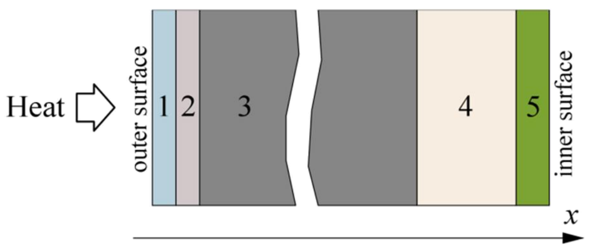

Figure 5 The structure of investigated multilayer material

In the modeling procedure the first temperature array is the experimental data obtained from measurement. The next dependencies are obtained due to the material layer properties with using of discrete model (4) for different temperatures of the outer surface. The proposed package of materials can be used to protect firefighters.

As the results of modeling, the temperature dependencies for outer and inner surfaces of the investigated material are shown in Figure 6.

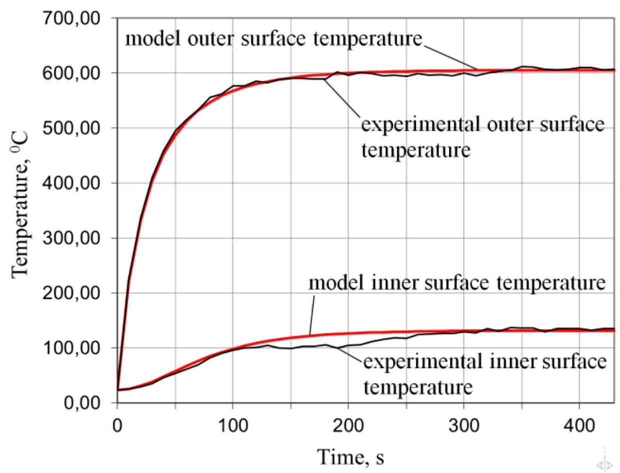

Figure 6 Temperatures at outer and inner surfaces under 800°C heat source temperature: black line - experimental data, red line - modeling results

Table 1 The parameters of thermal protective material layers

Layer	Material	Thickness [mm]	λ [W/m.K]	c [kJ/kg.K]	ρ [g/m^2]
1	Stainless steel wire mesh	0.5	204	0.921	1248
2	Metallized phenylon fabric	0.5	0.094	2.21	285
3	Non-woven carbon material	28	0.032	0.63	235
4	Woolen batting	4	0.061	2.42	495
5	Tarpaulin canvas	1	0.089	1.8	610

The model temperature values match with the experimental values. The maximum deviation of modeling results from experimental data is 4.73% due to small oscillations of measured temperature values shown in Figure 6. The slope of the inner surface temperature curve (Figure 6) from 100 s to 260 s is caused by moisture evaporation processes.

The heat transfer modeling results for all layers of material is shown in Figure 7 as a 3D graph.

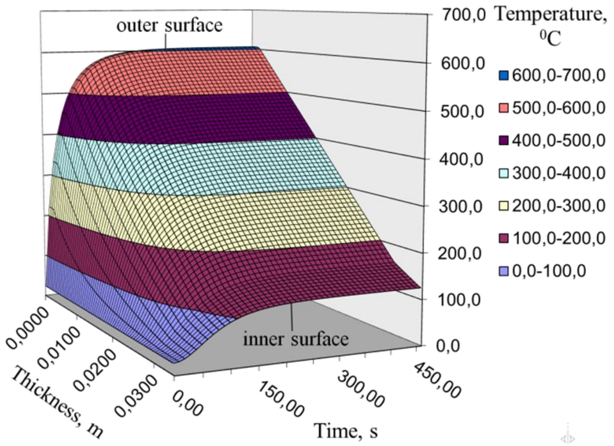

Figure 7 The heat transfer model for all layers

In accordance with the experiments' and modeling results the presented multilayer material has thermal protective properties shown in Table 2.

5 DISCUSSION

The described results show that presented multilayer material which consists of stainless steel wire mesh, metallized phenylon fabric, non-woven carbon material, woolen batting and tarpaulin canvas can be used for thermal protective clothing design.

The experiments' and modeling results show that in time domain heat transfer process can be divided into two periods. The first period corresponds to short-time thermal insulation capability and the second period shows the long-time thermal insulation capability of the proposed multilayer material.

As shown in Table 1, the short-time heat protection strongly depends on the heat source temperature. For 800°C heat source temperature this period is 32.8 s and for 500°C it increases to 60.4 s. The short-time heat protection depends on the speed of multilayer material response to the increase of outer surface temperature.

The long-time heat protection depends on the temperature of outer surface and provides slow temperature increase during a long time interval. If the outer surface temperature is less than 400°C then heat protection will be effective during more than 10 minutes.

Also it should be noted that the inner surface temperature increase curve has a slope from 100 s to 260 s (Figure 6) that is caused by moisture evaporation processes.

The presented modeling technique can be used in nondestructive testing of multilayer thermal insulation materials. The heat transfer modeling technique with discrete differentiation error estimation allows to avoid high discretization errors and errors which are caused by continuous function approximation operations.

The direction of future works is connected to development of discrete multilayer material modeling algorithms with automated minimization of errors that are caused by discretization of temperature data.

The other important purpose is the development of heat transfer modeling techniques which allow to describe the moisture evaporation and condensation processes at different material layers.

6 CONCLUSION

In this article we present the investigation of multilayer thermal protective material performance with using of discrete heat transfer model which is improved by discretization error estimation technique. The proposed model can be used in nondestructive testing of multilayer thermal protective materials.

The thermal protective properties of the presented multilayer material were obtained by laboratory experiments and confirmed by modeling on the base of discrete temperature dependencies' processing. In accordance with the obtained results the described multilayer material can be used for thermal protective clothing design. The proposed package of materials can be used to protect firefighters.

Table 2 Thermal protective material properties

Thermal protective properties	Heat source temperature [°C]				
	400	500	600	700	800
Time to reach 37°C temperature at the inner surface (seconds).	-	60.4	40.3	34.3	32.8
Time to reach 40°C temperature at the inner surface (seconds)	-	351.5	60.4	50.2	45.4
Difference between time to reach 37°C and time to reach 50°C temperature at the inner surface (seconds)	-	291.1	20.1	15.9	12.6
Inner surface temperature after 10 seconds heating time (°C)	20.6	20.9	21.6	22.5	24.1

7 REFERENCES

1. Song G., Mandal S., Rossi R.M.: Thermal protective clothing for firefighters, 1st ed., Woodhead Publishing, 2016, 242 p., ISBN: 9780081012857
2. Mandal S., Song G.: Characterizing thermal protective fabrics of firefighters' clothing in hot surface contact, Journal of Industrial Textiles 47(5), 2018, pp. 622-639, https://doi.org/10.1177/1528083716667258
3. Kothari V.K., Chakraborty S.: Thermal protective performance of clothing exposed to radiant heat, The Journal of The Textile Institute 106(12), 2015, pp. 1388-1393, https://doi.org/10.1080/00405000.2014.995929
4. He J., Wang M., Li J.: Determination of the thermal protective performance of clothing during bench-scale fire test and flame engulfment test: Evidence from a new index, Journal of Fire Science 33(3), 2015, pp. 218-231, https://doi.org/10.1177/0734904115581620
5. Kothari V.K., Chakraborty S.: Protective performance of thermal protective clothing assemblies exposed to different radiant heat fluxes, Fibers and Polymers 17(5), 2016, pp. 809-814, https://doi.org/10.1007/s12221-016-5656-z
6. Zhiying C., Yanmin W., Weiyuan Z.: Thermal protective performance and moisture transmission of firefighter protective clothing based on orthogonal design, Journal of Industrial Textiles 39(4), 2010, pp. 347-356, https://doi.org/10.1177/1528083709347126
7. Fu M., Yuan M.Q., Weng W.G.: Modeling of heat and moisture transfer within firefighter protective clothing with the moisture absorption of thermal radiation, International Journal of Thermal Science 96, 2015, pp. 201-210, https://doi.org/10.1016/j.ijthermalsci.2015.05.008
8. Liu S., Liu Z., E Bai X.: Comparative analysis of fibers for thermal protective clothing, Advanced Materials Research 627, 2013, pp. 29-32, https://doi.org/10.4028/www.scientific.net/AMR.627.29
9. Udayraj, Talukdar P., Das A., Alagirusamy R.: Heat and mass transfer through thermal protective clothing - A review, International Journal of Thermal Science 106, 2016, pp. 32-56, https://doi.org/10.1016/j.ijthermalsci.2016.03.006
10. Udayraj, Talukdar P., Das A., Alagirusamy R.: Simultaneous estimation of thermal conductivity and specific heat of thermal protective fabrics using experimental data of high heat flux exposure, Applied Thermal Engineering 107, 2016, pp. 785-796, https://doi.org/10.1016/j.applthermaleng.2016.07.051
11. Mandal S., Song G.: An empirical analysis of thermal protective performance of fabrics used in protective clothing, The Annals of Occupational Hygiene 58(8), 2014, pp. 1065-1077, https://doi.org/10.1093/annhyg/meu052
12. Onofrei E., Petrusic S., Bedek G., et al.: Study of heat transfer through multilayer protective clothing at low-level thermal radiation, Journal of Industrial Textiles 45(2), 2015, pp. 222-238, https://doi.org/10.1177/1528083714529805
13. Fu M., Weng W.G., Yuan H.Y.: Quantitative assessment of the relationship between radiant heat exposure and protective performance of multilayer thermal protective clothing during dry and wet conditions, Journal of Hazardous. Materials 276, 2014, pp. 383-392, https://doi.org/10.1016/j.jhazmat.2014.05.056
14. Yuan B., Ding S., Wang D., Wang G., et al.: Heat insulation properties of silica aerogel/glass fiber composites fabricated by press forming, Materials Letters 75, 2012, pp. 204-206, https://doi.org/10.1016/j.matlet.2012.01.114
15. Brendel H., Seifert G., Raether F.: Determination of thermal diffusivity of fibrous insulating materials at high temperatures by thermal wave analysis, International Journal of Heat and Mass Transfer 108, Part B, 2017, pp. 2514-2522, https://doi.org/10.1016/j.ijheatmasstransfer.2017.01.063
16. Xu J.Y., Sun Y.C., Li X.X., Chen R.X.: Influence of layer configuration on protecting effect of thermal protective clothing containing PCM, Advanced Materials Research 796, 2013, pp. 639-642, https://doi.org/10.4028/www.scientific.net/AMR.796.639
17. Bahadori R., Gutierrez H., Manikonda S., Meinke R.: Two-dimensional transient heat conduction in multi-layered composite media with temperature dependent thermal diffusivity using floating random walk Monte-Carlo method, International Journal of Heat and Mass Transfer 115, Part A, 2017, pp. 570-580, https://doi.org/10.1016/j.ijheatmasstransfer.2017.07.071
18. Bozzoli F., Mocerino A., Rainieri S., Vocale P.: Inverse heat transfer modeling applied to the estimation of the apparent thermal conductivity of an intumescent fire retardant paint, Experimental Thermal and Fluid Science 90, 2018, pp. 143-152, https://doi.org/10.1016/j.expthermflusci.2017.09.006
19. Tian M., Wang Z., Li J.: 3D numerical simulation of heat transfer through simplified protective clothing during fire exposure by CFD, International Journal of Heat and Mass Transfer 93, 2016, pp. 314-321, https://doi.org/10.1016/j.ijheatmasstransfer.2015.09.027
20. Hossain M.M. (Ed.): Heat and Mass Transfer - Modeling and Simulation, InTech, 2011, DOI: 10.5772/1431, ISBN: 978-953-307-604-1
21. Dorfman A.S.: Applications of Mathematical Heat Transfer and Fluid Flow Models in Engineering and Medicine, ASME Press and John Wiley & Sons, Ltd, 2017, ISBN: 978-1-119-32056-2
22. Bec J.V., Woodbury K.A.: Inverse heat conduction problem: Sensitivity coefficient insights, filter coefficients, and intrinsic verification, International Journal of Heat and Mass Transfer 97, 2016, pp. 578-588, https://doi.org/10.1016/j.ijheatmasstransfer.2016.02.034
23. Haddad H., Guessasma M., Fortin J.: Heat transfer by conduction using DEM-FEM coupling method, Computational Materials Science 81, 2014, pp. 339-347, https://doi.org/10.1016/j.commatsci.2013.08.033

24. Danko G.L.: Model Elements and Network Solutions of Heat, Mass and Momentum Transport Processes, Springer-Verlag, 2017, 251 p., DOI:10.1007/978-3-662-52931-7, ISBN: 978-3-662-52929-4
25. Nikiforakis N.: Computational Fluid Mechanics and Heat Transfer. Journal of Fluid and Mechanics 428, 2001, pp. 409-410, https://doi.org/10.1017/S0022112000003049
26. Abhishek K., Leyffer S., Linderoth J.T.: Modeling without categorical variables: A mixed-integer nonlinear program for the optimization of thermal insulation systems, Optimization and Engineering 11, 2010, pp. 185-212, https://doi.org/10.1007/s11081-010-9109-z
27. Kaveh Hariri Asli, Soltan Ali Ogli Aliyev: Fluid Mechanics and Heat Transfer: Advances in Nonlinear Dynamics Modeling, 1st ed. Apple Academic Press, 2015, 250 p., ISBN: 978-1771880848
28. Croft D.R., Lilley D.G.: Heat Transfer Calculations Using Finite Difference Equations, Elsevier Science & Technology, 1977, 283 p., ISBN: 978-0853347200
29. Langtangen H.P.: Finite Difference Computing with Exponential Decay Models, Springer International Publishing, 2016, 200 p., ISBN: 978-3-319-29438-4, DOI: 10.1007/978-3-319-29439-1
30. Niesen J.: On the Global Error of Discretization Methods for Ordinary Differential Equations, disertation thesis, University of Cambridge, 2004
31. Rangavajhala S., Sura V.S., Hombal V.K., Mahadevan S.: Discretization error estimation in multidisciplinary simulations, AIAA Journal 49(12), 2011, pp. 2673-2683, https://doi.org/10.2514/1.J051085
32. Ghattassi M., Roche J.R., Asllanaj F., Boutayeb M.: Galerkin method for solving combined radiative and conductive heat transfer, International Journal of Thermal Sciences 102, 2016, pp. 122-136, https://doi.org/10.1016/j.ijthermalsci.2015.10.011
33. Grady L.J., Polimeni J.R.: Discrete calculus: Applied Analysis on Graphs for Computational Science, Springer-Verlag London, 2010, 366 p., ISBN: 978-1-84996-289-6, DOI: 10.1007/978-1-84996-290-2
34. Langtangen H.P., Linge S.: Finite Difference Computing with PDEs. A Modern Software Approach, Springer International Publishing, 2017, 507 p., ISBN: 978-3-319-55455-6, DOI: 10.1007/978-3-319-55456-3
35. Roy C.J., Sinclair A.J.: On the generation of exact solutions for evaluating numerical schemes and estimating discretization error, Journal of Computational Physics 228, 2009, pp. 1790-1802., https://doi.org/10.1016/j.jcp.2008.11.008
36. Sarkar D., Jain A., Goldstein R.J., Srinivasan V.: Corrections for lateral conduction error in steady state heat transfer measurements, International Journal of Thermal Science 109 2016, pp. 413-423, https://doi.org/10.1016/j.ijthermalsci.2016.05.031
37. Celik I.B., Parsons D.R.: Prediction of discretization error using the error transport equation, Journal of Computational Physics 339, 2017, pp. 96-125, https://doi.org/10.1016/j.jcp.2017.02.058
38. Roy C.: Review of Discretization Error Estimators in Scientific Computing, 48th AIAA Aerospace Sciences Meeting Including the New Horizons Forum and Aerospace Exposition, 4-7 January 2010, Orlando, Florida, https://doi.org/10.2514/6.2010-126
39. Udayraj, Talukdar P., Das A., Alagirusamy R.: Estimation of radiative properties of thermal protective clothing, Applied Thermal Engineering 100 2016, pp. 788-797, https://doi.org/10.1016/j.applthermaleng.2016.02.088
40. Jiang Y.Y., Yanai E., Nishimura K., et al.: An integrated numerical simulator for thermal performance assessments of firefighters' protective clothing, Fire Safety Journal 45(5), 2010, pp. 314-326, https://doi.org/10.1016/j.firesaf.2010.06.003
41. Pignon B., Sobotka, V. Boyard N., Delaunay D.: Improvement of heat transfer analytical models for thermoplastic injection molding and comparison with experiments, International Journal of Heat and Mass Transfer 118, 2018, pp. 14-26, https://doi.org/10.1016/j.ijheatmasstransfer.2017.09.078
42. Gaetano A., Roncolato J., Montorfano D., et al.: Optimization by means of an analytical heat transfer model of a thermal insulation for CSP applications based on radiative shields, AIP Conference Proceedings 1734(1), 2016, https://doi.org/10.1063/1.4949067
43. Sidebotham G.: Heat Transfer Modeling. An Inductive Approach, Springer International Publishing, 2015, 516 p., ISBN: 978-3-319-14513-6, DOI: 10.1007/978-3-319-14514-3
44. Yan G., Ollivier-Gooch C.F.: Accuracy of discretization error estimation by the error transport equation on unstructured meshes, 53rd AIAA Aerospace Sciences Meeting, 5-9 January 2015, Kissimmee, Florida, https://doi.org/10.2514/6.2015-1264

RESEARCH OF THE INFLUENCE OF THE TREATMENT PROCESS OF THREE-CONE PACKING ON CRITICAL SPEEDS OF BOBBIN HOLDER OF THE WINDING MACHINE

B.S. Zavertannyi[1], O.O. Akymov[2], O.P. Manoilenko[1], M.A. Zenkin[3], Y.A. Kovalev[1] and S.A. Pleshko[1]

[1]*Kyiv National University of Technology and Design, Nemirovich-Danchenko st. 2, 01011 Kyiv, Ukraine*
[2]*State Research Institute for Testing and Certification of Arms and Military Equipment, Streletska Street 1, 14033 Chernihiv, Ukraine*
[3]*The National Technical University of Ukraine "Igor Sikorsky Kyiv Polytechnic Institute", Prosp. Peremohy 37, 03056 Kyiv, Ukraine*
botanuga@ukr.net, akimov.al.al@gmail.com, manojlenko.op@knutd.com.ua, nikolay_zenkin@ukr.net, kovalev-yri2012@yandex.ua, pleshko-s-a@ukr.net

Abstract: *The algorithm of critical speeds calculation of the winding mechanism with the account of three-cone packing was presented in the work. Computer simulation of the bobbin holder critical speeds of the winding mechanism in the process of packing is carried out. Dependences of change of critical speeds on the thickness of the packing and the angles of the generators inclination were obtained. Recommendations for designing new designs of winding mechanisms are given. The practical importance of the work is to determine the working speed of the equipment for rewinding threads, improving productivity, product quality. The use of the results obtained in the design and dynamic study accelerate the design process of rewinding equipment. The results are aimed at intensifying the rewinding and winding processes in the light industry.*

Keywords: *bobbin, critical winding speeds, bobbin holder, resonance, winding mechanism.*

1 INTRODUCTION

In today's realities, for the rapid pace of development of textile goods industrial production, there is a need to carry out on a large-scale research, design and practical work on the creation of new and improved equipment.

Textile processing plays a major role in the rewinding of yarns at the packaging level. Bobbin holders are intended for placement, alignment, retention of the thread carrier and transfer to it of rotation, which are applied on molding, reeling-exhausting, winding machines, rewinding machines, machines for receiving textured threads.

The rewinding process is one of the main stages of preparing the yarn, or yarn, for further processing. During rewinding, the quality of the thread obtained is monitored, different levels and densities of the packing length are developed, which requires increasing a number of requirements, especially with the introduction of new high-speed methods and mechanisms for producing the filaments. Therefore, a large number of light industry enterprises are equipped with cross-winding machines and automatic machines [1-3]. Along with rewinding machines, a similar design of the winding mechanism is used in winding machines [3]. Rewinders are very widely used in the weaving industry, in knitwear, ribbon. During operation of the winding mechanisms, there are a number of problems; the main is to limit the speed of rewinding, which leads to a decrease in equipment performance.

Increasing the speed of rewinding threads requires an increase in the spindle speed, which makes it necessary to calculate and analyze its critical speeds. Increasing the spindle speed is accompanied by an increase in the mechanism's vibration activity, which is important to take into account when upgrading the equipment and developing a new one [4], which also helps to reduce costs at the design stage. In this regard, there is a need to perform the simulation of winding processes on rewinding machines in order to analyze the critical spindle speeds. In [5, 6] the authors considered the dynamics of the movement of the thread and the winding drum, but did not pay attention to the oscillations of the winding mechanism. The conditions of thread movement are considered in detail. However, the critical speeds of the winding mechanism that affect the performance of the rewinding machine have not been determined.

Setting objectives. The purpose of the study is to develop an algorithm for calculating the critical and operating speeds of winding mechanisms of rewinding machines. Also, providing recommendations for improving the operating speed of equipment and the ability to use the results obtained in the design and dynamic study of rewinding equipment.

Objects and methods of research. The object of the study is the process of rewinding the bobbin thread. The subject of the study is the critical speed of the winding mechanisms. The known methods of analysis of natural frequencies of oscillations of spindles are applied in the work. The semi-rigid spindle method is based on the assumption that only the bobbin holder shaft is resilient, and the bobbin holder itself is considered to be absolutely rigid.

2 THEORETICAL SUBSTANTIATION

When designing high-speed winding mechanisms for winding textile threads on a bobbin, the values of the oscillation frequency and critical speed parameters that limit the range of working speeds of the rotors of the mechanisms are required.

One of the technical solutions is the use of a flexible shaft and the use of elastic supports in rewinding machines [4], which provides the necessary position of the range of operating speeds of equipment relative to critical speeds.

When calculating the critical velocities of bobbin holders, which have non-cylindrical elements in their composition, leads to significant errors in the calculation of the inertial parameters of the moving masses [4].

For practical calculations of the critical speeds of the winding mechanisms of textile machines, the method of "Semi-rigid spindle" is most widely used, which makes it possible to obtain two critical speeds of the winding rotor with an error not exceeding 10% [4, 7].

To determine the inertial parameters of the mandrel of the bobbin holder, it is divided into a number of simple elements Mi (cylindrical and conical shape). Thereby, the bobbin holder of the winding mechanism is formed by two conical elements (the bobbin locking mechanism, a conical thread carrier and a three-conical packing).

To simplify the calculation process and uniquely designate geometric parameters, all elements are considered conical. The appearance of the conical element and the designation of its main dimensions are shown in Figure 1.

The element on the plane is determined by the coordinates of the beginning and end of the element from the front support of the bobbin holder, hci - the coordinate of the position of the center of mass of the i-th element; ri, rvi, Ri, Rvi - the radii of a conic and i-th element.

In order to determine the effect of packing mass in the process of its accumulation on the critical velocity values, it is necessary to determine the mass-inertial parameters of the packing as a function of the thickness of the packing body.

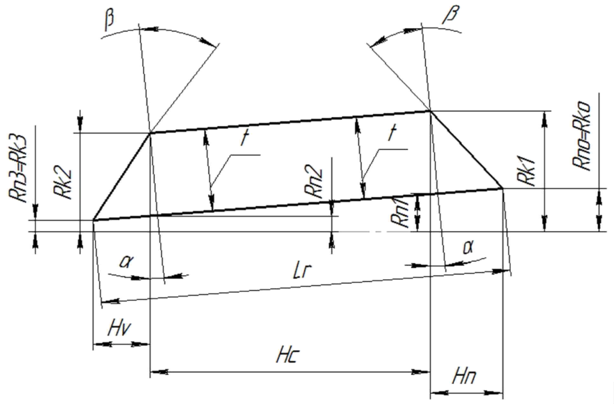

Figure 1 Geometric parameters of the packing section: $Rno, Rn1, Rn2, Rn3$ - the inner radii of cones; $Rko, Rk1, Rk2, Rk3$ - the outer radii of the cones; α - the angle of the cone of packing; β - the winding angle; t - is the thickness of the winding body; Lr - length of layout; Hv, Hc, Hn - the lengths of the upper, middle and lower sections of the packing respectively.

The relationship between the geometric dimensions of the package and the thickness of the winding body is determined by the ratios:

- length of packing areas [m]:

$$H_n = t \cdot (tg\alpha + tg\beta) \cdot \cos\alpha$$
$$H_v = t \cdot (tg\beta - tg\alpha) \cdot \cos\alpha \qquad (1)$$
$$H_c = Lr \cdot \cos\alpha - H_v - H_n$$

- packing cones radii [m]:

$$R_{n1} = R_{n0} - H_n \cdot tg\alpha$$
$$R_{k1} = R_{n1} + \frac{t}{\cos\alpha}$$
$$R_{n3} = R_{n0} - Lr \cdot \sin\alpha$$
$$R_{k3} = R_{n3} \qquad (2)$$
$$R_{k2} = R_{n3} + \frac{H_v}{tg(\beta - \alpha)}$$
$$R_{n2} = R_{k2} - \frac{t}{\cos\alpha}$$

- distance from the support to the items received [m]:

$$H_1 = H_0 + H_n$$
$$H_2 = H_1 + H_c \qquad (3)$$
$$H_3 = H_2 + H_v$$

Taking into account the parameters of the elements and dependencies (2, 3), the inertial parameters of the bobbin holder and the packing are determined from [8, 9]:

- is the volume of the i-th element of the bobbin holder Vi [m^3]:

$$V_i = \frac{\pi}{3} \cdot (X_{ki} - X_{ni}) \cdot \begin{bmatrix} \left[(R_i)^2 - (R_{vi})^2\right] + \\ + (R_i \cdot r_i - R_{vi} \cdot r_{vi}) + \left[(r_i)^2 - (r_{vi})^2\right] \end{bmatrix} \quad (4)$$

- mass of the bobbin holder Mo [kg]:

$$M_o = \sum_i V_i \cdot \rho_i \quad (5)$$

where ρi - the density of the material of the element.

- the coordinate of the position of the center of mass of the i-th element of the bobbin holder hci support [m]:

$$h_{ci} = \frac{\pi}{12} \cdot \frac{(X_{ki} - X_{ni})^2}{V_i} \cdot \begin{bmatrix} 3\left[(R_i)^2 - (R_{vi})^2\right] + \\ + 2(R_i \cdot r_i - R_{vi} \cdot r_{vi}) + \\ + \left[(r_i)^2 - (r_{vi})^2\right] \end{bmatrix} \quad (6)$$

- the coordinate of the position of the center of mass of the i-th element relative to the Xci support [m]:

$$X_{ci} = X_{ki} - h_{ci} \quad (7)$$

- polar moment of inertia of the coil holder Co [kg.m^2]:

$$C_o = \sum_i \frac{\pi}{10} \cdot M_i \cdot \frac{(X_{ki} - X_{ni})}{V_i} \cdot \begin{bmatrix} R_i \cdot (R_i + r_i) \times \\ \times \left[(R_i)^2 + (r_i)^2\right] + \\ + \left[(r_i)^4 - (r_{vi})^4\right] - \\ - R_{vi} \cdot (R_{vi} + r_{vi}) \times \\ \times \left[(R_{vi})^2 + (r_{vi})^2\right] \end{bmatrix} \quad (8)$$

where - Mi is the mass of the i-th element of the bobbin holder.

- moment of inertia of the element of the bobbin holder Ac [kg.m^2]:

$$A_c = \frac{1}{2} \cdot C_o + \sum_i M_i \cdot \begin{bmatrix} \frac{\pi}{30} \cdot \frac{(X_{ki} - X_{ni})^3}{V_i} \times \\ \times \begin{bmatrix} 6\left[(R_i)^2 - (R_{vi})^2\right] + \\ + 3(R_i \cdot r_i - R_{vi} \cdot r_{vi}) + \\ + \left[(r_i)^2 - (r_{vi})^2\right] \end{bmatrix} - \\ - (h_{ci})^2 \end{bmatrix} \quad (9)$$

- coordinate position of the mass center of the bobbin holder Hcm [m]:

$$H_{cm} = \frac{\sum_i M_i \cdot X_{ci}}{M_o} \quad (10)$$

- the equatorial moment of inertia of the bobbin holder Ao [kg.m^2]:

$$A_o = A_c + \sum_i M_i \cdot (H_{cm} - h_{ci})^2 \quad (11)$$

Impact coefficients are determined similarly [2, 4, 10]:

$$\delta_{11} = \frac{l_1 \cdot H_{cm}^2}{3E \cdot I_1} + \frac{a^2 \cdot (l_5 + 3l_3) + l_3^2 \cdot (l_3 + 3a)}{3E \cdot I_2}$$

$$\delta_{12} = \frac{l_1 \cdot H_{cm}}{3E \cdot I_1} + \frac{2a \cdot (l_5 + 3l_3) + 3l_3^2}{6E \cdot I_2} \quad (12)$$

$$\delta_{22} = \frac{l_1}{3E \cdot I_1} + \frac{l_5 + 3l_3}{3E \cdot I_2}$$

where l_1 - the length between the supports [m]; Hcm – the length from the front support to the center of mass [m]; $l3$ - the distance from the front support to the rear cone [m]; $l5$ - the distance between the front and rear cones [m]; E - modulus of elasticity (for Steel 45 E = 2 × 1011 N/m^2); a - the distance between the rear cone of the bobbin holder and its center of mass.

$$a = H_{cm} - l_3 \quad (13)$$

The mathematical model of free oscillations of the bobbin holder with supports has the following form [4, 7, 11, 12]:

$$\begin{cases} M\ddot{\eta} + m_{1\eta}\eta - m_{2\eta}\alpha = 0, \\ M\ddot{\zeta} + m_{1\zeta}\zeta - m_{2\zeta}\beta = 0, \\ A\ddot{\alpha} + C\dot{\beta} \cdot \omega - m_{2\eta}\eta + m_{3\eta}\alpha = 0, \\ A\ddot{\beta} - C\omega \cdot \dot{\alpha} - m_{2\zeta}\zeta + m_{3\zeta}\beta = 0. \end{cases} \quad (14)$$

where - M, A, C- inertial parameters of the bobbin holder; $\varphi, \eta, \zeta, \alpha, \beta$ - generalized coordinates [4]; $m_{1\eta}$, $m_{2\eta}$, $m_{3\eta}$, $m_{1\zeta}$, $m_{2\zeta}$, $m_{3\zeta}$ - coefficients of rigidity of the mechanical system in the horizontal and vertical directions.

3 THE SOLVING OF THE PROBLEM

The critical velocities based on the expressions given in [4] are determined from the problem on the natural vibrational frequencies with the matrix:

$$(M - iC)\overline{x} = \lambda K\overline{x} \quad (15)$$

where $\lambda = 1/\omega^2$, M - the matrix of inertial coefficients; C - the matrix of gyroscopic coefficients; K - the stiffness matrix.

Finding the values of the self-oscillations leads to the solution of the standard problem:

$$A\overline{y} = \lambda\overline{y} \quad (16)$$

Matrix of inertial coefficients:

$$M = diag(M_0, M_0, A_0, A_0) \quad (17)$$

The stiffness and gyroscopic coefficient matrices have the following form:

$$K = \begin{vmatrix} m_{1x} & 0 & -m_{2x} & 0 \\ 0 & m_{1y} & 0 & -m_{2y} \\ -m_{2x} & 0_1 & m_{3x} & 0 \\ 0 & -m_{2y} & 0 & m_{3y} \end{vmatrix}$$

$$C = \begin{vmatrix} 0000 \\ 0000 \\ 000C \\ 00C0 \end{vmatrix} \quad (18)$$

Substituting the input parameters and taking [13] into the program, the values of the critical velocities are given, which are given in Table 1.

Table 1 The values of the critical velocities

Marking		Critical speed values [rad/s]
During the start of the winding process	ω1 [s $^{-1}$]	683
	ω2 [s $^{-1}$]	7064
During the winding process	ω1 [s $^{-1}$]	334
	ω2 [s $^{-1}$]	5116

The value of the reduction of the first critical velocity in the packing process ranges from 683 rad/s to 334 rad/s. The value of the reduction of the second critical speed in the packing process is from 7064 rad/s to 5116 rad/s and is of no practical importance. The area of the working range of the winding speed of the filament must be up to the first critical speed, which ensures the receipt of quality packaging, uninterrupted operation of the winding mechanism.

The upper limit of the first operating angular velocity of the bobbin holder ω_p is defined by the following expression [10]:

$$\omega_p = 0.7 \cdot \omega_1$$

$$\omega_p = 0.7 \cdot 683 = 478\ s^{-1} \quad (19)$$

The maximum speed of the rewinding speed of the thread V [m/s]:

$$V = \omega_1 \cdot Rnc \quad (20)$$

where - Rnc is the average radius of conical packing [m] (for the machine BP-340 $Rnc = 0.031$ m).

$V = 478 \cdot 0.031 = 14.8\ m/s.$

The results of modeling the dependence of the first critical velocity on the thickness of the winding body are presented graphically in Figure 2. Figure 3 shows the dependence of the first critical speed on the thickness of the winding body at different winding angles.

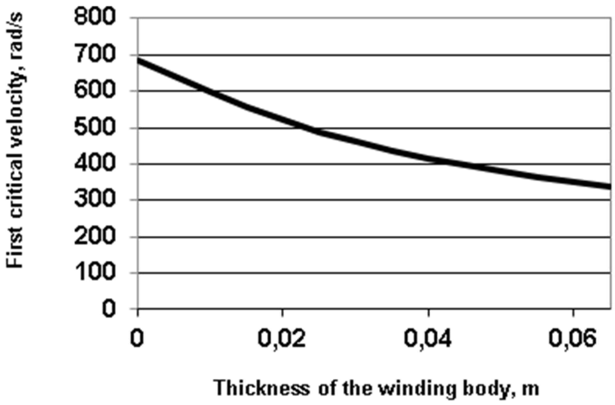

Figure 2 Dependence of the first critical velocity on the thickness of the winding body

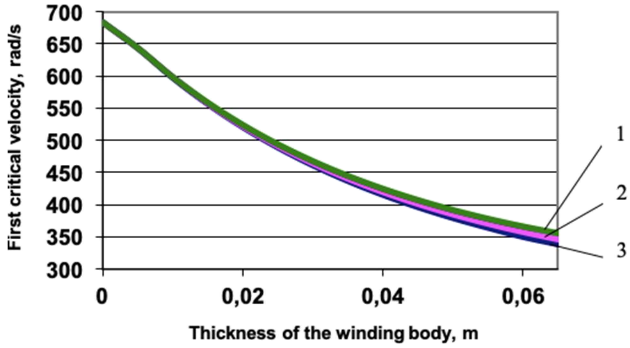

Figure 3 Dependence of the first critical velocity on the thickness of the winding body at different winding angles, 1 - 45°; 2 - 40°; 3 - 35°

The maximum speed of rewinding of threads for nylon fibers, achieved at the production, is 10.6 m/s [14].

The calculation shows that the working area of the bobbin holder is limited to the top angular speed of 478 rad/s. According to Figure 3, the value of the critical velocity changes with the change in the winding angle. This is due primarily to the change in the mass-inertia parameters of the packing and the design of the bobbin holder in general.

In order to facilitate the transition from the critical region to the working area of the speed of the bobbin holder, it is confirmed the expediency of using elastic supports of fastening of the spindle of the bobbin holder, which allows to increase the value of critical speeds, as well as to facilitate the transition through the critical speeds of rotation [10]. It is advisable to use an elastic shaft when designing winding mechanisms.

4 CONCLUSIONS

The method of calculation of the critical speeds of the winding mechanism with three-conical packing is presented in the work, the critical speeds of the process of winding the thread on the example of the BP-340 machine are determined. The analysis of the obtained results showed the possibility of increasing the operating speed of the equipment by 28%. The above calculation method allows to obtain the necessary results of critical velocity values by varying the materials of individual parts at the design stage, which facilitates the design stages of typical equipment.

5 REFERENCES

1. Akimov O.O., Manoilenko O.P., Zavertanniy B.S.: Ukrainian Patent UA 136674 U, B65H 54/00. A device for winding threads into bobbins, No. u201902866, publ. 08/27/2019, Bull. No. 16/2019
2. Zhmyhov I.N., Gal'brajh L.S., Akulich A.V.: Processes and equipment for the production of fibrous and film materials (Processy i oborudovanie proizvodstva voloknistyh i plenochnyh materialov), Higher school, 2013 (in Russian)
3. Regel'man E.Z., Rokotov N.V.: Reception mechanisms of machines for the production of chemical fibers (Priemnye mekhanizmy mashin dlya proizvodstva himicheskih volokon), Leningrad University Publishing House, 1988 (in Russian)
4. Ivanova T.P.: Technology and equipment for the preparation of threads for weaving: educational-methodical complex (Tekhnologiya i oborudovanie dlya podgotovki nitej k tkachestvu: uchebno-metodicheskij kompleks), UO «VGTU», Vitebsk, 2008 (in Russian)
5. Yakubitskaya I.A., Chugin V.V., Shcherban' V.Yu.: Dynamic analysis of the traversing conditions at the end sections of the groove in a winding drum, Izvestiya Vysshikh Uchebnykh Zavedenii (Technology of Textile Industry) 5, 1997, pp.33-36
6. Yakubitskaya I.A., Chugin V.V., Shcherban' V.Yu.: Differential equations for relative yarn movement in the end sections of the channel in the winding drum, Izvestiya Vysshikh Uchebnykh Zavedenii. (Technology of Textile Industry) 6, 1997, pp.50-54
7. Koritysskij Ya.I.: The dynamics of elastic systems of textile machines (Dinamika uprugih sistem tekstil'nyh mashin), Light and food industry, 1982 (in Russian)
8. Bat' M.I. et al.: Theoretical mechanics in examples and problems, vol. III (special chapters of mechanics) (Teoreticheskaya mekhanika v primerakh I zadachakh, t. III (spetsial'nye glavy mekhaniki)), training manual, The main editorial office of the physical and mathematical literature «Nauka», 1973 (in Russian)
9. Bashmetov V.S. et al.: Technology and equipment for the preparation of threads for weaving: training manual (Tekhnologiya i oborudovanie dlya podgotovki nitey k tkachestvu: uchebnoe posobie), Vitebsk: UO «VGTU» 2009 (in Russian)
10. Favorin M.V.: The moments of inertia of bodies. Reference book, (Momenty inertsii tel. Spravochnik), M.M. Gernet (Ed.), 2nd ed, „ Mechanical Engineering", 1977 (in Russian)
11. Chelomey V.N.: Vibrations in technology: A Manual, chapter 3: Vibrations of machines, structures and their elements (Vibratsii v tekhnike: Spravochnik. Mashinostroenie, T. 3 Kolebaniya mashin, konstruktsiy i ikh elementov), Dimentberg F.M., Kolesnikov K.S. (Eds), 1980 (in Russian)
12. Proshkov A.F.: Calculation and design of machines for the production of chemical fibers (Raschet I proektirovanie mashin dlya proizvodstva himicheskih volokon), textbook for students, Light and food industry, 1982 (in Russian)
13. Anisenko A.O.: Critical speeds of the bobbin holder with the three-conical packing of the BP–340 rewinding machine (Kritichni shvidkosti bobinotrimacha z tr'ohkonusnim pakuvannyam bobinazhno-peremotuval'noï mashini BP–340), thesis for advanced study of sciences, 27-28 May, 2011, CHDTU, Chernigiv, 2011 (in Ukraine)
14. Koroteeva L.I., et al.: Technological equipment of chemical yarn and fiber plants: a textbook (Tekhnologicheskoe oborudovanie zavodov khimicheskikh nitey i volokon: uchebnik), Publishing house "Legprombytizdat", 1987 (in Russian)

PARAMETRIZATION OF THE HIERARCHICAL STRUCTURE OF THE TREE OF PILLS EMERGENCE DURING PILLING FORMATION ON TEXTILE MATERIALS

Tetyana Zhylenko[1], Oksana Zakharkevich[2], Julia Koshevko[2] and Svitlana Kuleshova[2]

[1]Sumy State University, Department of Mathematical Analysis and Optimization Methods, 2 Rymskogo-Korsakova st., 40007 Sumy, Ukraine
[2]Khmelnytskyi National University, Department of Technology and Design of Garments, 11 Institytska st., 29016 Khmelnytskyi, Ukraine
t.zhylenko@phe.sumdu.edu.ua; zbir_vukladach@ukr.net; juliakoshevko@gmail.com; kuleshova_lana@ukr.net

Abstract: *The article deals with the development of a mathematical description of the distribution of pills on the surface of textile material, which will predict the change in aesthetic performance of the product during wearing by visualizing its appearance taking into account the surface characteristics of the fabric used. This, in turn, will facilitate the process of confection of materials in the manufacture of products that will not lose their appearance for a long time, and will encourage consumers to comply with the requirements of conscious fashion. The research has been conducted on the fabrics of the coat group, the raw materials of which are: lavsan, kapron; lavsan, nitron; wool, lavsan, nitron. In the process of research, it has been found out that under the action of wear factors for a short time the most probable is the formation of a cluster structure of the hierarchical tree of pills, which have a high branching. With the increasing time of the influence of factors formation of a weakly branched structure a pills' tree is again likely to occur.*

Keywords*: fabric, hierarchical structure, pilling, pills.*

1 INTRODUCTION

In the conditions of the growing public interest in sustainable development technologies, and as a consequence - the desire to extend the life of garments, a necessary condition for their design is the durability of materials and their appearance preservation over a long period of time.

One of the characteristics of textile materials that can significantly spoil the general look of the product is pilling [1]. Pilling is the tendency of the fabric to form on its surface loose balls of tangled fibers (pills), as a result of the product wearing. Therefore, this property is especially important for materials used for the manufacture of products with extended service life, namely: products-transformers, modular clothing (clothing-designer), which are developed within the concept of slow (conscious) fashion.

2 DISCUSSION OF IDEAS

The interest of world textile manufacturers in the problem of pilling is confirmed by a large number of studies of the process of pills formation [2, 3, 6-15], especially on the surface of knitted fabrics [1, 2, 9, 12, 14], as well as the development of special coatings and specific treatments of yarn and canvases that suspend the process of pilling on the surface of the canvas [7]. Laboratory tests only partially reproduce the processes of material wear from abrasion, which are observed during exploitation of the product [2]. Therefore, a significant amount of research is devoted to the development of new and improved methods for determining and estimation of pilling, which are mostly based on standard methods [4] and/or based on the use of computer technology applying photographic images of samples of materials after testing [8, 10, 11].

The essence of the standard method for determining pilling is the formation of hairiness on the fabric, and then pills, followed by counting the maximum number of pills on a certain area of the fabric. The test is carried out in two stages: the first is the formation of hairiness; the second is the formation of pills. Using a dissecting needle, the number of pills is counted. In this case, the test surface of the fabric is illuminated with a beam of light obliquely directed from the illuminator. It is possible to count pills under normal laboratory lighting.

However, in the world practice of textile materials science there are no examples of practical application of computer models of fabric behavior during exploitation due to a large number of factors influencing this process and the unknown nature of pills placement on the fabric surface during pilling. In this case, the "placement of pills" does not mean the general topography of the product pilling, and the direct placement of individual pills relating to each other. The presence of a mathematical description of this distribution will predict the change in the aesthetic features of the product during wear by visualizing of its look, taking into account the surface characteristics of the fabric used. This, in turn, will facilitate the process of materials confection when manufacturing the products that will not lose their look for a long time, and will encourage consumers to comply with the requirements of conscious fashion. Besides, these results will support the development of the expert systems for selecting fabrics to make transformable garments that are meant to be used during very long time and in different conditions [16].

3 MATERIALS AND METHODS

The research has been carried out according to the method of GOST 3810-72 on the device DIT-M, which has two heads and replaceable hoops. The experiments have been performed on fabrics of the coat group, the raw materials of which are: lavsan, kapron; lavsan, nitron; wool, lavsan, nitron.

Before the experiment fabric samples and abrasive material have been held in atmospheric conditions for at least 24 hours according to GOST 10681-75. Fabric samples have been filled face out. Experiments on fabrics have been done at a specific pressure of 1 kgf/sm^2 and a head rotation speed of 100 rpm.

In order to track the formation of pills on the surface of the material, every 100-500 cycles have been photographed using a digital microscope SigetaForward LCD (10-500x) (65503) (Figure 1). Studies have been performed during nearly 5000 cycles, as this is the maximum allowable limit for coat fabrics [16].

To process the obtained microscopic images, we will use numerical methods, representing pilling clusters as complex nets, in the study of which significant progress has recently been made [18]. For this purpose, we cover the images shown in Figure 1 by circles of the same size and we connect with ribs those ones that are in direct contact. As a result, we receive the nets (links, schemes) shown in Figure 2.

To develop a picture of the hierarchical structure of pills, we will compare each pill's nucleus with a node of a hierarchical tree, and we will represent the clustering process as the movement of a configuration point from lower (the most branched) levels to the top of the tree. There are many distributions of nodes according to the hierarchical levels of various trees [19-20].

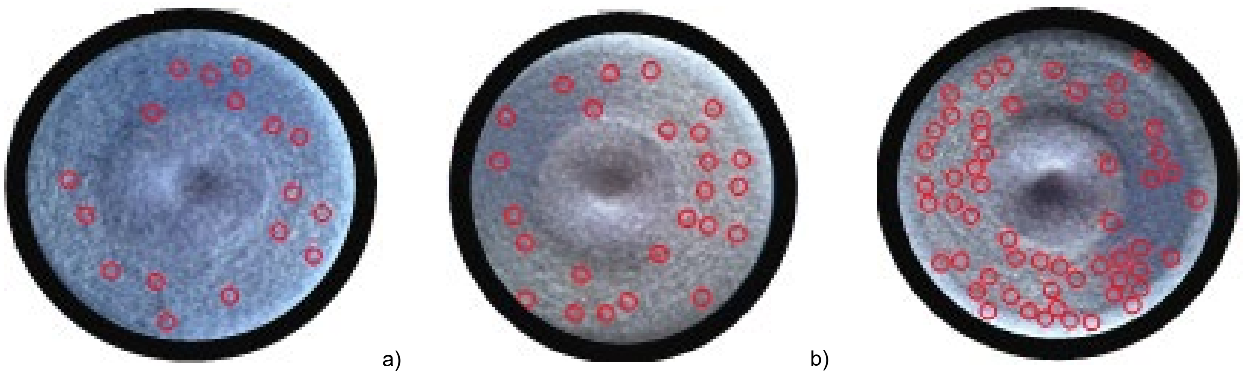

a) b) c)

Figure 1 Photo of a material sample (coat fabric) after 100, 500 and 5000 cycles of friction (a, b, c, respectively)

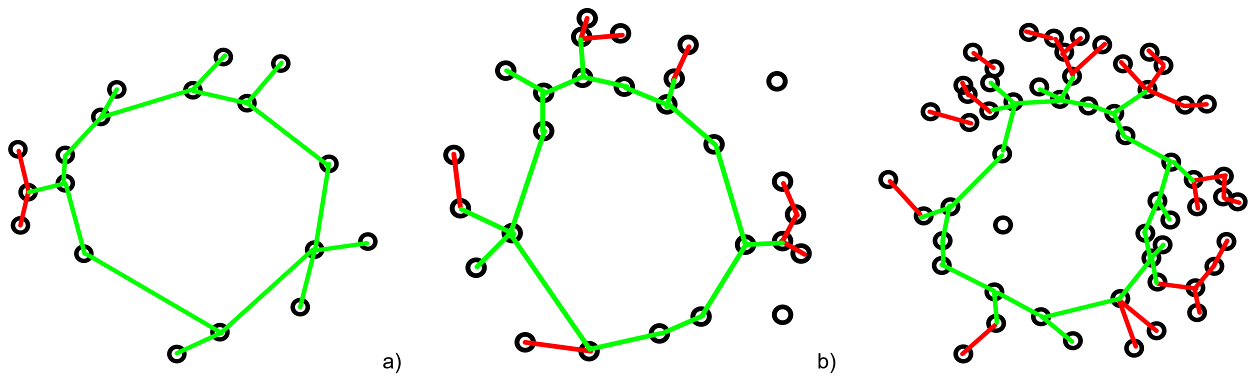

a) b) c)

Figure 2 The pills' nets on fabric surface after 100, 500 and 5000 cycles (a, b, c respectively)

Let us suppose that the maximum number of nodes *D* is located at the lower level and correspond to the distance in the ultra-metric space *k=0*. This level is correlated with a complete ensemble of individual nuclei, the number of which coincides with the number of nodes. The upper level of the hierarchical tree contains a single node that corresponds to a complete cluster of pills' nuclei and is determined by the maximum distance *k=K*. The task is reduced to determining the dependence *D(k)*, which defines the distribution of the number of tree nodes by hierarchical levels.

The main object of our consideration is a random tree. Let letter *h* - numbers the hierarchical levels in such a way that the minimum value corresponds to the top of the tree, and the maximum *h=K* corresponds to the lower level. Then the variable (1) determines the distance in the ultra-metric space, the points of which correspond to the nodes of the Cayley tree type. Moreover, the distance (1) between the nodes of this level is determined by the number of steps to their common ancestor, and the transition to continuous space is provided by the limits $r, K \to \infty$ [21].

$$k = K - h \tag{1}$$

For a random tree type we assume a graded distribution:

$$D_h = h^{\varepsilon}, \ \varepsilon > 0 \tag{2}$$

It is an intermediate case between exponential and linear correlations, which correspond to the limited distributions. Technically, a function *D(x)* is homogeneous, that is, meets the condition $D(hx) = h^{\varepsilon} D(x)$. Depending on the distance (1), this means $D(k) = D\left(1 - \frac{k}{K}\right)^{\varepsilon}$, where $D \equiv K^{\varepsilon}, \ \varepsilon > 1$.

Let us consider the statistical distribution of the pills' nuclei by the absolute values $\Psi(h)$ of their formation, depending on the level number which is indicated by letter *h*. The flow of probability of transition between levels *h* and *h+1* and in the limit *h>>1* is expressed by the generalized correlation:

$$j_h = \mu(\Psi) \cdot \frac{d\Psi}{dh} \tag{3}$$

Features of the type of fabric and its relation to the fiber defects are characterized by the presence of internal structural shift, the coefficient of effective mobility:

$$\mu(\Psi) = \mathrm{M}\Psi^{\lambda} \tag{4}$$

which is determined by a constant $M > 0$ and an indicator λ [22-23]. In steady-state conditions:

$$j_k D_k = J \tag{5}$$

substitution of equalities (2-4) into (5) gives the correlation:

$$\Psi(h) = \frac{D^{\alpha/\varepsilon}}{h^{\varepsilon}} \psi(h) \tag{6}$$

with indicator:

$$\alpha = \frac{\varepsilon - 1}{1 + \lambda} > 0 \tag{7}$$

and a factor $\psi(h)$ is determined by the equation:

$$\frac{dx}{dt} = \frac{\partial \Upsilon}{\partial x} \tag{8}$$

in which time, coordinate and scale are given by the next correlations respectively:

$$t = \alpha \ln h, \ x = \frac{\psi(h)}{\psi_0}, \ \psi_0 = \frac{1}{D}\left(\frac{J}{\alpha M}\right)^{\varepsilon/(\varepsilon-1)} \tag{9}$$

Part of the density of the generating functional reaches the maximum value at a point $x = 0$, and when $x > 1$ monotonically the value decreases.

$$\Upsilon_{\max} = \frac{0{,}5(1+\lambda)}{1-\lambda} \tag{11}$$

The above analysis shows that the process of hierarchical pilling starts with fluctuation overcoming the barrier (11) by subcritical nuclei of the lower level. This process is described by the equation:

$$\frac{dx}{dt} = -\frac{\partial \Upsilon}{\partial x} + \xi \tag{12}$$

with external additive interference $\xi = \xi(t)$, determined by the conditions:

$$\langle \xi(t) \rangle = 0, \ \langle \xi(t)\xi(t') \rangle = 2\delta(t - t') \tag{13}$$

where angle brackets mean averaging. In a formal point of view, equation (12) has a set *{x(t)}* of statistically distributed solutions, the probable density of which is given by a function $\varpi(t,x) = \langle \delta[x - x(t)] \rangle$. This function is determined by next equation [24-25]:

$$\frac{\partial \varpi}{\partial t} + \frac{\partial i}{\partial x} = 0, \ i = -\varpi \frac{\partial \Upsilon}{\partial x} - \frac{\partial \varpi}{\partial x} \tag{14}$$

When the probability flow *i* is equal to zero, the distribution function is reduced to the form:

$$\varpi_0(x) = \frac{e^{-\Upsilon(x)}}{S} \tag{15}$$

determined by formula (10). The statistical sum *Z* is set by the normalization, according to which:

$$S = \int_0^1 e^{\frac{x^2}{2} - \frac{x^{1-\lambda}}{1-\lambda}} dx \tag{16}$$

In accordance with distribution (15), the saddle-point method leads to a value $S \sim e^{-\bar{\Upsilon}}$.

As it can be seen from Figure 3, an increase in the indicator λ leads to a monotonic decrease in the statistical sum from the value of $S \approx 0.7$ at $\lambda=0$ to $S=0$ at $\lambda=1$. So, we can conclude that the behavior of the system acquires an anomalous character with an increase in the effective mobility index (4) to values $\lambda \rightarrow 1$.

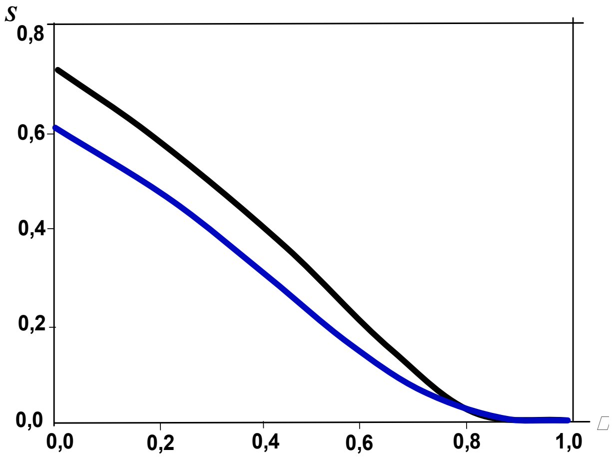

Figure 3 The dependence of the statistical sum (16) on the indicator of effective mobility (4) determined by formula (16) and correlation $S \sim e^{-\Upsilon_{\max}}$ (curves 1, 2 respectively)

When the probable stream takes a constant value $i_0 \neq 0$. According to the equation (14), the steady-state $\varpi(\psi)$ and equilibrium $\varpi_0(\psi)$ distribution functions are conected by the equality [26]:

$$\frac{\varpi(\psi)}{\varpi_0(\psi)} = i_0 \int\limits_{\psi/\psi_{\max}}^{\infty} \frac{dx}{\varpi_0(x)}, \tag{17}$$

where $\varpi \rightarrow 0$, when $\psi \rightarrow \infty$.

In the general case, the flow is inversely proportional to the statistical sum (16). Taking into consideration the correlation $S \sim e^{-\Upsilon}$, one can imply the value $i_0 \sim e^{-\Upsilon}$, according to which the stationary probable flow increases exponentially with the height (11) of the effective potential (10).

The stationary distribution function $\varpi(\psi)$ is determined by equation (17), according to which $\varpi(\psi) \approx \varpi_0(\psi)$ for and $\varpi(\psi) << \varpi_0(\psi)$ when $\psi >> \psi_{\max}$. Using equalities (17), (15) and (10) leads to the equation

$$\varpi(\psi) = i_0 \mathrm{e}^{\left(\frac{\psi^2}{2} - \frac{\psi^{1-\lambda}}{1-\lambda}\right)} \int_{\frac{\psi}{\psi_{\max}}}^{\infty} \mathrm{e}^{\frac{x^{1-\lambda}}{1-\lambda} - \frac{x^2}{2}}. \tag{18}$$

When $\lambda=0$ this equation is simplified to the form:

$$\varpi(\psi) = \sqrt{\frac{e\pi}{2}} i_0 \mathrm{e}^{\left(\frac{\psi^2}{2} - \psi\right)} \mathrm{erfc}\left(\frac{\psi - \psi_{\max}}{\sqrt{2}\psi_{\max}}\right) \tag{19}$$

4 EXPERIMENTAL

Since the ensemble of hierarchically subordinate pills' nuclei is a self-similar set, the probability density distribution $P_{HP}(\phi,k)$ is a homogeneous function of distance k in ultra-metric space [27]:

$$P_{HP}(\phi,k) = (K-k)^{\alpha} \varpi(\psi). \tag{20}$$

The index of the hierarchical level l is omitted; the dependence $\varpi(\psi)$ represents the stationary distribution. Equation (20) follows from correlations (6), (1). On the other hand, a decrease in probability density (20) with distance k in ultra-metric space reflects the hierarchical nature of the pilling process.

First, we will find the probability $\overline{\mathrm{P}}_{HP}(t)$ that at the moment of time t there will not be the emergence of pills. For this purpose, at each moment of time t we should carry out the integration over the distances s of the Debye's exponent $e^{-\frac{t}{t(k)}}$ with the relaxation time $t(k) \equiv t_0 e^{\phi(k)}$, the value of which is set by the height of the barrier:

$$\phi(k) = \frac{\psi(k)}{(K-k)} \tag{21}$$

which follows from equalities (6), (1) (t_0 is the microscopic time scale). Since the indicated Debye's process [20] is realized with a probability density (20), it should be used as a weight function for integration over k. As a result, the desired probability takes the form:

$$\overline{P}_{HP} = \int\limits_0^K \mathrm{e}^{-\left(\frac{t}{t_0}\right)\cdot e^{\frac{1}{\phi(k)}}} \cdot P_{HP}(\phi,k)\,dk \tag{22}$$

The correlation (1) allows us to proceed with integration over the numbers of hierarchical levels h, after which the use of equalities (20-22) leading to the formula:

$$\overline{P}_{HP} = \int\limits_0^K h^{\alpha} \cdot \mathrm{e}^{-\left(\frac{t}{t_0}\right)\cdot \mathrm{e}^{-h^{-\alpha}\psi(h)}} \cdot \varpi(\psi(h))\,dh \tag{23}$$

When $\lambda=0$ equation (8) lead to the formula:

$$\psi = (1 + h^{\alpha})\psi_{\mathrm{m}}, \tag{24}$$

where:

$$\psi_m = \psi_0 e^{\Upsilon_{\max}\cdot\frac{\varepsilon}{\varepsilon-1}} \tag{25}$$

As a result, probability (23) takes the form:

$$\overline{P}_{HP} = \int\limits_{\psi_m}^{\infty} \frac{\psi - \psi_m}{\psi_m} \cdot \mathrm{e}^{-\frac{t}{t_0}\cdot \mathrm{e}^{-\frac{\psi_m \psi}{\psi - \psi_m}}} \cdot \varpi(\psi)\,\mathrm{d}\psi, \tag{26}$$

where the distribution $\varpi(\psi)$ is set by formula (19).

The characteristic time scale $t_{ef} \gg t_0$ cannot be found within the framework of the approximation used.

The above calculations show that in the later stages $t \gg t_{ef}$ the probability $P_{HP}(t) = 1 - \overline{P}_{HP}(t)$ of hierarchical pilling is set by the asymptotic equation (27):

$$P_{HP}(t) \approx 1 - \frac{\sqrt{2\pi}}{\alpha} \psi_m^{1/\alpha} \left[\ln T_0\right]^{-\frac{2+3\alpha}{2\alpha}} \qquad (27)$$

where $T_0 = \dfrac{t}{t_{ef}}$.

Dependence (27) takes place under the following conditions:

- the inequality $\psi - \psi_m << \psi_m$ must be satisfied; on the other hand the maximum distance *K* is so large (*K*>>1) that the continuum approximation can be used;
- the probability density function $\varpi(\psi)$ in distribution (20) is approximated by a step function taking a value of $\varpi = \dfrac{1}{\psi_m}$ in the range from 0 to ψ_m.

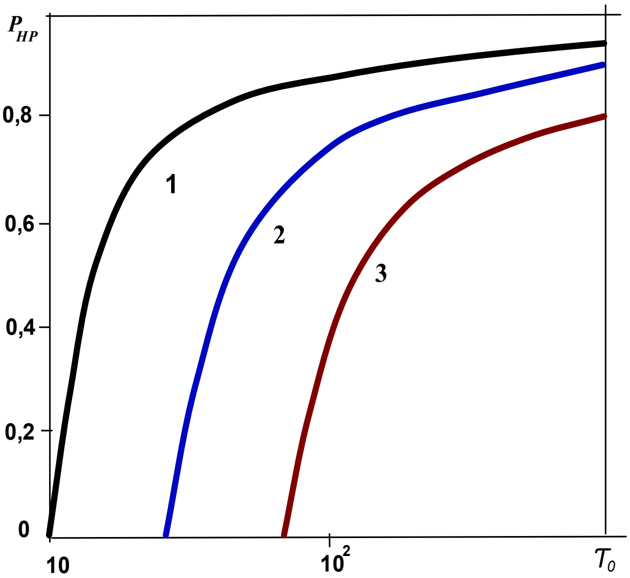

Figure 4 Temporal dependences of hierarchical pilling probability at λ=0 and branching indices such as α=1.25, 1.5, 1.75 (curves 1-3, respectively) obtained according to equality (27)

Dependence (27) is shown in Figure 4, from which it is seen that with increasing time, the probability of the formation of a hierarchical structure monotonically increases to a maximum value of $P_{HP}=1$. With decreasing branching of the hierarchical tree, when the exponential dependence index (2) takes on falling values $\varepsilon \to 1$, and the critical value (25) increases rapidly, the dependence $P_{HP}(t)$ shifts toward longer time. This means that a decrease in the branching of the hierarchical structure leads to a decrease in the probability of its formation.

The received time dependences of the probability of hierarchical pilling are shown in Figure 4. It can be seen from it that this clarification narrows down to a shift of the indicated dependences toward longer times, which is equivalent to a decrease in the time scale t_{ef}. Since the nature of the obtained dependences does not change, it can be concluded that method give qualitatively results.

5 RESULTS

The theoretical scheme presented above shows that the pills' nuclei create an ensemble of hierarchically subordinate objects distributed according to the values (6) of the transformation effect and distances in the ultra-metric space (1) that determine the cluster sizes. The stationary distribution of the pilling effect and the corresponding probability flow are determined by equalities (17). The behavior of the ensemble of pills' nuclei, defined by a homogeneous function (20), is determined by the effective potential (10), reaching the maximum value (11) at a critical value (25).

Regarding the experimental situation, it should be noted that the microscopic photographs shown in Figure 1c are characterized by not very large values of the branching index ε in correlation (2). On the other hand, there is no physical reason to assume that the effective mobility index λ (4) should take large values. Thus, we can assume that the conditions ε-1<<1 and λ=0 are satisfied. As a result, the critical value (25) of the specific pilling effect reaches exponentially large values ψ_m >>1 for weakly branching structures, where the exponent (7) takes small values α<<1.

According to the proposed scenario, the pilling process begins with overcoming the barrier (11) of the effective potential (10), which ensures the condition $\psi > \psi_m$ in time

$$t_m \approx t_0 e^{\Upsilon_m} \qquad (28)$$

With the further time passing, the phase formation is ensured by the propagation of the pills' nuclei, the process of which is reduced to the growth of the pilling effect (24), which proceeds in ultra-metric space. As a result, the long-term asymptotic behavior of the likelihood of forming a net structure of pills is determined by equation (27).

According to Figure 4 the probability of forming a net structure of pills monotonously increases over time, shifting toward longer times with decreasing branching structure. This allows us to explain the behavior of fabrics' pilling, which is observed in the photographs shown in Figure 1. Indeed, the figures show that, for short periods of the time of wearing clothing, the formation of a cluster structure with increased branching is most likely to occur. It is this behavior that Figure 1a demonstrates on which compact pills clusters are present. According to Figure 1b, with an increase in the time of wearing the clothes, the probability of the formation of a weakly branching structure becomes noticeable. In Figure 1c, this is confirmed by the formation of a well-developed net structure.

6 CONCLUSIONS

Thus, the main goal of the paper has been achieved and a mathematical description of the distribution of pills on the surface of textile material has been developed.

Such a description allows predicting the change in aesthetic performance of the product during operation by visualizing its appearance taking into account the surface characteristics of the fabric used.

This, in turn, will facilitate the process of confection of materials in the products' manufacture, which will not lose their look for a long time, and will encourage consumers to comply with the requirements of conscious fashion. The research has been conducted on the fabrics of the coat group, the raw materials of which are: lavsan, kapron; lavsan, nitron; wool, lavsan, nitron. In the process of research, it has been found out that under the action of wear factors for a short time the most probable is the formation of a cluster structure of the hierarchical tree of pills, which have a high branching. With the increasing time of the influence of factors formation of a weakly branched structure a pills' tree is again likely to occur.

The next step of the current research is to examine these results on the other groups of fabrics.

Another direction of research is to experiment on the correlation between fabric properties and parameters of the hierarchical structure of the tree of pills emergence during the pilling formation on textile materials. As a result, we aim to develop the simulation model of pilling formation.

7 REFFERENCES

1. Makhinya T.O., Galavska L.Ye.: Investigation of the influence of the type of raw material, weaving and abrasive surface of the pilling of knitwear, Proceedings of the II. International Scientific Conference of Textile and Fashion Technology KyivTex&Fashion, Kyiv, Ukraine, 2018, pp. 61-64 (in Ukrainian)
2. Ivasenko M.V., Baranova T.M.: Influence of pilling on change of aesthetic indicators of knitted products in the process of wearing, Technology and Design 2(7), 2013 (in Ukrainian)
3. Kuznetsova A.V., Dolgova E.Yu.: Perfection of the method of determining the peeling ability of the textile materials, Scientific Community of Students: Materials of the III. International Student Scientific-Practical Conference, Cheboksary, Russia, 2014, pp. 85-87 (in Russian)
4. Textile Materials. Determination of the Tendency of the Fabric to Tufted Surface and Pilling. Part 1. Methods of Pilling in Boxing: DSTU ISO 12945-1: 2005, National Standard of Ukraine, 12 (in Ukrainian)
5. Tukhanova V.Yu, Tikhonova T.P.: Determination of factors influencing the process of materials confectioning, Modern Science-Intensive Technologies. Regional Application 4 (44), 2015, pp. 204-209 (in Ukrainian)
6. Zubair M., Maqsood H., Neckar B.: Impact of filling yarns on woven fabric performance, Fibres & Textiles in Eastern Europe 24(5), 2016, pp. 50-54, DOI: 10.5604/12303666.1215527
7. Hussain T., Ahmed. S., Qayum A.: Effect of different softeners and sanforising treatment on pilling performance of polyester/viscose blended fabrics, Coloration Technology 124(6), 2008, pp. 375-378, https://doi.org/10.1111/j.1478-4408.2008.00166.x
8. Zhang J., Wang X., Palmer S.: Performance of an objective fabric pilling evaluation method, Textile Research Journal 80(16), 2010, pp. 1648-1657, https://doi.org/10.1177/0040517510361802
9. Sarioglu E., Celik N.: Investigation on regenerated cellulosic knitted fabric performance by using silicone softeners with different particle sizes, Fibres & Textiles in Eastern Europe 23(5), 2015, pp. 71-77, DOI: 10.5604/12303666.1161760
10. Zengbo X., Hongsui Y.: Fabric pilling object detection based on scale - space extremum, 2nd International Conference on Information Science and Control Engineering, 2015, pp. 383-386
11. Yu L., Wang R., Zhou J.: Performance of the pilling evaluation method based on the technique of DFF, Industria Textila 68(1), 2017, pp. 13-16
12. Coldea A., Dorin V.: Study regarding the physical-mechanical properties of knits for garments – pilling performance, 8th International Conference on Manufacturing Science and Education – MSE 2017 "Trends in New Industrial Revolution" 121, 2017, pp. 6-14
13. Özdemir H., Yavuzkasap D.: The effects of yarn and fabric structural parameters on the seam slippage, abrasion and pilling properties of double woven upholstery fabrics, Industria Textila 63(6), 2012, pp. 307-314
14. Li L., Zhu M., Wei X.: Pilling performance of cashmere knitted fabric of woollen ring yarn and mule yarn, Fibres & Textiles in Eastern Europe 22(1), 2014, pp. 74-75
15. Koshevko J., Kushevskiy N.: Design of energy-saving technology of shaping and fixing the shape of headdresses parts, Eastern-European Journal of Enterprise Technologies 3/6(81), 2016, pp. 16-26, DOI: 10.15587/1729-4061.2016.71242

16. Zakharkevich O., Zhylenko T., Koshevko Y., Kuleshova S., Ditkovska O., Shvets G.: Expert system to select the fabrics for transformable garments, Vlakna a textil (Fibres and Textiles) 25(2), 2018, pp. 105-112
17. Bersheda N., Koshevko Y.: Experimental study of material properties for products of transformers, XVII All-Ukrainian Scientific Conference of Young Scientists and Students "Scientific Developments of Youth at the Present stage" 1, Kyiv, Ukraine, 2018, pp. 318-319
18. Xu X., Wang J., Zhou Z., Garoni T.M., Deng Y.: Geometric structure of percolation clusters, Physical Review E 89, 2014, pp. 012120, DOI: 10.1103/PhysRevE.89.012120
19. Olemskoi A.I., Yushchenko O.V., Borisyuk V.N., Zhylenko T.I., Kosminska Yo.O., Perekrestov V.I.: Theory of hierarchical coupling, Physica A 391, 2012, pp. 3277-3284
20. Olemskoi A.I., Yushchenko O.V., Zhilenko T.I.: Investigation of conditions for a self-organized transition to the bistable regime of quasi-equilibrium condensation and stripping of the surface, Physics of the Solid State 53(4), 2011, pp. 845-853, https://doi.org/10.1134/S1063783411040287
21. Rammal R., Thoulouse G., Virasoro M.: Ultrametricity for physicists, Rev. Mod. Phys. 58, 1986, pp. 765-788, https://doi.org/10.1103/RevModPhys.58.765
22. Kharchenko D.O., Dvornichenko A.V.: Phase transitions induced by thermal fluctuations, The European Physical Journal B. 61, 2008, pp. 95-103, https://doi.org/10.1140/epjb/e2008-00035-y
23. Dvornichenko A.V., Kharchenko V.O.: Scaling properties of the growing monolayer on the disordered substrate, Physics Letters A 384(16), 2020, 126329, https://doi.org/10.1016/j.physleta.2020.126329
24. Risken H., Frank T.: The Fokker-Planck Equation, Berlin-Heidelberg: Springer-Verlag, 1996, 485 p., DOI: 10.1007/978-3-642-61544-3
25. Lifshits E.M., Pitaevsky L.P.: Physical Kinetics, 2nd ed., Moscow: Fizmatlit, 2002, 536 p.
26. Parzuski M., Maslov S., Parzuski M., Bak P.: Avalanche dynamics in evolution, growth, and depinning models, Phys. Rev. E. 53(1), 1996, pp. 414-443, DOI: 10.1103/physreve.53.414
27. Sornette D.: Critical Phenomena in Natural Sciences, New York: Springer-Verlag, 2006, 528 p.

INSTRUCTIONS FOR AUTHORS

The journal ,,**Vlákna a textil**" (**Fibres and Textiles**) is the scientific and professional journal with a view to technology of fibres and textiles, with emphasis to chemical and natural fibres, processes of fibre spinning, finishing and dyeing, to fibrous and textile engineering and oriented polymer films. The original contributions and works of background researches, new physical-analytical methods and papers concerning the development of fibres, textiles and the marketing of these materials as well as review papers are published in the journal.

Manuscript

The original research papers are required to be written in English language with summary. The advertisements will be published in a language according to the mutual agreement.

The first page of the manuscript has to contain:

The title of the article (16 pt bold, capital letters, centred)

The full *first name* (s) and also *surnames* of all authors (11 pt, bold, centred).

The complete address of the working place of the authors, e-mail of authors (9 pt, italic, centred)

Abstract (9 pt, italic)

Key words (9 pt, italic)

The manuscript has to be written in A4 standard form, in **Arial, 10 pt**.

The text should be in ***one-column format in single line spacing***.

Page margins: up and down 2.5 cm; left and right 2.0 cm.

Do not number the pages and do not use footnotes. Do not use business letterhead.

Figures, tables, schemes and photos (centered) should be numbered by Arabic numerals and titled over the table and under the figure or picture.

Photos and schemes have to be sufficiently contrastive and insert in text as pictures.

Mathematical formulae should be centred on line and numbered consecutively on the right margin.

Physical and technical properties have to be quantified in **SI units**, names and abbreviations of the chemical materials have to be stated according to the IUPAC standards.

References in the text have to be in square brackets and literature cited at the end of the text. References (9 pt), have to contain names of all authors.

[1] Surname N., Surname N.: Name of paper or Chapter, In Name of Book, Publisher, Place of Publication, YYYY, pp. xxx-yyy, ISBN

[2] Surname N., Surname N.: Name of paper, Name of Journal Vol. (No.), YYYY, pp. xxx-yyy, doi number

[3] Surname N., Surname, N.: Title of conference paper, Proceedings of xxx xxx, conference location, Month and Year, Publisher, City, Surname N. (Ed.), YYYY, pp. xxx-yyy

[4] Surname N., Surname N.: Name of Paper, Available from http://www.exact-address-of-site, Accessed: YYYY-MM-DD

The final template of manuscript is available on **http://www.vat.ft.tul.cz**

Authors are kindly requested to deliver the paper (in Word form) to be published together with information about at least 3 recommended reviewers from institutions others than the parent (name, e-mail, institution and department) by e-mail: marcela.hricova@stuba.sk

After successful review procedure there is charged fee (article processing charge) of EUR 100. All articles after review process are freely available online and this fee helps to cover the costs of taking a manuscript and turning it into a finished article.

Address of the Editor Office:

Marcela Hricová

Faculty of Chemical and Food Technology,

Slovak University of Technology in Bratislava

Radlinskeho 9

812 37 Bratislava,

Slovakia